

**ΕΘΝΙΚΟ ΚΑΙ ΚΑΠΟΔΙΣΤΡΙΑΚΟ ΠΑΝΕΠΙΣΤΗΜΙΟ
ΑΘΗΝΩΝ
ΣΧΟΛΗ ΕΠΙΣΤΗΜΩΝ ΥΓΕΙΑΣ
ΙΑΤΡΙΚΗ ΣΧΟΛΗ**

**ΠΑΝΕΠΙΣΤΗΜΙΑΚΟ ΓΕΝΙΚΟ ΝΟΣΟΚΟΜΕΙΟ «ΑΤΤΙΚΟΝ»
Δ' ΠΑΝΕΠΙΣΤΗΜΙΑΚΗ ΠΑΘΟΛΟΓΙΚΗ ΚΛΙΝΙΚΗ
ΔΙΕΥΘΥΝΤΗΣ: ΚΑΘΗΓΗΤΗΣ ΣΩΤΗΡΙΟΣ ΤΣΙΟΔΡΑΣ**

**Ο ΡΟΛΟΣ ΤΟΥ PD-1 ΣΤΗΝ ΕΝΕΡΓΟΠΟΙΗΣΗ ΤΩΝ
ΜΑΚΡΟΦΑΓΩΝ**

ΔΙΔΑΚΤΟΡΙΚΗ ΔΙΑΤΡΙΒΗ

ΑΝΘΟΣ ΧΡΙΣΤΟΦΙΔΗΣ

ΑΘΗΝΑ 2024

**NATIONAL AND KAPODISTRIAN UNIVERSITY OF
ATHENS
SCHOOL OF HEALTH SCIENCES
SCHOOL OF MEDICINE**

**«ATTIKON» UNIVERSITY HOSPITAL
4TH DEPARTMENT OF INTERNAL MEDICINE
DIRECTOR: PROFESSOR SOTIRIOS TSIODRAS**

**THE ROLE OF PD-1 IN MACROPHAGE
POLARIZATION AND FATE COMMITMENT**

DOCTORAL THESIS

ANTHOS CHRISTOFIDES, MD

ATHENS 2024

ΓΕΝΙΚΑ ΣΤΟΙΧΕΙΑ ΔΙΔΑΚΤΟΡΙΚΗΣ ΔΙΑΤΡΙΒΗΣ

Ημερομηνία αίτησης: 26/06/2020

Ημερομηνία ορισμού τριμελούς Συμβουλευτικής Επιτροπής: 27/07/2020

Μέλη τριμελούς Συμβουλευτικής Επιτροπής:

- Δημήτριος Τ. Μπούμπας, Καθηγητής Ιατρικής Σχολής, ΕΚΠΑ (Επιβλέπων)
- Βασιλική Α. Μπουσιώτη, Καθηγήτρια Ιατρικής Σχολής, Πανεπιστήμιο Harvard και BIDMC Κέντρο Καρκίνου, Beth Israel Deaconess Medical Center
- Παναγιώτης Βεργίνης, Αν. Καθηγητής Ιατρικής Σχολής, Πανεπιστήμιο Κρήτης

Ημερομηνία ορισμού θέματος: 05/08/2020

Πρόεδρος Ιατρικής Σχολής:

Νικόλαος Αρκαδόπουλος, Καθηγητής Ιατρικής Σχολής, ΕΚΠΑ

Επταμελής Εξεταστική Επιτροπή:

- Δημήτριος Τ. Μπούμπας, Καθηγητής Ιατρικής Σχολής, ΕΚΠΑ
- Βασιλική Α. Μπουσιώτη, Καθηγήτρια Ιατρικής Σχολής, Πανεπιστήμιο Harvard και BIDMC Κέντρο Καρκίνου, Beth Israel Deaconess Medical Center
- Παναγιώτης Βεργίνης, Αν. Καθηγητής Ιατρικής Σχολής, Πανεπιστήμιο Κρήτης
- Σωτήριος Τσιόδρας, Καθηγητής Ιατρικής Σχολής, ΕΚΠΑ
- Δημήτριος Βασιλόπουλος, Καθηγητής Ιατρικής Σχολής, ΕΚΠΑ
- Παναγιώτης Τσιριγώτης, Καθηγητής Ιατρικής Σχολής, ΕΚΠΑ
- Αντώνιος Φανουριάκης, επ. Καθηγητής Ιατρικής Σχολής, ΕΚΠΑ

Στη Μαρία μου, τη σύζυγο και φίλη μου,

Που με αγαπά και με στηρίζει στα δύσκολα και στα εύκολα.

Στον πατέρα και τη μάνα μου,

Που είναι πάντα δίπλα μου, που με έμαθαν να αγαπώ τη γνώση και την επιστήμη, που με αγαπούν χωρίς όρους και με στηρίζουν σε όλες μου τις αποφάσεις.

Στον μικρό μου αδερφό, τον Ιωάννη,

Που εκτός από αδερφός είναι φίλος και συνάδερφος μου.

Στον Δρ. Δημήτρη Μπούμπα,

Που με καθοδήγησε και με στήριξε σαν δεύτερος πατέρας.

Στη Δρ. Βασιλική Μπουσιώτη,

Που μου έδωσε την ευκαιρία να συνεχίσω το όνειρο μου στις ΗΠΑ,

που είναι παράλληλα μέντορας μου και καλή φίλη.

ΕΥΧΑΡΙΣΤΙΕΣ

Από τα πρώτα μου βήματα ως φοιτητής ιατρικής, με προσέλκυσε ιδιαίτερα η έρευνα και έτσι άρχισα να ασχολούμαι με ερευνητικά προγράμματα σε διάφορα εργαστήρια. Έμαθα τι σημαίνει επιστημονική διαδικασία και πορεία και κατάλαβα πόσο συναρπαστική είναι η δυνατότητα του να ανακαλύπτεις νέες γνώσεις.

Θέλω να ευχαριστήσω τον Δρ. Δημήτρη Μπούμπα που μου δίδαξε ότι η ανάπτυξη της νοοτροπίας ενός ερευνητή παράλληλα με την ανάπτυξη των ιατρικών γνώσεων θα μου επέτρεπε να γίνω καλύτερος γιατρός και ότι είναι πολύ σημαντικό να αναζητούμε την αιτία, για να κατανοούμε την επιστημονική επεξήγηση πίσω από τα ιατρικά προβλήματα των ασθενών μας.

Ως φοιτητής επιδίωξα να εργαστώ σε διάφορα επιστημονικά εργαστήρια τόσο στον ελληνικό χώρο όσο και στις ΗΠΑ. Αυτές οι ερευνητικές εμπειρίες με βοήθησαν να εκτιμήσω περισσότερο τη σύνδεση μεταξύ έρευνας και ιατρικής και διαμόρφωσαν την επιθυμία και τη δέσμευσή μου να ακολουθήσω μια καριέρα ως ιατρός-ερευνητής.

Σταθμός για μένα ήταν η γνωριμία μου με τη Δρ. Μπουσιώτη στο Beth Israel Deaconess Medical Center, του Harvard Medical School. Η πρώτη θητεία μου στο εργαστήριο της, όταν ήμουν ακόμη φοιτητής Ιατρικής, είχε συνέχεια αφού μετά την αποφοίτηση μου από την Ιατρική Σχολή του Πανεπιστημίου Αθηνών είχα την ευκαιρία να συνεχίσω μαζί της το μαγικό ταξίδι της έρευνας, αποκτώντας ταυτόχρονα όχι μόνο μία εξαιρετική επιστημονική σύμβουλο και μέντορα, αλλά και μία καλή φίλη.

Η ένταξη μου στο εργαστήριο της Δρ. Μπουσιώτη στην Ιατρική Σχολή του Χάρβαρντ, ως ερευνητής για τη διερεύνηση των μηχανισμών της ανοσολογίας των όγκων, ήταν μια συνειδητή

απόφαση. Πάντα με ενδιέφεραν οι τρόποι με τους οποίους το ανοσοποιητικό σύστημα θα μπορούσε να χρησιμοποιηθεί για την καταπολέμηση του καρκίνου. Τα τελευταία χρόνια, οι πρωτοποριακές ανακαλύψεις της ανοσολογίας έχουν αναδιαμορφώσει τη θεραπεία του καρκίνου.

Τέλος, θα ήθελα να ευχαριστήσω τον Δρ. Βεργίνη, για όλη τη βοήθεια, τη στήριξη, και τις πολύτιμες συμβουλές για την ολοκλήρωση αυτής της διδακτορικής διατριβής.

Οι ερευνητικές μου δραστηριότητες δεν μου φανερώνουν μόνο τα θαύματα της βασικής επιστήμης, αλλά με έχουν επίσης διδάξει πώς η έρευνα αποτελεί τη βάση για τη συνεχή εξέλιξη των πρωτοκόλλων περίθαλψης στην κλινική ιατρική.

Contents / Περιεχόμενα

- Curriculum Vitae / Βιογραφικό σημείωμα
- Abbreviations / Συντομεύσεις
- Abstract / Περίληψη
- Introduction / Εισαγωγή
 - I. Cancer Immunotherapy
 - II. Tumor Microenvironment (TME)
 - III. The gating strategy for immune cells of TME
 - IV. The role of PD-1 in myeloid cells
 - V. The PD-1 – SHP-2 interaction
- Papers / Επιστημονικά άρθρα
- Unanswered questions and future directions / αναπάντητα
ερωτήματα και μελλοντικοί στόχοι
- Key findings / Βασικά πορίσματα
- Citations / Αναφορές

Curriculum Vitae

Education

M.D Doctor in Medicine 2011-2018
Medical School, National and Kapodistrian University of Athens, Greece.

ECFMG Certified 2020

Post-Graduation Training

PhD in Medicine Aug. 2020 – Present
Medical School, National and Kapodistrian University of Athens, Greece.

Research Fellowship Dec. 2018- June 2022
Beth Israel Deaconess Medical Center, Harvard Medical School, Boston, MA, USA.

Medical Residency in Internal Medicine June 2022 – Present
Yale New Haven hospital, New Haven, Connecticut, USA.

Research Internships during Medical School

Department of Biology, Aug. – Sept 2012
University of Cyprus, Nicosia, Cyprus.

Motor Neuron Centre, Pathology and Cell Biology Department, Aug. 2013
University of Columbia. NY, USA.

Beth Israel Deaconess Medical Center / Harvard Medical School, Aug. 2015
Boston, MA, USA.

Electives, Internships and Observerships during Medical School

Observership in Medical and Radiation Oncology, Sept. – Dec. 2016
Bank of Cyprus Oncology Centre, Nicosia, Cyprus.

Observership in Interventional Radiology, Feb. 2018
Department of Radiology and Radiological Sciences, Johns Hopkins Medical School, Baltimore, USA.

Elective in Medical Oncology, Feb. – March
Department of Oncology, Johns Hopkins Medical School, Baltimore, USA. 2018

Work Related Courses

2nd Summer School in Biomedical Research & Management of the World Hellenic Biomedical Association May/ June 2013 (1st part: May 26-June 2, 2013, Monemvasia, Greece, 2nd part: June 3-4, 2013, Monemvasia/Sparta, Greece). 2013

Advanced Trauma Life Support: June 23-24, 2017, Athens, Greece. 2017

Advanced Life Support: July 07-08, 2018, Athens, Greece. 2018

HMX Pro Immunology—Immuno-oncology course offered by Harvard Medical School Office of Online Learning, External Education: June 9 – August 21. 2020

HMX Pro Immunology—Novel Therapies for Chronic Inflammation, Autoimmunity, and Allergy course offered by Harvard Medical School Office of Online Learning, External Education: January 12 – March 26. 2021

Awards

Special award by Dr. Michalis Koutsilieris to participate in “Physiology days in Mani” Conference (Award offered to students with grade 10/10 in Physiology), Mani, Greece (October 4-10, 2013). 2013

19th Basic Sciences Olympiad of Medical Knowledge, Member of the 3rd Prize winning team, Athens, Greece. 2015

Graduation of Athens Medical school with honors (GPA 8.93/10), Athens, Greece. 2018

ASH Annual Meeting & Exposition Abstract Achievement award. 2020/2021/2023

Teaching Assistantships - Research Supervisory - Training Responsibilities

Teaching assistant in Neuroanatomy Sept. 2013 –
Medical School, National and Kapodistrian University of Athens, Feb. 2014
Athens, Greece.

Supervision and teaching of laboratory interns Dec. 2018 –
Beth Israel Deaconess Medical Center / Harvard Medical School, June 2022
Boston, MA, USA.

Publications

1. Pneumaticos SG, **Christofides A**, Gkioka E, Kalogeropoulos T, Msaouel P, Koutsilieris M. Osteoprotegerin expression during the micro- and macrometastatic phases of the osteoblastic metastasis in prostate cancer: therapeutic implications. *Expert Opin Ther Targets*, 2013;17:1395-403. 10.1517/14728222.2013.834889
2. **Christofides A**, Kosmopoulos M, Piperi C. Pathophysiological mechanisms regulated by cytokines in gliomas. *Cytokine*, 2015;71:377-84. 10.1016/j.cyto.2014.09.008
3. Karantanos T, **Christofides A**, Barhdan K, Li L, Boussiotis VA. Regulation of T Cell Differentiation and Function by EZH2. *Front Immunol*, 2016;7:172. 10.3389/fimmu.2016.00172
4. **Christofides A**, Karantanos T, Bardhan K, Boussiotis VA. Epigenetic regulation of cancer biology and anti-tumor immunity by EZH2. *Oncotarget*, 2016;7:85624-40. 10.18632/oncotarget.12928
5. Kosmopoulos M, **Christofides A**, Drekolias D, Zavras PD, Gargalionis AN, Piperi C. Critical Role of IL-8 Targeting in Gliomas. *Curr Med Chem*, 2018;25:1954-67. 10.2174/0929867325666171129125712
6. Strauss L, Mahmoud MAA, Weaver JD, Tijaro-Ovalle NM, **Christofides A**, Wang Q, et al. Targeted deletion of PD-1 in myeloid cells induces antitumor immunity. *Sci Immunol*, 2020;5:10.1126/sciimmunol.aay1863
7. **Christofides A**, Tijaro-Ovalle NM, Boussiotis VA. Commentary on: Combination of Metabolic Intervention and T Cell Therapy Enhances Solid Tumor Immunotherapy. *Immunometabolism*, 2021;3:10.20900/immunometab20210016

8. **Christofides A**, Konstantinidou E, Jani C, Boussiotis VA. The role of peroxisome proliferator-activated receptors (PPAR) in immune responses. *Metabolism*, 2021;114:154338. 10.1016/j.metabol.2020.154338
9. **Christofides A**, Cao C, Pal R, Aksoylar HI, Boussiotis VA. Flow Cytometric Analysis for Identification of the Innate and Adaptive Immune Cells of Murine Lung. *J Vis Exp*, 2021;10.3791/62985
10. Sari-Ak D, Torres-Gomez A, Yazicioglu YF, **Christofides A**, Patsoukis N, Lafuente EM, et al. Structural, biochemical, and functional properties of the Rap1-Interacting Adaptor Molecule (RIAM). *Biomed J*, 2022;45:289-98. 10.1016/j.bj.2021.09.005
11. Yeo AT, Rawal S, Delcuze B, **Christofides A**, Atayde A, Strauss L, et al. Single-cell RNA sequencing reveals evolution of immune landscape during glioblastoma progression. *Nat Immunol*, 2022;23:971-84. 10.1038/s41590-022-01215-0
12. **Christofides A**, Strauss L, Yeo A, Cao C, Charest A, Boussiotis VA. The complex role of tumor-infiltrating macrophages. *Nat Immunol*, 2022;23:1148-56. 10.1038/s41590-022-01267-2
13. Yenyuwadee S, Aliazis K, Wang Q, **Christofides A**, Shah R, Patsoukis N, et al. Immune cellular components and signaling pathways in the tumor microenvironment. *Semin Cancer Biol*, 2022;86:187-201. 10.1016/j.semcancer.2022.08.004
14. **Christofides A**, Katopodi XL, Cao C, Karagkouni D, Aliazis K, Yenyuwadee S, et al. SHP-2 and PD-1-SHP-2 signaling regulate myeloid cell differentiation and antitumor responses. *Nat Immunol*, 2023;24:55-68. 10.1038/s41590-022-01385-x

Abstracts, Poster Presentations and Exhibits Presented at Professional Meetings (Presenter of every project was the first name)

1. **Anthos Christofides**, Natalia M Tijaro-Ovalle, Halil-Ibrahim Aksoylar, Rinku Pal, Mohamed A.A. Mahmoud, Laura Strauss, Nikolaos Patsoukis, Vassiliki A Boussiotis, Myeloid-Specific SHP-2 Ablation Induces Robust Anti-Tumor Immunity That Is Not Further Enhanced By PD-1 Blockade. Oral presentation at the 62nd American Society of Hematology Annual Meeting 2020, Dec 5-8.
2. **Anthos Christofides**, Natalia M. Tijaro-Ovalle, Ioannis Politkos, Haesook T. Kim, Vassiliki A. Boussiotis, Angiogenic Factors serve as regulators and predictors of immune

reconstitution after Umbilical Cord Blood Transplantation in Adults. Poster presentation at the Cell and Experimental Biology conference Dec 9-11, 2020.

3. **Anthos Christofides**, Carol Cao, Rinku Pal, Vassiliki A. Boussiotis, RIAM regulates myeloid cell fate commitment and macrophage polarization and controls tumor progression. Poster presentation at the Annual Meeting of the American Association of Immunologists, May 10-15, 2021.
4. **Anthos Christofides**, Rinku Pal, Halil-Ibrahim Aksoylar, Mahshid Arabi, Maciej M. Markiewski, Vassiliki A. Boussiotis, Cancer induces an immunosuppressive milieu in non-metastatic lungs. Poster presentation at the Annual Conference of the American Thoracic Society, May 14-19, 2021.
5. **Anthos Christofides**, Carol Cao, Qi Wang, Natalia M Tijaro-Ovalle, Eirini Konstantinidou, Rushil Shah, Chinmay Jani, Rinku Pal, Halil-Ibrahim Aksoylar, Nikolaos Patsoukis, Vassiliki A Boussiotis. PPAR α Ablation Suppresses T cell responses and Anti-Tumor Immunity By Compromising the Antigen-Presenting Properties of Tumor Associated Macrophages. Oral presentation at the 63rd American Society of Hematology Annual Meeting 2021, Dec 11-14.
6. Rushil Shah, **Anthos Christofides**, Halil-Ibrahim Aksoylar, Rinku Pal, Vassiliki A Boussiotis, Nikolaos Patsoukis, Loss of the nuclear receptor PPAR γ primes CD8⁺ T cells for exhaustion. presentation at the Annual Meeting of the American Association of Immunologists May 6-10 2022.
7. **Anthos Christofides**, Xanthi-Leda Katopodi, Carol Cao, Dimitra Karagkouni, Konstantinos Aliazis, Sasitorn Yenyuwadee, Rinku Pal, John Asara, Ioannis Vlachos, Nikolaos Patsoukis, Vassiliki A Boussiotis, SHP-2 Regulates Myeloid Cell Differentiation, Anti-Tumor Responses and Innate Immune Memory. Oral presentation at the 64th American Society of Hematology Annual Meeting 2022, Dec 10-13.
8. Rushil Shah, Xanthi-Leda Katopodi, **Anthos Christofides**, Rinku Pal, Ioannis Vlachos, Nikolaos Patsoukis, Vassiliki A Boussiotis, Loss of the Nuclear Receptor Ppar γ Primes T Effector (T_{EFF}) Differentiation of Antigen-Specific CD8⁺ T Cells. Poster presentation at the 64th American Society of Hematology Annual Meeting 2022, Dec 10-13.
9. Sasitorn Yenyuwadee, Konstantinos Aliazis, **Anthos Christofides**, Halil-Ibrahim Aksoylar, Rinku Pal, Vassiliki A Boussiotis, 42243 RIAM regulates T cell migration and activation in melanoma. Oral presentation at the Annual meeting of the American Academy of Dermatology 2023, March 17-21.
10. Konstantinos Aliazis, **Anthos Christofides**, Halil-Ibrahim Aksoylar, Rushil Shah, Rinku Pal, Nikolaos Patsoukis, Vassiliki A Boussiotis, Specific PD-1 Deletion on Regulatory T Cells Leads to Enhanced Anti-Tumor Responses. Poster presentation at the 65th American Society of Hematology Annual Meeting 2023, Dec 9-12.

11. **Anthos Christofides**, Rinku Pal, Nikolaos Patsoukis, Vassiliki A Boussiotis, Targeted Deletion of Ppar β/δ in Myeloid Cells Enhances Their Tumor-Promoting Function/ Poster presentation at the 65th American Society of Hematology Annual Meeting 2023, Dec 9-12.
12. Betul Ibis, **Anthos Christofides**, Konstantinos Aliazis, Rushil Shah, Rinku Pal, Vassiliki A Boussiotis, Ppar β/δ Has an Indispensable Role in T Cell Function and Anti-Tumor Response. Poster presentation at the 65th American Society of Hematology Annual Meeting 2023, Dec 9-12.
13. Rushil Shah, Konstantinos Aliazis, **Anthos Christofides**, Angelique A Pham, Rinku Pal, Vassiliki A Boussiotis, PD-1 Expression By Dendritic Cells Is a Key Regulator of T-Cell Immunity in Cancer. Poster presentation at the 65th American Society of Hematology Annual Meeting 2023, Dec 9-12.

Abbreviations

PD-1: Program Death protein 1

CTLA4: Cytotoxic T-Lymphocyte Associated protein 4

PD-L1 Program Death-Ligand 1

CD80: Cluster of Differentiation 80

CD86: Cluster of Differentiation 86

TIM-3: T cell Immunoglobulin and Mucin domain molecule 3

TIGIT: T cell Immunoreceptor with Ig and ITIM domains

LAG3: Lymphocyte-Activation gene 3

GITR: Glucocorticoid-induced tumor necrosis factor receptor-related protein

VISTA: V-domain Ig suppressor of T cell activation

FDA: Food and drug administration

CD28: Cluster of differentiation 28

TCR: T-cell receptor

MHC class II: Major histocompatibility complex class II

CAR T cell: Chimeric antigen receptor T cell

TILs: Tumor-infiltrating lymphocytes

CRS: Cytokine release syndrome

IL-2: Interleukin-2

IFN α : Interferon-alpha

IFN γ : Interferon-gamma

IL-7: Interleukin-7

IL-21: Interleukin-21

IL-12: Interleukin-12

GM-CSF: Granulocyte-macrophage colony-stimulating factor

CD3: Cluster of differentiation 3

TME: Tumor microenvironment

TAMs: Tumor associated macrophages

CD45: Cluster of differentiation 45

CD11b: Cluster of differentiation 11b

CD14: Cluster of differentiation 14

CD163: Cluster of differentiation 163

CX3CR1: C-X3-C Motif Chemokine Receptor 1

HLA-DR: Human Leukocyte Antigen – DR isotype

MDSCs: Myeloid-derived suppressor cells

DAMPs: Danger-associated molecular patterns

PMN-MDSCs: Polymorphonuclear - Myeloid-derived suppressor cells

M-MDSCs: Monocytic - Myeloid-derived suppressor cells

Ly6G: Lymphocyte antigen 6 complex, locus G

Ly6C: Lymphocyte antigen 6 complex, locus C

CD66: Cluster of differentiation 66

CD15: Cluster of differentiation 15

TADCs: Tumor associated DCs

cDC1: Classical Dendritic cell 1

cDC2: Classical Dendritic cell 2

pDCs: Plasmacytoid Dendritic cells

MoDCs: Monocyte-derived Dendritic cells

CD64: Cluster of differentiation 64

CD3: Cluster of differentiation 3

CD8: Cluster of differentiation 8

Grz B: Granzyme beta

CD4: Cluster of differentiation 4

LN: Lymph nodes

APCs: Antigen presenting cells

MHC class I: Major histocompatibility complex class I

Tregs: T regulatory cells

FOXP3: Forkhead box protein P3

CD25: Cluster of differentiation 25

SHP-2: SRC homology region 2 – containing protein tyrosine phosphatase 2

HOXA10: Homeobox A10

IRF8: Interferon regulatory factor 8

Abstract

Background

PD-1 is a checkpoint receptor that has been shown to inactivate T cells through SHP-2 recruitment. However, tumor bearing mice with conditional deletion of SHP-2 in T cells did not demonstrate any differences in tumor progression compared to wild type mice. Both PD-1 and SHP-2 are also expressed in myeloid cells, including the myeloid cells progenitors. PD-1 deletion in myeloid cells can induce differentiation of myeloid progenitors towards mature myeloid cells, while SHP-2 gain-of-function mutations are known to be implicated in Acute Myelogenous Leukemia, by preventing differentiation, through dephosphorylation of IRF-8 and HOXA10. Nevertheless, no PD-1/SHP-2 interaction has been described in primary healthy myelocytes. The goal of this study, is to investigate the PD-1 / SHP-2 interaction in myeloid cells in the context of tumor and the role of this axis in myeloid cell fate commitment and anti-tumor immunity.

Methods

We generated mice with conditional deletion of *Ptpn11* gene (encoding for Shp-2) in myeloid cells ($Shp2^{f/f}LysMCre$), or T cells ($Shp2^{f/f}LckCre$) and used $Shp2^{f/f}$ mice as control. We also used mice with myeloid-specific deletion of the *Pdcd1* gene (encoding for PD-1). Tumor cells were injected subcutaneously and tumor growth was monitored. We used two different tumor cell lines: MC17-51 fibrosarcoma and B16-F10 melanoma. At termination, tumors, spleens and bone marrows were collected, processed (details below), and immune populations were identified by flow cytometry. For cell isolation we used Fluorescence-Activated Cell Sorting (FACS) and magnetic beads and for signaling studies we used bone marrow cells cultured with GM-CSF and IL-3. Methods are described in detail below.

Results

Mice with myeloid-specific SHP-2 ablation had significantly decelerated tumor growth compared to mice with T cell-specific SHP-2 ablation or control mice, but did not gain extra benefit from PD-1 blockade. SHP-2 deletion in myeloid cells resulted in T cell activation and myeloid cell activation and differentiation, while MDSCs had diminished suppressive properties and monocytes acquired lasting anti-tumor properties. Furthermore, by using RNA sequencing and gene set enrichment analysis in TAMs and PMN MDSCs, we demonstrated that SHP-2 deletion enriched gene pathways related to activation, differentiation, phagocytosis and antigen presentation in both these myeloid cell types. Myeloid specific PD-1 ablation had very similar effects in T cells and myeloid cells, and RNAseq of PD-1 deficient TAMs showed greater than 50% overlap in gene expression with SHP-2 deficient TAMs. Furthermore, we determined that in myeloid cells, GM-CSF induced phosphorylation of PD-1, recruited SHP-2 to the GM-CSF receptor and facilitated PD-1-SHP-2 interaction. Finally, either PD-1 or SHP-2 deletion enhanced GM-CSF-dependent myeloid differentiation by abrogating SHP-2 mediated dephosphorylation of IRF8 and HOXA10.

Conclusion

With the current study, we showed that PD-1-SHP-2 interaction can play a role in the differentiation of bone marrow myelocytes and myeloid cell progenitors and, subsequently, can affect their function and anti-tumor immunity.

Περίληψη

Εισαγωγή

Το μόριο προγραμματισμένου θανάτου-1 (PD-1) είναι ένας υποδοχέας των σημείων ελέγχου του ανοσοποιητικού συστήματος, ο οποίος απενεργοποιεί τα Τ κύτταρα δια μέσου του SHP-2. Παρ'όλ'αυτά, η στοχευμένη διαγραφή του SHP-2 στα Τ κύτταρα σε ποντίκια με καρκινικούς όγκους δεν έδειξε κάποια διαφορά στην εξέλιξη των όγκων σε σχέση με τα ποντίκια στην ομάδα ελέγχου. Το PD-1, όπως και το SHP-2, εκφράζονται επίσης και στα μυελοκύτταρα, συμπεριλαμβανομένων και των πρώιμων μυελοκυττάρων στον μυελό των οστών. Η διαγραφή του PD-1 προκαλεί τη διαφοροποίηση των πρώιμων μυελοκυττάρων σε ώριμα μυελοκύτταρα. Αντιθέτως, μεταλλάξεις αυξημένης λειτουργικότητας του SHP-2 εμποδίζουν την διαφοροποίηση των μυελοκυττάρων μέσω της αποφωσφορυλίωσης του IRF-8 και του HOXA10, και ως εκ τούτου εμπλέκεται στην Οξεία Μυελογενή Λευχαιμία. Η αλληλεπίδραση του PD-1 με το SHP-2 δεν έχει ποτέ μελετηθεί στα μυελοκύτταρα. Ο σκοπός αυτής της μελέτης είναι να διερευνήσει αυτή την αλληλεπίδραση στα φυσιολογικά μυελοκύτταρα, και να μελετήσει τον ρόλο του άξονα PD-1/SHP-2 στην αντικαρκινική ανοσία.

Μεθοδολογία

Δημιουργήσαμε ποντίκια με στοχευμένη διαγραφή του γονιδίου *Ptprn11* (που κωδικοποιεί την πρωτεΐνη SHP-2) στα μυελοκύτταρα (*Shp2^{f/f} LysMCre*), ή στα Τ κύτταρα (*Shp2^{f/f} LckCre*) και χρησιμοποιήσαμε τα *Shp2^{f/f}* ποντίκια ως ομάδα ελέγχου. Ομοίως, χρησιμοποιήσαμε ποντίκια με στοχευμένη διαγραφή του γονιδίου *Pdcd1*, που κωδικοποιεί την πρωτεΐνη PD-1. Χρησιμοποιήσαμε 2 διαφορετικές καρκινικές κυτταρικές σειρές: MC17-51 κύτταρα ινομυοσαρκώματος και B16-F10 κύτταρα μελανώματος. Μετά την ευθανασία των ποντικών, οι

όγκοι, οι σπλήνες και οι μυελοί των οστών απομονώθηκαν και επεξεργάστηκαν (όπως περιγράφεται πιο κάτω) και οι διάφοροι πληθυσμοί του ανοσολογικού συστήματος ταυτοποιήθηκαν με κυτταρομετρία ροής. Για απομόνωση κυττάρων χρησιμοποιήσαμε κυτταρομετρία ροής ενεργοποιούμενης από φθορισμό (FACS) και μαγνητικά σφαιρίδια, και για τη μελέτη σηματοδότησης χρησιμοποιήσαμε κύτταρα μυελού των οστών σε καλλιέργεια με παράγοντα διέγερσης αποικιών από κοκκιοκύτταρα-μακροφάγα (GM-CSF) και ιντερλευκίνη 3 (IL-3). Η μεθοδολογία περιγράφεται λεπτομερώς πιο κάτω.

Αποτελέσματα

Τα ποντίκια με στοχευμένη διαγραφή του SHP-2 στα μυελοκύτταρα είχαν σημαντική επιβράδυνση στην ανάπτυξη του όγκου, σε σχέση με τα ποντίκια με διαγραφή του SHP-2 στα T κύτταρα ή τα ποντίκια της ομάδας ελέγχου, χωρίς όμως να έχουν επιπλέον όφελος όταν τους χορηγήθηκαν αναστολείς του PD-1. Η στοχευμένη διαγραφή του SHP-2 στα μυελοκύτταρα είχε ως αποτέλεσμα την ενεργοποίηση των T κυττάρων, την ενεργοποίηση και διαφοροποίηση των μυελοκυττάρων, την άμβλυνση των κατασταλτικών ιδιοτήτων των κατασταλτικών κυττάρων της μυελικής σειράς (MDSCs) και την απόκτηση αντι-καρκινικών ιδιοτήτων μακράς διάρκειας από τα μονοκύτταρα. Επιπρόσθετα, χρησιμοποιώντας RNA-seq σε μακροφάγα που βρίσκονται μέσα στον όγκο (TAMs) και σε MDSCs με χαρακτηριστικά πολυμορφύρητων, δείξαμε ότι η διαγραφή του SHP-2 ενίσχυσε τα γονιδιακά μονοπάτια που σχετίζονται με την ενεργοποίηση, διαφοροποίηση, φαγοκυττάρωση και αντιγονοπαρουσίαση από αυτά τα κύτταρα. Η στοχευμένη διαγραφή του PD-1 στα μυελοκύτταρα είχε όμοια λειτουργικά αποτελέσματα στα T κύτταρα και στα μυελοκύτταρα με αυτά που παρατηρήσαμε μετά από τη διαγραφή του SHP-2, ενώ RNA-seq σε TAMs από ποντίκια με στοχευμένη διαγραφή του PD-1 στα μυελοκύτταρα έδειξε περισσότερο

από 50% επικάλυψη σε γονιδιακή έκφραση με τα TAMs που απομονώθηκαν από ποντίκια που τα στοχευμένη διαγραφή του SHP-2 στα μυελοκύτταρα. Δείξαμε επίσης ότι στα μυελοκύτταρα, η φωσφορυλίωση του PD-1 από το GM-CSF στρατολόγησε το SHP-2 και οδήγησε σε αλληλεπίδραση PD-1-SHP-2. Τέλος, η διαγραφή είτε του PD-1, είτε του SHP-2 είχε σαν συνεπεια τη διαφοροποίηση των μυελοκυττάρων μέσω της καταστολής της αποφωσφορυλίωσης του IRF8 και του HOXA10 από το SHP-2.

Συμπέρασμα

Με την μελέτη αυτή, αποδείξαμε ότι η αλληλεπίδραση του PD-1 με το SHP-2 σε κύτταρα της μυελικής σειράς , παίζει ρόλο στη διαφοροποίηση και την ενεργοποίηση τους, και ως εκ τούτου μπορεί να επηρεάσει την αντικαρκινική ανοσία.

Introduction

I. Cancer immunotherapy

Cancer is the second most common cause of death worldwide [1] . As a result of the scientific evolution the last decades and the development of new or more efficient therapies, the prognosis of cancer has been improved significantly, and, nowadays, many types of cancers, can be treated or even cured [2]. Initially, chemotherapy, surgery and radiotherapy were the milestones of cancer treatment. However, the improved understanding of the immune system, and the ability to utilize and redirect immune cells against tumor cells, started a new field in cancer therapy, which is now widely known as “cancer immunotherapy”. Many different types of immunotherapy approaches have been developed including check-point inhibitors, adoptive cell immune therapy, cancer vaccines, cytokine therapies, oncolytic virus immunotherapy and bispecific antibodies [3].

1. Immune Checkpoint inhibitors

Immune checkpoints are molecules physiologically expressed by the immune cells and their role is to dynamically regulate immune response. The most well-known and studied immune checkpoints are the T cell inhibitory receptors PD-1 and CTLA-4 and their ligands are PD-L1 or PD-L2 and CD80 or CD86, respectively [4]. Other checkpoints with similar role include TIM-3, TIGIT and LAG-3, GITR and VISTA [5-22]. In the context of tumor, immune checkpoint engagement results in cytotoxic T cell inactivation/exhaustion and subsequently tumor cells escape [23].

- PD-1/PD-L1 inhibitors: PD-1 expression is induced by T cell receptor (TCR)-mediated activation of T cells. For PD-1-mediated inactivation of T cells in the tumor microenvironment, PD-1-PD-L1 engagement is required. PD-L1 is expressed in tumor cells, or other myeloid cells of the tumor microenvironment, especially dendritic cells. The PD-1–PD-L1 blockade by using either PD-1 or PD-L1 inhibitors is thought to reverse PD-1-induced inactivation, enhancing the anti-cancer properties of T cells (figure 1a) [24-26]. Pembrolizumab, Nivolumab and Cemiplimab are the FDA approved anti-PD-1 antibodies, while Atezolizumab, Avelumab and Durvalumab are the anti-PD-L1 FDA approved antibodies, and they are considered, nowadays, standard of care treatment for many malignancies [27].

Recently, it was shown that PD-1 is also expressed in myeloid cells of the tumor microenvironment, but mostly in myeloid progenitors in the bone marrow [28,29]. The role of PD-1 in myeloid cells will be discussed later in the project.

- CTLA4 inhibitors: Similarly to PD-1, CTLA4 has a crucial physiological role in inducing peripheral tolerance and preventing autoimmunity, as indicated by studies with CTLA-4 deficient mice. CTLA4 is the high affinity receptor for CD80 and CD86, is expressed upon T cell activation and suppresses activated T cells by competing with CD28 for binding on CD80 and CD86 expressed on antigen presenting cells. Hence, CTLA4 interaction with CD80/CD86 blocks T cell activation (figure 1b) [24-26,30,31]. Additionally, in antigen presenting cells, CD80 can interact with PD-L1 *in cis*, whereas the engagement between CTLA-4 expressed on Treg and CD80 depletes CD80 from APC, by trogocytosis, exposing free PD-L1 to bind with PD-1 *in trans* and

inhibit T cell activation [32]. Ipilimumab is the FDA approved anti-CTLA4 medication that is used for the treatment of cancer [33].

Checkpoint inhibitors in cancer immunotherapy work by blocking interactions that physiologically maintain tolerance and prevent autoimmunity. As a consequence, immune-related adverse effects (irAEs) of checkpoint inhibitors result in the development of autoimmune conditions in almost every organ [31]. The description of irAEs induced by checkpoint inhibitors is beyond the scope of our present study; such conditions are extensively described in recent reviews [26,31].

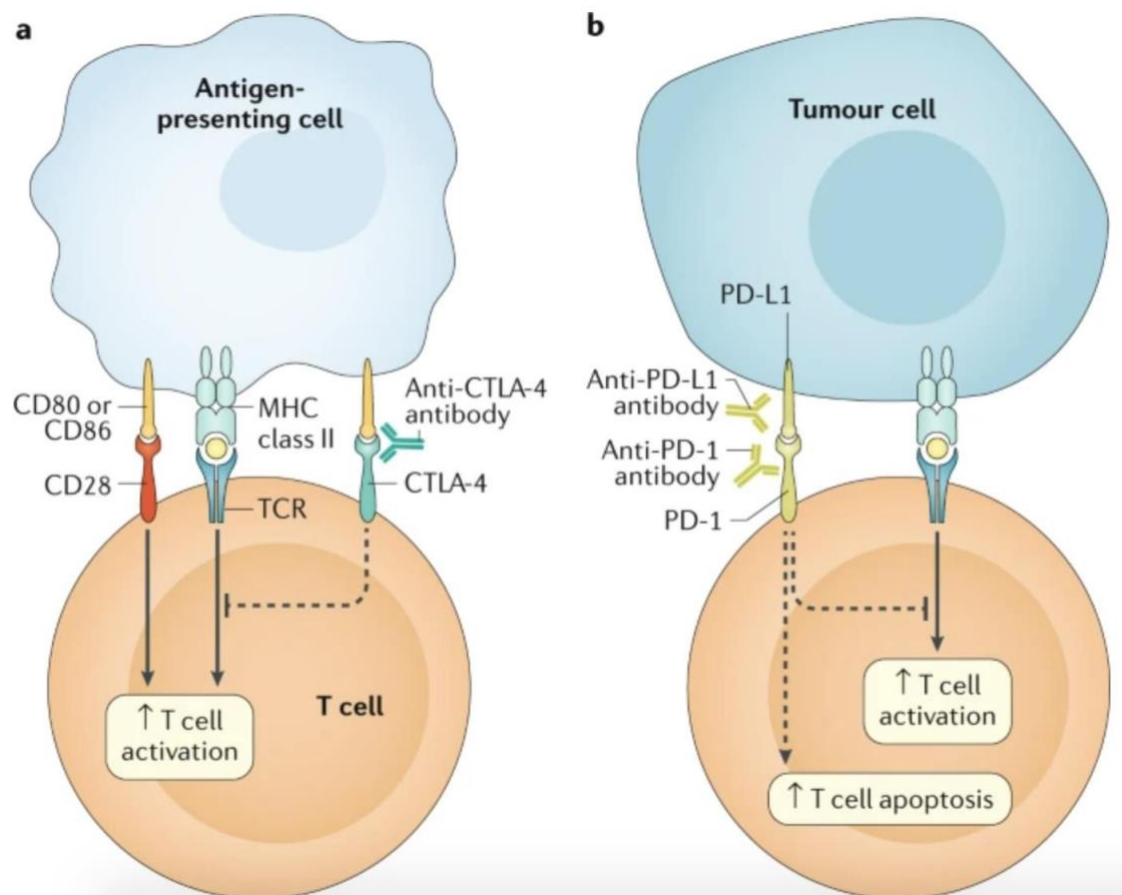


Figure 1. Mechanism of action of check-point inhibitors. Figure from Immune-related adverse events of checkpoint inhibitors, Nature Reviews Disease Primers, 2020 [26].

2. Adoptive cell immune therapy

The two main types of adoptive cell immune therapy are chimeric antigen receptor (CAR)-T cell immunotherapy and tumor-infiltrating lymphocytes (TILs) immunotherapy [34].

In CAR-T cells immunotherapy, T cells are collected from the peripheral blood of the patient. These T cells are genetically modified *in vitro*, with the incorporation of synthetic receptors that allow the recognition and binding to specific antigens, after the reinjection to the patient. Details about the structure and the *in vitro* modification of CAR-T cells are beyond the purpose of this study. CAR-T cell therapies have been approved for some types of hematologic malignancies. It is a very promising and innovating approach to cancer treatment, however their efficacy is limited by: a) severe toxicities including cytokine release syndrome (CRS), hemophagocytic lymphohistiocytosis and macrophage activation syndrome, and immune effector cell-associated neurotoxicity syndrome, b) development of resistance by tumor cells by decreasing or eliminating the targeted antigen, c) development of a hostile tumor microenvironment that limits the trafficking of the CAR-T cells near the tumor cells and creates an immunosuppressive environment that interferes with CAR-T cells function, d) expression of targeted antigens in healthy tissues resulting in “on-target off-tumor effect” [34-38].

In TIL therapy, T cells located in the tumor microenvironment that have been already exposed to tumor cells and tumor antigens, are collected directly from the tumor upon tumor resection, expanded *in vitro* and re-injected to the patient with the goal of detecting and killing the remaining tumor cells. TIL therapy has been applied with good results in

various solid tumors, mostly melanoma. As opposed to CAR-T cells, TILs can detect multiple antigens and tumor neoantigens and not only a single antigen which CAR-T cells are engineered to recognize. However, like with CAR-T cells, a hostile and immunosuppressive tumor microenvironment can limit the effect of adoptively transferred TILs. In TIL immunotherapy, tumor resection is required for the collection of the immune cells, which can be sometimes very challenging. In addition, even though immune cells have been exposed to tumor antigens, cancer cells have the ability to alter/change their surface antigens, escaping from the “immune cell attack”. Lastly, similar to CAR-T cell therapy, the phenomenon of on-target-off-tumor effect due to binding and recognition of targets in healthy tissues cannot be avoided. [34,39-41].

3. Cancer vaccines

The principle on which cancer vaccines are based is to expose host immune cells to antigens expressed by the tumor cells and re-direct them against tumor. The cancer vaccine antigens can be classified into “predefined” and “anonymous”. Predefined antigens include either personalized antigens that can be found in the tumor of certain individuals and used in a personalized manner, or shared antigens that can be expressed in the tumors of many individuals with cancer. On the other hand, in anonymous antigen vaccines, APCs are exposed either *ex vivo* to tumor antigens after excisional biopsy and then injected to patients, or are directly injected at the tumor site and are exposed to tumor antigens in the tumor microenvironment [42].

4. Cytokine cancer therapies

Cytokines are small molecules-messengers produced and secreted by immune, non-immune cells or cancer cells and have a central role in the regulation of the immune system [43,44]. Cytokines have a crucial role in tumor immunology through promoting or inhibiting tumor growth. Cancer inhibiting cytokines can prevent tumor growth by activating cytotoxic immune cells, expanding immune cells with anti-tumor capacity and inhibiting important processes for tumor progression such as angiogenesis. On the other hand, cancer promoting cytokines can accelerate tumor development by inducing cancer cell proliferation and immune escape, inhibiting tumor cell apoptosis and contributing to angiogenesis and epithelial to mesenchymal transition [45]. Given their central role in tumor immunology, several cytokines have been already approved for cancer treatment including IL-2 for metastatic renal cell cancer and melanoma and IFN α for melanoma and some hematologic malignancies while some other cytokines such as IFN γ , IL-7, IL-21, IL-12 and GM-CSF are currently in clinical trials [43,46-48].

5. Other types of cancer immunotherapies:

- Oncolytic virus therapy: Oncolytic viruses can infect malignant cells and induce tumor cell lysis, and further activation of the adaptive and innate immune system [49]
- Monoclonal antibodies: Monoclonal antibodies are in vitro generated recombinant proteins that bind specific epitopes in vivo resulting in enhanced immune response against cancer cells via antibody depended cellular cytotoxicity, phagocytosis, or complement-depended cytotoxicity [50]

- Bispecific antibodies: Bispecific antibodies are molecules with two binding sites that can recognize and bind two different epitopes simultaneously. The one epitope is usually CD3, the universal T cell molecule co-expressed with TCR, and the other epitope is a target expressed on cancer cells, with the goal of bringing together T cells and target cells, enhancing cytotoxicity [51,52].

II. Tumor Microenvironment (TME)

The TME is a very complex, diverse and dynamic environment, that consists of tumor and non-tumor cells. The non-tumor component of TME includes immune cells, fibroblasts and structural cells that compose the extracellular matrix and the blood vessels. The cell types and the function of TME vary based on the type of the tumor, the organ and the stage of the tumor [53].

The immune cells of the TME can affect tumor development either by creating a very immunosuppressive microenvironment that favors tumor progression and metastasis, or a TME with activated immune cells which mediate anti-tumor properties and limit tumor progression. The diverse properties of the tumor immune microenvironment make it a potential therapeutic target [53,54].

The main populations of immune cells in the TME are:

1. Tumor associated Macrophages (TAMs)

TAMs are the most abundant immune cells of the TME. In mice, TAMs can be identified as CD45⁺CD11b⁺F4/80⁺, while in humans as CD11b⁺CD14⁺CD163⁺CX3CR1⁺HLA-DR⁺. TAMs consist of a very heterogeneous population with either pro-tumorigenic or anti-tumorigenic capacity. Pro-tumorigenic Compared to normal macrophages, TAMs have lessened antigen presentation capacity with MHC-II downregulation, , and support tumor growth by creating a suppressive environment, inhibiting anti-tumorigenic immune populations of the TME,

contributing to angiogenesis, and secreting growth factors that can be utilized by tumor cells. Furthermore, metalloproteases produced and secreted by TAMs, can expedite tumor metastasis by promoting tumor migration and intravasation. On the other hand, anti-tumorigenic macrophages are professional antigen presenting cells, with high MHC-II expression, and superior phagocytic/tumor killing properties. Interestingly, anti-tumorigenic TAMs can become pro-tumorigenic and vice versa, a phenomenon called plasticity. Plasticity is a potential therapeutic target in tumor immunotherapy [55,56].

2. Myeloid-derived suppressor cells (MDSCs)

Tumor cells, and tumor infiltrating immune cells are a constant source of cytokines and danger-associated molecular patterns (DAMPs), that can enter the circulation and directly stimulate the bone marrow, resulting in the production of immature myeloid cells, named myeloid-derived suppressor cells (MDSCs). Produced during a process called emergency myelopoiesis, MDSCs are phenotypically similar to their mature myeloid counterparts but have immunosuppressive function instead of functioning as protective innate immune cells. There are two major categories of MDSCs: a. the polymorphonuclear MDSCs (PMN-MDSCs), that are phenotypically identical to fully mature neutrophils and b. the monocytic MDSCs (M-MDSCs), that are that are phenotypically identical to fully mature monocytes. MDSCs can suppress T-cell activation, leading to a highly immunosuppressed tumor microenvironment and subsequently to tumor progression [54,55]. In addition, studies have shown that MDSCs can accumulate in organs distal to primary tumor, and contribute to the formation of the metastatic niches [57]. In mice, PMN-MDSCs can be identified as $CD11b^+Ly6G^+Ly6C^{lo}$ and the M-MDSCs as $CD11b^+Ly6G^-Ly6C^{hi}$

while in humans, PMN-MDSCs as $CD11b^+CD14^-CD15^+/CD66b^+$ and M-MDSCs as $CD14^+CD15^-HLA-DR^{lo/-}$ [58].

3. Tumor associated DCs (TADCs)

Dendritic cells, a small minority of tumor infiltrating myeloid cells, are the main antigen-presenting cells in the TME, responsible for bridging adaptive and innate tumor immunity. After tumor antigen uptake, TADCs migrate to tumor drainage lymph nodes (TDLN), where they can present such antigens to naïve T cells, resulting in T cell activation. Like other tumor infiltrating myeloid cells, TADCs can also demonstrate pro-tumorigenic properties. PD-L1 and PD-L2 on the surface of DCs can interact with PD-1 on T cells, resulting in inhibition of T cell activation and proliferation. Furthermore, TME may suppress DCs either by inhibiting their production from bone marrow, preventing their accumulation in the tumor, preventing their migration towards the TDLNs or directly inhibiting their function. The DC are categorized in classical DC (cDC) type 1 (cDC1) and type 2(cDC2), plasmacytoid DCs (pDCs) and monocyte-derived DCs, which are the four different DC subsets identified in both humans and mice. In mice, DCs can be identified as $CD45^+CD11b^+F4/80^+MHCII^+CD11C^+$ while in humans as $CD45^+CD11b^+HLA-DR^{hi}CD11c^{hi}CD14^-CD64^-$ [54,59-62]. Further description of each of these groups is beyond the purpose of this project.

4. Tumor Infiltrating Lymphocytes (TILs)

Another extremely important cell component of TME is the TIL population $CD3^+CD8^+$ T cells are the main cytotoxic cells T cells of TME which can recognize and directly kill tumor cells by releasing perforin, Grz B and IFN γ . On the other hand, $CD3^+CD4^+$ T cells have a more regulatory

role, by providing help to CD8⁺ CTL but also by mediating direct anti-tumor cytolytic function as it is currently increasingly identified. . As described above, the first step before T cell activation and migration from tumor drainage LNs towards the TME is the tumor antigen presentation by professional APCs, such as TADCs. During antigen presentation two different signals are required for activation of naive T cells, known as signal 1 and signal 2. During signal 1, APCs present antigen on MHC-I or MHC-II which are recognized by the T-cell receptor of CD8⁺ and CD4⁺ T cells, respectively. Signal 2 comprises of interaction of costimulatory molecules expressed on APC, with cognate receptors expressed on T cells. The B7 molecules (CD80 and CD86) expressed on APCs, which interact with CD28 expressed on T cells, form the prototype and most extensively studied components of Signal 2. This process is counter-regulated by inhibitory checkpoints and has been the target of many immunotherapeutic medications, as described above. Activated T cells, such as tumor infiltrating T cells, express higher levels of checkpoint inhibitor molecules compared to naïve T cells, as a result of activation after antigen encounter. These markers are persistently expressed during T cell exhaustion, a phenomenon characterized by the inability of T cells to proliferate and acquire effector function, resulting in cancer escape from the immune system and subsequently, uncontrolled tumor progression. Notably, checkpoint inhibitor blocking immunotherapy has been shown to prevent or even reverse T cell exhaustion [54,63-66].

5. Tregs

Forkhead box protein P3 (FOXP3) positive regulatory T cells (Tregs), identified in both mice and humans as CD4⁺CD25⁺FOXP3⁺, are a subset of CD4⁺ T cells with immunosuppressive properties. In healthy individuals, Tregs are responsible for maintaining homeostasis by promoting immune tolerance and preventing autoimmunity [67]. In the context of tumor, the importance of Tregs is

demonstrated by Treg depletion in experimental tumor models, which results in tumor rejection or deceleration of growth. Tregs, can suppress anti-tumor immunity via many different mechanisms, including CTLA-4 mediated interference in T cells-APCs interaction, production and secretion of immunosuppressive cytokines such as TGF- β and IL-10, and consumption of activating cytokines such as IL-2 [68].

III. Gating strategy for immune cells of the TME

As described above, TME is a complex environment consisting of different populations of immune and non-immune cells. The identification of myeloid (Figure 2) and T cell (Figure 3) populations by flow cytometry requires the use of antibodies against many different protein markers.

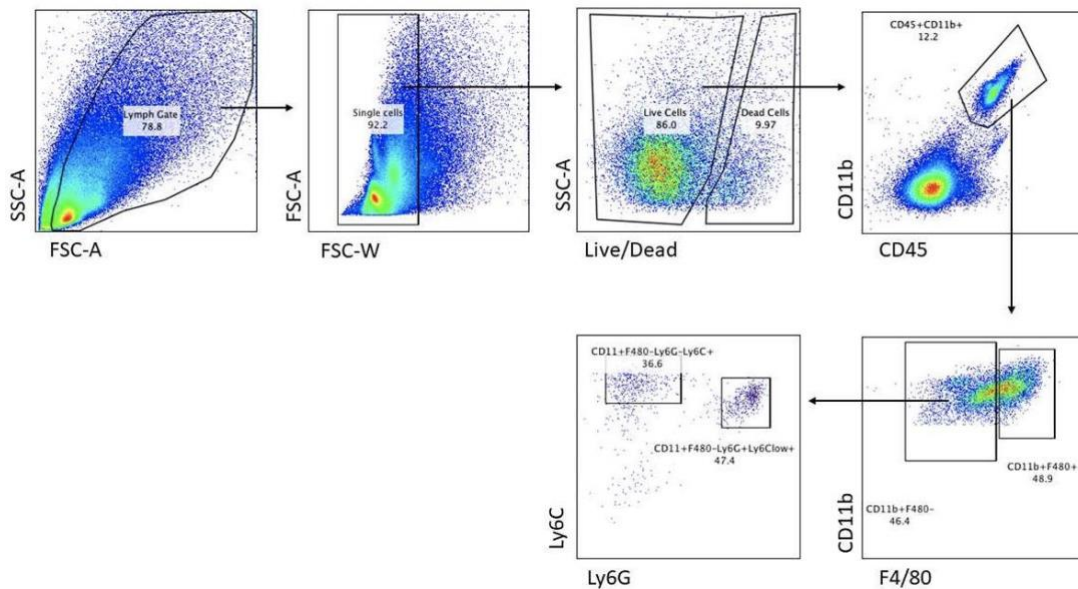


Figure 2. Gating strategy for identification of myeloid cells in the TME using flow cytometry.

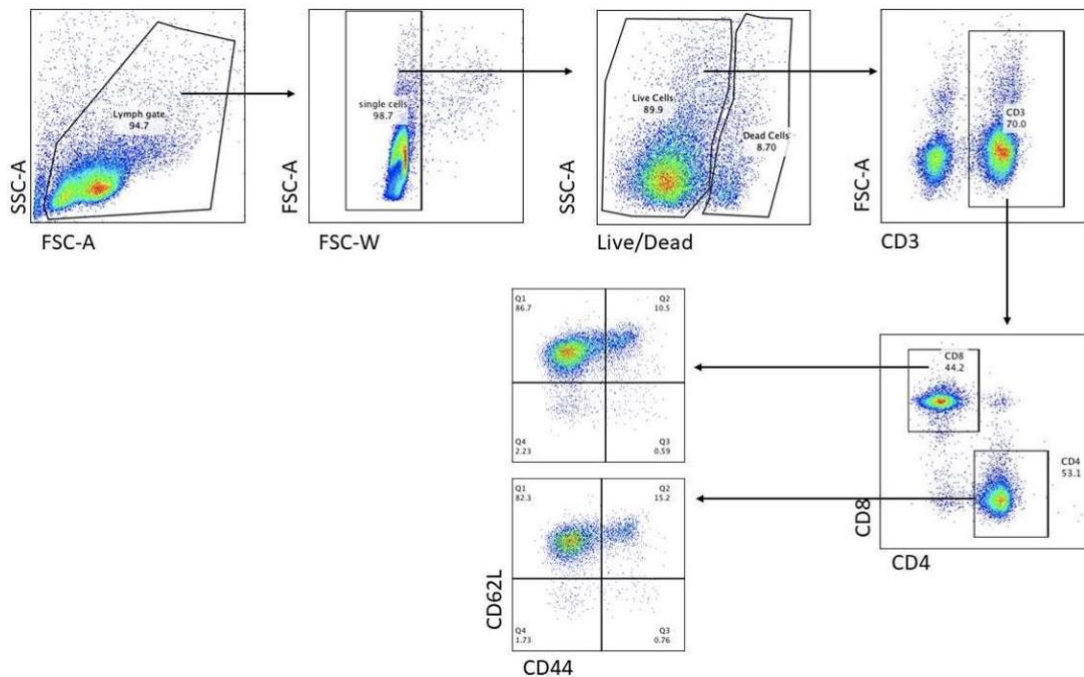


Figure 3. Gating strategy for identification of T cells in the TME using flow cytometry.

IV. The role of PD-1 in myeloid cells

PD-1 has been discovered in Kyoto University by Tasuku Honjo and his colleagues [69]. It is a T cell inhibitory checkpoint and, as described above, together with its ligand PD-L1, form one of the most extensively studied pathways and molecules/targets for tumor immunotherapy. In the TME, PD-L1, expressed in tumor cells and antigen presenting cells, interacts with, and activates PD-1 on tumor infiltrating T cells. PD-1 activation in T cells blunts their anti-tumor properties, resulting in tumor immune escape and tumor progression. The use of blocking antibodies, either against PD-1 or PD-L1, has been showed to improve anti-tumor immunity [24,25].

PD-1 has been historically considered as T cell inhibitory checkpoint [70]. However, recent studies have identified PD-1 expression in myeloid cells of the tumor microenvironment [29] and myeloid

progenitors in the BM [28]. PD-1 expression in TAMs has been shown to be negatively associated with M1 polarization and phagocytosis [29]. This finding raises the question about the role of PD-1 in the myeloid cells. To address this question, genetically modified mice with selective deletion of PD-1 in the T cell or the myeloid compartment were generated and mice were injected subcutaneously with tumor cells. Interestingly, mice with PD-1 deletion in the myeloid compartment developed significantly smaller tumors. In the same study, it was demonstrated that the anti-tumor capacity of all major myeloid populations of the TME, MDSCs, DCs, and TAMs, is enhanced after deletion of PD-1 in the myeloid compartment. After PD-1 deletion, MDSCs became less suppressive, while macrophages and dendritic cells from the tumor microenvironment acquired improved antigen presentation properties [28].

Finally, PD-1 deletion in the myeloid progenitors of the bone marrow, affected myeloid cell differentiation, suggesting that PD-1 can change the fate of myeloid cells very early in the differentiation cascade. PD-1 is expressed in myeloid progenitors including common myeloid progenitors and granulocyte/macrophage progenitors. During emergency myelopoiesis, progenitors are accumulated in the bone marrow and give rise to MDSCs. PD-1 deletion prevented the accumulation of immature progenitors and the subsequent generation of MDSCs, resulting in improved anti-tumor response [28].

V. The PD-1 – SHP-2 interaction

PD-1 engagement in T cells results in T cells inactivation, and in the context of tumor, to decreased anti-tumor immunity [24,25]. At the molecular level, PD-1 ligation results in recruitment and activation of SHP-2 phosphatase [71-74]. PD-1 deletion in myeloid cells resulted in greater anti-tumor immunity compared to PD-1 deletion in T cells [28]. However, PD-1 deletion in T cell

compartment also improved anti-tumor responses compared to control mice [28]. Based on this, and given that PD-1 mediates its effect through interaction with SHP-2, one would expect a similar effect after ablation of SHP-2 in T cells. Surprisingly, SHP-2 deletion in T cells neither changed tumor progression nor did alleviate the benefit of PD-1 blocking antibody [75].

As opposed to T cells, the PD-1 – SHP-2 interaction has never been explored in mature myeloid cells or myeloid progenitors. PD-1 deletion in the myeloid progenitors resulted in myeloid cell differentiation and prevented accumulation of immature cells [28]. On the other hand, SHP-2 gain-of-function mutations in myeloid progenitors result in differentiation arrest and development of acute myelogenous leukemia [76]. This effect of constitutively activated SHP-2 is mediated through altering the phosphorylation and function of transcription factors HOXA10 and IRF8 [77-79]. IRF8 is a transcription factor with a central role in myeloid differentiation towards DCs and monocytes and away from granulocytes. IRF8 phosphorylation is essential for IRF8 nuclear translocation, and SHP-2 phosphatase can block myelocyte differentiation by dephosphorylating IRF8 [78,80]. Similarly, HOXA proteins are known for their role in myeloid progenitor differentiation. Phosphorylation of HOXA10 decreases its affinity to promoters where it mediates repressive function, resulting in the expression of target genes essential for myeloid differentiation. SHP-2 mediated dephosphorylation of HOXA10 promotes its binding affinity, resulting in suppression of target genes and subsequently blockade of myeloid differentiation [77,81].

Papers

SHP-2 and PD-1-SHP-2 signaling regulate myeloid cell differentiation and antitumor responses

Received: 23 December 2021

Accepted: 3 November 2022

Published online: 29 December 2022

 Check for updates

Anthos Christofides^{1,2,3,10,14}, **Xanthi-Lida Katopodi**^{4,5,6,14}, **Carol Cao**^{1,2,7},
Dimitra Karagkouni^{4,5,6}, **Konstantinos Aliazis** ^{1,2,3}, **Sasitorn Yenyuwadee**^{1,2,3,11},
Halil-Ibrahim Aksoylar^{1,2,3}, **Rinku Pal**^{1,2,3}, **Mohamed A. A. Mahmoud**^{1,2,12},
Laura Strauss^{1,2,3,13}, **Natalia M. Tijaro-Ovalle**^{1,2,10}, **Louis Boon**⁸, **John Asara**³,
Ioannis S. Vlachos^{4,5,6,9}, **Nikolaos Patsoukis**^{1,2,3} & **Vassiliki A. Boussiotis** ^{1,2,3}



The inhibitory receptor PD-1 suppresses T cell activation by recruiting the phosphatase SHP-2. However, mice with a T-cell-specific deletion of SHP-2 do not have improved antitumor immunity. Here we showed that mice with conditional targeting of SHP-2 in myeloid cells, but not in T cells, had diminished tumor growth. RNA sequencing (RNA-seq) followed by gene set enrichment analysis indicated the presence of polymorphonuclear myeloid-derived suppressor cells and tumor-associated macrophages (TAMs) with enriched gene expression profiles of enhanced differentiation, activation and expression of immunostimulatory molecules. In mice with conditional targeting of PD-1 in myeloid cells, which also displayed diminished tumor growth, TAMs had gene expression profiles enriched for myeloid differentiation, activation and leukocyte-mediated immunity displaying >50% overlap with enriched profiles of SHP-2-deficient TAMs. In bone marrow, GM-CSF induced the phosphorylation of PD-1 and recruitment of PD-1-SHP-2 to the GM-CSF receptor. Deletion of SHP-2 or PD-1 enhanced GM-CSF-mediated phosphorylation of the transcription factors HOXA10 and IRF8, which regulate myeloid differentiation and monocytic-moDC lineage commitment, respectively. Thus, SHP-2 and PD-1-SHP-2 signaling restrained myelocyte differentiation resulting in a myeloid landscape that suppressed antitumor immunity.

To escape immunosurveillance, cancer cells have developed mechanisms that mask their immunogenic features, such as expression of ligands for inhibitory receptors that directly inhibit T cell responses by engaging immune inhibitory receptors, such as PD-1 (ref. 1). Tumors alter myeloid cells, which constitute a considerable cellular fraction of the microenvironment, to suppress antitumor responses. However, tumor-infiltrating myeloid cells may also contain immunostimulatory subsets, such as tumor-associated macrophages (TAMs) that produce

proinflammatory cytokines and type 1 classical dendritic cells. Conversely, immunosuppressive myeloid cells include protumorigenic TAMs² and immature myeloid-derived suppressor cells (MDSCs)³.

The inhibitory receptor PD-1 blocks T cell activation through a process attributed to the recruitment of the phosphatase SHP-2 to its cytoplasmic tail⁴. Because of this, it was expected that deletion of SHP-2 would abrogate the inhibitory pathway activated downstream of PD-1 receptor. However, T cell-specific deletion of SHP-2 did not improve

antitumor immunity and did not alter antitumor responses of these mice to PD-1 antibody treatment⁵ but instead had a detrimental effect on tumor progression⁶. PD-1 is also expressed in common myeloid progenitors (CMPs) and granulocyte/macrophage progenitors (GMPs), which accumulate during cancer-driven emergency myelopoiesis and give rise to immunosuppressive MDSC and TAMs⁷. In tumor-bearing mice with myeloid-specific deletion of PD-1, diminished accumulation of MDSCs was observed in the spleen and tumors, while the output of differentiated effector myeloid cells with monocytic lineage dominance was increased⁷. The molecular mechanisms behind these observations remain unclear.

Temporal activation of SHP-2 is critical for myeloid cell fate. Gain of function mutations in SHP-2 with constitutive phosphatase activation prevent myeloid differentiation and lead to the accumulation of immature myelocytes and development of leukemia⁸. The transcription factors HOXA, which regulate hematopoiesis, are SHP-2 targets⁹. *HOXA* genes are maximally expressed in committed myeloid progenitors and their dysregulation is associated with leukemia¹⁰. Tyrosine phosphorylation of the HOXA10 homeodomain during growth factor-induced myelopoiesis decreases its binding affinity for target gene promoters and abrogates HOXA10-induced transcriptional repression, which allows differentiation¹¹. SHP-2 also regulates the phosphorylation of the transcription factor IRF8, which is essential for the development of monocytes and DCs from monocyte-DC progenitors (MDPs), while inhibiting neutrophil differentiation¹². IRF8 phosphorylation at Tyr95 in the conserved IRF domain is mandatory for nuclear translocation and function. SHP-2 dephosphorylates IRF8 and prevents its nuclear localization¹³. Loss of functional IRF8 leads to the generation of MDSCs¹⁴.

Here we showed that in bone marrow myelocytes, GM-CSF induced PD-1 phosphorylation, interaction with SHP-2 and PD-1-SHP-2 recruitment to the GM-CSF receptor. Conditional ablation of either SHP-2 or PD-1 in myeloid cells resulted in augmented phosphorylation of HOXA10 and IRF8 in vitro and enhanced differentiation, activation, phagocytosis and inflammatory responses in myeloid cells of tumor-bearing mice, leading to diminished tumor growth.

Results

Myeloid-specific SHP-2 targeting suppresses tumor growth

To dissect the role of PD-1-SHP-2 in antitumor immune responses, we crossed *Shp2^{fl/fl}* mice with mice expressing Cre recombinase under the control of the lysozyme (*LysM*) promoter to induce selective depletion of *Ptfn11* in myeloid cells (*Shp2^{fl/fl}LysM^{Cre}*) or under the control of the distal *Lck* promoter to induce selective depletion of *Ptfn11* in mature T cells (*Shp2^{fl/fl}Lck^{Cre}*). We monitored tumor growth longitudinally for 2 weeks starting on day 7 post subcutaneous implantation of B16-F10 melanoma cells. *Shp2^{fl/fl}LysM^{Cre}* mice had substantially reduced tumor growth compared to *Shp2^{fl/fl}* mice, while tumor growth in *Shp2^{fl/fl}Lck^{Cre}* was similar to *Shp2^{fl/fl}* mice (Fig. 1a). Based on the expression of CD44, CD8⁺ T cells in tumor-draining lymph nodes (dLN) of *Shp2^{fl/fl}LysM^{Cre}* mice had a more activated state compared to their counterparts in *Shp2^{fl/fl}Lck^{Cre}* and control *Shp2^{fl/fl}* mice (Fig. 1b,c; gating strategy, Supplementary Fig. 1). CD44^{hi}CD62L^{lo} T effector cells (hereafter T_{EF} cells) and CD44^{hi}CD62L^{hi} central memory T-like cells (T_{CM}-like cells) from tumor-bearing *Shp2^{fl/fl}LysM^{Cre}* mice had increased expression of IFN- γ (Fig. 1d), indicating a state of activation and effector function. In contrast, based on the expression of CD44 and IFN- γ , no difference was observed in the activation of dLN CD8⁺ T cells from *Shp2^{fl/fl}Lck^{Cre}* mice compared to *Shp2^{fl/fl}* tumor-bearing mice (Fig. 1b–d).

MDSCs isolated on day 14–16 post-implantation from *Shp2^{fl/fl}LysM^{Cre}* mice bearing B16-F10 tumors had substantially diminished immunosuppressive capacity compared to *Shp2^{fl/fl}Lck^{Cre}* and *Shp2^{fl/fl}* MDSCs (Fig. 1e), and lower expression of CD38 (Fig. 1f–h), an indicator of immunosuppressive MDSC¹⁵. PD-1 is expressed in myeloid progenitors and immature myeloid cells in tumor-bearing mice and its ablation switch the fate of myeloid cells toward inflammatory monocytes and

DC⁷. To examine whether PD-1-SHP-2 signaling operated in myeloid cells, tumor-bearing mice were treated with PD-1 antibody on days 9, 11 and 13 after tumor inoculation. *Shp2^{fl/fl}* mice displayed a considerable reduction of tumor growth compared to mice receiving control IgG2a (Fig. 2a). In contrast, *Shp2^{fl/fl}LysM^{Cre}* mice, which had diminished tumor growth compared to *Shp2^{fl/fl}* mice, did not substantially benefit from treatment with PD-1 antibody compared to IgG2a (Fig. 2b,c). In addition, the numbers and expression of CD38⁺ MDSC were diminished by PD-1 antibody compared to IgG2a treatment in tumor-bearing *Shp2^{fl/fl}* mice, but not in *Shp2^{fl/fl}LysM^{Cre}* mice (Fig. 2d–f). *Shp2^{fl/fl}LysM^{Cre}* tumor-bearing mice also exhibited enhanced T cell activation (Fig. 2g,h) and recruitment of CD4⁺ and CD8⁺ T_{EF} cells in dLN (Fig. 2i,j). Treatment with PD-1 antibody increased the activation of CD8⁺ T cells (Fig. 2g,h) and the numbers of CD4⁺ and CD8⁺ T_{EF} cells in *Shp2^{fl/fl}*, but not in *Shp2^{fl/fl}LysM^{Cre}* tumor-bearing mice (Fig. 2i,j), which had more T_{EF} cells in dLN in both IgG2a and PD-1 Ab treatment groups (Fig. 2i). As such, myeloid-specific SHP-2 deletion induced potent antitumor immunity, which was only marginally improved by PD-1 blocking immunotherapy.

Myeloid-specific SHP-2 deficiency alters the lineage fate of MDSCs

To study the effects of SHP-2 ablation in myeloid cells in more detail, we used an MC17-51 fibrosarcoma mice tumor model, which induces robust cancer-mediated emergency myelopoiesis, leading to considerable output of bone marrow-derived MDSCs and TAMs¹⁶. On week 2 post subcutaneous tumor inoculation, tumor growth in *Shp2^{fl/fl}LysM^{Cre}* mice, but not in *Shp2^{fl/fl}Lck^{Cre}* mice (Fig. 3a,b and Extended Data Fig. 1a,b), was substantially diminished compared to *Shp2^{fl/fl}* mice. MDSCs in the mice consist of two major subsets, CD11b⁺Ly6C^{hi}Ly6G⁻ monocytic (M-MDSC) and CD11b⁺Ly6C^{lo}Ly6G⁺ polymorphonuclear (PMN-MDSC) cells, which have similar morphology and phenotype to normal monocytes and neutrophils, respectively, but distinct functions³. We did not observe quantitative differences in tumor-infiltrating myeloid cells (Fig. 3c), but *Shp2^{fl/fl}LysM^{Cre}* mice had an increased fraction of M-MDSC in tumors (Fig. 3d,e; gating strategy, Supplementary Fig. 2) and an increased ratio of M-MDSC/PMN-MDSC (Fig. 3f) compared to control *Shp2^{fl/fl}* tumor-bearing mice. A similar increase of M-MDSC tumor-infiltrating myeloid cells was observed in B16-F10 tumor-bearing *Shp2^{fl/fl}LysM^{Cre}* mice, which also developed smaller tumors (Extended Data Fig. 1c–g) compared to *Shp2^{fl/fl}* tumor-bearing mice. There was an increase in number of CD4⁺ and CD8⁺ T_{EF} cells (Fig. 3g,h) and an increase in the fraction activated CD44⁺CD8⁺ T cells (Fig. 3i,j) in dLN, a systemic increase of CD4⁺ and CD8⁺ T_{EF} and T_{CM}-like cells (Fig. 3k,l) and enhanced T cell activation (Fig. 3m,n) in the spleen of *Shp2^{fl/fl}LysM^{Cre}* compared to *Shp2^{fl/fl}* MC17-51 tumor-bearing mice. No differences were noted in the expression of checkpoint receptors including PD-1, PD-L1, CTLA-4, TIGIT or ICOS in CD4⁺ and CD8⁺ T cells between tumor-bearing *Shp2^{fl/fl}* and *Shp2^{fl/fl}LysM^{Cre}* (Supplementary Fig. 3) or in the numbers and activation of T_{reg} cell in dLNs (Supplementary Fig. 4a,b). Thus, myeloid-specific SHP-2 ablation led to increased tumor infiltration by Ly6C^{hi} monocytes and concomitant recruitment and activation of T_{EF} and T_{CM} cells.

SHP-2 deficiency induces MDSC differentiation and activation

At day 15 post MC17-51 tumor injection, PMN-MDSC from *Shp2^{fl/fl}LysM^{Cre}* mice had diminished immunosuppressive function (Fig. 4a) and lower expression of CD38 (Fig. 4b,c). M-MDSC from *Shp2^{fl/fl}LysM^{Cre}* mice also had substantially lower immunosuppressive capacity (Supplementary Fig. 4c) compared to the respective MDSCs from *Shp2^{fl/fl}* mice. M-MDSC in tumors from *Shp2^{fl/fl}LysM^{Cre}* mice had higher expression of MHC II, CD86 and IFN- γ than their counterparts in *Shp2^{fl/fl}* mice (Fig. 4d–g), consistent with an activated and proinflammatory phenotype with improved antigen presentation and costimulation capacity in M-MDSC. Tumor PMN-MDSC in *Shp2^{fl/fl}LysM^{Cre}* mice had higher expression of IFN- γ than their counterparts in *Shp2^{fl/fl}* mice (Fig. 4f,g), indicating that, in the context of cancer, deletion of SHP-2 switched the differentiation of

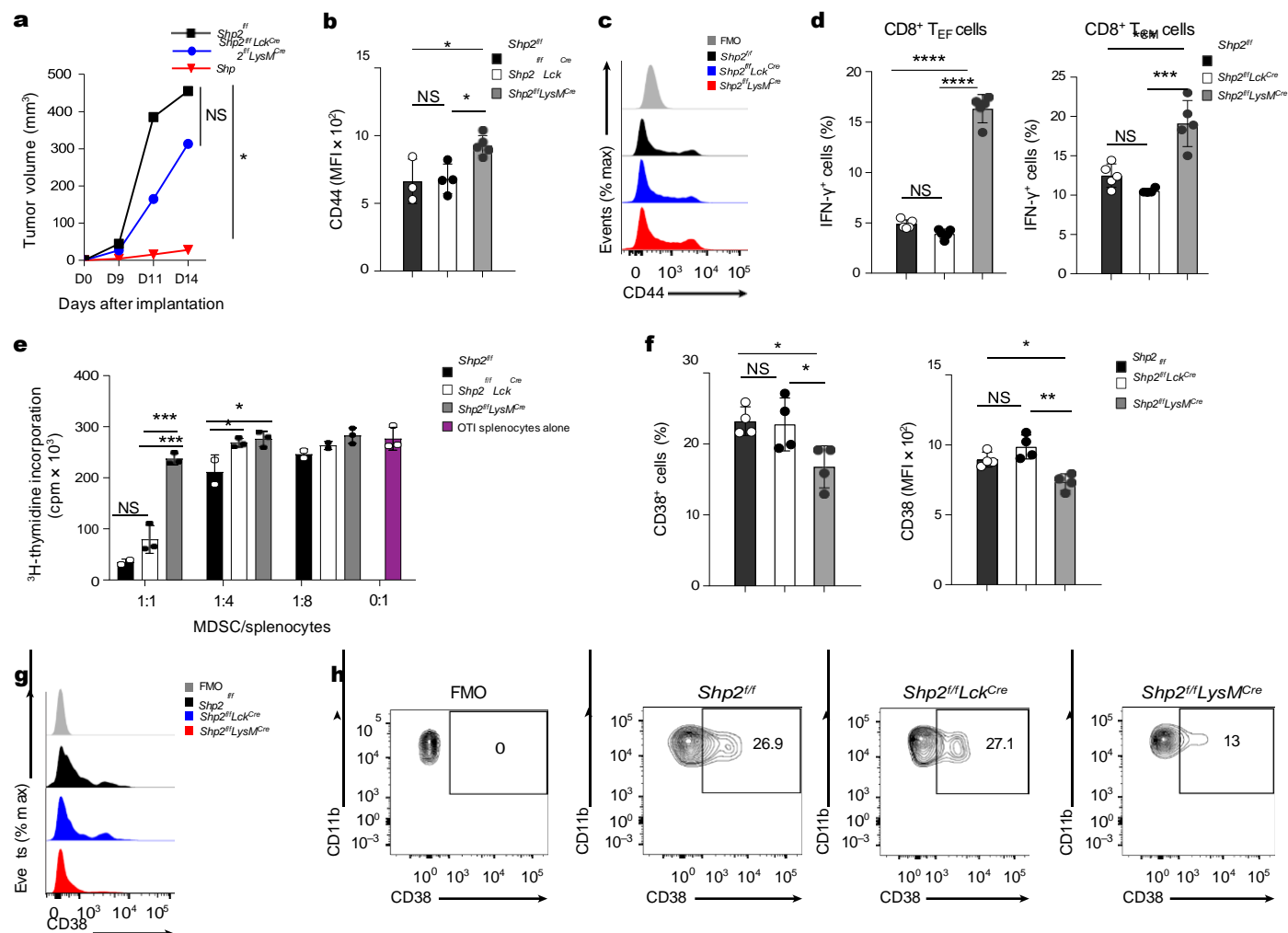


Fig. 1 | Myeloid-specific SHP-2 deletion diminished tumor progression and suppressive function of MDSC. **a**, Tumor volume in *Shp2^{fl/fl}*, *Shp2^{fl/fl}Lck^{Cre}* and *Shp2^{fl/fl}LysM^{Cre}* mice inoculated with B16-F10 melanoma cells (1×10^5 cells per mouse) and monitored longitudinally on each day of assessment. Data shown are means of $n = 6$ mice per group and are from one of three independent experiments with reproducible results. **b–c**, Quantification (**b**) and representative flow cytometry (**c**) of expression of CD44 in CD8⁺ T cells isolated from dLNs of mice as in **a**. **d**, Expression of IFN-γ assessed in CD8⁺ T_{EM} and T_{CM} cells from dLN in mice as in **a**. Mean fluorescence intensity (MFI) ± s.d. results are shown. Results are representative of four independent experiments with $n = 8$ mice per group. **e**, Thymidine incorporation in OTI splenocytes (2×10^5

cells per well) stimulated with OVA_{257–264} after the addition of graded numbers of GR1⁺ MDSCs cells isolated from the spleens of tumor-bearing *Shp2^{fl/fl}*, *Shp2^{fl/fl}Lck^{Cre}* and *Shp2^{fl/fl}LysM^{Cre}* mice. Mean ± s.d. of cpm values are shown. Results are representative of three separate experiments using $n = 9$ mice per group and four technical replicates per condition. **f, g**, Representative flow cytometry histograms (**g**) and contour plots (**h**) of CD38 expression on splenic MDSC from *Shp2^{fl/fl}*, *Shp2^{fl/fl}Lck^{Cre}* and *Shp2^{fl/fl}LysM^{Cre}* tumor-bearing mice. Mean percentage ± s.d., MFI ± s.d. % positive cells results are representative of two independent experiments with $n = 4$ and $n = 6$ mice per group and reproducible results. * $P = 0.0023–0.0465$, *** $P = 0.0001–0.0007$, **** $P < 0.0001$, ANOVA.

myeloid cells toward proinflammatory neutrophils, and monocytes with enhanced antigen presentation and T cell costimulation capacity.

Upon tumor entry, M-MDSC converts into TAMs that promote tumor progression³. To determine the molecular features of the myeloid compartment in tumor-bearing mice, we isolated PMN-MDSC from spleens and TAMs from tumors of *Shp2^{fl/fl}* and *Shp2^{fl/fl}LysM^{Cre}* mice on day 15 post MC17-51 tumor implantation and analyzed their gene expression profile by RNA sequencing (RNA-seq). Gene expression analysis showed that among the 17,746 expressed genes, a total of 1,240 genes (842 upregulated and 286 downregulated) were differentially expressed between *Shp2^{fl/fl}* and *Shp2^{fl/fl}LysM^{Cre}* MDSC (Fig. 4h,i and Supplementary Table 1). Genes involved in leukocyte differentiation and function¹⁷ were among the top differentially expressed in *Shp2^{fl/fl}LysM^{Cre}* MDSCs compared to *Shp2^{fl/fl}* MDSC (Fig. 4i). These included multilineage hematopoietic progenitor genes such as *Klf1*, *Gata2* and *Egr1* and the neutrophil transcription factors *Cebpe* and *Gfi1* (Fig. 4i,j and

Supplementary Table 1), consistent with the GMP origin of PMN-MDSC³. A number of granule genes typically expressed by mature neutrophils, in particular, the primary granule proteases neutrophil elastase (*Ela*), proteinase 3 (*Prtn3*), cathepsin G (*Ctsg*) and myeloperoxidase (*Mpo*)¹⁷ (Fig. 4i,j), and genes expressed in mature, fully differentiated granulocytes, such as *S100a8* and *Camp*¹⁷ (Fig. 4i and Supplementary Table 1) were highly expressed in PMN-MDSC from tumor-bearing *Shp2^{fl/fl}LysM^{Cre}* compared to *Shp2^{fl/fl}* mice.

Over-representation and gene set enrichment analysis (GSEA) indicated that relative to those isolated from *Shp2^{fl/fl}* tumor-bearing mice, gene expression profiles of myeloid cells from *Shp2^{fl/fl}LysM^{Cre}* tumor-bearing mice were enriched for processes involved in the regulation of PRC2-EZH2 targets, phagosome formation, myeloid cell differentiation, neutrophil-mediated immunity, Notch signaling and HOXA targets, and were dominated by functions of antigen processing and presentation, myeloid cell migration, mitosis and autophagy (Fig. 4k,l

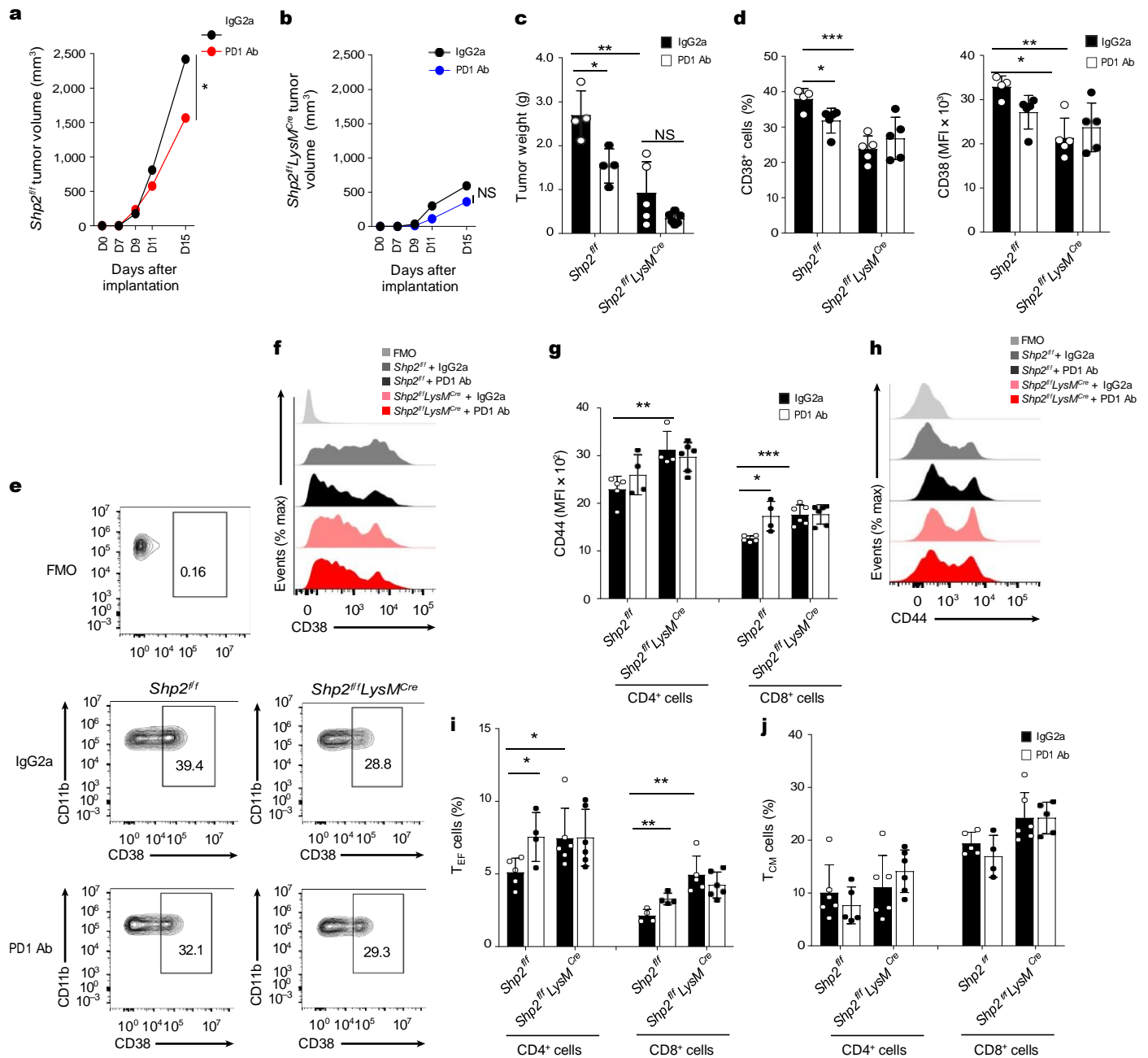


Fig. 2 | PD-1 blockade induced antitumor responses in *Shp2^{ff}* mice but not in *Shp2^{ff}LysM^{Cre}* mice. a–c, Tumor size in *Shp2^{ff}* (a) and *Shp2^{ff}LysM^{Cre}* mice (b) inoculated with B16-F10 melanoma (3×10^5 cells per mouse) and treated with PD-1 blocking antibody or IgG2a control on days 9, 11 and 13 after tumor inoculation and measured starting on day 7 (a, b) or day 15 (c). Results show means \pm s.d. are representative of three experiments $n = 4$ mice per group and two experiments with $n = 5$ mice per group. d–f, Quantification (d) and representative flow

cytometry (e, f) of CD38 expression in spleen PMN-MDSC isolated from mice as in a, g, h, Quantification (g) and representative histograms (h) of CD44 expression in CD4⁺ and CD8⁺ T cells of dLN. i, j, Frequency of CD4⁺ and CD8⁺ T_{EF} cells (i) and CD4⁺ and CD8⁺ T_{CM}-like cells (j) in dLN on *Shp2^{ff}* versus *Shp2^{ff}LysM^{Cre}* mice treated with IgG2a or PD-1 Ab mean percentage \pm s.d. are shown. Results are from one of three separate experiments with five mice per group. * $P = 0.017$ – 0.028 , ** $P = 0.0047$ – 0.0075 , *** $P = 0.0006$, unpaired two-sided t test.

and Extended Data Fig. 2a). Consistent with these, transcripts of the IFN I-inducible genes *Rsad2*, *Ifit2* and *Cmpk2*, which is required for NLRP3 inflammasome activation downstream of IFNRI signaling¹⁸, were substantially elevated (Fig. 4i and Supplementary Table 1), while the expression of *Trem2*, a myeloid receptor that transmits intracellular signals promoting immunosuppression function in myeloid cells¹⁹, was substantially decreased (Fig. 4i, j and Supplementary Table 1) in *Shp2^{ff}LysM^{Cre}* MDSC compared to *Shp2^{ff}* MDSC. *Shp2^{ff}LysM^{Cre}* MDSCs also exhibited lower expression of *Msr1*, which promotes neutrophil netosis, a protumorigenic process, and *Xbp1*, a classical marker of the unfolded protein response, which polarizes tumor-infiltrating myeloid cells to

highly immunosuppressive MDSC²⁰ (Fig. 4i, j and Supplementary Table 1). Thus, myeloid cells in tumor-bearing *Shp2^{ff}LysM^{Cre}* mice were skewed away from immunosuppressive MDSC and displayed features of differentiated neutrophils and properties of neutrophil-mediated immunity.

SHP-2 deficiency reshapes the intratumoral macrophage infiltrate

Next, we examined the transcriptional properties of TAMs isolated from tumors of *Shp2^{ff}LysM^{Cre}* and *Shp2^{ff}* mice at day 15 post-tumor implantation. Differential gene expression analysis showed that among 16,749 expressed genes, a total of 7,307 genes (3,650 upregulated and

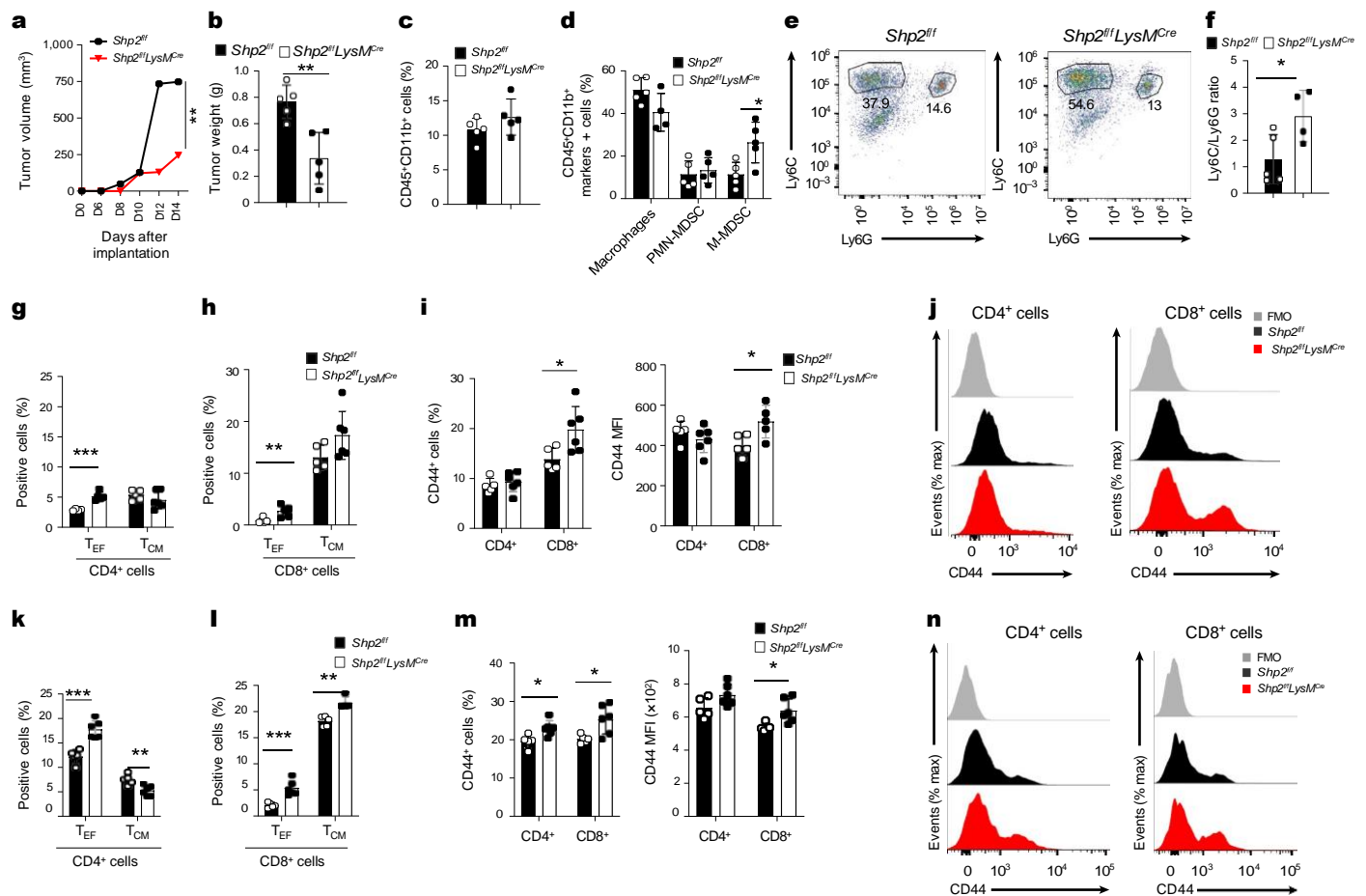


Fig. 3 | Myeloid-specific SHP-2 deletion alters the MDSC. **a, b**, In *Shp2^{fl/fl}* and *Shp2^{fl/fl}LysM^{Cre}* mice, tumor volume was monitored for 14 days (**a**) and tumor weight was assessed on day 14 (**b**) post inoculation with MC17-51 cells. **c–e**, Percentage of CD45⁺CD11b⁺ cells (**c**), macrophages, CD11b⁺Ly6C^{hi}Ly6G[−] monocytic MDSCs (M-MDSCs) and CD11b⁺Ly6C^{lo}Ly6G⁺ PMN-MDSCs (**d**), and representative pseudocolor plots (**e**) in tumors from mice as in **a**. **f**, The ratio of M-MDSC/PMN-MDSC in the tumors of *Shp2^{fl/fl}* and *Shp2^{fl/fl}LysM^{Cre}* tumor-bearing

mice as in **a**. **g–n**, Frequency of CD4⁺ T_{EF} cells (**g**, **k**) and CD8⁺ T_{EF} cells (**h**, **l**) and representative flow cytometry (**j**, **n**) and quantification (**i**, **m**) of CD44 expression in CD4⁺ and CD8⁺ T_{EF} cells in dLN (**g–j**), and the spleen (**k–n**) of tumor-bearing mice as in **a**. Mean percentage ± s.d. are shown. Results are representative of three separate experiments with four mice per group and two experiments with seven mice per group. **P* = 0.0166–0.0293, ***P* = 0.0019–0.0085, ****P* = 0.0003–0.00085, unpaired two-sided *t* test.

3,657 downregulated) were differentially expressed between TAMs from *Shp2^{fl/fl}LysM^{Cre}* and *Shp2^{fl/fl}* tumor-bearing mice (Fig. 5a,b, Supplementary Table 2, Extended Data Fig. 2b and Supplementary Fig. 5). TAMs from *Shp2^{fl/fl}LysM^{Cre}* mice had enhanced expression of genes with important roles in monocyte, macrophage or DC differentiation and function, such as the transcription factors *Irf8*, *Klf4* and *Zeb2* (Fig. 5b,c and Supplementary Table 2), monocyte signature genes (*Cfp*, *Ly86* and *Csf1R*; Supplementary Table 2) and DC specification genes, such as the transcription factor *Baft3* (Fig. 5b,c and Supplementary Table 2), which together with *Irf8* is required for DC differentiation²¹, and the immunostimulatory molecules *CD86* and *CD83* and *Csf1*, *Siglec1*, *Clec10* and *Slamf7* (Fig. 5b and Supplementary Table 2), which have been associated with moDC differentiation^{22,23}. Although our experimental system was not geared to investigate DC differentiation, these findings indicated that TAMs in *Shp2^{fl/fl}LysM^{Cre}* mice had enhanced gene expression programs identifying monocytes differentiated from MDPs, which can give rise to Ly6C⁺ classical and moDC-producing monocytes and DC²⁴. We noted increased expression of *Nos2* (Fig. 5b), which characterizes inflammatory macrophages differentiated from Ly6C^{hi} monocytes²⁵; *STING* (encoded by *Tmem173*) (Supplementary Table 2), a pattern recognition receptor that transmits signals activating IFN type I responses²⁶; IFN type I-induced proinflammatory genes *Ifi12*, *Ifi13* and *Cmpk2* (Fig. 5b); and TLRs and TLR downstream signaling mediators

such as *Unc93b1* and *Wdfy1* (Fig. 5b,c and Supplementary Table 2) in TAMs of *Shp2^{fl/fl}LysM^{Cre}* tumor-bearing mice, indicating an enhanced proinflammatory program. Conversely, compared to TAMs isolated from *Shp2^{fl/fl}* mice, TAMs of *Shp2^{fl/fl}LysM^{Cre}* had diminished expression of inhibitory genes such as *Havcr2* (encoding for Tim3), *Prdm1*, *Trem2* and *Wnt* (Fig. 5b,c), all of which have detrimental immunosuppressive roles in myelocyte-mediated antitumor function^{19,27,28}.

Pathway enrichment analysis and GSEA showed that TAMs from *Shp2^{fl/fl}LysM^{Cre}* mice were enriched for genes of macrophage differentiation and activation, phagocytosis, TLR and NF-κB signaling, cytokine and chemokine activity, IL-1 response, cell killing, antigen-presenting function and autophagy (Fig. 5d,e and Extended Data Fig. 2b), which are associated with antitumor properties of TAMs²⁹. The differentially expressed cytokine production pathways included enhanced production of IL-10, IL-17, type I IFN and IFN-γ (Fig. 5f,g), proinflammatory IL-6, IL-1α, IL-1β and IL-18 (Fig. 5h and Supplementary Fig. 2b). Several chemokines—including *Pf4* (*CXCL4*), which acts as a chemoattractant for neutrophils and monocytes and enhances T memory cell responses and *CXL2* and *CXL3*, which collectively promote monocyte, DC, NK and T cell recruitment and macrophage activation, thereby mediating a proinflammatory immune response—were upregulated in *Shp2^{fl/fl}LysM^{Cre}* TAMs compared to *Shp2^{fl/fl}* TAMs (Extended Data Fig. 2b and Supplementary Table 2). TAMs from *Shp2^{fl/fl}LysM^{Cre}* mice had an

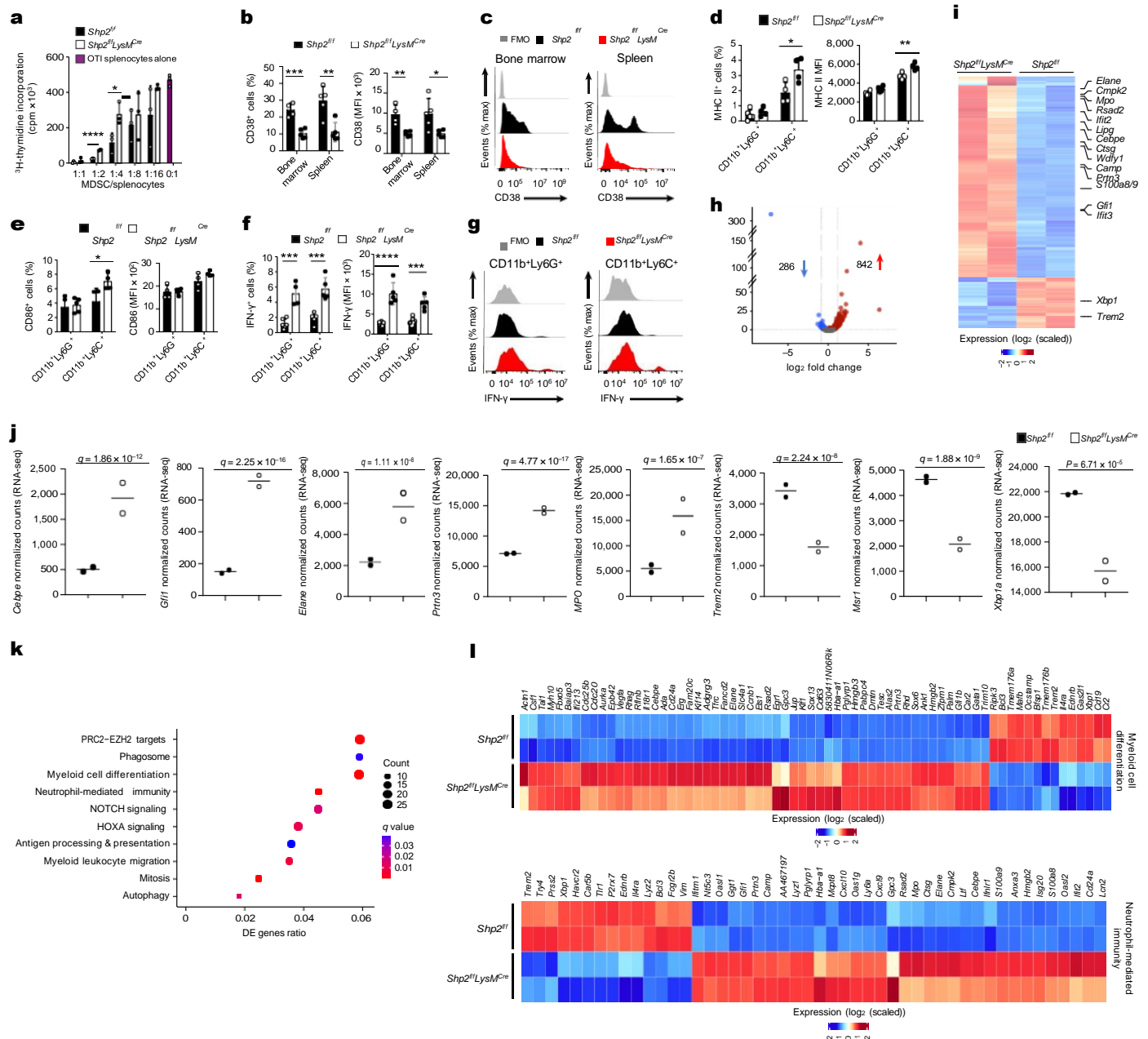


Fig. 4 | SHP-2 deletion promotes myeloid cell differentiation to mature leukocytes with enhanced neutrophil-mediated immunity. **a**, ³H-thymidine incorporation (cpm) in OTI splenocytes stimulated with OVA_{257–264} cocultured with PMN-MDSC isolated from *Shp2^{fl/fl}* and *Shp2^{fl/fl}LysM^{Cre}* mice at day 15 post inoculation of MC17-51 tumor cells. Mean ± s.d. of cpm values is shown. *****P* < 0.0001 cpm counts obtained by addition of *Shp2^{fl/fl}* versus *Shp2^{fl/fl}LysM^{Cre}* PMN-MDSC, unpaired *t* test. Results are representative of three separate experiments using 8–10 mice per group, and three technical replicates per condition. **b,c**, Quantification (**b**) and representative histograms (**c**) of CD38 expression in PMN-MDSC from spleen and BM in mice as in **a**. Mean percentage ± s.d. **d–g**, Quantification of MHC II (**d**) and CD86 (**e**) expression in tumor-infiltrating CD11b⁺Ly6C^{lo}Ly6G⁺ and CD11b⁺Ly6C^{hi}Ly6G⁺ cells and quantification (**f**) and representative histograms (**g**) of IFN-γ expression in

tumor-infiltrating CD11b⁺Ly6C^{lo}Ly6G⁺ and CD11b⁺Ly6C^{hi}Ly6G⁺ cells in mice as in **a**. Results are from one of three independent experiments with *n* = 5 mice per group. **h,i**, Volcano plot of differentially expressed (DE) genes (**h**) and heat map (**i**) of top 600 DE genes in PMN-MDSC cells isolated from spleens of *Shp2^{fl/fl}* and *Shp2^{fl/fl}LysM^{Cre}* tumor-bearing mice and analyzed by bulk RNA-seq (*q* < 0.05 for all DEGs, log₂(FC) > 0 and log₂(FC) < 0 for upregulated and downregulated genes, respectively). **j**, Expression of the indicated genes in PMN-MDSC from *Shp2^{fl/fl}* and *Shp2^{fl/fl}LysM^{Cre}* tumor-bearing mice (data from RNA-seq dataset). **k**, Bubble plot of substantially enriched pathways (*q* < 0.1) in cells from *Shp2^{fl/fl}LysM^{Cre}* mice sorted by GeneRatio. **l**, Heat maps of differentially expressed genes involved in myeloid cell differentiation and neutrophil-mediated immunity (*q* < 0.05). **P* = 0.026, ****P* = 0.0034–0.004, *****P* < 0.0001, unpaired *t* test.

enhanced signature of multiple metabolic pathways, including lipid, carbohydrate and amino acid transport, cholesterol metabolism and energy metabolism (Fig. 5i). Enhanced metabolic activity, characterized by glucose and glutamine metabolism, increased levels of amino acids and anabolic lipid metabolism were also observed in phagocytes generated from the bone marrow of *Shp2^{fl/fl}LysM^{Cre}* and *Shp2^{fl/fl}* mice by

culture with GM-CSF (Extended Data Fig. 3). Consistent with these findings, GSEA using Gene Ontology Biological Processes Pathways gene sets showed that TAMs from *Shp2^{fl/fl}LysM^{Cre}* mice were characterized by highly expressed signatures of leukocyte activation, chemotaxis, migration, cytokine production and inflammatory response (Extended Data Fig. 4a).

To examine whether the properties of myeloid cells from *Shp2^{fl/fl}/LysM^{Cre}* mice had a direct role in the improved antitumor responses, we examined antitumor responses after T cell depletion in *Shp2^{fl/fl}* and *Shp2^{fl/fl}/LysM^{Cre}* mice. T cell depletion increased tumor growth in *Shp2^{fl/fl}* mice but only marginally increased tumor growth in *Shp2^{fl/fl}/LysM^{Cre}* mice, indicating that non-T cell types had a more prominent role in mediating antitumor responses in *Shp2^{fl/fl}/LysM^{Cre}* mice (Extended Data Fig. 4b,c). These results indicated that myeloid cells from *Shp2^{fl/fl}/LysM^{Cre}* tumor-bearing mice developed a program of enhanced proinflammatory differentiation and features consistent with enhanced antigen processing and presentation leading to T cell activation but also had an ability to mediate T cell-independent antitumor function.

SHP-2 ablation induces lasting antitumor properties in monocytes

Next, we investigated whether the neutrophils and monocytes in tumor-bearing *Shp2^{fl/fl}/LysM^{Cre}* mice mediated lasting antitumor protection indicative of trained immunity. At day 9 post MC17-51 tumor injection, a time at which tumors had similar size in *Shp2^{fl/fl}* and *Shp2^{fl/fl}/LysM^{Cre}* mice, we collected CD45⁺CD11b⁺Ly6C^{hi}Ly6G⁻ monocytes and CD45⁺CD11b⁺Ly6C^{lo}Ly6G⁺ neutrophils from the bone marrow of tumor-bearing *Shp2^{fl/fl}/LysM^{Cre}* mice, mixed them with an equal number of MC17-51 tumor cells and injected them subcutaneously into naïve wild-type (WT) mice³⁰. There was no difference in tumor growth in WT mice that received neutrophils from *Shp2^{fl/fl}/LysM^{Cre}* tumor-bearing mice compared to mice that were injected with MC17-51 tumors alone, whereas WT mice that received monocytes from *Shp2^{fl/fl}/LysM^{Cre}* tumor-bearing mice had substantially reduced tumor growth compared to those that were injected with MC17-51 tumors alone (Fig. 6a,b). These findings indicated that bone marrow CD45⁺CD11b⁺Ly6C^{hi}Ly6G⁻ monocytes in *Shp2^{fl/fl}/LysM^{Cre}* mice had an antitumor function that could be transferred to new hosts.

Development of trained immunity in other models has been associated with an expansion of distinct types of hematopoietic progenitors or mature myeloid cell subsets³¹. Quantification of distinct subsets of myeloid progenitors and mature myeloid cells in the bone marrow of tumor-bearing *Shp2^{fl/fl}* and *Shp2^{fl/fl}/LysM^{Cre}* mice at day 9 post implantation of MC17-51 tumors, before isolation of monocytes and neutrophils for adoptive transfer, showed similar number of Lin⁻ myeloid progenitors including Flt3⁺CD115^{lo} CMP, FLT3⁺CMP, MDP, GMP, GP, MP+cMoP or mature differentiated Lin⁺ myeloid cells, including total CD45⁺CD11b⁺ myeloid cells, CD11b⁺Ly6C^{hi}Ly6G⁻ monocytes and CD11b⁺Ly6C^{lo}Ly6G⁺ granulocytes at this timepoint (Fig. 6c,d and Extended Data Fig. 5). These observations indicated that bone marrow monocytes in *Shp2^{fl/fl}/LysM^{Cre}* tumor-bearing mice were imprinted with antitumor properties, while the number of bone marrow myeloid progenitors were not altered.

SHP-2 and PD-1-SHP-2 signaling impede phosphorylation of HOXA10 and IRF8

Next, we examined whether phosphorylation of the SHP-2 targets HOXA10 and IRF8 was altered in SHP-2 deficient bone marrow myeloid cells. Flow cytometric analysis of bone marrow Lin⁻ myeloid progenitor cells cultured with GM-CSF+IL-3 for 3 days indicated that the percentage of Lin⁻ myeloid progenitors had decreased while that of Lin⁺ cells had increased (Extended Data Fig. 6a), and ≥ 95% of the Lin⁺ cells were CD45⁺CD11b⁺ myelocytes (Extended Data Fig. 6b), indicating differentiation of myeloid progenitors. In cell lysates from *Shp2^{fl/fl}/LysM^{Cre}* and *Shp2^{fl/fl}* bone marrow cultured for 48 h with GM-CSF+IL-3, HOXA10 or IRF8 immunoprecipitation followed by immunoblot with a phosphotyrosine antibody showed enhanced HOXA10 or IRF8 phosphorylation in myelocytes from *Shp2^{fl/fl}/LysM^{Cre}* myelocytes compared to *Shp2^{fl/fl}* (Fig. 7a,b). When cultured with GM-CSF with or without IL-3, myeloid progenitors and their progeny express PD-1 and PD-L1 (Extended Data Fig. 6c,d)⁷. PD-1 immunoprecipitation followed by SHP-2 immunoblot

detected a robust PD-1-SHP-2 interaction in GM-CSF+IL-3-cultured myelocytes from *Shp2^{fl/fl}* but not *Shp2^{fl/fl}/LysM^{Cre}* mice (Fig. 7a,b).

Erk and mTOR are targets of PD-1 in T cells³², and the GM-CSF-mediated activation of Erk and mTOR was reported to be enhanced in PD-1-deficient CMPs and GMPs during culture⁷. During culture of primary bone marrow, PD-1 and PD-L1 were expressed at low levels in both Lin⁻ and Lin⁺ cells before treatment with GM-CSF+IL-3 and were upregulated after treatment (Fig. 7e and Extended Data Fig. 6c,d). In T cells, SHP-2 is recruited to the cytoplasmic tail of PD-1 after tyrosine phosphorylation by TCR-mediated activation of Src kinases Fyn and Lck^{33,34}. In the myeloid lineage, the β subunit of the GM-CSF receptor (GM-CSFR) represents a major signaling subunit and is tyrosine phosphorylated in response to cytokine stimulation³⁵. The Src kinase Lyn can directly associate with GM-CSFR β subunit. Immunoprecipitation with PD-1 antibody followed by immunoblot with phospho-specific PD-1 antibody, which recognizes pY248, a site within the conserved ITSM motif of PD-1 cytoplasmic tail known to be phosphorylated by Src family kinases leading to PD-1 interaction with SHP-2 in T cells^{33,34}, showed that GM-CSF induced pY248 and PD-1 interaction with SHP-2 (Fig. 7d,e). Sequential immunoblot with GM-CSFRβ-specific and Lyn-specific antibodies showed that both proteins were detected in PD-1 immunoprecipitates (Fig. 7d,e). Thus, GM-CSF-mediated signaling in myeloid cells induced the recruitment of PD-1 and SHP-2 phosphatase to GM-CSFRβ, a major signaling receptor involved in myelocyte activation, proliferation and differentiation.

Phosphorylation of HOXA10 and IRF8 was increased in whole bone marrow cells from *Pdcd1^{fl/fl}/LysM^{Cre}* mice, in which the *Pdcd1* gene (encoding PD-1) is deleted selectively in the myeloid compartment, cultured with GM-CSF+IL-3 for 48 h (Fig. 7f,g) or in WT bone marrow cells cultured with GM-CSF+IL-3 for 48 h in the presence of a PD-L1 blocking antibody, but not in the presence of an isotype-matched control antibody (Extended Data Fig. 7). These results indicated that PD-1-SHP-2 signaling suppressed HOXA10 and IRF8 phosphorylation, which have important roles in myeloid differentiation and lineage fate commitment^{9,13}.

PD-1 ablation alters the properties of monocytes and TAMs

SHP-2 has multiple interactors but is the only direct interacting partner for PD-1 identified to date³⁶. Next, we examined whether the myeloid-specific PD-1 deletion induced the generation of monocytes with antitumor properties and molecular signatures similar to SHP-2 deficiency. *Pdcd1^{fl/fl}/LysM^{Cre}* mice had smaller tumors during longitudinal monitoring after implantation with MC17-51 tumor cells compared to control *Pdcd1^{fl/fl}* mice (Extended Data Fig. 8a,b), consistent with previous observations in different tumor models⁷. The percentage of IRF8⁺ M-MDSC (Extended Data Fig. 8c) and TAMs (Extended Data Fig. 8d) and the expression of CD80 and CD86 in TAMs (Extended Data Fig. 8e) was increased in *Pdcd1^{fl/fl}/LysM^{Cre}* tumor-bearing mice compared to *Pdcd1^{fl/fl}* tumor-bearing mice.

To determine whether PD-1 deficient monocytes had the ability to develop trained immunity and lasting antitumor protection, CD45⁺CD11b⁺Ly6C^{hi}Ly6G⁻ monocytes isolated from the bone marrow of *Pdcd1^{fl/fl}/LysM^{Cre}* or *Pdcd1^{fl/fl}* mice on day 9 post injection with MC17-51 tumor cells, when tumors had comparable size between the two groups, were mixed with an equal number of MC17-51 tumor cells and injected subcutaneously into naïve WT mice. There was no difference in tumor growth between WT mice implanted with MC17-51 tumor cells alone and recipients of monocytes from tumor-bearing *Pdcd1^{fl/fl}* mice, whereas recipients of monocytes from tumor-bearing *Pdcd1^{fl/fl}/LysM^{Cre}* mice had substantially reduced tumor growth (Fig. 8a,b), indicating that PD-1-deficient monocytes could mediate tumor control. Similar numbers of bone marrow Lin⁻ myeloid progenitors, including Flt3⁺CD115^{lo} CMP, FLT3⁺CMP, MDP, GMP, GP and MP+cMoP, or mature differentiated Lin⁺ myeloid cells, including total CD45⁺CD11b⁺ myeloid cells, CD11b⁺Ly6C^{hi}Ly6G⁻ monocytes and CD11b⁺Ly6C^{lo}Ly6G⁺ granulocytes,

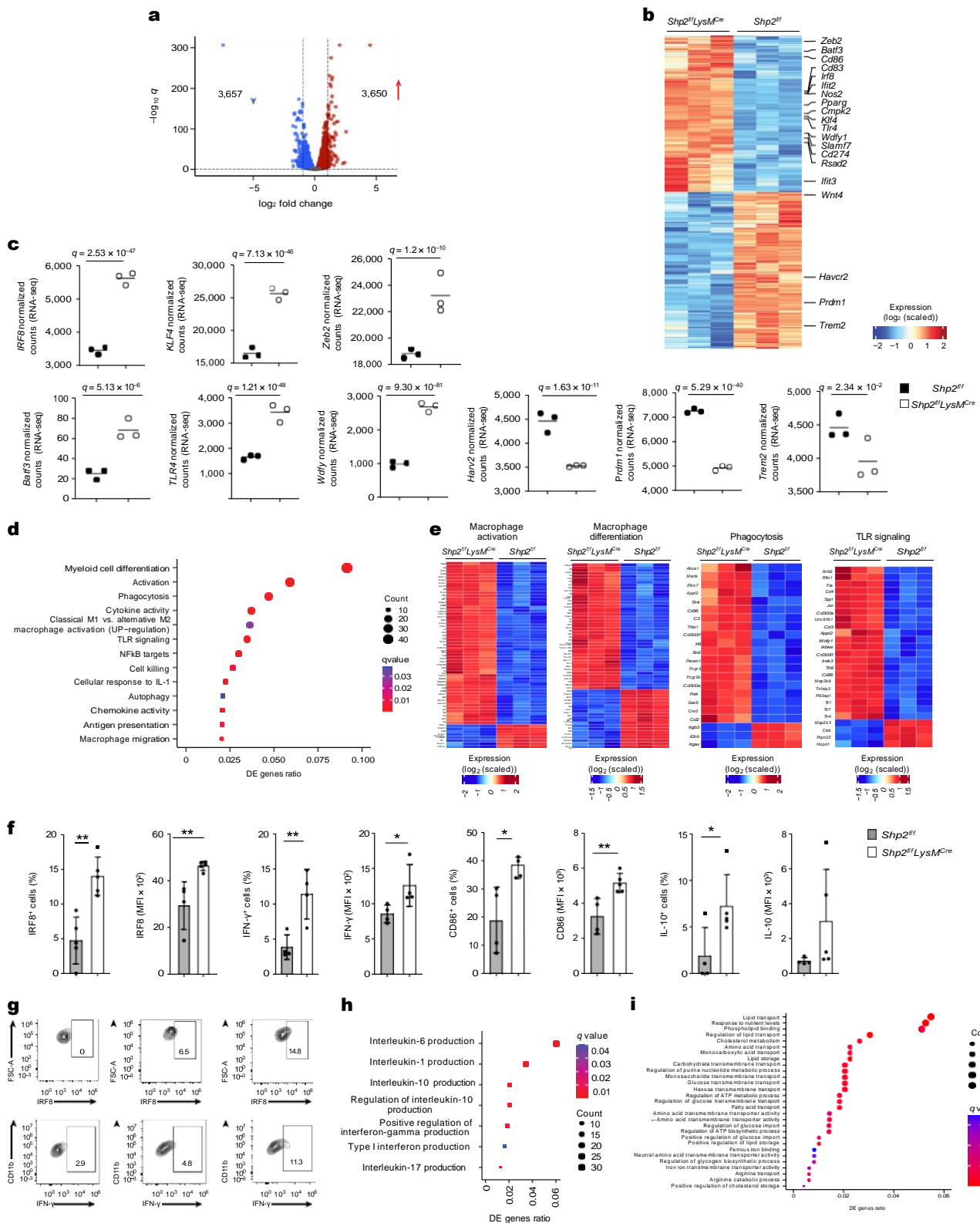


Fig. 5 | SHP-2 deletion increases monocyte and DC specification gene transcripts and imprints an effector differentiation program in TAMs. **a, b**, Volcano plot of DE genes (**a**) and heat map (**b**) of the top 6,500 DE genes in TAMs isolated from MC17-51 tumor-bearing *Shp2^{fl/fl}* and *Shp2^{fl/fl}LysM^{Cre}* mice and analyzed by RNA-seq. $\log_2(\text{FC}) > 0$ and $\log_2(\text{FC}) < 0$ for upregulated and downregulated genes, $q < 0.05$ for all DEGs, respectively). **c**, Expression of the indicated genes by TAMs from *Shp2^{fl/fl}* and *Shp2^{fl/fl}LysM^{Cre}* tumor-bearing mice (data from RNA-seq dataset). **d**, Bubble plot of substantially enriched pathways ($q < 0.1$) in TAMs of *Shp2^{fl/fl}LysM^{Cre}* mice sorted by GeneRatio. **e**, Heat maps of

differentially expressed genes related to macrophage differentiation, macrophage activation, phagocytosis and TLR signaling in TAMs from *Shp2^{fl/fl}* and *Shp2^{fl/fl}LysM^{Cre}* tumor-bearing mice ($q < 0.05$). **f, g**, Quantification of IRF8, IFN- γ , CD86 and IL-10 expression (**f**) and representative flow cytometry of IRF8 and IFN- γ expression (**g**) in TAMs of tumor-bearing *Shp2^{fl/fl}* and *Shp2^{fl/fl}LysM^{Cre}* mice. Results are representative of four independent experiments with four to six mice per group. **h, i**, Bubble plot of cytokine pathways (**h**) and metabolic pathways (**i**) substantially enriched in TAMs ($q < 0.1$) from *Shp2^{fl/fl}LysM^{Cre}* mice sorted by GeneRatio.

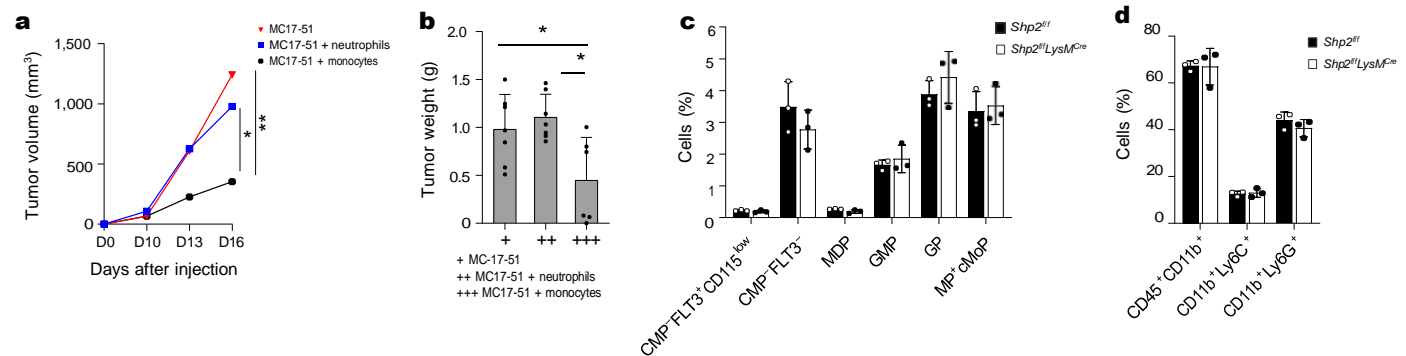


Fig. 6 | SHP-2 ablation induces lasting antitumor properties in monocytes.

a, Tumor size in naïve WT mice subcutaneously injected with MC17-51 tumor cells with or without injection with CD45⁺CD11b⁺Ly6C^{hi}Ly6G⁻ monocytes or CD45⁺CD11b⁺Ly6C^{lo}Ly6G⁺ neutrophils isolated from the bone marrow of *Shp2*^{fl/fl}/*LysM*^{Cre} mice on day 9 post inoculation of MC17-51 tumors. **b**, Tumor weight on day 15 in mice as in **a**. Results show mean + s.d. Results are from one of two experiments with $n = 10$ mice per group. * $P = 0.0104$ – 0.0387 , ** $P = 0.0033$,

ANOVA. **c, d**, The indicated subsets of Lin⁻ myeloid progenitors (**c**) and mature CD45⁺CD11b⁺ myeloid cells and the subsets of CD45⁺CD11b⁺Ly6C^{hi}Ly6G⁻ monocytes (CD11b⁺Ly6C⁺) and CD45⁺CD11b⁺Ly6C^{lo}Ly6G⁺ neutrophils (CD11b⁺Ly6C⁻) were assessed in the bone marrow of *Shp2*^{fl/fl} and *Shp2*^{fl/fl}/*LysM*^{Cre} tumor-bearing mice on day 9 before collection of monocytes or neutrophils from *Shp2*^{fl/fl}/*LysM*^{Cre} tumor-bearing mice for transfer into the new hosts. Results are from one of three separate experiments with $n = 5$ mice per group.

were detected in *Pdcd1*^{fl/fl}/*LysM*^{Cre} and *Pdcd1*^{fl/fl} tumor-bearing mice at day 9 post-tumor inoculation (Extended Data Fig. 8f,g).

Next, we performed RNA-seq in TAMs isolated from *Pdcd1*^{fl/fl}/*LysM*^{Cre} and *Pdcd1*^{fl/fl} tumor-bearing mice. Differential gene expression analysis showed that among 16,552 expressed genes, a total of 1,766 genes (846 upregulated and 920 downregulated) were differentially expressed between TAMs from *Pdcd1*^{fl/fl}/*LysM*^{Cre} and *Pdcd1*^{fl/fl} mice (Fig. 8c,d and Supplementary Table 3). *Pdcd1*^{fl/fl}/*LysM*^{Cre} TAMs had enhanced expression of genes consistent with myeloid cell differentiation, such as *Myadm*; inflammatory activation, such as *Klf7*, the dectin-2 family of C-type lectin receptors *Clec4e*, *Clec4d* and *Clec4n*; and the paracaspase *Malt1* (Fig. 8d,e and Supplementary Table 3), which together with *Clec4n* are indispensable determinants of responses to PD-1 blocking immunotherapy³⁷. There was also increased expression of *Itgax* (CD11c), *Nr4a2*, *Nr4a3*, *Egr2*, *Egr3*, *Bhlhe40* and *CD24* transcripts, which are related to DC maturation²¹ (Fig. 8d,e and Supplementary Table 3), indicating that *Pdcd1*^{fl/fl}/*LysM*^{Cre} TAMs were derived from monocytes differentiated from MDPs that could give rise to Ly6C⁺ classical and moDC-producing monocytes, and DC²⁴.

Consistent with an activated macrophage profile, there was an increase of *CD80*, *CD86* (Fig. 8d and Supplementary Table 3), inflammatory mediators, including the TLR downstream mediators *Wdfy1* and *CD180* (Fig. 8d,e, Supplementary Table 3 and Extended Data Fig. 9a), and multiple proinflammatory cytokines, including *IL-6*, *IL-1a*, *IL-1b* and *IL-23a* (Fig. 8d and Supplementary Table 3). Conversely, there was a diminished expression of genes that convey immunosuppressive functions of TAMs such as *Trem2*, *Mertk*, *CD163* and *Mrc1* (CD206) (Fig. 8d,e and Supplementary Table 3). Compared to *Pdcd1*^{fl/fl} TAMs, *Pdcd1*^{fl/fl}/*LysM*^{Cre} TAMs had increased expression of *Jarid2* (Fig. 8d), a histone methyltransferase acting as an accessory subunit for the core PRC, recruiting PRC2 complex to target genes and epigenetically regulating gene expression³⁸. *Pdcd1*^{fl/fl}/*LysM*^{Cre} TAMs had increased expression of *Hif1a* (Fig. 8d and Supplementary Table 3), which promotes glycolysis under hypoxia but also serves as an indispensable metabolic mediator of trained immunity³⁹ and pyruvate dehydrogenase phosphatase 1 (*Pdp1*) (Fig. 8d,e and Supplementary Table 3), which regulates the activation of pyruvate dehydrogenase complex converting pyruvate to acetyl-CoA for entry to the TCA cycle and synthesis of itaconate, serving a critical metabolic step required by proinflammatory macrophages to sustain cytokine production⁴⁰. In parallel, there was decreased expression of *Cpt1a*, which regulates mitochondrial entry of long-chain fatty acids promoting fatty acid oxidation, and a concomitant increase of *Hmgcs1* (Fig. 8d,e and Supplementary Table 3), the enzyme catalyzing

condensation of acetyl-CoA with acetoacetyl-CoA to form HMG-CoA that is converted into mevalonate, the precursor of cholesterol synthesis and a mediator of trained immunity⁴¹.

GSEA of the top 500 differentially expressed genes showed that *Pdcd1*^{fl/fl}/*LysM*^{Cre} TAMs were highly enriched for genes involved in leukocyte activation and differentiation, chemotaxis, protein secretion and inflammatory response, phagocytosis, cytokine and chemokine activity, DC differentiation and maturation, and response to type I IFNs (Fig. 8f and Extended Data Fig. 9a), all functions associated with antitumor properties of TAMs^{42,43}. In addition, there was high enrichment for genes of signaling pathways, including the MAPK cascade, kinase activity, Erk1/2 cascade, Ras and second messenger mediated signaling, NF- κ B, calcium ion transport, PI3K, PKB, phospholipase activity and tyrosine kinase activity (Fig. 8f), signaling pathways targeted by PD-1 in T cells³². *Pdcd1*^{fl/fl}/*LysM*^{Cre} TAMs were also highly enriched for genes involved in oxidative stress response, phospholipid binding and lipid transport, glucose homeostasis, amino acid metabolism and fatty acid biosynthetic processes (Fig. 8f). Thus, myeloid-specific PD-1 ablation resulted in the generation of TAMs with enhanced signaling and anabolic metabolism.

Comparison of gene expression and GSEA in transcriptomics indicated multiple genes displaying similar changes in *Shp2*^{fl/fl}/*LysM*^{Cre} and *Pdcd1*^{fl/fl}/*LysM*^{Cre} TAMs (Fig. 8d and Supplementary Table 4). Among the commonly upregulated genes were macrophage activation markers such as *Myadm*, *Itgax*, the C-type lectin receptors *Clec4e*, *Clec4d* and *Clec4n*, type I IFN-induced genes such as *Ifi205*, *Rsd2* and *Ifit1*, the small GTPase *Rap1a* and the Rap1-interacting partner *RIAM* (*Apbb1ip*), which has an indispensable role in phagocytosis⁴⁴, TLR signaling mediators such as *Wdfy1* and *CD180*, macrophage activation genes such as *KLF7* and *CD86*, and metabolic regulators including *Hif1a*, *Pdp1* and *Hmgcs1* (Fig. 8d and Supplementary Table 4).

Among pathways enriched in the differentially upregulated genes in *Shp2*^{fl/fl}/*LysM*^{Cre} TAMs, 22% overlapped with pathways enriched in *Pdcd1*^{fl/fl}/*LysM*^{Cre} TAMs (Fig. 8g), consistent with multiple signaling interactions of SHP-2 besides PD-1. Conversely, 59% of the pathways enriched in *Pdcd1*^{fl/fl}/*LysM*^{Cre} TAMs overlapped with pathways enriched in *Shp2*^{fl/fl}/*LysM*^{Cre} TAMs (Fig. 8g), indicating that the majority of PD-1-mediated functions in TAMs were mediated through SHP-2. Common functional pathways enriched in both datasets included genes involved in myeloid cell activation, chemotaxis, proliferation and differentiation, synapse organization and cell adhesion, leukocyte-mediated immunity, TLR signaling and production of inflammatory and effector cytokines (Fig. 8h). Common signaling pathways were also enriched

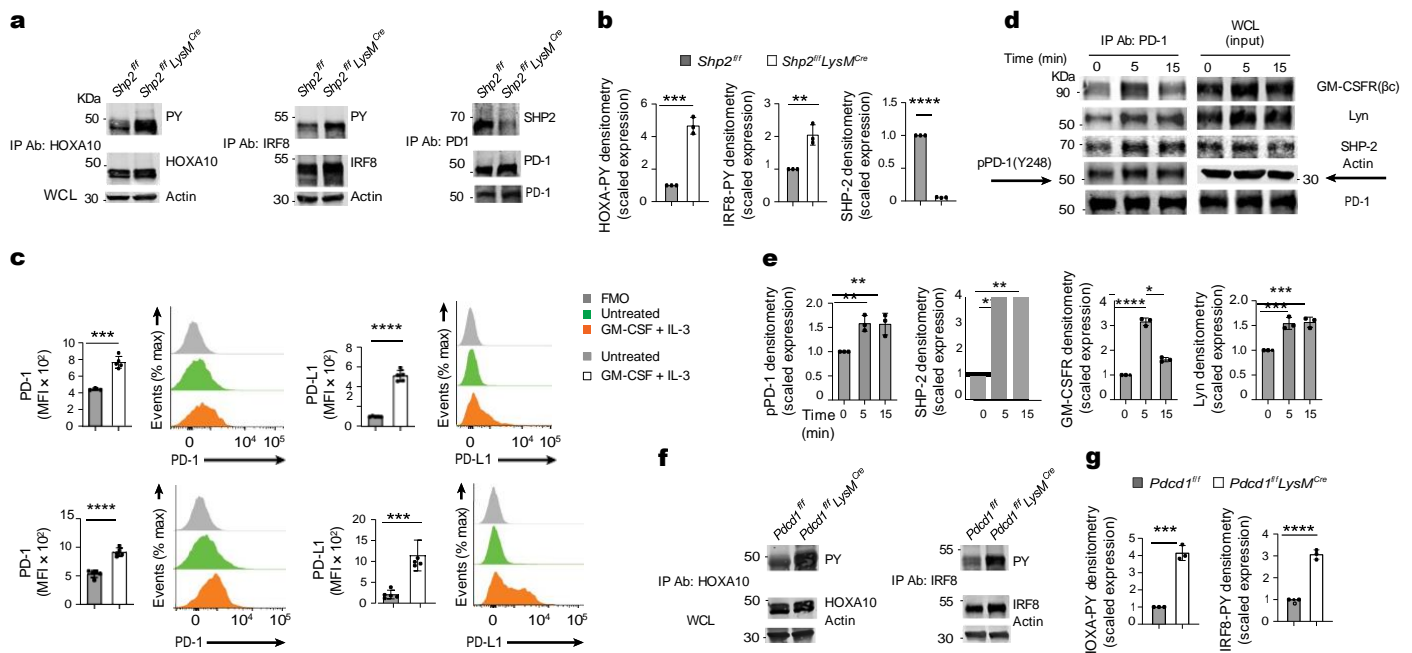


Fig. 7 | Ablation of SHP-2 or PD-1 enhances GMC-SF-mediated phosphorylation of HOXA1- and IRF8. **a**, Immunoprecipitation with agarose-conjugated antibodies specific for HOXA10, IRF8 or PD-1 followed by SDS-PAGE and immunoblot with antibodies specific for pY or HOXA10, IRF8 or PD-1, respectively, in cell lysates from *Shp2^{fl/fl}* and *Shp2^{fl/fl}LysM^{Cre}* bone marrow cells cultured for 48 h with GM-CSF (10 ng ml⁻¹) and IL-3 (5 ng ml⁻¹). Expression of actin in whole-cell lysates was examined as input. **b**, Abundance of phosphorylated HOXA10, IRF8 or PD-1 normalized to immunoprecipitated HOXA10, IRF8 or PD-1 and expressed as fold change over the value obtained in *Shp2^{fl/fl}* cells, defined as one. Results are representative of three experiments. **c**, Expression of PD-1 and PD-L1 in Lin⁻ (top) and Lin⁺ (bottom) cells following 48 h of the bone marrow from C57BL/6 WT mice as in **a**. MFI ± s.d. and representative histograms are shown. Results are from one of five experiments with four to six mice per group. **d**, Immunoprecipitation with agarose-conjugated PD-1 antibody followed by SDS-PAGE and immunoblot with the indicated antibodies in cell lysates from

C57BL/6 WT bone marrow cells cultured as in **a**, rested for 3 h and then either left untreated or stimulated with GM-CSF (40 ng ml⁻¹) for the indicated time points. **e**, The abundance of PD-1 phosphorylated at Y248 (pPD-1), SHP-2, GM-CSFR(β) and Lyn coprecipitated with PD-1 from the cell lysates was normalized to immunoprecipitated PD-1 and was expressed as fold change over the value obtained in nonstimulated cells at the zero timepoint (defined as one). Expression of indicated proteins in whole-cell lysates was also examined. Results from one of two experiments are shown. **f**, Immunoprecipitation with agarose-conjugated HOXA10-specific antibody or agarose-conjugated IRF8-specific antibodies followed by SDS-PAGE and immunoblot with antibodies specific for pY followed by immunoblot with HOXA10 or IRF8 in bone marrow cells from *Pcd1^{fl/fl}* and *Pcd1^{fl/fl}LysM^{Cre}* mice cultured as in **a**. Expression of actin in whole-cell lysates was examined as input. **g**, Quantification of phosphorylated HOXA10 and IRF8 was assessed as in **b**. Results from one of two experiments are shown (**f, g**). ***P* = 0.0025–0.0084, ****P* = 0.0004–0.0084, *****P* < 0.0001, *t*-test.

in the gene sets of *Pcd1^{fl/fl}LysM^{Cre}* and *Shp2^{fl/fl}LysM^{Cre}* TAMs, including Ras pathway activation, kinase activation, MAPK and Erk1/2 cascade, second messenger-mediated signaling, calcium ion homeostasis, calcium-mediated signaling and NF-κB activation (Extended Data Fig. 9b). Thus, TAMs in *Pcd1^{fl/fl}LysM^{Cre}* and *Shp2^{fl/fl}LysM^{Cre}* mice were governed by molecular mediators that converged in multiple common signaling pathways and biological processes.

IRF8 programs the differentiation of monocytes and DC through epigenetic regulation of distinct sets of enhancers in cooperation with other transcription factors⁴⁵. We examined the expression of genes recently identified to be induced by IRF8 in mature phagocytic cells of the monocyte/DC lineage⁴⁵. In TAMs from *Shp2^{fl/fl}LysM^{Cre}* mice, 891 (24%) of the 3,650 upregulated genes were IRF8 targets (Fig. 8i and Supplementary Table 5) and in TAMs from *Pcd1^{fl/fl}LysM^{Cre}* mice, 221 (26%) of the 846 upregulated genes were IRF8 targets (Fig. 8j and Supplementary Table 5). Common and distinct IRF8-regulated genes were upregulated in *Shp2^{fl/fl}LysM^{Cre}* and *Pcd1^{fl/fl}LysM^{Cre}* TAMs (Fig. 8i,j) consistent with the ability of IRF8 to cooperate with common and distinct transcription factors in different cells, based on differential concentrations of IRF8 and the differential presence of cooperating transcription factors⁴⁵. Among the common IRF8 targets upregulated in *Shp2^{fl/fl}LysM^{Cre}* and *Pcd1^{fl/fl}LysM^{Cre}* TAMs were the scavenger receptor *CD36*, the costimulatory molecule *CD86*, the volume-regulated anion channel *Lrrc8c*, which regulates STING activation and production of type I interferons, the enzyme *Hmgcs1*, the transcription factor *Egr2*,

the antioxidant mediator *Tmx4*, macrophage activation genes such as *Vcan* and *Clec4n* and the cytokine IL-10 (Fig. 8i,j and Supplementary Table 5). Among IRF8-target genes upregulated selectively in *Shp2^{fl/fl}LysM^{Cre}* TAMs were the transcription factors *Nr4a1*, *Maff* and *Zeb2* (Fig. 8i), whereas among IRF8 targets upregulated specifically in *Pcd1^{fl/fl}LysM^{Cre}* TAMs were the costimulatory molecule *CD80*, the member of the tetraspanin family *CD9*, the epigenetic regulator *Jarid2*, and the transcription factor *Cebpe* (Fig. 8j), suggesting enhanced IRF8 function in SHP-2 and PD-1 deficient TAMs. These results showed that TAMs in *Pcd1^{fl/fl}LysM^{Cre}* mice had a transcriptomic profile associated with inflammatory differentiation and activation, accompanied by enhanced signaling and metabolic reprogramming and considerable enrichment of IRF8-regulated genes, and that molecular signatures of TAMs in *Pcd1^{fl/fl}LysM^{Cre}* and *Shp2^{fl/fl}LysM^{Cre}* mice converged in multiple common signaling pathways and biological processes.

IL-10 is involved in the enhanced antitumor immunity

Although considered an immunosuppressive mediator, IL-10 can have a proimmunogenic role with considerable implications in antitumor immunity⁴⁶. Because IL-10, an IRF8-regulated gene⁴⁵, was upregulated in TAMs of *Shp2^{fl/fl}LysM^{Cre}* and *Pcd1^{fl/fl}LysM^{Cre}* mice, we examined its role in the altered immunological properties of myeloid cells and the enhanced antitumor responses in *Shp2^{fl/fl}LysM^{Cre}* and *Pcd1^{fl/fl}LysM^{Cre}* mice. In WT, *Shp2^{fl/fl}LysM^{Cre}* and *Pcd1^{fl/fl}LysM^{Cre}* mice treated with IL-10 neutralizing antibody or isotype control on day 9, 11 and 13 post injection with

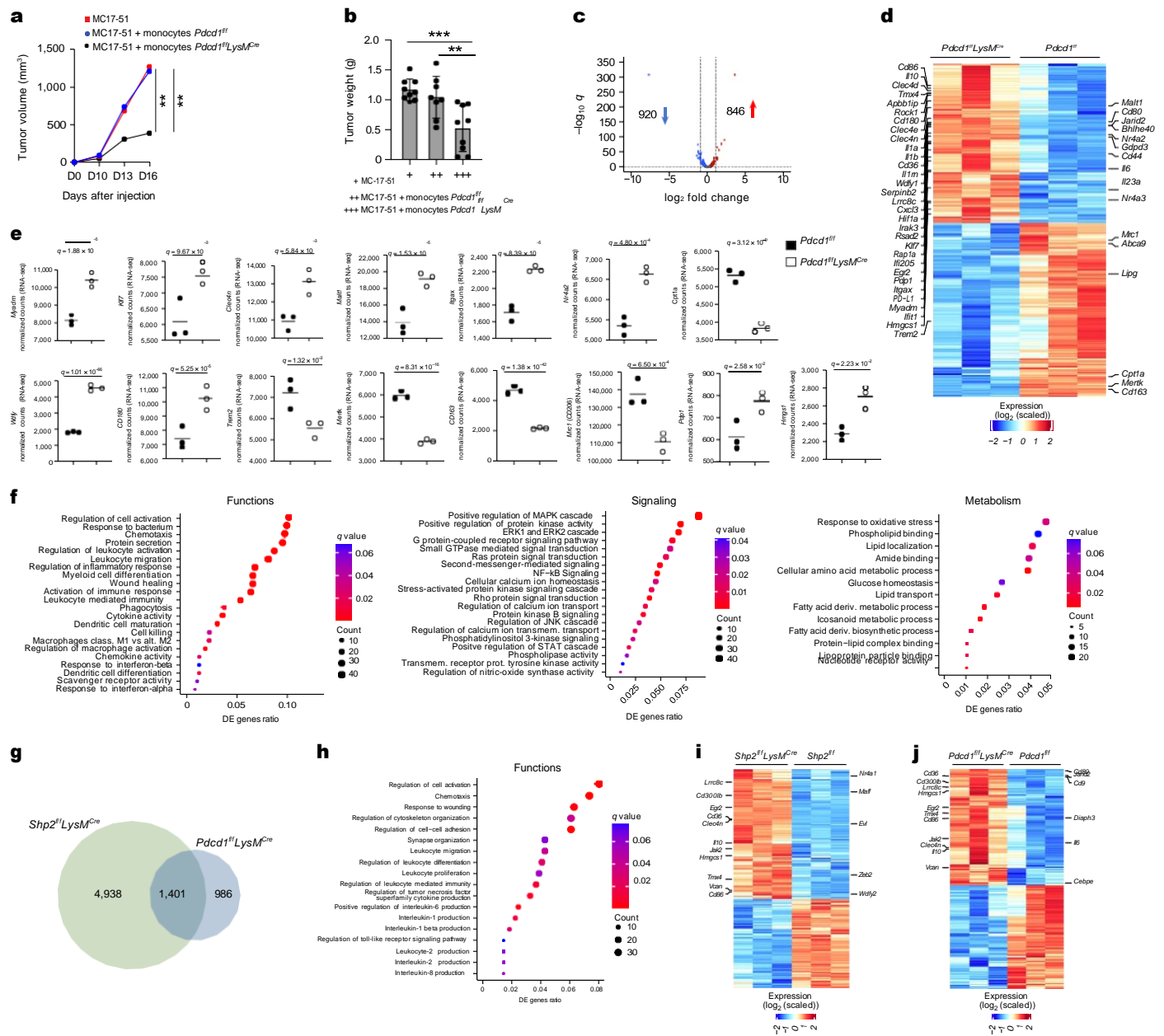


Fig. 8 | PD-1 deletion altered signaling and metabolism, and imprinted an effector function program in TAMs. **a, b,** Tumor size in naïve WT mice subcutaneously injected with MC17-51 tumor cells with or without CD45⁺CD11b⁺Ly6C^{hi}Ly6G⁻ monocytes isolated from the bone marrow of *Pdcd1^{fl/fl}LysM^{Cre}* and *Pdcd1^{fl/fl}* mice on day 9 post inoculation of MC17-51 tumors. **b,** Tumor weight on day 15 in mice as in **a.** Results show mean + s.d. Results are from one of two experiments with *n* = 10 mice per group. ***P* = 0.0055–0.0079, ****P* = 0.0006, ANOVA. **c, d,** Volcano plot of DE genes (**c**) and heat map (**d**) of 1,766 genes differentially expressed in TAMs isolated from MC17-51 tumor-bearing *Pdcd1^{fl/fl}* and *Pdcd1^{fl/fl}LysM^{Cre}* mice and analyzed by RNA-seq. $\log_2(\text{FC}) > 0$ and $\log_2(\text{FC}) < 0$ for upregulated and downregulated genes, *q* < 0.05 for all DEGs, respectively).

e, Expression of the indicated genes in TAMs from *Pdcd1^{fl/fl}* and *Pdcd1^{fl/fl}LysM^{Cre}* tumor-bearing mice (data from RNA-seq dataset). **f,** Bubble plot of substantially enriched functional, signaling and metabolic pathways (*q* < 0.1) among the top 500 DE genes in TAMs of *Pdcd1^{fl/fl}LysM^{Cre}* mice compared to *Pdcd1^{fl/fl}* mice sorted by GeneRatio. **g,** Venn Diagrams depicting the overlap of substantially enriched pathways between upregulated DE genes in *Shp2^{fl/fl}LysM^{Cre}* and *Pdcd1^{fl/fl}LysM^{Cre}* TAMs. **h,** Bubble plot of common pathways enriched in among the top 500 DE genes in *Shp2^{fl/fl}LysM^{Cre}* and *Pdcd1^{fl/fl}LysM^{Cre}* TAMs. **i, j,** Heat maps of the top 6,500 DE genes in TAMs of tumor-bearing *Shp2^{fl/fl}LysM^{Cre}* mice (**i**) and heat maps of the top 1,766 DE genes in TAMs of *Pdcd1^{fl/fl}LysM^{Cre}* mice (**j**). Representative common (left) and distinct (right) IRF8-upregulated genes are annotated.

MC17-51 tumor cells, there was no difference in tumor growth between IL-10 Ab-treated and isotype-treated WT mice, while IL-10 Ab-treated *Shp2^{fl/fl}LysM^{Cre}* and *Pdcd1^{fl/fl}LysM^{Cre}* mice had substantially enhanced tumor growth compared to their counterparts treated with isotype control Ig (Extended Data Fig. 10a,b). IL-10 Ab treatment did not alter the diminished suppressor function of MDSCs from *Shp2^{fl/fl}LysM^{Cre}* and *Pdcd1^{fl/fl}LysM^{Cre}* mice (Extended Data Fig. 10c,d). The fractions of

myeloid subsets (Extended Data Fig. 10e) and expression of MHC II, CD80 or CD86 were similar in TAMs from IL-10 Ab- or isotype-treated *Shp2^{fl/fl}LysM^{Cre}* or *Pdcd1^{fl/fl}LysM^{Cre}* mice (Extended Data Fig. 10f), indicating that IL-10 was not responsible for the diminished suppressor function of SHP-2- or PD-1-deficient myeloid cells in this experimental system. However, IL-10 had an active role in the enhanced antitumor immunity induced by SHP-2 or PD-1 targeting in myeloid cells.

Discussion

Here we showed that SHP-2 and the PD-1-SHP-2 axis regulated myeloid cell differentiation and fate commitment and function in cancer. Myeloid-specific SHP-2 or PD-1 ablation-induced myeloid cells with enriched gene expression profiles of enhanced differentiation, activation, phagocytosis and features of effector differentiation. Monocytes from *Shp2^{fl/fl}LysM^{Cre}* and *Pdcd1^{fl/fl}LysM^{Cre}* tumor-bearing mice had a direct impact on controlling tumor growth and could transfer antitumor immunity into naïve hosts.

SHP-2 and the PD-1-SHP-2 signaling restrained the GM-CSF-mediated phosphorylation of HOXA10 and IRF8, which induce myeloid differentiation and monocyte/DC lineage commitment, respectively. During GM-CSF signaling, PD-1 interacted with Lyn and was phosphorylated at Y248 within the conserved ITSM motif, a site that is phosphorylated by Src family kinases in T cells leading to PD-1 interaction with SHP-2 (ref. 34), indicating canonical PD-1-SHP-2 signaling axis was operative in myeloid cells, similarly to what has been previously established for B and T lymphocytes³². This myeloid-specific PD-1-SHP-2 axis might be particularly important in the context of cancer, where growth factors released by cancer cells induce emergency myelopoiesis, and directly upregulate PD-1 and PD-L1 expression in myeloid progenitors and their progeny, thereby posing a signaling restraint to their effector differentiation. This might be the earliest critical signaling target of the PD-1-PD-L1 pathway in the context of cancer, because soluble factors produced by cancer cells can act systemically at early stages of the cancer immunity cycle, before local tumor growth and infiltration by immune cells that are subject to inhibitory signals in the tumor microenvironment.

We found that targeting SHP-2 in myeloid cells resulted in enhanced differentiation of neutrophils and TAMs generated from bone marrow-derived monocytes in tumors. Both cell types were characterized by enriched gene signatures and pathways linked to effector differentiation, leukocyte-mediated immunity, cytokine and chemokine production. TAM-mediated chemokine production and chemotaxis have been reported to have a tumor-promoting effect by recruiting immunosuppressive myeloid cells to tumors⁴⁷. In contrast, chemokine production signatures of TAMs in *Shp2^{fl/fl}LysM^{Cre}* and *Pdcd1^{fl/fl}LysM^{Cre}* tumor-bearing mice were associated with diminished tumor growth. This outcome might be explained by the differentiated state of SHP-2-deficient and PD-1-deficient myelocytes that were skewed away from protumorigenic MDSCs and TAMs and, instead, had enhanced effector functions promoting antitumor immune responses.

The impact of inhibiting SHP-2 in myeloid cells has been previously reported by using allosteric inhibitors of SHP-2 such as SHP099, TNO155 (ref. 48) and RMC4550 (ref. 49) to target cancer cells where SHP-2 is activated downstream of RTK/Ras signaling and functions as an oncogene. Combined approaches of SHP-2 allosteric inhibitors and pharmacologic RTK inhibitors or KRAS^{G12C}-GDP inhibitors have been employed with the main purpose to target signaling vulnerabilities in cancer⁵⁰. Such treatments also altered immune cells of the TME but remained elusive whether this was due to a direct effect of these compounds on immune cells or a consequence of inhibiting cancer growth. Our studies, employing a genetic approach, showed an increase of differentiated granulocytes and TAMs with signatures of effector differentiation and leukocyte-mediated immunity indicating a direct effect in myeloid cells after SHP-2 ablation.

IL-10, an IRF8-regulated gene⁴⁵, was increased in SHP-2-deficient and PD-1-deficient TAMs, whereas IL-10 neutralization compromised the enhanced antitumor immunity of *Shp2^{fl/fl}LysM^{Cre}* and *Pdcd1^{fl/fl}LysM^{Cre}* mice. Myeloid-specific SHP-2 ablation was reported to enhance IL-10-mediated immunosuppression in gut macrophages protecting mice from intestinal inflammation and carcinogenesis⁵¹. In our system, we did not find detectable effects of IL-10 in the immunosuppressive function of MDSCs or the activation state of TAMs. IL-10 is currently

emerging as a previously unappreciated regulator of antitumor function and a master switch of tumor-promoting inflammation to antitumor immunity⁴⁶. This might be mediated by IL-10-receptor-mediated recruitment and engagement of STAT3, diminishing procarcinogenic IL-6-mediated STAT3 signaling. IL-10 might have direct effects on T cells because pegylated IL-10 induced systemic activation and polyclonal expansion of CD8⁺ T cells in cancer patients⁵².

Besides IL-10, TAMs from *Shp2^{fl/fl}LysM^{Cre}* and *Pdcd1^{fl/fl}LysM^{Cre}* mice had increased transcripts of other genes that counteract protumorigenic inflammation, compared to *Shp2^{fl/fl}* and *Pdcd1^{fl/fl}* TAMs. For instance, there was an increase in *IRAK3*, which functions as a negative regulator of MyD88-mediated proinflammatory activation downstream of TLR/IL-1R⁵³. We also found a common increase in the expression of *Zbtb18*, a zinc finger transcriptional repressor recently identified to bind promoter/enhancer elements of genes encoding class I PI3K regulatory subunits, limiting their expression⁵⁴. Because TLR/IL-1R and PI3K-mediated signaling in myeloid cells promote protumorigenic inflammation⁵⁵, our findings uncovered several mechanisms capable of mediating fine-tuning of proinflammatory signaling in SHP-2 and PD-1 deficient TAMs.

IRF8 has a decisive role in the differentiation of monocytes and DC via epigenetic regulation of distinct sets of enhancers in cooperation with other transcription factors. High, low and null IRF8 expression promotes the differentiation of conventional DC, monocytes and neutrophils, respectively⁴⁵. In the absence of SHP-2- or PD-1-mediated signals, bone marrow myeloid cells had enhanced IRF8 phosphorylation, which is required for IRF8 function⁴³. IRF8 expression is fine-tuned at various differentiation stages of the myeloid lineage. Its expression starts at the multipotent progenitor stage, substantially increases in MDP and further increases in CDP and cells differentiating into the DC lineage, whereas it remains relatively low or downregulated in the monocytic lineage⁴⁵. In addition to transcription, IRF8 abundance is regulated by post-transcriptional mechanisms through Notch⁵⁶ and c-Cbl ubiquitin ligase⁵⁷. Future studies are required to determine how IRF8 abundance and function are regulated in the context of cancer and PD-1-SHP-2 signaling.

Our results showed that monocytes isolated from the bone marrow of SHP-2 and PD-1 deficient tumor-bearing mice could transfer antitumor capacity to naïve hosts, a feature previously attributed to the development of trained immunity. Neutrophils might also develop anticancer-protective trained immunity³⁰; however, in our system, we found that monocytes but not neutrophils conferred antitumor protection. Of note, IL-1 β that drives training of monocyte precursors³¹ was highly increased in SHP-2 and PD-1 deficient TAMs, potentially explaining the preferential development of training in monocytes by blockade of the PD-1-SHP-2 signaling. It is tempting to speculate that the long-lasting effects of PD-1-based immunotherapy in some, but not all, patients might be related to the development of immunotherapy-mediated monocyte differentiation and trained immunity versus generation of immunosuppressive MDSCs and TAMs during cancer-driven emergency myelopoiesis. Future studies will investigate these new directions of central regulation of antitumor responses to cancer immunotherapy in patients.

In conclusion, our results provide multiple levels of evidence that SHP-2 and the PD-1-SHP-2 axis pose a signaling restraint to the differentiation and monocyte/DC lineage in the context of cancer, resulting in a myeloid landscape that compromises antitumor immunity.

Online content

Any methods, additional references, Nature Portfolio reporting summaries, source data, extended data, supplementary information, acknowledgements, peer review information; details of author contributions and competing interests; and statements of data and code availability are available at <https://doi.org/10.1038/s41590-022-01385-x>.

References

1. Baumeister, S. H., Freeman, G. J., Dranoff, G. & Sharpe, A. H. Coinhibitory pathways in immunotherapy for cancer. *Annu. Rev. Immunol.* **34**, 539–573 (2016).
2. Cassetta, L. & Pollard, J. W. Tumor-associated macrophages. *Curr. Biol.* **30**, R246–R248 (2020).
3. Veglia, F., Sanseviero, E. & Gabrilovich, D. I. Myeloid-derived suppressor cells in the era of increasing myeloid cell diversity. *Nat. Rev.* **21**, 485–498 (2021).
4. Yokosuka, T. et al. Programmed cell death 1 forms negative costimulatory microclusters that directly inhibit T cell receptor signaling by recruiting phosphatase SHP2. *J. Exp. Med.* **209**, 1201–1217 (2012).
5. Rota, G. et al. Shp-2 is dispensable for establishing T cell exhaustion and for PD-1 signaling in vivo. *Cell Rep.* **23**, 39–49 (2018).
6. Zhang, T. et al. Loss of SHP-2 activity in CD4⁺ T cells promotes melanoma progression and metastasis. *Sci. Rep.* **3**, 2845 (2013).
7. Strauss, L. et al. Targeted deletion of PD-1 in myeloid cells induces antitumor immunity. *Sci. Immunol.* **5**, eaay1863 (2020).
8. Tartaglia, M. et al. Somatic mutations in PTPN11 in juvenile myelomonocytic leukemia, myelodysplastic syndromes and acute myeloid leukemia. *Nat. Genet.* **34**, 148–150 (2003).
9. Lindsey, S. et al. Activation of SHP2 protein-tyrosine phosphatase increases HoxA10-induced repression of the genes encoding gp91(PHOX) and p67(PHOX). *J. Biol. Chem.* **282**, 2237–2249 (2007).
10. Alharbi, R. A., Pettengell, R., Pandha, H. S. & Morgan, R. The role of HOX genes in normal hematopoiesis and acute leukemia. *Leukemia* **27**, 1000–1008 (2013).
11. Eklund, E. A., Jalava, A. & Kakar, R. Tyrosine phosphorylation of HoxA10 decreases DNA binding and transcriptional repression during interferon gamma-induced differentiation of myeloid leukemia cell lines. *J. Biol. Chem.* **275**, 20117–20126 (2000).
12. Kurotaki, D. et al. IRF8 inhibits C/EBPalpha activity to restrain mononuclear phagocyte progenitors from differentiating into neutrophils. *Nat. Commun.* **5**, 4978 (2014).
13. Zhu, C., Lindsey, S., Konieczna, I. & Eklund, E. A. Constitutive activation of SHP2 protein tyrosine phosphatase inhibits ICSBP-induced transcription of the gene encoding gp91PHOX during myeloid differentiation. *J. Leukoc. Biol.* **83**, 680–691 (2008).
14. Netherby, C. S. et al. The granulocyte progenitor stage is a key target of IRF8-mediated regulation of myeloid-derived suppressor cell production. *J. Immunol.* **198**, 4129–4139 (2017).
15. Karakasheva, T. et al. CD38⁺ M-MDSC expansion characterizes a subset of advanced colorectal cancer patients. *JCI Insight* **3**, e97022 (2018).
16. Strauss, L. et al. RORC1 regulates tumor-promoting 'emergency' granulo-monocytopenia. *Cancer Cell* **28**, 253–269 (2015).
17. Olsson, A. et al. Single-cell analysis of mixed-lineage states leading to a binary cell fate choice. *Nature* **537**, 698–702 (2016).
18. Zhong, Z. et al. New mitochondrial DNA synthesis enables NLRP3 inflammasome activation. *Nature* **560**, 198–203 (2018).
19. Molgora, M. et al. TREM2 modulation remodels the tumor myeloid landscape enhancing anti-PD-1 immunotherapy. *Cell* **182**, 886–900 (2020).
20. Condamine, T. et al. Lectin-type oxidized LDL receptor-1 distinguishes population of human polymorphonuclear myeloid-derived suppressor cells in cancer patients. *Sci. Immunol.* **1**, aaf8943 (2016).
21. Grajales-Reyes, G. E. et al. Baf3 maintains autoactivation of Irf8 for commitment of a CD8 α^+ conventional DC clonogenic progenitor. *Nat. Immunol.* **16**, 708–717 (2015).
22. Gao, Y. et al. Single-cell analysis reveals the heterogeneity of monocyte-derived and peripheral type-2 conventional dendritic cells. *J. Immunol.* **207**, 837–848 (2021).
23. Briseno, C. G. et al. Distinct transcriptional programs control cross-priming in classical and monocyte-derived dendritic cells. *Cell Rep.* **15**, 2462–2474 (2016).
24. Yanez, A. et al. Granulocyte-monocyte progenitors and monocyte-dendritic cell progenitors independently produce functionally distinct monocytes. *Immunity* **47**, 890–902 (2017).
25. Menezes, S. et al. The heterogeneity of Ly6C(hi) monocytes controls their differentiation into iNOS⁺ macrophages or monocyte-derived dendritic cells. *Immunity* **45**, 1205–1218 (2016).
26. Gajewski, T. F., Schreiber, H. & Fu, Y. X. Innate and adaptive immune cells in the tumor microenvironment. *Nat. Immunol.* **14**, 1014–1022 (2013).
27. Dixon, K. O. et al. TIM-3 restrains anti-tumour immunity by regulating inflammasome activation. *Nature* **595**, 101–106 (2021).
28. Spranger, S., Bao, R. & Gajewski, T. F. Melanoma-intrinsic beta-catenin signalling prevents anti-tumour immunity. *Nature* **523**, 231–235 (2015).
29. Guiducci, C., Vicari, A. P., Sangaletti, S., Trinchieri, G. & Colombo, M. P. Redirecting in vivo elicited tumor infiltrating macrophages and dendritic cells towards tumor rejection. *Cancer Res.* **65**, 3437–3446 (2005).
30. Kalafati, L. et al. Innate immune training of granulopoiesis promotes anti-tumor activity. *Cell* **183**, 771–785 (2020).
31. Christ, A. et al. Western diet triggers NLRP3-dependent innate immune reprogramming. *Cell* **172**, 162–175 (2018).
32. Boussiotis, V. A. Molecular and biochemical aspects of the PD-1 checkpoint pathway. *N. Engl. J. Med.* **375**, 1767–1778 (2016).
33. Hui, E. et al. T cell costimulatory receptor CD28 is a primary target for PD-1-mediated inhibition. *Science* **355**, 1428–1433 (2017).
34. Patsoukis, N. et al. Interaction of SHP-2 SH2 domains with PD-1 ITSM induces PD-1 dimerization and SHP-2 activation. *Commun. Biol.* **3**, 128 (2020).
35. Hansen, G. et al. The structure of the GM-CSF receptor complex reveals a distinct mode of cytokine receptor activation. *Cell* **134**, 496–507 (2008).
36. Celis-Gutierrez, J. et al. Quantitative interactomics in primary T cells provides a rationale for concomitant PD-1 and BTLA coinhibitor blockade in cancer immunotherapy. *Cell Rep.* **27**, 3315–3330 (2019).
37. Yang, N. et al. Knockout of immunotherapy prognostic marker genes eliminates the effect of the anti-PD-1 treatment. *NPJ Precis. Oncol.* **5**, 37 (2021).
38. Li, G. et al. Jarid2 and PRC2, partners in regulating gene expression. *Genes Dev.* **24**, 368–380 (2010).
39. Cheng, S. C. et al. mTOR- and HIF-1 α -mediated aerobic glycolysis as metabolic basis for trained immunity. *Science* **345**, 1250684 (2014).
40. Meiser, J. et al. Pro-inflammatory macrophages sustain pyruvate oxidation through pyruvate dehydrogenase for the synthesis of itaconate and to enable cytokine expression. *J. Biol. Chem.* **291**, 3932–3946 (2016).
41. Bekkering, S. et al. Metabolic induction of trained immunity through the mevalonate pathway. *Cell* **172**, 135–146 (2018).
42. Diamond, M. S. et al. Type I interferon is selectively required by dendritic cells for immune rejection of tumors. *J. Exp. Med.* **208**, 1989–2003 (2011).
43. Lecoultré, M., Dutoit, V. & Walker, P. R. Phagocytic function of tumor-associated macrophages as a key determinant of tumor progression control: a review. *J. Immunother. Cancer* **8**, e001408 (2020).

44. Medrano-Fernandez, I. et al. RIAM (Rap1-interacting adaptor molecule) regulates complement-dependent phagocytosis. *Cell. Mol. Life Sci.* **70**, 2395–2410 (2013).
45. Murakami, K. et al. A RUNX-CBF β -driven enhancer directs the Irf8 dose-dependent lineage choice between DCs and monocytes. *Nat. Immunol.* **22**, 301–311 (2021).
46. Saraiva, M., Vieira, P. & O'Garra, A. Biology and therapeutic potential of interleukin-10. *J. Exp. Med.* **217**, e20190418 (2020).
47. Halama, N. et al. Tumoral immune cell exploitation in colorectal cancer metastases can be targeted effectively by anti-CCR5 therapy in cancer patients. *Cancer Cell* **29**, 587–601 (2016).
48. Chen, Y. N. et al. Allosteric inhibition of SHP2 phosphatase inhibits cancers driven by receptor tyrosine kinases. *Nature* **535**, 148–152 (2016).
49. Quintana, E. et al. Allosteric inhibition of SHP2 stimulates antitumor immunity by transforming the immunosuppressive environment. *Cancer Res.* **80**, 2889–2902 (2020).
50. Fedele, C. et al. SHP2 inhibition diminishes KRASG12C cycling and promotes tumor microenvironment remodeling. *J. Exp. Med.* **218**, e20201414 (2021).
51. Xiao, P. et al. Phosphatase Shp2 exacerbates intestinal inflammation by disrupting macrophage responsiveness to interleukin-10. *J. Exp. Med.* **216**, 337–349 (2019).
52. Naing, A. et al. PEGylated IL-10 (pegilodecakin) induces systemic immune activation, CD8(+) T cell invigoration and polyclonal T cell expansion in cancer patients. *Cancer Cell* **34**, 775–791 (2018).
53. Kobayashi, K. et al. IRAK-M is a negative regulator of toll-like receptor signaling. *Cell* **110**, 191–202 (2002).
54. Xie, B. et al. The zinc finger protein Zbtb18 represses expression of class I phosphatidylinositol 3-kinase subunits and inhibits plasma cell differentiation. *J. Immunol.* **206**, 1515–1527 (2021).
55. Schmid, M. C. et al. Receptor tyrosine kinases and TLR/IL1Rs unexpectedly activate myeloid cell PI3kgamma, a single convergent point promoting tumor inflammation and progression. *Cancer Cell* **19**, 715–727 (2011).
56. Xu, H. et al. Notch-RBP-J signaling regulates the transcription factor IRF8 to promote inflammatory macrophage polarization. *Nat. Immunol.* **13**, 642–650 (2012).
57. Xiong, H. et al. Ubiquitin-dependent degradation of interferon regulatory factor-8 mediated by Cbl down-regulates interleukin-12 expression. *J. Biol. Chem.* **280**, 23531–23539 (2005).

Publisher's note Springer Nature remains neutral with regard to jurisdictional claims in published maps and institutional affiliations.

Open Access This article is licensed under a Creative Commons Attribution 4.0 International License, which permits use, sharing, adaptation, distribution and reproduction in any medium or format, as long as you give appropriate credit to the original author(s) and the source, provide a link to the Creative Commons license, and indicate if changes were made. The images or other third party material in this article are included in the article's Creative Commons license, unless indicated otherwise in a credit line to the material. If material is not included in the article's Creative Commons license and your intended use is not permitted by statutory regulation or exceeds the permitted use, you will need to obtain permission directly from the copyright holder. To view a copy of this license, visit <http://creativecommons.org/licenses/by/4.0/>.

© The Author(s) 2022

¹ Division of Hematology–Oncology, Beth Israel Deaconess Medical Center, Boston, MA, USA. ²Department of Medicine, Beth Israel Deaconess Medical Center, Harvard Medical School, Boston, MA, USA. ³Cancer Center, Beth Israel Deaconess Medical Center, Boston, MA, USA. ⁴Department of Pathology, Beth Israel Deaconess Medical Center, Harvard Medical School, Boston, MA, USA. ⁵Harvard Medical School Initiative for RNA Medicine, Beth Israel Deaconess Medical Center, Boston, MA, USA. ⁶Broad Institute of MIT and Harvard, Cambridge, MA, USA. ⁷Harvard College, Cambridge, MA, USA. ⁸JJP Biologics, Warsaw, Poland. ⁹Cancer Research Institute, Beth Israel Deaconess Medical Center, Boston, MA, USA. ¹⁰Present address: Department of Medicine, Yale University, New Haven, CT, USA. ¹¹Present address: Department of Dermatology, Faculty of Medicine Siriraj Hospital, Mahidol University, Bangkok, Thailand. ¹²Present address: Heidelberg University, German Cancer Research Center (DKFZ), Heidelberg, Germany. ¹³Present address: Sanofi / Tidal, Cambridge, MA, USA. ¹⁴These authors contributed equally: Anthos Christofides, Xanthi-Lida Katopodi. ✉ e-mail: vboussio@bidmc.harvard.edu

Methods

Mice

All mice procedures were approved by the Institutional Animal Care and Use Committee at Beth Israel Deaconess Medical Center (Boston MA) and were in accordance with the National Institutes of Health Guidelines for the Care and Use of Animals. An approved active protocol is in place for the investigator (046-2019). The studies are compliant with the maximum tumor size permitted by the committee and tumors were never allowed to ulcerate. Mice with conditional targeting of the *Ptprn11* gene (encoding for Shp-2) were kindly provided by Dr. Gen-Sheng Feng (University of California, San Diego) and have been previously described⁵⁸. Mice with conditional targeting of the *Pdcd1* gene (encoding for PD-1) have been previously described⁷. Mice expressing Cre recombinase under the control of the distal Lck promoter (Strain, 012837) and mice expressing Cre recombinase under the control of the lysozyme (LysM) promoter (Strain, 004781), C57BL/6 mice and OTI-TCR transgenic mice (C57BL/6-Tg(TcrαTcrβ)1100Mjb/J) were purchased from Jackson Laboratory (Bar Harbor, Maine).

Tumor cell lines and tumor experiments

B16-F10 melanoma and MC17-51 fibrosarcoma cell lines were purchased from ATCC. B16-F10 cell line was subcloned and subclones with intermediate growth rate were selected for use. Eight to twelve weeks old mice were used for tumor implantation, and B16-F10 melanoma (1×10^5 or 3×10^5 cells per mouse, as described in individual experiments) or MC17-51 fibrosarcoma (4×10^4 or 1×10^5 cells per mouse) were injected subcutaneously in the left flank under isoflurane anesthesia. For adoptive transfer of monocytes or neutrophils into naïve hosts, CD45⁺CD11b⁺Ly6C^{hi}Ly6G⁻ monocytes and CD45⁺CD11b⁺Ly6C⁻Ly6G⁺ neutrophils were magnetically collected from the bone marrow of tumor-bearing mice 9 days after implantation of MC17-51 tumors. Further, 0.75×10^5 monocytes or 0.75×10^5 neutrophils were mixed with equal number of MC17-51 cells and were injected subcutaneously in new WT C57BL/6 hosts. Starting from day 9, tumor size was monitored every 2 days by a caliper fitted with a Vernier scale. The tumor volume was calculated by the following formula: tumor volume = $0.5 \times \text{width}^2 \times \text{length}$. Mice were killed on days 14–16 after tumor implantation and bone marrows, spleens, tumors and tumor-draining lymph nodes were collected. At termination, tumor weight was also measured. For antibody treatment experiments, 250 μg of either InVivoMab anti-PD-1 (clone RMP1-14, BioXCELL) or IgG2a control (clone 2A3, BioXCell) diluted in sterile PBS were injected intraperitoneally in a volume of 100 μl per mice on days 9, 11 and 13 after tumor inoculation and the mice were euthanized at day 15. For T cell depletion, mice were injected on day 1 relatively to tumor inoculation, and subsequently every third day with 200 μg of InVivoMab antimouse CD3 ϵ (clone 145-2C11 f(ab')₂ fragments, Bio X Cell) or hamster IgG f(ab')₂ fragments (BioXCell). For treatment with anti-IL-10 antibody, mice were treated with 250 μg of either InVivoMab anti-IL-10 (clone JES5-2A5, BioXCell) or rat IgG1 control (clone HRPN, BioXCell) on days 9, 11 and 13 after tumor inoculation.

Cell purification and processing

Single-cell suspensions were made from spleens, tumor-draining lymph nodes, and tumors as previously described⁷. Briefly, tumors were digested by 1 mg ml⁻¹ of Collagenase I in incomplete RPMI and then filtered through 70 μl strainers, while the spleens and the tumor-draining lymph nodes were directly filtered through 70 μl strainers. For flow cytometry studies, 1×10^6 were resuspended in 1X PBS supplemented with 2.5% FBS and plated in 96-well round bottom plates. Surface staining was performed at 4 °C for 25–30 min with the flow antibodies listed in Supplementary Table 7. For intracellular staining, Foxp3/transcription factor permeabilization/staining Buffer set (Thermo Fischer Scientific) was used according to the manufacturer's instructions. Intracellular staining was performed at 4 °C for 35–45 min with flow antibodies listed in Supplementary Table 3. Cells were acquired

using Becton Dickinson LSR Fortessa or Beckman-Coulter Cytoflex flow cytometer and analyzed with FlowJo software.

Suppression assay

MDSC-mediated suppression was assessed using previously established methodology⁷. Briefly, splenic MDSCs were isolated from the spleens of mice bearing B16-F10 melanoma or MC17-51 fibrosarcoma, by using the EasySep Mouse (CD11b⁺GR1⁺) isolation kit (Stemcell Technologies, 19867), or the MDSC isolation kit (Miltenyi Biotech, 130-094-538) to separate GR1^{hi}Ly6G⁺Ly6C⁻ (PMN-MDSC) and GR1^{dim}Ly6G⁻Ly6C⁺ (M-MDSC) cells. Serial dilutions of MDSCs (2×10^5 , 1×10^5 , 0.5×10^5 , 0.25×10^5 and 0.125×10^5) were plated in flat bottom 96-well plates with 2×10^5 splenocytes per well isolated from OTI-TCR transgenic mice and 250 ng ml⁻¹ of ovalbumin peptide (OVA₂₅₇₋₂₆₄) for 72 h. As a control, OTI splenocytes were incubated with OVA peptide (OVA₂₅₇₋₂₆₄) without MDSC. ³H-thymidine was added for the last 16 h of a 72 h culture, and thymidine incorporation was measured by MicroBeta plate counter (Perkin Elmer).

Cell culture and signaling

For signaling experiments, bone marrow cells from C57BL/6 WT mice or *Shp2*^{fl/fl} and *Shp2*^{fl/fl}*LysM*^{Cre} mice were cultured for 48 h in Iscove's media supplemented with 10% FBS, 2 mmol l⁻¹ glutamine, 100 units per ml penicillin–streptomycin, 10 mM Hepes and 20 μM β -mercaptoethanol, in the presence of GM-CSF (10 ng ml⁻¹) and IL-3 (5 ng ml⁻¹) (both purchased from Peprotech). Where indicated, a PD-L1 blocking antibody (MIH5) (10 μg ml⁻¹) was added to the cultures for the entire period of incubation. For studies of GM-CSF-mediated short-term signaling activation, 48 h after culture as described above, cells were rested for 3 h at 37 °C in RPMI 1640 containing 10 mM HEPES. Cells were then either left unstimulated or resuspended at 10×10^6 cells per ml in prewarmed RPMI 1640 containing 10 mM HEPES and were stimulated with GM-CSF (40 ng ml⁻¹). At the indicated time points, the reaction was stopped by adding cold PBS and placement on ice.

Immunoprecipitation and immunoblotting

To prepare lysates, cells were washed in PBS and lysed as previously described in ref. 34. Briefly, cells were resuspended and lysed in lysis buffer containing 50 mM Tris–HCl, pH 7.4, 150 mM NaCl, 2 mM MgCl₂, 10% glycerol and 1% NP-40 supplemented with 2 mM sodium orthovanadate, 1 mM sodium fluoride, 1 mM phenylmethylsulfonyl fluoride and protease Inhibitor Cocktail (Thermo Fischer Scientific). Cell lysates were resolved by SDS-PAGE, transferred on nitrocellulose membrane, and analyzed by western blotting with the indicated antibodies. The following antibodies were used for western blotting: SHP-2 (D50F2) 3397T, Cell Signaling Technology; Lyn (H-6) sc-7274 AF790, Santa Cruz Biotechnology; HoxA10 (E-11) sc-271428 AF680, Santa Cruz Biotechnology; ICSBP (IRF8) (E-9) sc-365042 AF680, Santa Cruz Biotechnology; Pdcd-1 (RMP1-30) sc-56200 AF680, Santa Cruz Biotechnology; IL-3/IL-5/GM-CSFR β (A-3) sc-398246, Santa Cruz Biotechnology; p-Tyr (PY99) sc-7020 AF790, Santa Cruz Biotechnology. The rabbit polyclonal antiphospho-Y248 (ITSM) PD-1 (pPD-1) antibody was developed in our laboratory³⁴. For conjugation of pPD-1 Ab, the Li-COR IRDye 800CW protein labeling kit for high molecular weight and microscale reactions (829-08881) was used. Immunoprecipitations were performed with agarose-conjugated antibodies HoxA10 (E-11) sc-271428 AC, Santa Cruz Biotechnology; ICSBP (IRF8) (E-9) sc-365042 AC, Santa Cruz Biotechnology; Pdcd-1 (RMP1-30) sc-56200 AC, Santa Cruz Biotechnology. Briefly, 20 μl of agarose slurry/sample was first washed three times with lysis buffer and then resuspended in 40 μl of buffer. For each IP sample, 40 μl of washed agarose-conjugated Ab were mixed with 500–1000 μg of cell lysates and incubated overnight at 4 °C with gentle rotation. The agarose slurry was then washed three times with lysis buffer and boiled for 5 min in denaturing sample buffer followed by a quick spin. The supernatant was analyzed by SDS-PAGE, transferred to

a nitrocellulose membrane and blotted with the indicated antibodies. Images were visualized, acquired and quantified with Li-COR Odyssey CLx imaging system. The abundance of phosphorylated HOXA10 and IRF8 was normalized to the immunoprecipitated HOXA10 and IRF8, respectively, and was expressed as fold change over the value obtained in *Shp2^{fl/fl}* cells, defined as one. Expression of actin in whole-cell lysates was used as input. The abundance of SHP-2 coprecipitated with PD-1 was normalized to the immunoprecipitated PD-1 and was expressed as a fold change over the value obtained in *Shp2^{fl/fl}* cells, defined as one. Expression of PD-1 in whole-cell lysates was used as input.

RNA-seq and analysis

For RNA-seq, PMN-MDSCs (GR1^{hi}Ly6G⁺Ly6C⁻) were isolated from the spleens of MC17-51 fibrosarcoma bearing and *Shp2^{fl/fl}LysM^{Cre}* and *Shp2^{fl/fl}* mice by magnetic bead isolation. TAMs were isolated from the same mice by cell sorting after using the Live/Dead Fixable Far Read Dead Cell Stain kit (Thermo Fischer Scientific; L34973) to identify live cells, staining with antibodies specific for CD45, CD11b, F4/80 and Ly6G and gating on CD45⁺CD11b⁺F4/80⁺Ly6G⁻ live cells. Total RNA was isolated from the cells using the Qiagen RNeasy Mini Kit (Qiagen, 74104). For each sample, 400 ng of total RNA was then used in Illumina's TruSeq Stranded mRNA Library kit (20020594) for polyA mRNA isolation and library construction. Libraries were sequenced on Illumina NextSeq 500 as paired-end 42-nt reads (Active Motif). Raw sequencing reads were quality-checked using FastQC (v0.11.5)⁵⁹ and data were pre-processed with Cutadapt (v2.5)⁶⁰ for adapter removal following best practices⁶¹. Gene expression quantification was performed by aligning against the GRCh38 genome using STAR (v2.7.3a)⁶² and quantifying reads against Ensembl v98 (ref. 63) annotated gene loci with featureCounts (Subread 1.6.2)⁶⁴. Differential gene expression analysis was performed using DESeq2 (v1.24.0)⁶⁵, while ClusterProfiler (v3.12.0)⁶⁶ was used for downstream functional investigations. Plots were generated in R using ggplot2 (v3.3.3)⁶⁷, EnhancedVolcano (v1.8.0)⁶⁸ and ComplexHeatmap (v2.6.2)⁶⁹. Storey's *q* value was used to control family-wise error rate⁷⁰. Sequencing data have been deposited in the Gene Expression Omnibus database under the accession numbers GSE187394 and GSE206207.

Metabolite analysis

Phagocytes were differentiated from bone marrow of *Shp2^{fl/fl}* and *Shp2^{fl/fl}LysM^{Cre}* mice by culture in Iscove's media supplemented with 10% fetal bovine serum, 2 mmol l⁻¹ glutamine, 100 units per ml penicillin–streptomycin, 10 mM Hepes and 20 μM beta-mercaptoethanol, in the presence of GM-CSF (40 ng ml⁻¹)⁷¹. Polar metabolites were quantitatively profiled by a positive/negative ion-switching, targeted liquid chromatography–tandem mass spectrometry (LC–MS/MS) based metabolomics platform using a 5500 QTRAP hybrid triple quadrupole mass spectrometer (AB/SCIEX) via selected reaction monitoring (SRM) as described previously⁷². Briefly, Lin^{neg} bone marrow cells were cultured with G-CSF and GM-CSF (40 ng ml⁻¹ each) for 48 h using triplicate samples for each condition and sample type. After methanol extraction using 80% (vol/vol) methanol (–80 °C) was carried out, pellets were lyophilized using a SpeedVac concentrator using no heat. Twenty microliter of LC–MS grade water was added to resuspend each sample just before LC–MS/MS analysis and 5 μl of sample was injected onto the autosampler of the LC system (Shimadzu) using an amide HILIC column (Waters). Once the SRM data for ~285 metabolites were acquired, peaks were integrated using a software platform for peak area integration MultiQuant 2.1 (AB/SCIEX). Data analysis was performed using online MetaboAnalyst 3.0 software.

Real-time quantitative PCR

Total RNA extraction was prepared with the RNeasy Mini Kit from Qiagen, Valencia, CA, according to the manufacturer's instructions, and 50 ng of RNA was subjected to quantitative PCR (qPCR) analysis for the

target genes *Clec4n* and *Cxcl3* using AB 7,000 qPCR machine (Applied Biosystems Roche). FAM-conjugated gene-specific primers for target genes and the TaqMan One-Step RT-PCR Master Mix reagents and the VIC-TAMRA-conjugated 18S RNA housekeeping gene control primers were from Applied Biosystems/Roche.

Statistics and reproducibility

RNA-seq statistical analysis was completed as described above. All other statistical analyses were performed using GraphPad Prism (GraphPad Software v.9.3.0). Values are given as mean ± s.d. as indicated. Numbers of experimental replicates are given in the figure legends. When two groups were compared, significance was determined using an unpaired two-tailed *t*-test. For comparing more than two groups, one-way analysis of variance was applied. *P* < 0.05 are considered as statistically significant (**P* < 0.05, ***P* < 0.01, ****P* < 0.001, *****P* < 0.0001). No statistical methods were used to predetermine sample sizes, and our sample sizes were similar to those reported in the previous publications^{7,16,19}. Mice were assigned randomly to the various experimental groups described. Equal numbers of male and female mice were used in all experiments. Data collection and analysis were not performed blind to the conditions of the experiments. Data distribution was assumed to be normal, but this was not formally tested. No data points were excluded from the analyses.

Reporting summary

Further information on research design is available in the Nature Portfolio Reporting Summary linked to this article.

Data availability

All data generated or analyzed during this study are included in this published article (and its supplementary information files). Sequencing data have been deposited in the Gene Expression Omnibus database under the accession numbers GSE187394 and GSE206207 and are publicly available. Source data are provided with this paper.

References

- Zhang, E. E., Chapeau, E., Hagihara, K. & Feng, G. S. Neuronal Shp2 tyrosine phosphatase controls energy balance and metabolism. *Proc. Natl Acad. Sci.* **101**, 16064–16069 (2004).
- Martin, M. Cutadapt removes adapter sequences from high-throughput sequencing reads. *EMBnet J.* **17**, 10–12 (2011).
- Andrews, S. A quality control tool for high throughput sequence data. <http://www.bioinformatics.babraham.ac.uk/projects/fastqc/> (2010).
- Conesa, A. et al. A survey of best practices for RNA-seq data analysis. *Genome Biol.* **17**, 13 (2016).
- Dobin, A. et al. STAR: ultrafast universal RNA-seq aligner. *Bioinformatics* **29**, 15–21 (2013).
- Yates, A. D. et al. Ensembl 2020. *Nucleic Acids Res.* **48**, D682–D688 (2020).
- Liao, Y., Smyth, G. K. & Shi, W. featureCounts: an efficient general purpose program for assigning sequence reads to genomic features. *Bioinformatics* **30**, 923–930 (2014).
- Love, M. I., Huber, W. & Anders, S. Moderated estimation of fold change and dispersion for RNA-seq data with DESeq2. *Genome Biol.* **15**, 550 (2014).
- Yu, G., Wang, L. G., Han, Y. & He, Q. Y. clusterProfiler: an R package for comparing biological themes among gene clusters. *OMICS* **16**, 284–287 (2012).
- Wickham, H. ggplot2: elegant graphics for data analysis. <https://ggplot2.tidyverse.org> (2009).
- Blighe, K., Rana, S. & Myles, L. EnhancedVolcano: publication-ready volcano plots with enhanced colouring and labeling. <https://github.com/kevinblighe/EnhancedVolcano> (2020).

69. Gu, Z., Eils, R. & Schlesner, M. Complex heatmaps reveal patterns and correlations in multidimensional genomic data. *Bioinformatics* **32**, 2847–2849 (2016).
70. Storey, J. D. & Tibshirani, R. Statistical significance for genomewide studies. *Proc. Natl Acad. Sci.* **100**, 9440–9445 (2003).
71. Di Gioia, M. et al. Endogenous oxidized phospholipids reprogram cellular metabolism and boost hyperinflammation. *Nat. Immunol.* **21**, 42–53 (2020).
72. Yuan, M., Breitkopf, S. B., Yang, X. & Asara, J. M. A positive/negative ion-switching, targeted mass spectrometry-based metabolomics platform for bodily fluids, cells, and fresh and fixed tissue. *Nat. Protoc.* **7**, 872–881 (2012).

Acknowledgements

This work was supported by NIH/NCI under grants CA238263 and CA229784 (to V.A.B.).

Author contributions

A.C. performed most experiments, wrote sections of the manuscript and prepared figures; C.C., K.A., S.Y., I.A., M.A.A.M., L.S., N.M.T. and R.P. performed experiments; X.L.K., D.K. and I.S.V. performed bioinformatics analysis and prepared figures; L.B. provided reagents; J.A. did metabolomics; N.P. did experiments, participated in the experimental design and wrote sections of the manuscript and V.A.B. designed the project, guided participants, did experiments and wrote the manuscript. All authors read, edited and approved the manuscript.

Competing interests

V.A.B. has patents on the PD-1 pathway licensed by Bristol-Myers Squibb, Roche, Merck, EMD-Serono, Boehringer Ingelheim, AstraZeneca, Novartis and Dako. All the other authors declare no competing interests.

Additional information

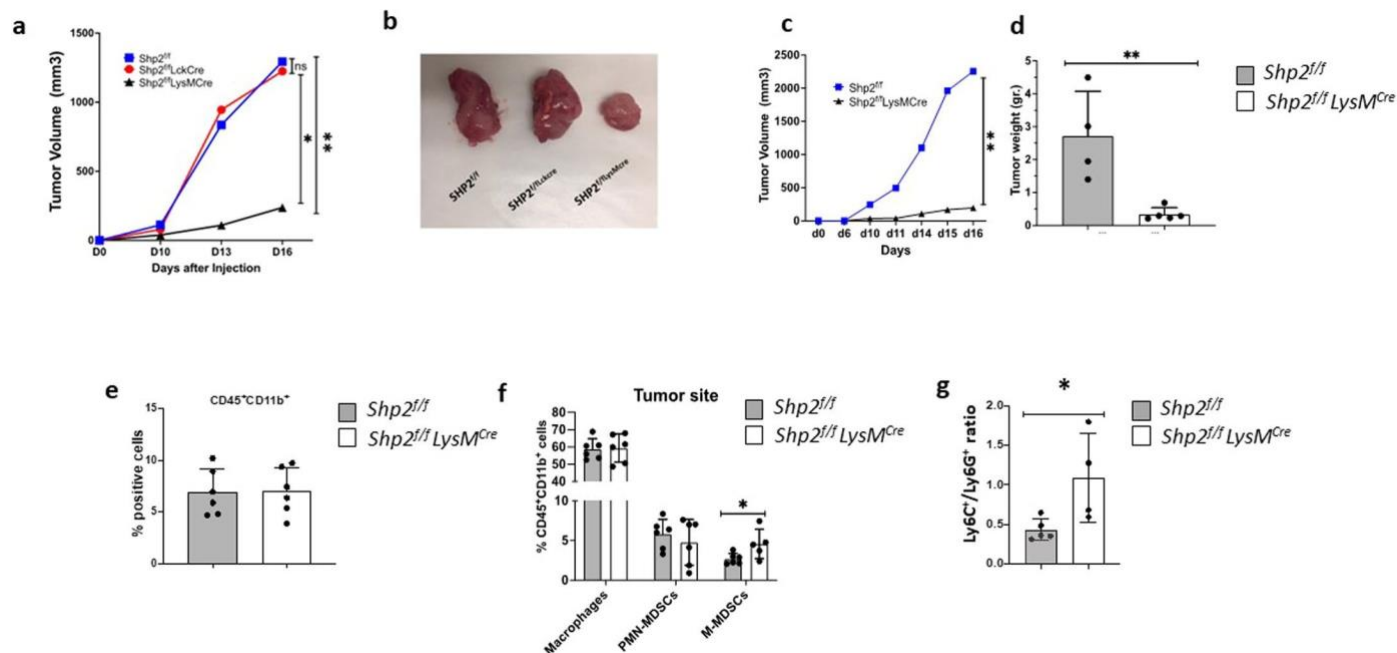
Extended data is available for this paper at <https://doi.org/10.1038/s41590-022-01385-x>.

Supplementary information The online version contains supplementary material available at <https://doi.org/10.1038/s41590-022-01385-x>.

Correspondence and requests for materials should be addressed to Vassiliki A. Boussiotis.

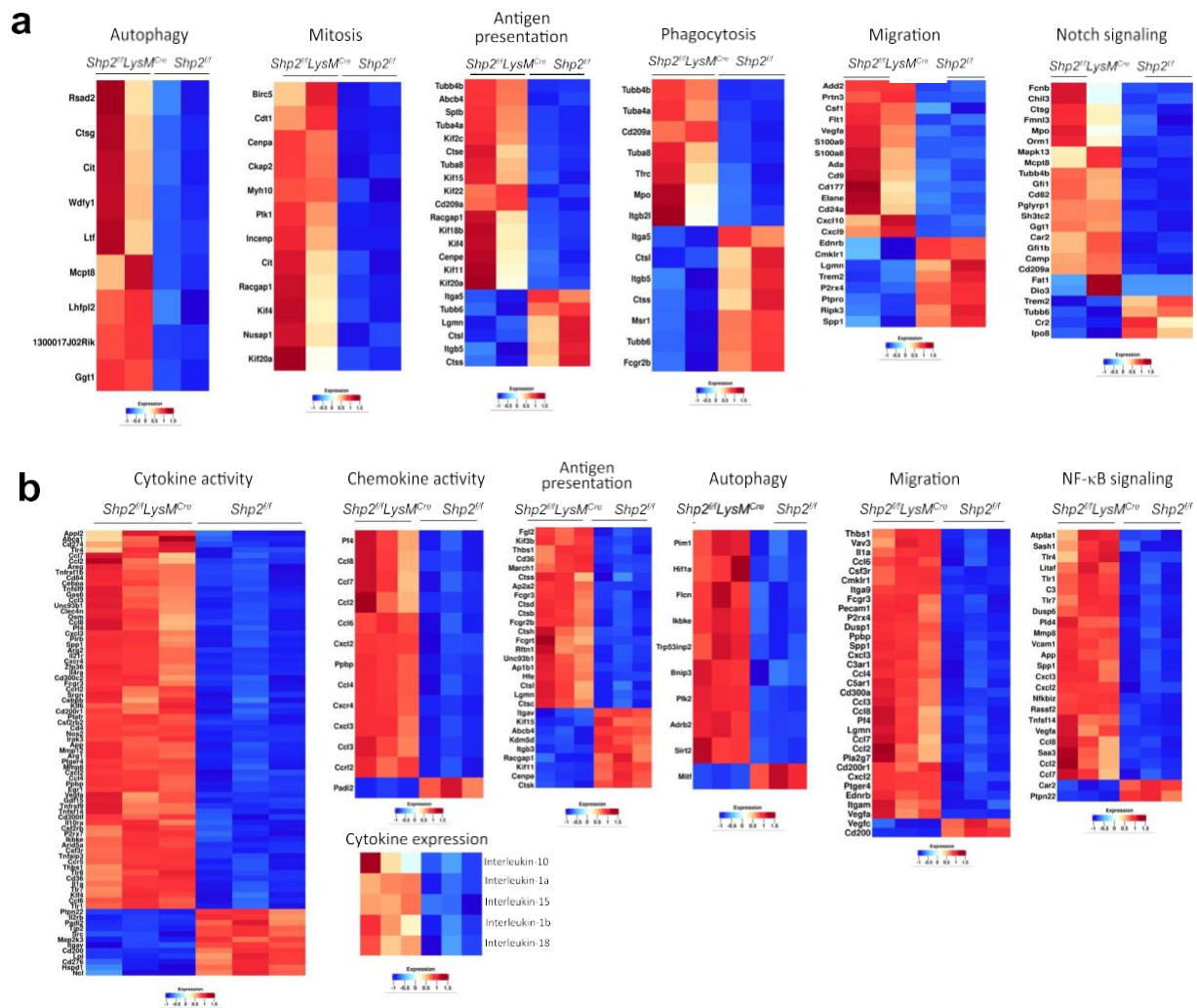
Peer review information *Nature Immunology* thanks Cecilia Garlanda and the other, anonymous, reviewer(s) for their contribution to the peer review of this work. (if applicable to your journal): Ioana Visan was the primary editor of this article and managed its editorial process and peer review in collaboration with the rest of the editorial team. Peer reviewer reports are available.

Reprints and permissions information is available at www.nature.com/reprints.



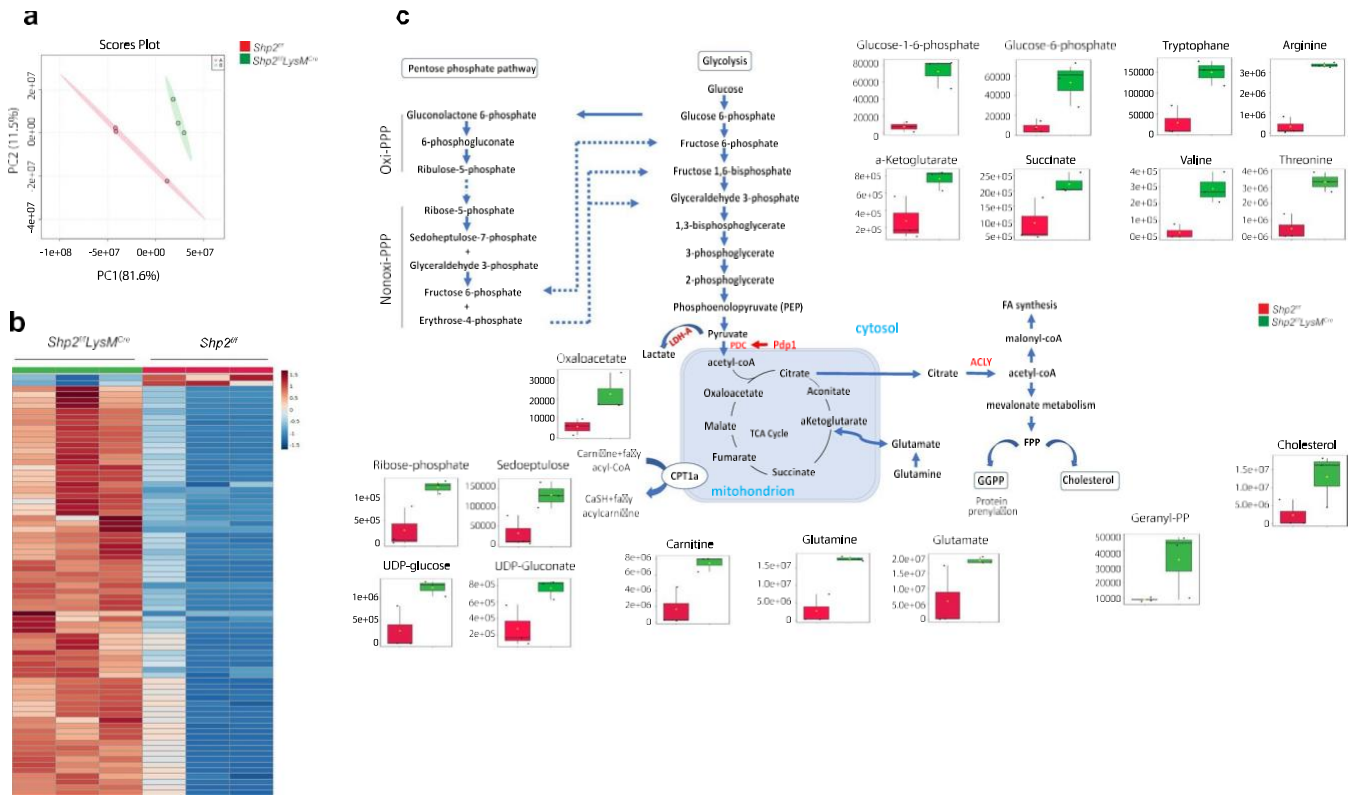
Extended Data Fig. 1 | Myeloid-specific SHP-2 depletion diminishes tumor growth. **a**, *Shp2^{fl/fl}*, *Shp2^{fl/fl}Lck^{Cre}*, and *Shp2^{fl/fl}LysM^{Cre}* mice were inoculated with MC17-51 fibrosarcoma cells, tumor volume was monitored longitudinally, and comparisons were made on each day of assessment. Data shown are means of $n = 6$ mice per group and are representative of three independent experiments. (* $p < 0.05$, ** $p < 0.01$), ANOVA. **b**, Representative images of tumors isolated at day 15 from each of the three experimental group are shown. **c**, **d**, *Shp2^{fl/fl}* and *Shp2^{fl/fl}LysM^{Cre}* mice were inoculated with B16-F10 melanoma cells, tumor volume was

monitored longitudinally (**c**) and tumor weight was measured at termination on day 16 (**d**). Data are means of $n = 5$ mice per group and are representative from one of four independent experiments. (* $p < 0.05$, ** $p < 0.01$), unpaired t-test two tailed. **e-g**, The frequencies of CD45⁺CD11b⁺ myeloid cells (**e**), the fractions of macrophages, PMN-MDSC and M-MDSC (**f**) and the ratio of M-MDSC/PMN-MDSC (**g**) in tumors were assessed. Data are representative of means \pm SD are shown. Results from one representative of 4 independent experiments with $n = 4$ mice per group are shown (* $p < 0.05$, ** $p < 0.01$), unpaired t-test two tailed.



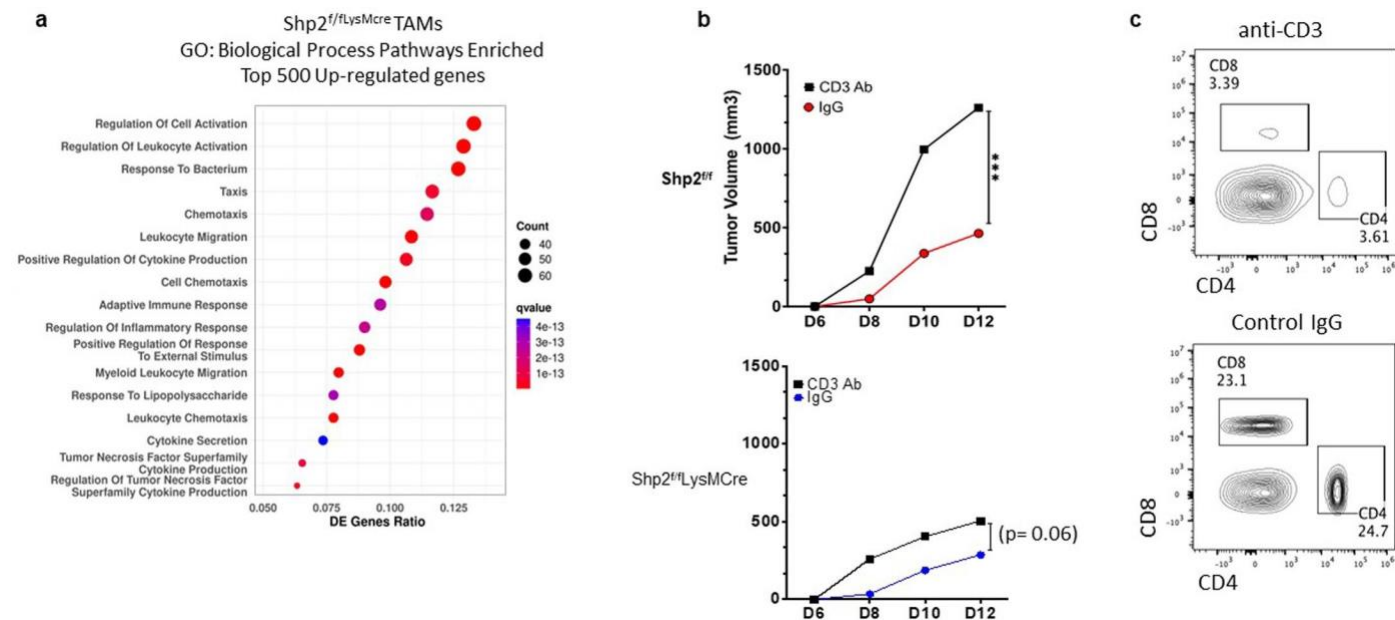
Extended Data Fig. 2 | Distinct transcription signatures in PMN-MDSC and TAMs of *Shp2^{fl}/LysM^{Cre}* tumor-bearing mice compared to *Shp2^{fl}* tumor-bearing mice. a, b, *Shp2^{fl}/LysM^{Cre}* and *Shp2^{fl}* mice were injected with MC17-51 cancer cells and 15 days later, PMN-MDSC (a) were isolated from the spleens,

TAMs (b) were isolated from tumors, and RNA-seq was performed followed by pathway enrichment analysis of DEG. Heat maps of DEG for enriched pathways are shown. Differential gene expression analysis was performed using DESeq2.



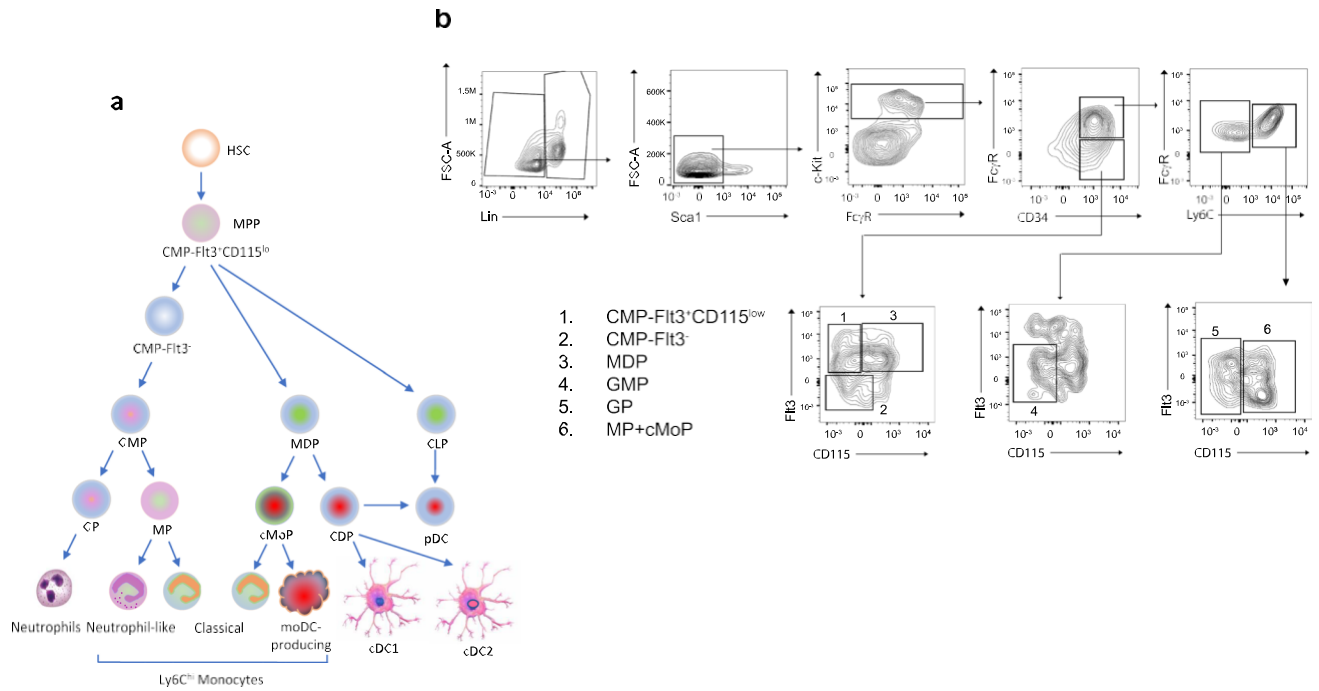
Extended Data Fig. 3 | Phagocytes from *Shp2^{fl/fl}/LysM^{Cre}* and *Shp2^{fl/fl}* mice have distinct metabolic activities. **a**, Phagocytes were generated from primary bone marrow cells of *Shp2^{fl/fl}/LysM^{Cre}* and *Shp2^{fl/fl}* mice using GM-CSF and metabolite analysis was performed after 48 hours of culture. Principal component analysis (PCA). **b**, Unsupervised hierarchical clustering of top 75 metabolites ($\log_2FC \geq 1$). **c**, Individual graphs of relative peak intensity of representative intermediate

metabolites of glycolysis, PPP and TCA cycle. Results from one representative of two independent experiments are shown. The amounts of the indicated metabolites were plotted in whisker boxes. The lower and upper sides of the box indicate the first and third quartile, respectively. The horizontal line inside the box indicates the median value, whereas the lower and upper bars indicate the minimum and maximum of distribution, respectively.

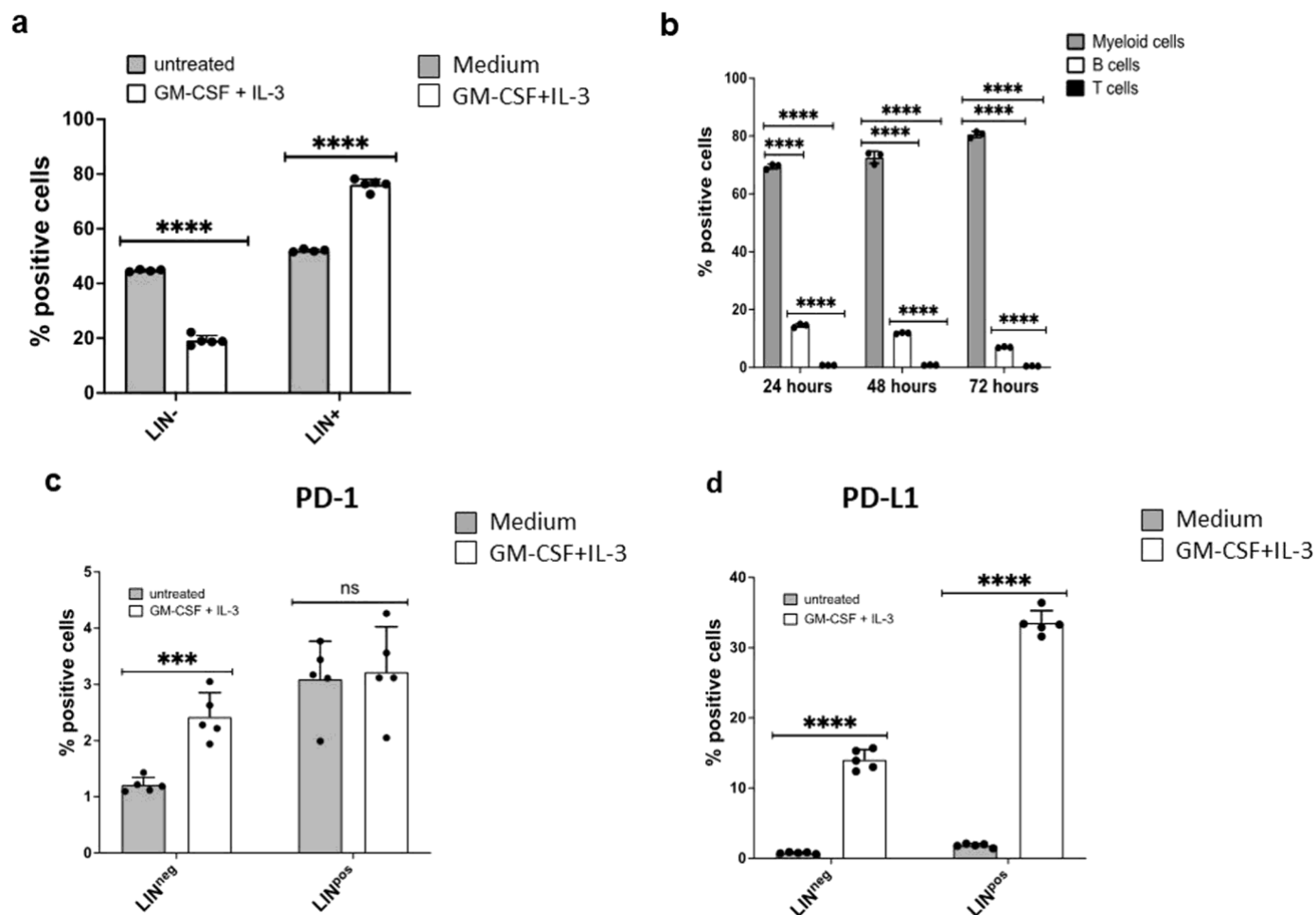


Extended Data Fig. 4 | Myeloid cells of *Shp2^{f/f}/LysM^{Cre}* mice have distinct molecular and functional properties. **a**, GO Biological Processes Pathways enriched among top 500 upregulated genes in TAMs from *Shp2^{f/f}/LysM^{Cre}* MC17-51 tumor-bearing mice compared to *Shp2^{f/f}* MC17-51 tumor-bearing mice, collected at day 15 after tumor implantation. Differential gene expression analysis was performed using DESeq2 and ClusterProfiler (v3.12.0) was utilized for downstream functional investigations. **b**, **c**, *Shp2^{f/f}* and *Shp2^{f/f}/LysM^{Cre}* mice injected with MC17-51 fibrosarcoma were treated with either anti-CD3 antibody or control IgG at day -1 relative to tumor injection and subsequently

every third day, and tumor growth was monitored for 12 days (**b**). Results show means of tumor volume and are representative of one from two independent experiments with $n = 10$ mice per group, (***) $p < 0.001$ unpaired t-test two tailed. **c**, At termination, expression of lymph node CD4⁺ and CD8⁺ T cells was assessed by flow cytometry. One representative histogram of each treatment condition generated from *Shp2^{f/f}/LysM^{Cre}* mice is shown. (In this experiment, the number of injected MC17-51 cells was reduced by 50% because, after T cell depletion, tumors in *Shp2^{f/f}* mice rapidly exceeded the permitted size).

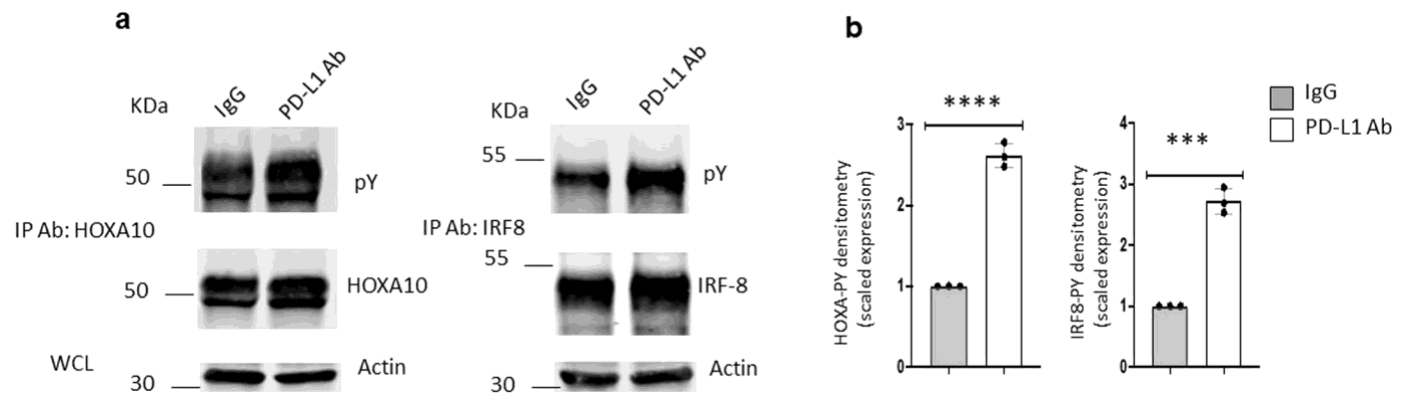


Extended Data Fig. 5 | Differentiation and identification of myeloid progenitors. a, b, Model for myeloid cell differentiation (a) and gating strategy (b) for characterization of bone marrow Lin⁻ myeloid progenitors. Identification of the progenitor subsets numbered in the histograms is shown.



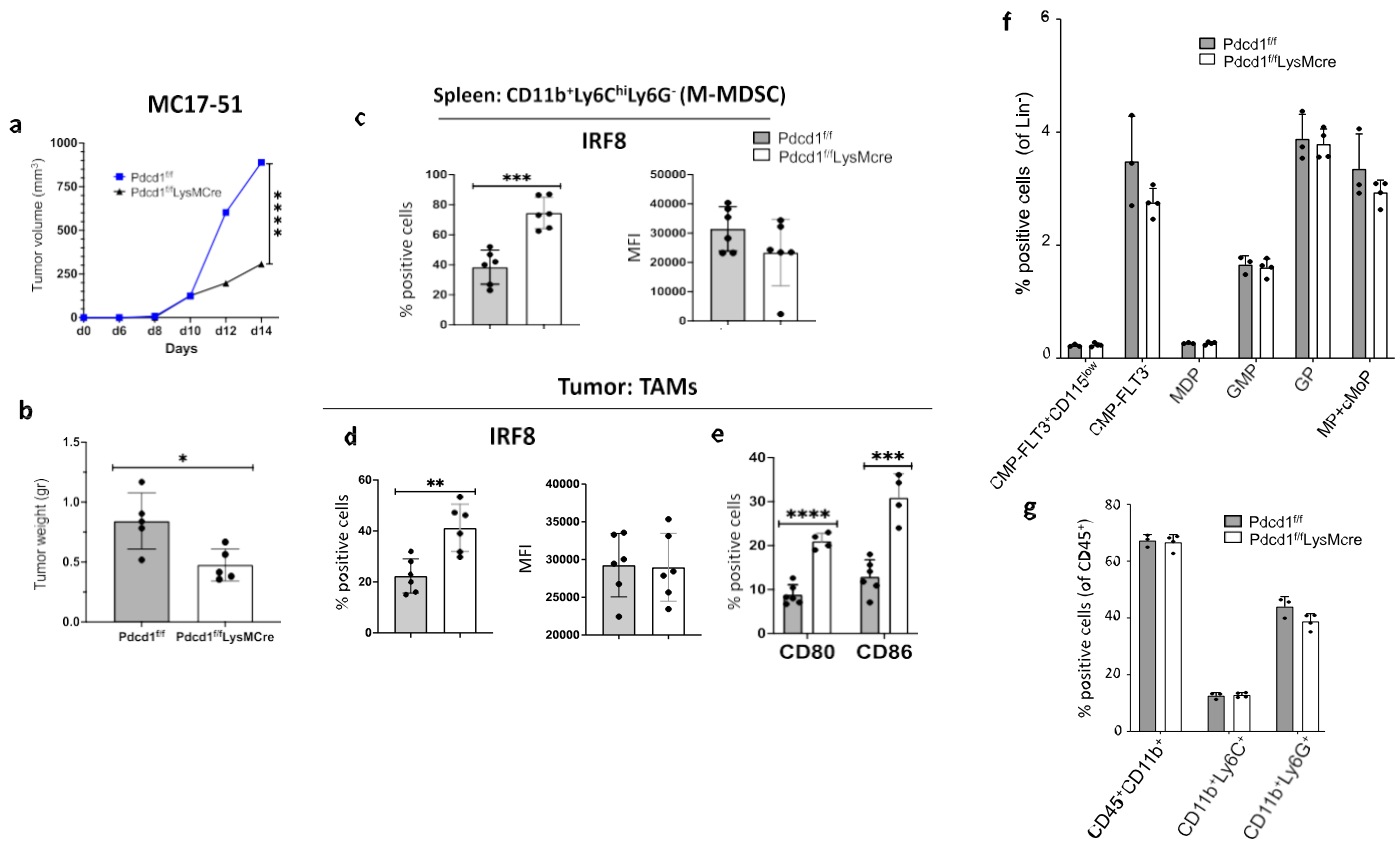
Extended Data Fig. 6 | Culture of bone marrow cells with GM-CSF + IL-3 induces PD-1 and PD-L1 expression in Lin⁻ and Lin⁺ myelocytes. a b, Bone marrow cells from WT C57BL/6 mice were cultured with GM-CSF (10 ng/ml) and IL-3 (5 ng/ml) for 24, 48 and 72 hours. Changes in the Lin⁻ and Lin⁺ populations were examined at 48 hours of culture (a). The frequency of the differentiated myeloid cells (CD45⁺CD11b⁺), B cells (B220⁺) and T cells (CD3⁺) was assessed

by flow cytometry at the indicated time points (b). c, d, Expression of PD-1 (c) and PD-L1 (d) in Lin⁻ and Lin⁺ subsets examined by flow cytometry at 72 hours of culture. Results are from one of five independent experiments with n = 5 biological replicates per group (**p < 0.01, ***p < 0.005, ****p < 0.001) unpaired t-test two tailed.



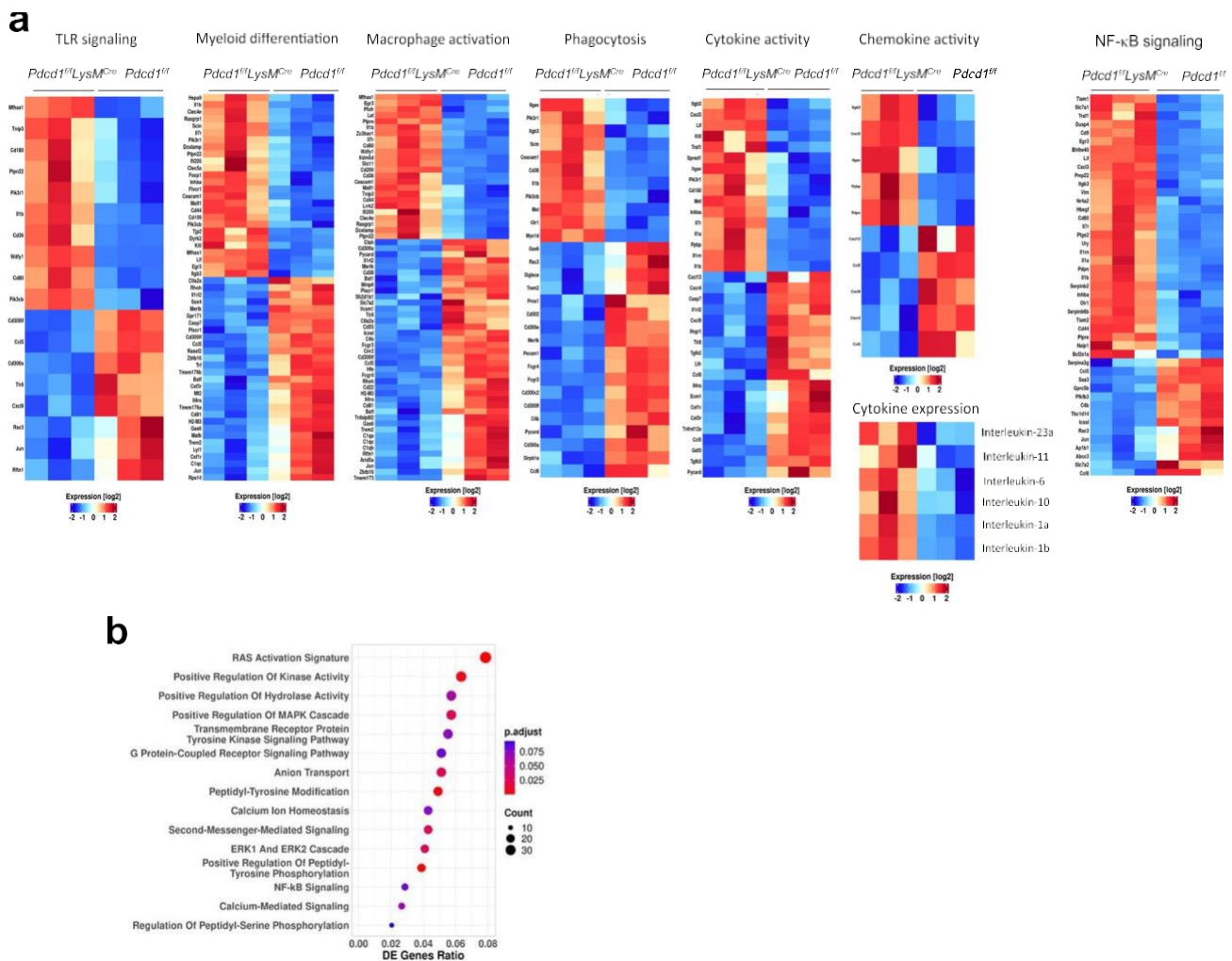
Extended Data Fig. 7 | Enhanced HOXA10 and IRF8 phosphorylation in myeloid cells during culture with GM-CSF and IL-3 in the presence of anti-PD-L1 blocking antibody. a, b, Bone marrow cells from C57BL/6 wild-type mice were cultured for 48 hr in the presence of GM-CSF (10 ng/ml) and IL-3 (5 ng/ml), with either IgG control or anti-PD-L1 blocking antibody (MIH5) (10 μ g/ml). Cell lysates were prepared and immunoprecipitation was done with agarose-conjugated HOXA10-specific antibody or agarose-conjugated IRF8-specific antibody followed by SDS-PAGE and immunoblot with anti-PY and HOXA10 antibodies or anti-PY and IRF8 antibodies (a). The abundance of

phosphorylated HOXA10 was normalized to immunoprecipitated HOXA10 and the abundance of phosphorylated IRF8 was normalized to immunoprecipitated IRF8 and were expressed as fold change over the relevant values obtained in cells cultured without PD-L1 blocking antibody (defined as 1) (b). Expression of actin in whole cell lysates was also examined as input. Images were visualized, acquired and quantified with Li-COR Odyssey CLx imaging system. Results are from one of three independent experiments. Values of three separate quantifications per condition are shown.



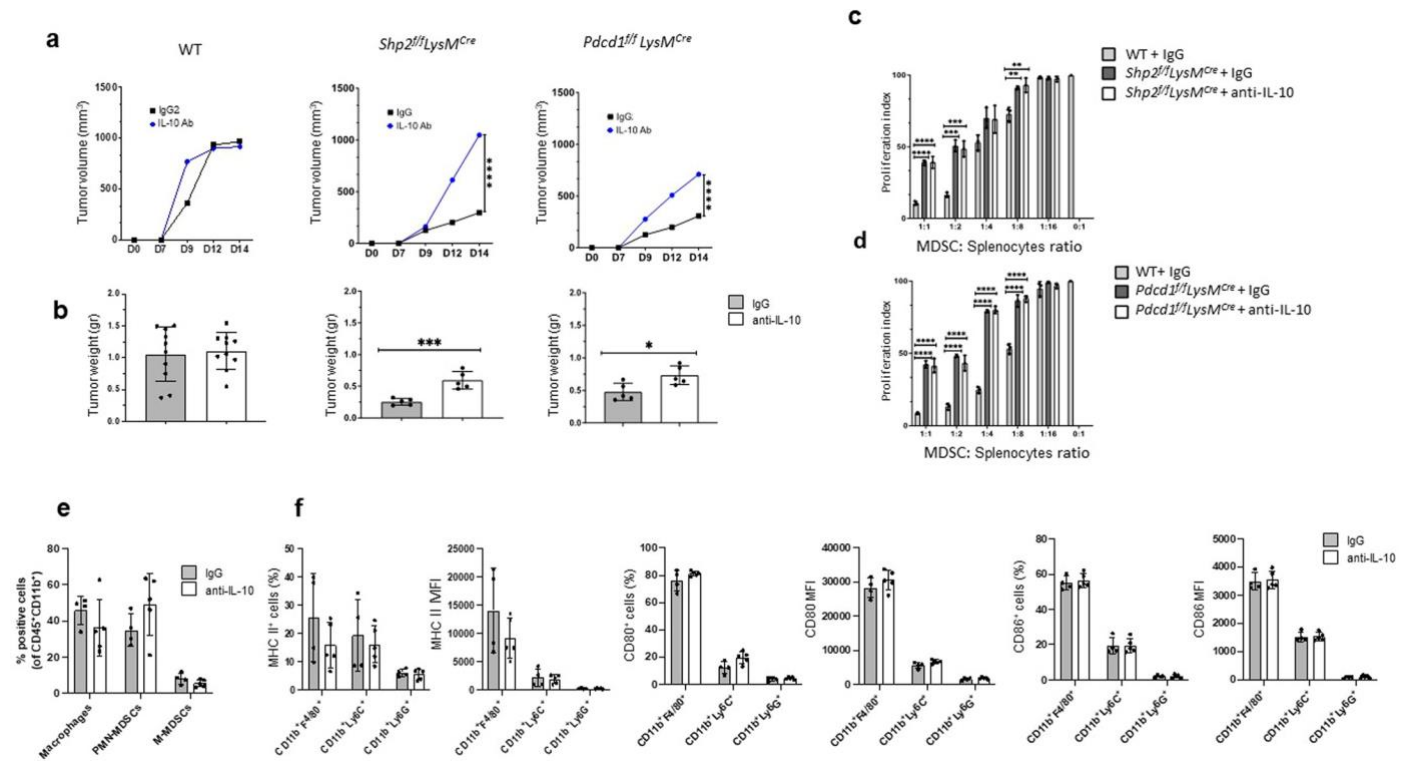
Extended Data Fig. 8 | Myeloid-specific deletion of PD-1 induces antitumor immunity, and increased numbers of IRF8⁺ M-MDSC and TAMs, and CD80⁺ and CD86⁺ TAMs. **a, b,** *Pdc1^{fl/fl}* and *Pdc1^{fl/fl}LysM^{Cre}* mice were inoculated with MC17-51 cells. Tumor volume was monitored longitudinally (**a**) and tumor weight (**b**) was measured at termination on day 15 after injection. Results show means of tumor volume (**a**) and means \pm SD of tumor weight (**b**) and are representative of four independent experiments with $n = 6$ mice per group, (** $p < 0.01$, **** $p < 0.0001$), unpaired t-test two tailed. **c-e,** M-MDSC (**c**), and TAMs (**d, e**) were

examined for the expression of IRF8, CD80 and CD86 by flow cytometry. Means \pm SD of % positive cells and MFI are shown. Results are from one representative of four independent experiments with $n = 6$ mice per group (** $p < 0.01$, **** $p < 0.0001$) unpaired t-test two tailed. **f, g,** At day 9 after tumor implantation, bone marrow was collected and flow cytometry was used to identify the subsets of Lin⁻ myeloid progenitors (**f**) using the gating strategy shown in Extended Data Fig. 5, the mature CD45⁺CD11b⁺ myeloid cells, and the subsets of Ly6C^{hi}Ly6G⁻ and Ly6C^{lo}Ly6G⁺ cells (**g**).



Extended Data Fig. 9 | Distinct transcription signatures in TAMs of *Pdc1fl/LysMCre* tumor-bearing mice compared to *Pdc1fl* tumor-bearing mice TAMs. a, *Pdc1fl/LysMCre* and *Pdc1fl* mice were injected with MC17-15 cancer cells and 15 days later, TAMs were isolated from tumors and RNA-seq was performed followed by pathway enrichment analysis of DEG. Heat maps of DEG for enriched pathways are shown. b, *Shp2fl/LysMCre* and *Pdc1fl/LysMCre* mice were injected

with MC17-51 fibrosarcoma and at day 15 after injection, TAMs were collected from tumors and RNA-seq was performed followed by GO analysis of DEG. GO Biological Processes of common signaling pathways enriched among top 500 DEG in TAMs from *Shp2fl/LysMCre* and *Pdc1fl/LysMCre* tumor-bearing mice are shown. Differential gene expression analysis was performed using DESeq2 and ClusterProfiler (v3.12.0) was utilized for downstream functional investigations.



Extended Data Fig. 10 | IL-10 neutralization compromises the enhanced anti-tumor responses of *Shp2^{fl}/LysM^{Cre}* and *Pdc1^{fl}/LysM^{Cre}* mice. a-f, Wild type, *Shp2^{fl}/LysM^{Cre}* and *Pdc1^{fl}/LysM^{Cre}* mice were injected with MC17-51 cancer cells and were subsequently treated with anti-IL-10 Ab or control IgG1 on days 9, 11, and 13 after tumor inoculation. Tumor volume (a) was monitored longitudinally and tumor weight (b) was measured at termination on day 15 after injection. Results are representative of two separate experiments with n = 10 mice per group. At day 15 after tumor injection, GR1⁺MDSC were isolated from the spleens of wild-type mice treated with IgG, and from *Shp2^{fl}/LysM^{Cre}* (c) and *Pdc1^{fl}/LysM^{Cre}* (d) tumor-bearing mice treated with anti-IL-10 Ab or IgG and were cultured at various

ratios with splenocytes from OTI transgenic mice (2×10⁵cells/well) stimulated with OVA₂₅₇₋₂₆₄. Results show Means ± SEM of cpm values of ³H-thymidine incorporation and are representative of two separate experiments with n = 4 mice per group. At day 15 after tumor injection, the fractions of the indicated cell populations (e), and the expression of MHC II, CD80 and CD86 (f) at the tumor site, were examined by flow cytometry. Data show Means ± SD and are representative from one of two independent experiments with n = 5 *Shp2^{fl}/LysM^{Cre}* mice per group (*p < 0.05, **p < 0.01, ***p < 0.001, ****p < 0.0001) unpaired t-test two tailed.

Reporting Summary

Nature Portfolio wishes to improve the reproducibility of the work that we publish. This form provides structure for consistency and transparency in reporting. For further information on Nature Portfolio policies, see our [Editorial P](#) and the [E Policy Checklist](#).

Statistics

For all statistical analyses, confirm that the following items are present in the figure legend, table legend, main text, or Methods section.

n/a Confirmed

The exact sample size (n) for each experimental group/condition, given as a discrete number and unit of measurement

A statement on whether measurements were taken from distinct samples or whether the same sample was measured repeatedly

The statistical test(s) used AND whether they are one- or two-sided

“ “ *Only common tests should be described solely by name, describe more complex techniques in the Methods section.*

A description of all covariates tested

A description of any assumptions or corrections, such as tests of normality and adjustment for multiple comparisons

A full description of the statistical parameters including central tendency (e.g. means) or other basic estimates (e.g. regression coefficient) AND variation (e.g. standard deviation) or associated estimates of uncertainty (e.g. confidence intervals)

“ “ For null hypothesis testing, the test statistic (e.g. F , t , r) with confidence intervals, effect sizes, degrees of freedom and P value noted
Give P values as exact values whenever suitable.

For Bayesian analysis, information on the choice of priors and Markov chain Monte Carlo settings

For hierarchical and complex designs, identification of the appropriate level for tests and full reporting of outcomes

Estimates of effect sizes (e.g. Cohen's d , Pearson's r), indicating how they were calculated

Our web collection on [s/ot/s/hi/s_ or b/o/o_ /st/s](#) hontons articles on man a ffile ohms above.

Software and code

Policy information about [availability of computer code](#)

Data collection

Flow cytometry data were analyzed with Flowjo 10.4 Software. For Metabolite analysis, polar metabolites were quantitatively profiled by a positive/negative ion-switching, targeted liquid chromatography tandem mass spectrometry (LC-MS/MS) based metabolomics platform using a 5500 QTRAP hybrid triple quadrupole mass spectrometer (AB/SCIEX) via selected reaction monitoring (SRM). Once the SRM data for 285 metabolites were acquired, peaks were integrated using a software platform for peak area integration MultiQuant 2.1 (AB/SCIEX). Data analysis was performed using online MetaboAnalyst 3.0 software. Raw sequencing reads were quality-checked using FastQC (v0.11.5) and data were pre-processed with Cutadapt (v2.5) for adapter removal following best practices. Gene expression quantification was performed by aligning against the GRCh38 genome using STAR (v2.7.3) and quantifying reads against Ensembl v98 annotated gene loci with featureCounts (Subread 1.6.2). Differential gene expression analysis was performed using DESeq2 (v1.24.0), while ClusterProfiler (v3.12.0) was utilized for downstream functional investigations. Plots were generated in R using ggplot2 (v3.3.3), EnhancedVolcano (v1.8.0), and ComplexHeatmap (v2.6.2). Storey's q value was utilized to control family-wise error rate. All other statistical analyses were performed using GraphPad Prism (GraphPad Software v.9.4.0)

Data analysis

For manuscripts utilizing custom algorithms or software that are central to the research but not yet described in published literature, software must be made available to editors and reviewers. We strongly encourage code deposition in a community repository (e.g. GitHub). See the Nature Portfolio [guidelines for submitting code & software](#) for further information.

Data

Policy information about [availability of data](#)

All manuscripts must include a [data](#) statement. This statement should provide the following information, where applicable:

- Accession codes, unique identifiers, or web links for publicly available datasets
- A description of any restrictions on data availability
- For clinical datasets or third party data, please ensure that the statement adheres to our [data sharing policy](#)

All data generated or analyzed during this study are included in this published article (and its supplementary information files). Sequencing data have been deposited at the Gene Expression Omnibus database under the accession numbers GSE187394 and GSE206207 and are publicly available.

Human research participants

Policy information about [studies involving human research](#) and [Sex and Gender in Research](#)

Reporting on sex and gender N/A

Population characteristics N/A

Recruitment N/A

Ethics oversight N/A

Note that information on the approval of the study protocol must also be provided in the manuscript.

Field-specific reporting

Please select the one below that is the best fit for your research. If you are not sure, read the appropriate sections before making your selection.

Life sciences

Behavioural & social sciences

Ecological, evolutionary & environmental sciences

For a reference copy of the document with all sections see [nature.com/documents/nr-reporting-summary-flat.pdf](https://www.nature.com/documents/nr-reporting-summary-flat.pdf)

Life sciences study design

All studies must disclose on these points even when the disclosure is negative

Sample size	No statistical methods were used to predetermine sample sizes, and our sample sizes were similar to those reported in previous publications. Strauss, L. et al. Targeted deletion of PD-1 in myeloid cells induces antitumor immunity. <i>Sci Immunol</i> 5, doi:10.1126/sciimmunol.aay1863 (2020). Strauss, L. et al. RORC1 Regulates Tumor-Promoting "Emergency" Granulo-Monocytopenia. <i>Cancer cell</i> 28, 253-269, doi:10.1016/j.ccr.2015.07.006 (2015). Molgora, M. et al. TREM2 Modulation Remodels the Tumor Myeloid Landscape Enhancing Anti-PD-1 Immunotherapy. <i>Cell</i> 182, 886-900 e817, doi:10.1016/j.cell.2020.07.013 (2020).
Data exclusions	No datapoints were excluded from the analyses.
Replication	All experiments were reproducible and were repeated at least three times
Randomization	Mice were assigned randomly to the various experimental groups described. Equal numbers of male and female mice were used in all experiments.
Blinding	Blinding was not used because the studies involved several genetically engineered mouse strains which are hard to breed in high numbers. For this reason, every available mouse should be used judiciously.

Reporting for specific materials, systems & methods

We require information from authors about some types of materials, experimental systems and methods used in many studies. Here, indicate whether each material, system or method listed is relevant to your study. If you are not sure if a list item applies to your research, read the appropriate section before selecting a response.

Materials & experimental systems**Methods**

n/a Involved in the study

- Antibodies
- Eukaryotic cell lines
- Palaeontology and archaeology
- Animals and other organisms
- Clinical data
- Dual use research of concern

n/a Involved in the study

- ChIP-seq
- Flow cytometry
- MRI-based neuroimaging

Antibodies

Antibodies used All antibodies used are described in the methods section and in a supplementary table (Supplementary Table 7). All antibodies were used according to the recommendations of the manufacturer unless indicated otherwise.

Validation

Eukaryotic cell lines

Policy information about [cell lines and Sex and Gender in Research](#)

Cell line source(s) B16-F10 and MC17-51 cell lines were used and were obtained from ATCC.

Authentication Authentication is provided by the vendor

Mycoplasma contamination All cell lines were tested negative for mycoplasma contamination. In our laboratory, we perform a regular screening for mycoplasma on a monthly basis.

Commonly misidentified lines (See [_____](#) register) N/A

Animals and other research organisms

Policy information about [studYes involving animals](#); [ARRIVE guidelines](#) recommended for reporting animal research, and [Sex and Gender in Research](#)

Laboratory animals Mouse

Wild animals N/A

Reporting on sex Equal number of male and female mice were used assigned in all experimental groups. This approach was employed because, the study does not involve a disease with distinct prevalence between sex groups.

Field—collected samples N/A

Ethics oversight All mice procedures were approved by the Institutional Animal Care and Use Committee (IACUC) at Beth Israel Deaconess Medical Center (Boston MA), and were in accordance with National Institutes of Health Guidelines for the Care and Use of Animals.

Note that full information on the approval of the study protocol must also be provided in the manuscript.

Flow Cytometry**Plots**

Confirm that:

- The axis labels state the marker and fluorochrome used (e.g. CD4-FITC).
- The axis scales are clearly visible. Include numbers along axes only for bottom left plot of group (a 'group' is an analysis of identical markers).
- All plots are contour plots with outliers or pseudocolor plots.
- A numerical value for number of cells or percentage (with statistics) is provided.

Methodology

Sample preparation Samples were prepared from live animals.

Instrument

Flow cytometry samples were acquired using Becton Dickinson LSR Fortessa or Beckman-Coulter Cytoflex. For metabolite analysis, polar metabolites were quantitatively profiled by a positive/negative ion-switching, targeted liquid chromatography tandem mass spectrometry (LC-MS/MS) based metabolomics platform using a 5500 QTRAP hybrid triple quadrupole mass spectrometer (AB/SCIEX) via selected reaction monitoring (SRM). Once the SRM data for ~285 metabolites were acquired, peaks were integrated using a software platform for peak area integration MultiQuant 2.1 (AB/SCIEX). Raw sequencing reads were quality-checked using FastQC (v0.11.5) and data were pre-processed with Cutadapt (v2.5) for adapter removal following best practices. Gene expression quantification was performed by aligning against the GRCh38 genome using STAR (v2.7.3a) and quantifying reads against Ensembl v98 annotated gene loci with featureCounts (Subread 1.6.2). Differential gene expression analysis was performed using DESeq2 (v1.24.0), while ClusterProfiler (v3.12.0) was utilized for downstream functional investigations. Plots were generated in R using ggplot2 (v3.3.3), EnhancedVolcano (v1.8.0), and ComplexHeatmap (v2.6.2). Storey's q value was utilized to control family-wise error rate. Gene sets used for Gene Set Enrichment. Signals on western blots were visualized, acquired and quantified with Li-COR Odyssey CLx imaging system. For assessment of cell proliferation 3H-thymidine incorporation was measured using a MicroBeta plate counter (TriLux Perkin Elmer).

Software

Cells were acquired using Becton Dickinson LSR Fortessa or Beckman-Coulter Cytoflex Flow cytometer and analyzed with FlowJo Software.

Cell population abundance

No cell sorting was used in any of the experiments




Gating strategy

All detailed relevant information regarding gating strategy is provided in Supplementary figures.

Tick this box to confirm that a figure exemplifying the gating strategy is provided in the Supplementary Information.



The complex role of tumor-infiltrating macrophages

Anthos Christofides^{1,2,3}, Laura Strauss^{1,2,3,5}, Alan Yeo³, Carol Cao^{1,2,4}, Alain Charest^{2,3}  and Vassiliki A. Boussiotis^{1,2,3}  

Long recognized as an evolutionarily ancient cell type involved in tissue homeostasis and immune defense against pathogens, macrophages are being re-discovered as regulators of several diseases, including cancer. Tumor-associated macrophages (TAMs) represent the most abundant innate immune population in the tumor microenvironment (TME). Macrophages are professional phagocytic cells of the hematopoietic system specializing in the detection, phagocytosis and destruction of bacteria and other harmful micro-organisms, apoptotic cells and metabolic byproducts. In contrast to these healthy macrophage functions, TAMs support cancer cell growth and metastasis and mediate immunosuppressive effects on the adaptive immune cells of the TME. Cancer is one of the most potent insults on macrophage physiology, inducing changes that are intimately linked with disease progression. In this Review, we outline hallmarks of TAMs and discuss the emerging mechanisms that contribute to their pathophysiological adaptations and the vulnerabilities that provide attractive targets for therapeutic exploitation in cancer.

Macrophages are professional phagocytic cells specialized in the detection, phagocytosis and destruction of harmful organisms, apoptotic cells, insult-related debris, and metabolic byproducts, providing immediate defense¹. After ingesting pathogens through phagocytosis, macrophages can directly present peptide antigens through the major histocompatibility complex class II (MHCII) to activate T helper cells. In contrast to dendritic cells (DCs), which present antigens in the lymph nodes and activate naive T cells, macrophages present antigens within tissues and cannot induce naive T cell activation². Macrophages detect pathogen-associated molecular patterns (PAMPs), such as bacterial products, and damage-associated molecular patterns (DAMPs) produced in response to trauma, ischemia, or tissue damage. For this process, they use a system of pattern recognition receptors (PRRs), such as Toll-like receptors (TLRs), which can bind specifically to pathogen components like bacterial lipopolysaccharides (LPS), RNA, DNA, or extracellular proteins, leading to the activation of signaling cascades and production of inflammatory mediators³. As a consequence, macrophages release soluble factors, such as cytokines, enzymes, or metabolites that affect other immune cell types. These steps can be subverted, resulting in a causal association of macrophages with diseases⁴.


In the adult host, macrophages originate mainly from blood monocytes produced from bone marrow (BM) myeloid progenitors, which leave the circulation to differentiate into macrophages in tissues. Macrophages generated during earlier stages of ontogeny, mainly from the yolk sac or fetal liver, also exist in various tissues⁵. These embryonic-derived macrophages persist throughout life as tissue-resident macrophages (TRMs) and participate in cancer evolution and metastasis. The adult bone marrow gives rise to Ly6C⁻ (nonclassical) patrolling monocytes that detect pathogens and maintain vessel integrity^{6,7}, and to Ly6C⁺ (classical) inflammatory monocytes, which are recruited to sites of infection, tissue injury and tumors. The Ly6C⁺ monocytes continuously replenish DCs in a process controlled by FLT3, generating monocyte-derived DCs (moDCs)^{5,8}. Despite their distinct origins, the differentiation and expansion of all monocyte and macrophage lineages are regulated by CSF1R (a receptor of colony stimulating factor 1) and its ligands,

IL-34 and CSF1 (refs. ^{9,10}). In some organs, such as kidney, liver, brain, and lung, macrophages originating from BM-derived monocytes co-exist with embryonically derived TRMs. Lineage-tracing studies have shown that microglia are primarily derived from the yolk-sac progenitors, whereas Kupffer cells of the liver have a mixed origin, from the yolk sac and fetal liver^{11,12}. Major embryonically derived TRM populations are found in skin, spleen, pancreas, liver, brain, and lung¹³. In such tissues, the distinct origin of macrophages is of particular importance in the context of cancer, where TRMs and bone-marrow-derived TAMs differentially accumulate in primary versus metastatic tumors^{14,15}.

TAMs are the most abundant immune population of the TME, representing ~50% of hematopoietic cells, and have heterogeneous properties spanning from anti-tumorigenic to pro-tumorigenic¹⁶. Antitumorigenic TAMs retain properties of antigen-presenting cells (APC), including high expression of MHCII, phagocytotic, and tumor-killing activity. Antitumorigenic TAMs secrete proinflammatory cytokines that support and activate adaptive immune cells¹⁷. In contrast, pro-tumorigenic TAMs are immunosuppressive and are characterized by low expression of MHCII and expression of inhibitory molecules such as PD-1, PD-L1, VISTA, B7-H4 and Tim3 (refs. ^{18–24}). Cues in the TME, including tumor-secreted soluble factors and metabolites, have been extensively studied and have been found to have an instrumental role in promoting the pro-tumorigenic features of TAMs, while suppressing the anti-tumorigenic features²⁵. The inherent ability of TAMs to alter their properties, defined as plasticity, can cause significant changes that result in the generation of TAM subsets characterized by distinct abilities to support tumor growth and metastasis^{26,27}. The distinct properties of TAMs are potential therapeutic targets (reviewed in ref. ²⁸).

Classical and patrolling monocytes

In tumor-bearing hosts, there is an increased output of classical Ly6C⁺ monocytes from BM myeloid progenitors, specifically common myeloid progenitors (CMPs) and granulocyte-macrophage progenitors (GMPs), which expand during cancer-mediated emergency myelopoiesis (Fig. 1a)²⁹. Strong activation signals, such as

¹Division of Hematology-Oncology, Beth Israel Deaconess Medical Center, Harvard Medical School, Boston, MA, USA. ²Department of Medicine, Beth Israel Deaconess Medical Center, Harvard Medical School, Boston, MA, USA. ³Cancer Center, Beth Israel Deaconess Medical Center, Harvard Medical School, Boston, MA, USA. ⁴Harvard College, Cambridge, MA, USA. ⁵Present address: Sanofi /Tidal, Cambridge, MA, USA.  e-mail: vboussio@bidmc.harvard.edu

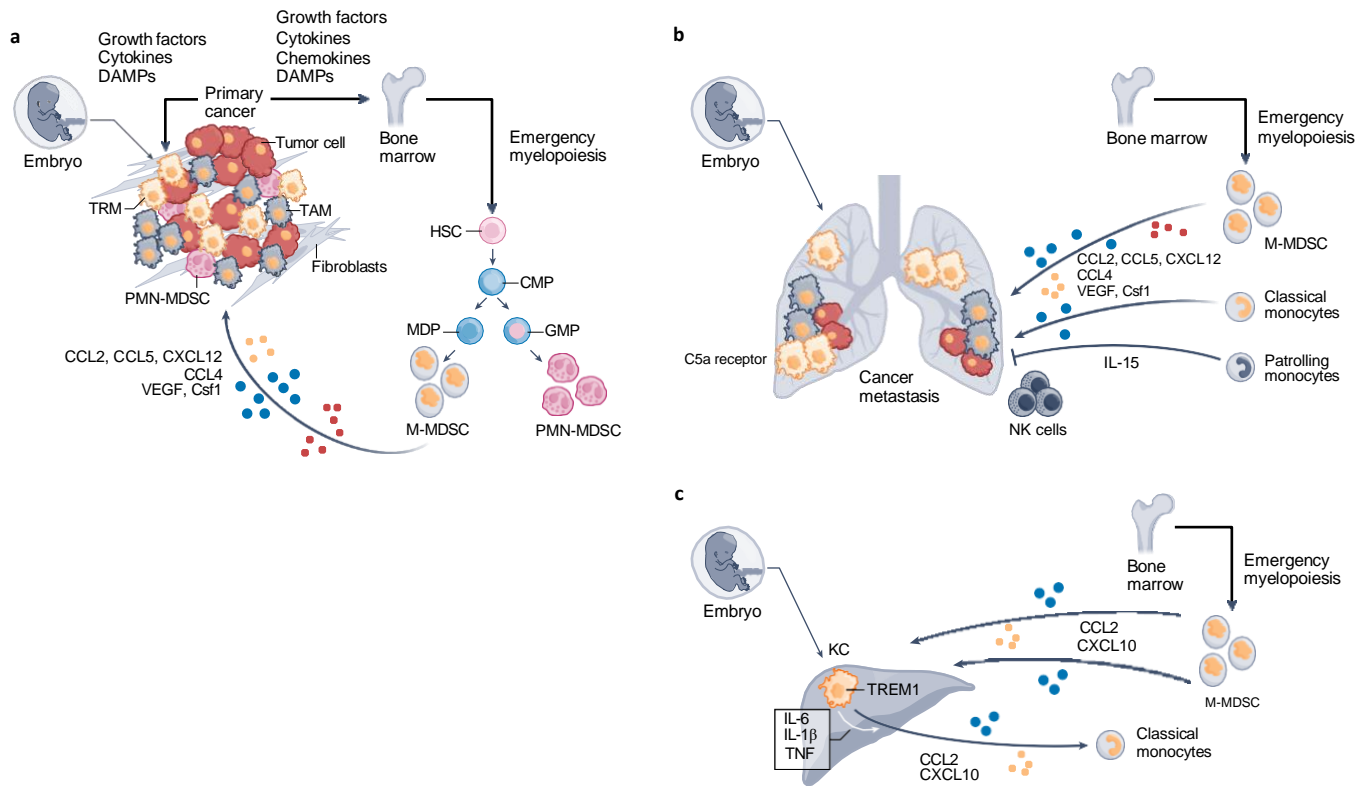


Fig. 1 | In tumor-bearing hosts, tumor-released factors drive increased production and output of classical Ly6C^+ monocytes and MDSCs from myeloid progenitors of the BM. **a–c**, After egress, BM-derived monocytes, M-MDSCs, and PMN-MDSCs are recruited to the primary tumor (**a**) and metastasis sites (**b,c**) through chemotactic factors produced by cancer cells, tumor-associated fibroblasts, and TAMs. After localizing at the tumor, BM-derived monocytes and M-MDSCs differentiate to TAMs and promote cancer growth. In contrast to classical monocytes that give rise to TAMs, nonclassical patrolling monocytes seem to have a protective role against cancer progression because they accumulate at the sites of lung metastasis, produce IL-15, and orchestrate the recruitment and activation of NK cells, thereby inhibiting cancer invasion and growth. During cancer evolution, tissue-resident macrophages (TRMs) derived from embryonic hematopoietic organs, such as alveolar macrophages in the lung (**b**) and KCs in the liver (**c**) are the first to be subject to the effects of cancer-produced soluble factors, as well as other TME insults (**a**). They undergo early inflammatory changes, assist in the recruitment of BM-derived monocytes, and contribute to the generation of TAMs. In metastatic sites, TRMs might foster formation of the premetastatic niche (**b,c**). C5a receptor, complement receptor 5a. Growth factors: M-CSF, GM-CSF; cytokines: IL-6, IL-1, IL-8; chemokines: CCL2, CCL5, CXCL12, CCL4; DAMPs: DNA, RNA, exosomes, uric acid, ATP, metabolites. HSC, hematopoietic stem cell; MDP, monocyte-DC progenitor.

those mediated by PAMPs, lead to a transient expansion and differentiation of myeloid progenitors to mature monocytes and granulocytes to protect the host. In contrast, during emergency myelopoiesis driven by continuous low-level stimulation mediated by cancer-derived growth factors, cytokines, and DAMPs, myeloid progenitors undergo modest expansion, with hindered differentiation leading to the accumulation of myeloid cells with immunosuppressive and tumor-promoting properties, named myeloid-derived suppressor cells (MDSCs). In mice, MDSCs consist of two major subsets, $\text{CD11b}^+\text{Ly6C}^{\text{hi}}\text{Ly6G}^-$ monocytic MDSCs (M-MDSCs) and $\text{CD11b}^+\text{Ly6C}^{\text{lo}}\text{Ly6G}^+$ polymorphonuclear MDSCs (PMN-MDSCs), which have a similar morphology and phenotype to normal monocytes and neutrophils, respectively. In humans, M-MDSCs are identified as $\text{CD11b}^+\text{CD14}^-\text{CD15}^+/\text{CD66b}^+$, and PMN-MDSCs as $\text{CD14}^+\text{CD15}^+\text{HLA-DR}^{\text{lo}}$ myelocytes (reviewed in ref. ³⁰). After egress from the BM, monocytes (or M-MDSCs) are recruited to the TME via chemokines of the CC and CXC families, such as CCL2, CCL5, and CXCL12 (Fig. 1a)³¹ that are produced by cancer cells early during tumorigenesis.

The recruitment and retention of BM-derived monocytes to metastatic sites are primarily regulated by the CCR2–CCL2 axis^{32,33} (Fig. 1b,c). As determined by studies in xenograph metastatic models, BM-derived human monocytes also migrate to tumor sites in a CCR2-dependent manner, where they differentiate to macrophages

and promote cancer growth³⁴. Although CCL2-mediated recruitment is dominant, factors such as the inducer of vascular growth, VEGFA, and Csf1 can also mediate recruitment of monocytes and conversion to TAMs^{35,36}. CCL5 may stimulate monocyte production and recruitment to tumors³⁷, whereas CCL4 (ref. ³⁸) produced by TAMs can recruit BM-derived monocytes.

Nonclassical ‘patrolling’ monocytes, identified as $\text{CX3CR1}^{\text{hi}}\text{Ly6C}^-$ in mice and $\text{CX3CR1}^{\text{hi}}\text{CD14}^{\text{dim}}\text{CD16}^+$ in humans, are also generated in the BM. Patrolling monocytes have a protective role against cancer progression and mediate metastasis immunosurveillance^{39,40}. In the tumor-bearing host, patrolling monocytes accumulate at the sites of metastasis and orchestrate IL-15-mediated recruitment and activation of NK cells, thereby inhibiting cancer invasion and growth (Fig. 1b)⁴⁰. Mice lacking patrolling monocytes have impaired activation and accumulation of NK cells and develop multiple pulmonary metastases⁴⁰. Although patrolling monocytes are initially protective, the effect of BM-derived TAMs gradually becomes dominant, resulting in progression of primary and metastatic tumors^{33,39}. Under these conditions, inhibiting recruitment of BM-derived monocytes can reduce both primary tumor and metastatic burden³⁴.

Tissue-resident macrophages

All healthy tissues harbor TRMs, which support defense, homeostasis, maintenance of tissue integrity, and wound healing⁵. During

cancer evolution, TRMs are the first to be subject to the effects of cancer-produced soluble factors and other TME insults. They undergo early inflammatory changes, assist the recruitment of BM-derived monocytes and contribute to the generation of TAMs. The involvement of TRMs in tumor progression is distinct in various cancer types. For example, in a breast cancer mouse model, the numbers of TRMs progressively decreased over time, while the numbers of TAMs generated from BM-derived monocytes concomitantly increased. In this context, ablation of TRMs did not impact tumor growth, whereas ablation of circulating monocytes resulted in the reduction of tumor size⁴¹. In contrast, in a mouse model of pancreatic cancer, TRMs expanded during tumor progression and acquired a transcriptional profile favoring a profibrotic program typical of pancreatic adenocarcinoma, which was not disrupted by depletion of BM-derived macrophages but was reversed by depletion of TRMs⁴². In a lung cancer model, macrophages of both origins contributed to tumor growth and progression⁴³. Thus, the role of TRMs in cancer growth seems to be organ-specific.

Conversion of BM-derived monocytes to TAMs

Recruitment of myeloid cells in tumors and subsequent conversion to TAMs requires integrin activation (Fig. 2). Cytokines and chemokines produced in the TME, including GM-CSF, IL-1 β , SDF1 α , VEGF, CSF1, and CCL2, promote emergency myelopoiesis, leukocyte trafficking to tumor, and extravasation by activating receptor-mediated signaling events that induce inside-out conformational changes of α _v β 1 integrin. Blockade of this pathway inhibits tumor inflammation and growth⁴⁴. Specifically, IL-1 β , SDF1 α , and VEGF activate G-protein-coupled receptors (GPCRs), receptor tyrosine kinases (RTKs), and TLR/IL-1R, leading to activation of Ras and its downstream target phosphoinositide 3-kinase γ (PI3K γ), the PI3K isoform predominantly expressed in myeloid cells⁴⁵. PI3K γ activates Bruton's tyrosine kinase (BTK), phospholipase C (PLC), and RasGrp/CalDAG-GEFs, leading to the activation of Rap1 and its downstream effector RIAM⁴⁵. The Rap1-RIAM module regulates reorganization of cytoskeletal actin, talin conformational changes, and integrin activation^{46,47}, guiding leukocyte adhesion and migration⁴⁸. Inhibition of this signaling cascade can decrease monocyte recruitment and TAM accumulation in tumors⁴⁵. Activation of PI3K γ mediates generation of TAMs by suppressing the activation of the transcription factor NF- κ B and promoting c/EBP β -mediated signaling⁴⁹. However, the integrin α _v β 2 (CD11b/CD18), which is abundantly expressed in myelocytes does not appear to have any impact in the recruitment of monocytes to tumors and generation of TAMs⁵⁰. Global deletion of CD11b in *Itgam*^{-/-} mice did not compromise the ability of myeloid cells to accumulate in tumors, but CD11b-deficient myeloid cells or wild-type myeloid cells treated with a CD11b blocking antibody in vitro had an elevated expression of immunosuppressive genes and a simultaneous decrease of immunostimulatory genes⁵⁰, suggesting that loss of α _v β 2 function might compromise the properties of myeloid cells by unidentified mechanisms.

Although it is difficult to define when the recruited monocytes become TAMs, it is well-documented that tissue engagement changes the transcriptional profile of the recruited monocytes⁵¹. The precise mechanisms that drive this conversion are incompletely understood. It has been proposed that hypoxia-mediated enhancement of CD45 phosphatase activity in M-MDSCs alters activity of STAT3 and promotes TAM differentiation⁵². The enhanced phosphatase activity is induced by disruption of CD45 protein dimerization, an effect mediated by the sialic acid in the TME⁵². TAMs display distinct transcriptional profiles compared with circulating monocytes. Distinct transcriptional profiles have also been identified between TAMs and macrophages residing in adjacent healthy tissues⁵¹. In mouse models of breast cancer with lung metastatic disease, transcriptomics studies showed that newly recruited

BM-derived monocytes convert into a precursor Ly6C^{hi}CD11b^{hi} cell population, which produces the chemokine ligand CCL3, and recruit metastasis-facilitating macrophages³².

It is possible that subsets of TAMs within the same tumor have unique functional roles in supporting cancer growth (Fig. 2). A subset of TAMs that express the angiopoietin receptor Tie2 accumulate in the perivascular areas, where they support angiogenesis, tumor growth, and tumor relapse after chemotherapy^{53,54}. A distinct population of TAMs are recruited through the semaphorin 3A (Sema3A)-neuropilin-1 (Nrp1) pathway to avascular, hypoxic tumors areas, where they acquire pro-angiogenic and immunosuppressive properties. After accumulation in hypoxic niches, Nrp1 is downregulated and Sema3A entraps TAMs locally through plexinA1-plexinA4-mediated stop signals²⁶. The pro-angiogenic properties of TAMs in the hypoxic niches also rely on their metabolism. REDD1, a negative regulator of mTOR that is upregulated in TAMs in hypoxic niches, prevents glycolysis and promotes the formation of abnormal blood vessels, contributing to tumor metastasis²⁷. Other TAMs differentiate into metastasis-associated macrophages that are able to escort cancer cells at distal sites and facilitate their engraftment to form metastasis³⁴. Conversely, IRF8, a transcription factor with a decisive role in monocyte and moDC lineage commitment, imprints a macrophage program that prevents metastasis⁵⁵. Certain TAM subsets produce proteases such as metalloproteases (MMPs), which promote not only tissue remodeling, facilitating monocyte migration, but also cancer cell migration, intravasation, and relocation in distal sites, initiating metastatic foci⁵⁶. The differential molecular properties of the spatially distinct subsets of TAMs might represent attractive targets for therapeutic intervention.

BM-derived macrophages and TRMs in primary and metastatic cancer

Since TRMs colonize tissue-specific niches during embryonic development and have self-renewal capacity^{5,13}, they are present in metastases-targeted organs prior to cancer growth and might mediate local tissue alterations that facilitate metastasis. This hypothesis was investigated in depth in a metastatic breast cancer mouse model by looking at the alveolar macrophages⁵⁷, the TRMs of the lung⁵. Alveolar macrophages accumulated in premetastatic lungs through complement C5a receptor-mediated proliferation, reduced the number and maturation of lung dendritic cells, suppressed type 1 helper T (T_H1) responses and enhanced lung metastases (Fig. 1b). Depletion of alveolar macrophages reversed immunosuppression, strengthened local T_H1 cell responses, and reduced metastatic burden. Thus, TRMs might foster the formation of the premetastatic niche and support development of metastatic disease⁵⁷. Consistent with this notion, in three different lung cancer models it was found that BM-derived macrophages facilitated metastatic tumor spreading, whereas TRMs supported proliferation of cancer cells at the primary tumor site⁴³.

In liver Kupffer cells (KCs), the local TRMs, TREM-1-mediated activation results in secretion of proinflammatory cytokines, including IL-6, IL-1 β , TNF, CCL2, and CXCL10, leading to inflammatory liver injury and subsequent carcinogenesis (Fig. 1c)⁵⁸. CCL2 is highly expressed in individuals with hepatocellular carcinoma (HCC), whereas blockade of the CCL2-CCR2 pathway in a mouse model of HCC prevented TAM accumulation and tumor growth, suggesting a role for KCs in regulating the immunological TME profile in HCC⁵⁹. In addition, KCs might protect against metastasis of colorectal carcinoma (CRC) to the liver, as indicated by the increased number of metastases in livers of KC-deficient mice⁶⁰.

Some of the most informative studies regarding the contribution of TRMs and BM-derived macrophages in primary versus metastatic cancer growth have been generated in the context of brain cancer. In the homeostatic central nervous system (CNS), innate immunity is solely accomplished by parenchymal microglia, and to a

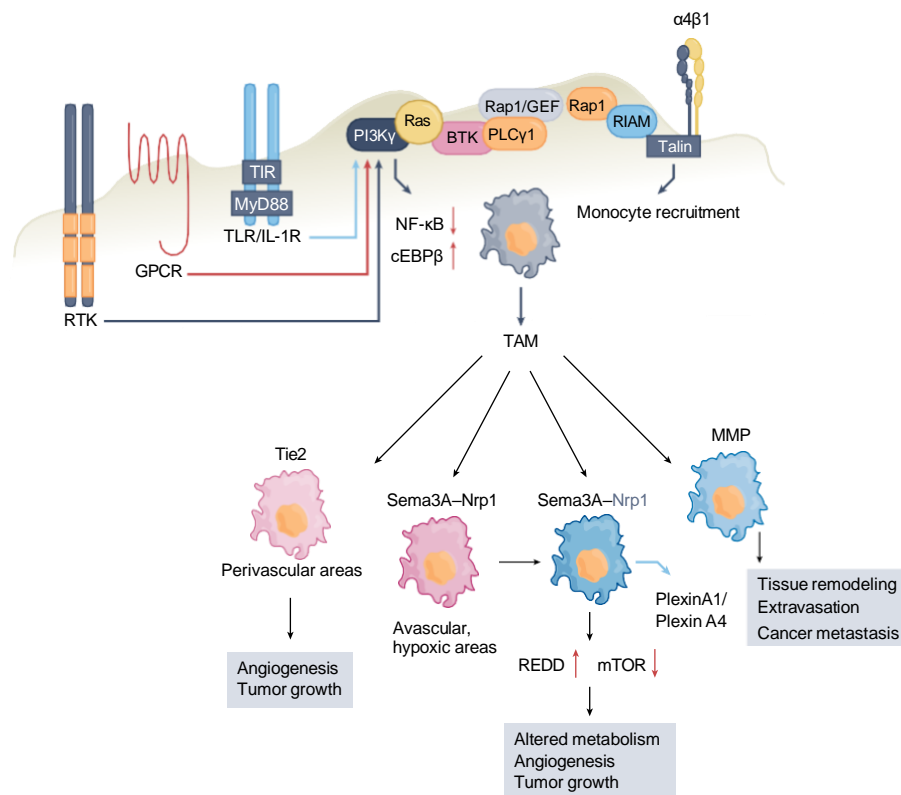


Fig. 2 | Recruitment of BM-derived monocytes in tumors and subsequent conversion to TAMs requires activation of $\alpha_4\beta_1$ integrin. IL-1 β , SDF1 α , and VEGF activate receptor tyrosine kinases (RTK), G-protein-coupled receptors (GPCR), and TLR/IL-1R, leading to activation of Ras and its downstream target phosphoinositide 3-kinase γ (PI3K γ), initiating a signaling cascade that leads to integrin activation. Activation of PI3K γ inhibits signaling through the transcription factor NF- κ B while promoting *c/EBP β* -mediated signaling leading to the generation of immunosuppressive TAMs. Various subsets of TAMs within the same tumor have unique functional roles in supporting cancer growth. TAMs expressing the angiopoietin receptor Tie2 accumulate at the perivascular areas, where they support angiogenesis and tumor growth. TAMs are recruited to avascular, hypoxic tumor areas through the semaphorin 3A (Sema3A)–neuropilin-1 (Nrp1) pathway, where Nrp1 is downregulated and Sema3A entraps TAMs locally through plexinA1–plexinA4-mediated stop signals. Upregulation of REDD1, a negative regulator of mTOR, prevents glycolysis and promotes angiogenesis. Certain TAM subsets produce MMPs, which promote tissue remodeling, thereby facilitating monocyte and cancer cell migration, intravasation, and metastasis.

lesser degree by border-associated macrophages (BAMs). Microglia are a unique population of myeloid mononuclear phagocytic cells that originate during embryogenesis from erythromyeloid progenitors in the yolk sac^{11,61} and are divergent from BAMs (reviewed in ref. ⁶²). Microglia play a dynamic role in brain wiring during CNS development by phagocytosing apoptotic neurons and by selectively remodeling synapses. Microglia accomplish these tasks by surveying the environment, sensing changes in brain function and physiology, and responding accordingly⁶³. Genes representing the microglial sensing system are well-defined^{64,65}, and responses of microglia to pathologies vary widely, depending on their location within the CNS. High-resolution single-cell RNA-sequencing studies of mouse and human microglia indicated the existence of highly heterogeneous populations of microglia under normalcy⁶⁶.

Primary brain cancers (which originate within the CNS) are composed of histopathologically and molecularly distinct neoplasms⁶⁷, and their tumor immune microenvironment demonstrates remarkable heterogeneity⁶⁸. Glioblastoma, the most common primary malignant brain cancer, is molecularly well characterized. Glioblastoma is considered highly immunosuppressive, with minimal cytotoxic lymphoid infiltration and the presence of considerable numbers of suppressive myeloid cells, such as macrophages, microglia, and MDSCs. Microglia, BAMs, and BM-derived TAMs constitute up to 40% of the tumor cellular composition. Microglia and monocyte-derived TAMs are

heterogeneous populations in terms of their localization within the tumor and their functions. Extensive transcriptional analyses in mouse brain tumors indicated that microglia and TAMs share both proinflammatory M1-like and anti-inflammatory M2-like phenotypes⁶⁹; in human glioblastoma, they additionally display expression profiles of non-polarized M0 macrophages⁷⁰.

Detailed analyses of the immune populations in primary and metastatic human brain tumors^{14,15} have found that glioblastomas are populated by TRMs, microglia, and BM-derived TAMs, whereas metastatic brain tumors are populated predominantly by BM-derived TAMs, consistent with findings in a mouse model of proneural glioma⁷¹. In addition, the TME of human glioblastoma imposed a distinct pattern of gene regulation on microglia and BM-derived macrophages compared with that found in metastatic tumors^{14,15}. These findings provide evidence for tumor-specific roles in the transcriptional imprinting of recruited monocyte-derived and TRMs in tumors and set the basis for further investigation.

Macrophage diversity in cancer

The inherited ability of macrophages to develop distinct adaptations to slight alterations of microenvironmental stimuli, including an intratumoral gradient of nutrients, metabolites, or oxygen, leads to a significant diversity of TAMs among different cancer types, but also within the same tumor⁷². The diversity of TAMs was previously streamlined in the simplified concept that TAMs have a

polarization program resembling M2 macrophages and are skewed away from M1-polarized phenotype³. Classical M1 polarization has been defined by the expression of CD80, CD86, MHCII, iNOS, and CD68, correlated with the tumoricidal function of TAMs that could engulf cancer cells and recruit T cells. Conversely, M2 polarization has been characterized by the expression of CD206, CD204, VEGF, CD163, and Arg-1 and is associated with an immune quiescent profile³. The M1–M2 programs were thought to rely mainly on metabolism, because proinflammatory M1 macrophages are supported by glycolysis whereas anti-inflammatory M2 macrophages utilize mainly fatty acid oxidation (FAO)⁷³. Although this concept is no longer considered appropriate, most studies continue to utilize M1–M2-associated markers for characterization of TAMs, because there is extensive experience based on the correlation between their expression and prognosis in tumor models and human cancers^{25,74}. It is becoming increasingly clear that macrophage metabolism is much more complex than the selective utilization of glucose or fatty acids as an energy source. It is now known that lipid utilization goes beyond fatty acid catabolism in FAO, and has an essential role in the ability of TAMs to function as potent APCs. Cancer-produced β -glucosylceramide drives reshuffling of lipid composition on the ER membrane, leading to IRE1-dependent ER stress responses⁷⁵. The co-engagement of the IRE1–XBP1 and IRE1–STAT3 pathways during the ER stress response promoted pro-tumorigenic polarization and pro-survival properties of TAMs. Conversely, targeting IRE1–XBP1 and IRE1–STAT3 signaling or preserving lipid composition of the ER membrane by genetic and pharmacological approaches diminished the pro-tumorigenic ability of TAMs and inhibited tumor progression⁷⁵. Thus, metabolic adaptations with significant impact on TAM function depend on lipid composition in a manner independent of their utilization as an energy source.

The significance of nutrients in TAM diversity is highlighted by the role of glutamine, which is indispensable for cellular functions, such as nucleotide and amino acid production, redox balance, and protein glycosylation. Small-molecule inhibitor blocking of glutamine metabolism reduced tumor growth and metastases in a mouse model of breast cancer by enhancing macrophage activation and inhibiting MDSC generation⁷⁶. Targeting glutamine metabolism with an inhibitor of the enzyme glutamine synthetase, which generates glutamine from glutamate, converted TAMs into effector APCs, which mediated potent anti-tumor function in three highly metastatic mouse models⁷⁷. An integrated high-throughput transcriptional-metabolic profiling showed that an immunosuppressive M2-like macrophage profile is supported by glutamine catabolism and is compromised by glutamine deprivation⁷⁸. Consistent with these findings, production of α -ketoglutarate (α KG) via glutaminolysis is important for M2-like activation of macrophages, including engagement of FAO and epigenetic reprogramming of M2 genes⁷⁹. This M2-promoting mechanism is further modulated by a high α KG/succinate ratio, whereas a low ratio strengthens the M1-like phenotype⁷⁹. The immunometabolic properties of TAMs correlate not only with TAM functional diversity, but also cancer prognosis. For example, diversity of MHCII^{lo} and MHCII^{hi} TAM subsets correlate with distinct metabolic signatures and abilities to utilize lactate, a metabolite that is abundantly present in the TME. In MHCII^{lo} TAMs, lactate supports oxidative metabolism, increases L-arginine metabolism, and enhances their T cell suppressive capacity⁸⁰. These observations underline the significance, and the complexity, of targeting the metabolic function of the diverse TAM subsets for therapeutic purposes.

During the past few years, progress in genomics, single-cell RNA-sequencing, and time-of-flight (CyTOF) technologies has revealed the previously unsuspected diversity of TAMs. Macrophages can now be classified into multiple distinct clusters based on distinct combinations of genes expressed. Spatial distribution of TAMs correlates with their distinct gene profiles and specific

functional properties in many cancers, including lung, renal, brain breast, and ovarian cancer, head and neck carcinoma, melanoma, and colorectal cancer^{14,15,72,81–84}. The evolution of such technologies might guide the development of new therapies targeting unique properties of tumorigenic TAMs⁸⁵.

TAMs in inflammation and immunosuppression

The association between inflammation and cancer has been extensively documented and is currently considered an integral component of cancer evolution (reviewed in refs. ^{86,87}). Tumors were proposed to behave as wounds that do not heal⁸⁸; indeed, several features of tissue injury and healing identified in wounds characterize the TME, including infiltration by inflammatory cells such as neutrophils, monocytes, and macrophages, tissue remodeling, and enhanced coagulation⁸⁸. However, in contrast with the sequential process of tissue injury, inflammation, and healing observed in wounds, features that characterize injury and healing co-exist and persist in the TME⁸⁶. Cancer-related inflammation is likely initiated by soluble factors, such as hematopoietic growth factors (for example, M-CSF, GM-CSF), cytokines (for example, IL-6, IL-1, IL-8), and chemokines (for example, CCL2, CCL5, CXCL12) produced as a consequence of the oncogenes whose expression is induced by driver mutations (Fig. 3), including KRAS^{G12D} (ref. ⁸⁹), p53 (ref. ⁹⁰), BRAF^{V600E} (ref. ⁹¹), and BRCA1 (ref. ⁹²).

An additional mechanism responsible for cancer-related inflammation involves the generation of DAMPs that are produced by cancer cells owing to rapid replication and apoptosis, nutrient starvation, and hypoxia (Fig. 3). These DAMPs are recognized by PRRs expressed by monocytes, macrophages, other cells of the innate immune system, and cancer cells, and initiate proinflammatory cascades. Exosomes released from cancer, containing tumor DNA, recognized by STING and AIM2 (refs. ^{93,94}), or RNA, recognized by TLR3 (ref. ⁹⁵), induce monocyte recruitment to the primary tumor and the metastatic niche⁹⁶. These pathways, along with NLRP3, which recognizes ATP⁹⁷, induce production of inflammatory cytokines and chemokines, recruiting T cells. At the early stages of the anti-tumor immune response, T cells can successfully eliminate cancer by cell-mediated killing, which in turns generates a third level of inflammatory mediators in the TME. The cancer-produced cytokines and DAMPs also act on the BM progenitors to induce emergency myelopoiesis, giving rise to immunosuppressive PMN-MDSCs and M-MDSCs, the latter being recruited into the tumor to become TAMs (Fig. 3)⁵².

Paradoxically, the proinflammatory pathways that promote the cancer-related inflammation and generation of immunosuppressive TAMs are the same mediators of protective proinflammatory immune responses in macrophages against pathogens, such as those regulated by type I IFN induced by viral infections⁹⁸. These pathways also have an instrumental role in the recruitment and retention of CD8⁺ T cells in tumors, an outcome that can be recapitulated by treatment with type I IFN or DNA-damaging chemo- and radiotherapies⁹⁹, but can be hijacked by the tumor to initiate cancer-related inflammation and immunosuppression¹⁰⁰. Notch signaling, which is involved in myeloid cell development and hematopoiesis and is needed for the differentiation of M1-like effector macrophages^{101,102}, is also involved in the differentiation of TRMs into TAMs⁴¹. PI3K, a critical regulator of effector immune responses, acts as a mediator of cancer-related inflammation⁴⁹.

Although the precise mechanisms of this paradox remain poorly understood, activation of proinflammatory pathways in TAMs might concomitantly lead to increased expression of inhibitory receptors and ligands, thereby favoring immunosuppression (Fig. 3). After phagocytosis of cancer cells by macrophages, AIM2, which is activated by tumor DNA, cleaves cGAS and upregulates PD-L1 and IDO, overriding the anti-tumor function of macrophages⁹⁴. In response to TLR signaling or phagocytosis of cancer cells, TAMs

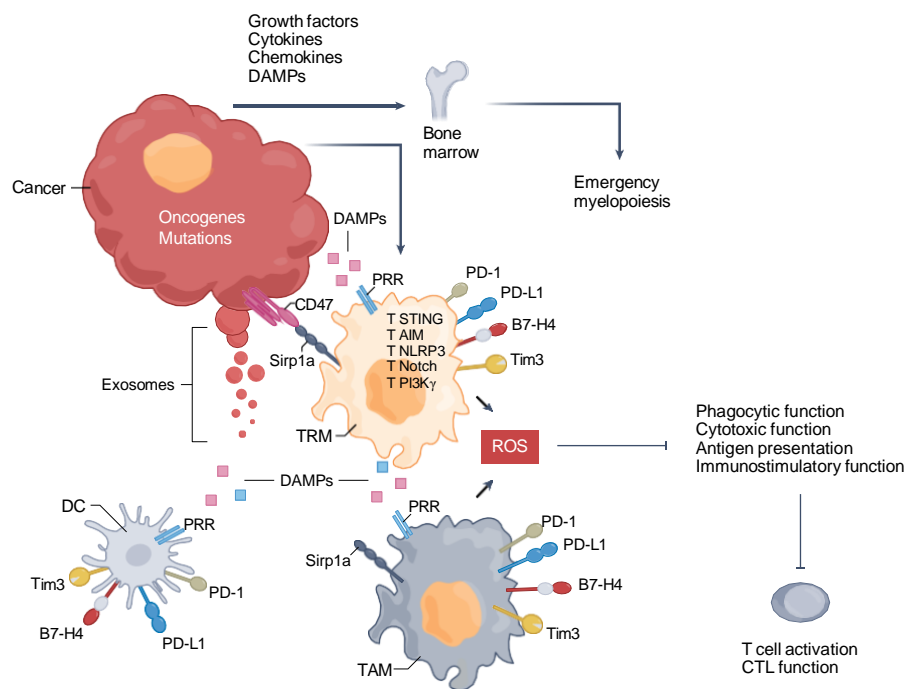


Fig. 3 | Cancer-related inflammation is initiated by hematopoietic growth factors, cytokines, and chemokines produced by cancer cells as a consequence of oncogene-mediated malignant transformation. There is proinflammatory activation from DAMPs produced by cancer cells due to rapid replication and apoptosis, nutrient starvation, and hypoxia. Exosomes released from cancer cells, containing tumor DNA or RNA, contribute to the proinflammatory TME. Cytokines activate immune and cancer cells, whereas DAMPs are recognized by pattern recognition receptors (PRRs) expressed by macrophages and other cells of the innate immune system, such as dendritic cells (DCs), as well as cancer cells, to initiate proinflammatory cascades. In response to inflammatory activation, TAMs express Tim3, Tim4, PD-1, and PD-L1 checkpoint inhibitors, which can inhibit macrophage functions and synergize with the Sirp1a–CD47 pathway to inhibit phagocytosis of cancer cells. Cancer-produced cytokines and DAMPs also act on BM progenitors through cytokine and growth factor receptors and PRRs to induce myelopoiesis, which gives rise to immature immunosuppressive PMN-MDSCs and M-MDSCs, the latter being recruited into the tumor to become TAMs. CTL, cytotoxic T lymphocyte.

also express Tim3, Tim4, PD-1, and PD-L1, which can inhibit macrophage functions including phagocytosis, inflammasome activation, and production of effector cytokines^{18–21,103}, and synergize with Sirp1a, which transmits phagocytosis-inhibitory signals after engagement by CD47 (ref. ¹⁰⁴). Such mechanisms might perpetuate proinflammatory activation but impaired effector function of TAMs while inhibiting T cell activation through co-inhibitory receptors and TAM-generated reactive oxygen species (Fig. 3). Macrophages might be subjected to PD-L1-mediated inhibition as macrophage-specific blockade of PD-L1 can induce macrophage activation and proliferation¹⁰⁵.

Expression of PD-1 is induced by TLR signaling in myeloid cells and is correlated with impaired M1-like polarization¹⁰⁶. In the context of infection, PD-1 expression in macrophages suppresses the innate inflammatory response to sepsis¹⁰⁷ and inhibits the phagocytosis of *Mycobacterium tuberculosis*¹⁰⁸. PD-1 upregulation in TAMs during tumor progression compromises their phagocytic potency in a mouse model of colon cancer¹⁸. In peripheral blood monocytes from individuals with chronic lymphocytic leukemia (CLL), PD-L1- or antibody-mediated triggering of PD-1 hampers BTK signaling, glycolysis, and phagocytosis²⁰. Conversely, selective PD-1 ablation¹⁹ or macrophage-specific PD-1 blockade¹⁸ in murine tumor models, or PD-1 blockade in monocytes from people with CLL²⁰, significantly enhance anti-tumor responses. Thus, checkpoint inhibitors have an active role in the immunosuppressive properties of TAMs, but it is poorly understood under what conditions, and in which TAM subsets, these inhibitory mediators are expressed and operate. Studies in this direction might provide opportunities for tumor immunotherapy.

Resolution of inflammation

An attractive hypothesis regarding the mechanisms involved in TAM-mediated inflammation in cancer is that unidentified modifications might occur in the regulation of proinflammatory pathways during cancer evolution. According to the concept of cancer immunoeediting, the immune system can control cancer development during the phase of immunosurveillance and elimination, when cancer cells are successfully recognized and cleared (Fig. 4)¹⁰⁹. Macrophages have a central role in this process by mediating phagocytosis and clearance of cancer cells¹¹⁰ and the presentation of cancer neoantigens to T cells². Under immune-mediated pressure, cancer cells undergo immunoeediting, which results initially in an immune equilibrium phase and, subsequently, full bypassing of the mechanisms of antigen recognition and anti-tumor immune response, leading to tumor escape¹⁰⁹. It is possible that, during the immune equilibrium phase, the properties of TAMs gradually change as their proinflammatory pathways are increasingly activated (Fig. 4), but lose their efficacy. For example, PRR signaling, which is controlled by posttranslational, metabolic, and epigenetic modifications^{111,112}, might operate differently during immune equilibrium and immune escape than during elimination. In support of this hypothesis, only acute engagement of pro-immune inflammatory pathways during immune escape can override the continuing cancer-promoting inflammation and elicit anti-tumor immunity¹¹³. Under such conditions, inflammasome activation with oxidized phospholipids can induce strong and long-lasting protection against cancer and eradicate various tumors that are resistant to standard checkpoint immunotherapy¹¹³.

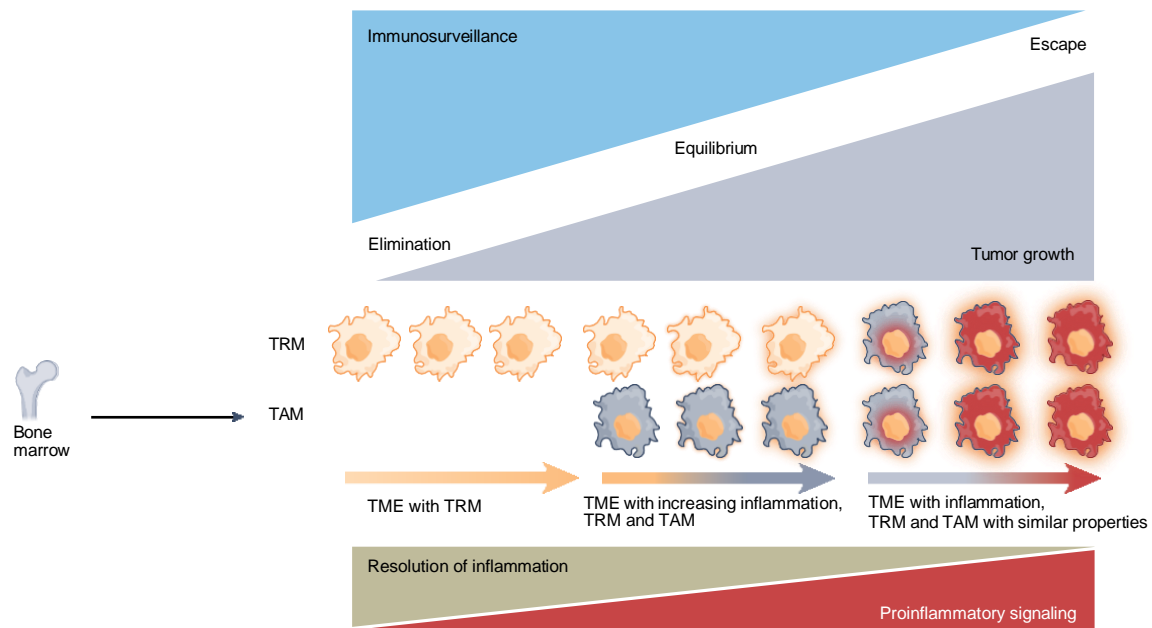


Fig. 4 | Changes of TAMs during cancer immunoeediting. During the elimination phase, macrophages eliminate cancer cells by phagocytosis and activation of anti-tumor T cell responses by presentation of tumor-associated antigens, whereas these immune functions are compromised during cancer progression to immune equilibrium and escape. While TRMs predominate during elimination, BM-derived TAMs increasingly enter the tumor during the immune equilibrium phase, leading to increasing local inflammation. During the immune escape phase, in response to tissue residence and cues of the TME, TRMs and BM-derived TAMs acquire similar properties, characterized by enhanced proinflammatory and diminished pro-resolving signaling.

Because macrophages have a physiological role in mediating resolution of inflammation and promoting tissue remodeling and healing², it is possible that the cancer-promoting proinflammatory effects of TAMs are mediated by impaired mechanisms of inflammation resolution (Fig. 4). During physiologic immune responses, nuclear hormone receptors program an anti-inflammatory and pro-resolving function in macrophages¹¹⁴. The nuclear hormone receptor PPAR γ has an important role in this process and mediates resolution of inflammation by inducing expression of the scavenger receptor CD36 and the nuclear hormone receptor LXR^{115,116}. Notably, LXR activation can suppress cancer growth in multiple murine tumor models¹¹⁷. Macrophages also promote inflammation resolution by production of pro-resolving cytokines. Following tissue injury or infection, eicosanoids initiate the inflammation process. The prostaglandins PGE2 and PGI2, which are involved in vasodilation, and the leukotriene LTB4, which is involved in chemotaxis and adhesion, stimulate the recruitment of neutrophils as first responders. Subsequently, lipoxins, resolvins, protectins, and maresins, collectively called specialized pro-resolving mediators (SPMs), are produced¹¹⁸. Switching from eicosanoids to SPMs mediates a ‘stop signal’ to the acute inflammatory response. SPMs counteract the proinflammatory mediators and stimulate the recruitment of monocytes, which become resolving macrophages, clear apoptotic cells by efferocytosis and promote antigen presentation and engagement of adaptive immune responses¹¹⁹. In a mouse tumor model, debris of various cancer cell types killed by chemotherapy or targeted therapy induced production of proinflammatory cytokines by TAMs and tumor growth, whereas administration of SPMs induced inflammation resolution, T cell activation, and suppression of cancer growth¹²⁰. Thus, a plausible scenario might be that, during the immune equilibrium phase, the anti-inflammatory pathways of TAMs are progressively suppressed and eventually lose efficacy during cancer immune escape (Fig. 4). A spatiotemporally aberrant and unconcerted activation of proinflammatory and pro-resolving mechanisms of TAMs might have a central role in pro-tumorigenic inflammation.

Concluding remarks

Macrophages have an essential and indispensable role in homeostasis and immunity, but lose their protective functions and become TAMs in the context of cancer. TAMs arise from TRMs localized at the tumor site and BM-derived monocytes that are recruited to tumors. TAMs provide a protective niche for cancer growth and invasion at primary and metastatic sites. TAMs are highly heterogeneous, and the significance and therapeutic potential of their diversity are evolving. Although TAMs might have either a supportive or a suppressive role in anti-tumor immunity, they most frequently enhance tumor growth by promoting angiogenesis and immunosuppression through hijacking proinflammatory pathways naturally programmed to provide protective immune responses. Altered signaling and metabolic properties support the immunosuppressive functions of TAMs. The immunological, biochemical, and metabolic aberrations can serve as targets of novel precision therapies for reprogramming and switching macrophage function from pro-tumorigenic TAMs to anti-tumorigenic and protective APCs. On this road, the great challenge remains of spatially guiding such interventions to achieve tumor-specific outcomes without compromising responses of healthy innate and adaptive immune cells.

Received: 19 January 2022; Accepted: 10 June 2022;

Published online: 25 July 2022

References

1. Watanabe, S., Alexander, M., Misharin, A. V. & Budinger, G. R. S. The role of macrophages in the resolution of inflammation. *J. Clin. Investig.* **129**, 2619–2628 (2019).
2. Hirayama, D., Iida, T. & Nakase, H. The phagocytic function of macrophage-enforcing innate immunity and tissue homeostasis. *Int. J. Mol. Sci.* **19**, 92 (2017).
3. Martinez, F. O., Sica, A., Mantovani, A. & Locati, M. Macrophage activation and polarization. *Front. Biosci.* **13**, 453–461 (2008).
4. Wynn, T. A., Chawla, A. & Pollard, J. W. Macrophage biology in development, homeostasis and disease. *Nature* **496**, 445–455 (2013).
5. Ginhoux, F. & Guilliams, M. Tissue-resident macrophage ontogeny and homeostasis. *Immunity* **44**, 439–449 (2016).

6. Carlin, L. M. et al. Nr4a1-dependent Ly6C_{low} monocytes monitor endothelial cells and orchestrate their disposal. *Cell* **153**, 362–375 (2013).
7. Auffray, C. et al. Monitoring of blood vessels and tissues by a population of monocytes with patrolling behavior. *Science* **317**, 666–670 (2007).
8. Geissmann, F. et al. Development of monocytes, macrophages, and dendritic cells. *Science* **327**, 656–661 (2010).
9. Wang, Y. et al. IL-34 is a tissue-restricted ligand of CSF1R required for the development of Langerhans cells and microglia. *Nat. Immunol.* **13**, 753–760 (2012).
10. Wei, S. et al. Functional overlap but differential expression of CSF-1 and IL-34 in their CSF-1 receptor-mediated regulation of myeloid cells. *J. Leukoc. Biol.* **88**, 495–505 (2010).
11. Ginhoux, F. et al. Fate mapping analysis reveals that adult microglia derive from primitive macrophages. *Science* **330**, 841–845 (2010).
12. Ginhoux, F. & Merad, M. Ontogeny and homeostasis of Langerhans cells. *Immunol. Cell Biol.* **88**, 387–392 (2010).
13. Schulz, C. et al. A lineage of myeloid cells independent of Myb and hematopoietic stem cells. *Science* **336**, 86–90 (2012).
14. Klemm, F. et al. Interrogation of the microenvironmental landscape in brain tumors reveals disease-specific alterations of immune cells. *Cell* **181**, 1643–1660 (2020).
15. Friebel, E. et al. Single-cell mapping of human brain cancer reveals tumor-specific instruction of tissue-invading leukocytes. *Cell* **181**, 1626–1642 (2020).
16. Robinson, A., Han, C. Z., Glass, C. K. & Pollard, J. W. Monocyte regulation in homeostasis and malignancy. *Trends Immunol.* **42**, 104–119 (2021).
17. Mantovani, A., Marchesi, F., Jaillon, S., Garlanda, C. & Allavena, P. Tumor-associated myeloid cells: diversity and therapeutic targeting. *Cell Mol. Immunol.* **18**, 566–578 (2021).
18. Gordon, S. R. et al. PD-1 expression by tumour-associated macrophages inhibits phagocytosis and tumor immunity. *Nature* **545**, 495–499 (2017).
19. Strauss, L. et al. Targeted deletion of PD-1 in myeloid cells induces antitumor immunity. *Sci. Immunol.* **5**, eaay1863 (2020).
20. Qorraj, M. et al. The PD-1/PD-L1 axis contributes to immune metabolic dysfunctions of monocytes in chronic lymphocytic leukemia. *Leukemia* **31**, 470–478 (2017).
21. Dixon, K. O. et al. TIM-3 restrains anti-tumour immunity by regulating inflammasome activation. *Nature* **595**, 101–106 (2021).
22. Seo, W. I. et al. Expression of VISTA on tumor-infiltrating immune cells correlated with short intravesical recurrence in non-muscle-invasive bladder cancer. *Cancer Immunol. Immunother.* **70**, 3113–3122 (2021).
23. Lin, H. et al. Host expression of PD-L1 determines efficacy of PD-L1 pathway blockade-mediated tumor regression. *J. Clin. Investig.* **128**, 805–815 (2018).
24. Dangaj, D. et al. Novel recombinant human b7-h4 antibodies overcome tumoral immune escape to potentiate T-cell antitumor responses. *Cancer Res.* **73**, 4820–4829 (2013).
25. Sica, A. et al. Macrophage polarization in tumour progression. *Semin. Cancer Biol.* **18**, 349–355 (2008).
26. Casazza, A. et al. Impeding macrophage entry into hypoxic tumor areas by Sema3A/Nrp1 signaling blockade inhibits angiogenesis and restores antitumor immunity. *Cancer Cell* **24**, 695–709 (2013).
27. Wenes, M. et al. Macrophage metabolism controls tumor blood vessel morphogenesis and metastasis. *Cell Metab.* **24**, 701–715 (2016).
28. Mantovani, A., Marchesi, F., Malesci, A., Laghi, L. & Allavena, P. Tumour-associated macrophages as treatment targets in oncology. *Nat. Rev. Clin. Oncol.* **14**, 399–416 (2017).
29. Manz, M. G. & Boettcher, S. Emergency granulopoiesis. *Nat. Rev.* **14**, 302–314 (2014).
30. Veglia, F., Sanseviero, E. & Gabrilovich, D. I. Myeloid-derived suppressor cells in the era of increasing myeloid cell diversity. *Nat. Rev.* **21**, 485–498 (2021).
31. Mantovani, A. et al. Chemokines in the recruitment and shaping of the leukocyte infiltrate of tumors. *Semin. Cancer Biol.* **14**, 155–160 (2004).
32. Kitamura, T. et al. CCL2-induced chemokine cascade promotes breast cancer metastasis by enhancing retention of metastasis-associated macrophages. *J. Exp. Med.* **212**, 1043–1059 (2015).
33. Ma, R. Y. et al. Monocyte-derived macrophages promote breast cancer bone metastasis outgrowth. *J. Exp. Med.* **217**, e20191820 (2020).
34. Qian, B. Z. et al. CCL2 recruits inflammatory monocytes to facilitate breast-tumour metastasis. *Nature* **475**, 222–225 (2011).
35. Lin, E. Y., Nguyen, A. V., Russell, R. G. & Pollard, J. W. Colony-stimulating factor 1 promotes progression of mammary tumors to malignancy. *J. Exp. Med.* **193**, 727–740 (2001).
36. Lin, E. Y. et al. Vascular endothelial growth factor restores delayed tumor progression in tumors depleted of macrophages. *Mol. Oncol.* **1**, 288–302 (2007).
37. Ban, Y. et al. Targeting autocrine CCL5–CCR5 axis reprograms immunosuppressive myeloid cells and reinvigorates antitumor immunity. *Cancer Res.* **77**, 2857–2868 (2017).
38. De la Fuente Lopez, M. et al. The relationship between chemokines CCL2, CCL3, and CCL4 with the tumor microenvironment and tumor-associated macrophage markers in colorectal cancer. *Tumour Biol.* **40**, 1010428318810059 (2018).
39. Hanna, R. N. et al. Patrolling monocytes control tumor metastasis to the lung. *Science* **350**, 985–990 (2015).
40. Kubo, H., Mensurado, S., Goncalves-Sousa, N., Serre, K. & Silva-Santos, B. Primary tumors limit metastasis formation through induction of IL15-mediated cross-talk between patrolling monocytes and NK cells. *Cancer Immunol. Res.* **5**, 812–820 (2017).
41. Franklin, R. A. et al. The cellular and molecular origin of tumor-associated macrophages. *Science* **344**, 921–925 (2014).
42. Zhu, Y. et al. Tissue-resident macrophages in pancreatic ductal adenocarcinoma originate from embryonic hematopoiesis and promote tumor progression. *Immunity* **47**, 323–338 (2017).
43. Loyher, P. L. et al. Macrophages of distinct origins contribute to tumor development in the lung. *J. Exp. Med.* **215**, 2536–2553 (2018).
44. Schmid, M. C. et al. Combined blockade of integrin- α 4 β 1 plus cytokines SDF-1 α or IL-1 β potently inhibits tumor inflammation and growth. *Cancer Res.* **71**, 6965–6975 (2011).
45. Schmid, M. C. et al. Receptor tyrosine kinases and TLR/IL1Rs unexpectedly activate myeloid cell PI3K γ , a single convergent point promoting tumor inflammation and progression. *Cancer Cell* **19**, 715–727 (2011).
46. Lafuente, E. M. et al. RIAM, an Ena/VASP and Profilin ligand, interacts with Rap1-GTP and mediates Rap1-induced adhesion. *Dev. Cell* **7**, 585–595 (2004).
47. Cho, E. A. et al. Phosphorylation of RIAM by src promotes integrin activation by unmasking the PH domain of RIAM. *Structure* **29**, 320–329 (2021).
48. Patsoukis, N. et al. The adaptor molecule RIAM integrates signaling events critical for integrin-mediated control of immune function and cancer progression. *Sci. Signal* **10**, eaam8298 (2017).
49. Kaneda, M. M. et al. PI3K γ is a molecular switch that controls immune suppression. *Nature* **539**, 437–442 (2016).
50. Schmid, M. C. et al. Integrin CD11b activation drives anti-tumor innate immunity. *Nat. Commun.* **9**, 5379 (2018).
51. Cassetta, L. et al. Human tumor-associated macrophage and monocyte transcriptional landscapes reveal cancer-specific reprogramming, biomarkers, and therapeutic targets. *Cancer Cell* **35**, 588–602 (2019).
52. Kumar, V. et al. CD45 phosphatase inhibits STAT3 transcription factor activity in myeloid cells and promotes tumor-associated macrophage differentiation. *Immunity* **44**, 303–315 (2016).
53. Hughes, R. et al. Perivascular M2 macrophages stimulate tumor relapse after chemotherapy. *Cancer Res.* **75**, 3479–3491 (2015).
54. Chen, L. et al. Tie2 expression on macrophages is required for blood vessel reconstruction and tumor relapse after chemotherapy. *Cancer Res.* **76**, 6828–6838 (2016).
55. Twum, D. Y. et al. IFN regulatory factor-8 expression in macrophages governs an antimetastatic program. *JCI Insight* **4**, e124267 (2019).
56. Gui, P. et al. The protease-dependent mesenchymal migration of tumor-associated macrophages as a target in cancer immunotherapy. *Cancer Immunol. Res.* **6**, 1337–1351 (2018).
57. Sharma, S. K. et al. Pulmonary alveolar macrophages contribute to the premetastatic niche by suppressing antitumor T cell responses in the lungs. *J. Immunol.* **194**, 5529–5538 (2015).
58. Wu, J. et al. The proinflammatory myeloid cell receptor TREM-1 controls Kupffer cell activation and development of hepatocellular carcinoma. *Cancer Res.* **72**, 3977–3986 (2012).
59. Li, X. et al. Targeting of tumour-infiltrating macrophages via CCL2/CCR2 signalling as a therapeutic strategy against hepatocellular carcinoma. *Gut* **66**, 157–167 (2017).
60. Matsumura, H. et al. Kupffer cells decrease metastasis of colon cancer cells to the liver in the early stage. *Int. J. Oncol.* **45**, 2303–2310 (2014).
61. Goldmann, T. et al. Origin, fate and dynamics of macrophages at central nervous system interfaces. *Nat. Immunol.* **17**, 797–805 (2016).
62. Hoeffel, G. & Ginhoux, F. Fetal monocytes and the origins of tissue-resident macrophages. *Cell. Immunol.* **330**, 5–15 (2018).
63. Nimmerjahn, A., Kirchhoff, F. & Helmchen, F. Resting microglial cells are highly dynamic surveillants of brain parenchyma in vivo. *Science* **308**, 1314–1318 (2005).
64. Butovsky, O. et al. Identification of a unique TGF- β -dependent molecular and functional signature in microglia. *Nat. Neurosci.* **17**, 131–143 (2014).
65. Hickman, S. E. et al. The microglial sensome revealed by direct RNA sequencing. *Nat. Neurosci.* **16**, 1896–1905 (2013).
66. Masuda, T. et al. Spatial and temporal heterogeneity of mouse and human microglia at single-cell resolution. *Nature* **566**, 388–392 (2019).
67. Louis, D. N., Wiestler, O. D. & Cavenee, W. K. World Health Organization Classification of Tumours of the Central Nervous System. 5th ed. (International Agency for Research on Cancer, 2021).
68. Boussiotis, V. A. & Charest, A. Immunotherapies for malignant glioma. *Oncogene* **37**, 1121–1141 (2018).
69. Szulzewsky, F. et al. Glioma-associated microglia/macrophages display an expression profile different from M1 and M2 polarization and highly express Gpnmb and Spp1. *PLoS ONE* **10**, e0116644 (2015).

70. Gabrusiewicz, K. et al. Glioblastoma-infiltrated innate immune cells resemble M0 macrophage phenotype. *JCI Insight* **1**, e85841 (2016).
71. Pyonteck, S. M. et al. CSF-1R inhibition alters macrophage polarization and blocks glioma progression. *Nat. Med.* **19**, 1264–1272 (2013).
72. Donadon, M. et al. Macrophage morphology correlates with single-cell diversity and prognosis in colorectal liver metastasis. *J. Exp. Med.* **217**, e20191847 (2020).
73. O'Neill, L. A. & Pearce, E. J. Immunometabolism governs dendritic cell and macrophage function. *J. Exp. Med.* **213**, 15–23 (2016).
74. Jayasingam, S. D. et al. Evaluating the polarization of tumor-associated macrophages into M1 and M2 phenotypes in human cancer tissue: technicalities and challenges in routine clinical practice. *Front. Oncol.* **9**, 1512 (2019).
75. Di Conza, G. et al. Tumor-induced reshuffling of lipid composition on the endoplasmic reticulum membrane sustains macrophage survival and pro-tumorigenic activity. *Nat. Immunol.* **22**, 1403–1415 (2021).
76. Oh, M. H. et al. Targeting glutamine metabolism enhances tumor-specific immunity by modulating suppressive myeloid cells. *J. Clin. Invest.* **130**, 3865–3884 (2020).
77. Menga, A. et al. Glufosinate constrains synchronous and metachronous metastasis by promoting anti-tumor macrophages. *EMBO Mol. Med.* **12**, e11210 (2020).
78. Jha, A. K. et al. Network integration of parallel metabolic and transcriptional data reveals metabolic modules that regulate macrophage polarization. *Immunity* **42**, 419–430 (2015).
79. Liu, P. S. et al. α -ketoglutarate orchestrates macrophage activation through metabolic and epigenetic reprogramming. *Nat. Immunol.* **18**, 985–994 (2017).
80. Geeraerts, X. et al. Macrophages are metabolically heterogeneous within the tumor microenvironment. *Cell Rep.* **37**, 110171 (2021).
81. Zilionis, R. et al. Single-cell transcriptomics of human and mouse lung cancers reveals conserved myeloid populations across individuals and species. *Immunity* **50**, 1317–1334 (2019).
82. Azizi, E. et al. Single-cell map of diverse immune phenotypes in the breast tumor microenvironment. *Cell* **174**, 1293–1308 e1236 (2018).
83. Chevrier, S. et al. An immune atlas of clear cell renal cell carcinoma. *Cell* **169**, 736–749 e718 (2017).
84. Tirosh, I. et al. Dissecting the multicellular ecosystem of metastatic melanoma by single-cell RNA-seq. *Science* **352**, 189–196 (2016).
85. Artyomov, M. N. & Van den Bossche, J. Immunometabolism in the single-cell era. *Cell Metab.* **32**, 710–725 (2020).
86. Mantovani, A., Allavena, P., Sica, A. & Balkwill, F. Cancer-related inflammation. *Nature* **454**, 436–444 (2008).
87. Nakamura, K. & Smyth, M. J. Targeting cancer-related inflammation in the era of immunotherapy. *Immunol. Cell Biol.* **95**, 325–332 (2017).
88. Dvorak, H. F. Tumors: wounds that do not heal. Similarities between tumor stroma generation and wound healing. *N. Engl. J. Med.* **315**, 1650–1659 (1986).
89. Bayne, L. J. et al. Tumor-derived granulocyte-macrophage colony-stimulating factor regulates myeloid inflammation and T cell immunity in pancreatic cancer. *Cancer Cell* **21**, 822–835 (2012).
90. Ubertini, V. et al. Mutant p53 gains new function in promoting inflammatory signals by repression of the secreted interleukin-1 receptor antagonist. *Oncogene* **34**, 2493–2504 (2015).
91. Sumimoto, H., Imabayashi, F., Iwata, T. & Kawakami, Y. The BRAF–MAPK signaling pathway is essential for cancer-immune evasion in human melanoma cells. *J. Exp. Med.* **203**, 1651–1656 (2006).
92. Mehta, A. K. et al. Targeting immunosuppressive macrophages overcomes PARP inhibitor resistance in BRCA1-associated triple-negative breast cancer. *Nat. Cancer* **2**, 66–82 (2021).
93. Dou, Z. et al. Cytoplasmic chromatin triggers inflammation in senescence and cancer. *Nature* **550**, 402–406 (2017).
94. Su, S. et al. Immune checkpoint inhibition overcomes ADCP-induced immunosuppression by macrophages. *Cell* **175**, 442–457 e423 (2018).
95. Liu, Y. et al. Tumor exosomal RNAs promote lung pre-metastatic niche formation by activating alveolar epithelial TLR3 to recruit neutrophils. *Cancer Cell* **30**, 243–256 (2016).
96. Keklikoglou, I. et al. Chemotherapy elicits pro-metastatic extracellular vesicles in breast cancer models. *Nat. Cell Biol.* **21**, 190–202 (2019).
97. Di Virgilio, F., Sarti, A. C., Falzoni, S., De Marchi, E. & Adinolfi, E. Extracellular ATP and P2 purinergic signalling in the tumour microenvironment. *Nat. Rev. Cancer* **18**, 601–618 (2018).
98. Hubel, P. et al. A protein-interaction network of interferon-stimulated genes extends the innate immune system landscape. *Nat. Immunol.* **20**, 493–502 (2019).
99. Mowat, C., Mosley, S. R., Namdar, A., Schiller, D. & Baker, K. Anti-tumor immunity in mismatch repair-deficient colorectal cancers requires type I IFN-driven CCL5 and CXCL10. *J. Exp. Med.* **218**, e20210108 (2021).
100. West, A. J. et al. Inflammasome-associated gastric tumorigenesis is independent of the NLRP3 pattern recognition receptor. *Front. Oncol.* **12**, 830350 (2022).
101. Radtke, F., Fasnacht, N. & Macdonald, H. R. Notch signaling in the immune system. *Immunity* **32**, 14–27 (2010).
102. Wang, Y. C. et al. Notch signaling determines the M1 versus M2 polarization of macrophages in antitumor immune responses. *Cancer Res.* **70**, 4840–4849 (2010).
103. Chiba, S. et al. Tumor-infiltrating DCs suppress nucleic acid-mediated innate immune responses through interactions between the receptor TIM-3 and the alarmin HMGB1. *Nat. Immunol.* **13**, 832–842 (2012).
104. Matlung, H. L., Szilagy, K., Barclay, N. A. & van den Berg, T. K. The CD47–SIRP α signaling axis as an innate immune checkpoint in cancer. *Immunological Rev.* **276**, 145–164 (2017).
105. Hartley, G. P., Chow, L., Ammons, D. T., Wheat, W. H. & Dow, S. W. Programmed cell death ligand 1 (PD-L1) signaling regulates macrophage proliferation and activation. *Cancer Immunol. Res.* **6**, 1260–1273 (2018).
106. Chen, W., Wang, J., Jia, L., Liu, J. & Tian, Y. Attenuation of the programmed cell death-1 pathway increases the M1 polarization of macrophages induced by zymosan. *Cell Death Dis.* **7**, e2115 (2016).
107. Huang, X. et al. PD-1 expression by macrophages plays a pathologic role in altering microbial clearance and the innate inflammatory response to sepsis. *Proc. Natl. Acad. Sci. USA* **106**, 6303–6308 (2009).
108. Shen, L. et al. PD-1/PD-L pathway inhibits M.tb-specific CD4⁺ T-cell functions and phagocytosis of macrophages in active tuberculosis. *Sci. Rep.* **6**, 38362 (2016).
109. Schreiber, R. D., Old, L. J. & Smyth, M. J. Cancer immunoeediting: integrating immunity's roles in cancer suppression and promotion. *Science* **331**, 1565–1570 (2011).
110. Lecoultre, M., Dutoit, V. & Walker, P. R. Phagocytic function of tumor-associated macrophages as a key determinant of tumor progression control: a review. *J. Immunother. Cancer* **8**, e001408 (2020).
111. Liu, J., Qian, C. & Cao, X. Post-translational modification control of innate immunity. *Immunity* **45**, 15–30 (2016).
112. Bene, K., Halasz, L. & Nagy, L. Transcriptional repression shapes the identity and function of tissue macrophages. *FEBS Open Bio.* **11**, 3218–3229 (2021).
113. Zhivaki, D. et al. Inflammasomes within hyperactive murine dendritic cells stimulate long-lived T cell-mediated anti-tumor immunity. *Cell Rep.* **33**, 108381 (2020).
114. Christofides, A., Konstantinidou, E., Jani, C. & Boussiotis, V. A. The role of peroxisome proliferator-activated receptors (PPAR) in immune responses. *Metabolism* **114**, 154338 (2021).
115. Chawla, A. et al. A PPAR γ -LXR-ABCA1 pathway in macrophages is involved in cholesterol efflux and atherogenesis. *Mol. Cell* **7**, 161–171 (2001).
116. Moore, K. J. et al. The role of PPAR γ in macrophage differentiation and cholesterol uptake. *Nat. Med.* **7**, 41–47 (2001).
117. Tavazoie, M. F. et al. LXR/ApoE activation restricts innate immune suppression in cancer. *Cell* **172**, 825–840 (2018).
118. Serhan, C. N. Pro-resolving lipid mediators are leads for resolution physiology. *Nature* **510**, 92–101 (2014).
119. Libreros, S. et al. A new E-series resolvin: RvE4 stereochemistry and function in efferocytosis of inflammation-resolution. *Front. Immunol.* **11**, 631319 (2020).
120. Sulciner, M. L. et al. Resolvins suppress tumor growth and enhance cancer therapy. *J. Exp. Med.* **215**, 115–140 (2018).

Acknowledgements

This work was supported by NIH grants R01CA238263 (V.A.B.) and R01CA229784 (A. Charest and V.A.B.).

Author contributions

A. Christofides, L.S., A.Y., and C.C. wrote the main sections of the manuscript. A. Charest generated sections of the manuscript related to glioblastoma. V.A.B. generated sections of the manuscript, prepared figures, guided the co-authors and was responsible for the organization of the document.

Competing interests

V.A.B. has patents on the PD-1 pathway licensed by Bristol-Myers Squibb, Roche, Merck, EMD-Serono, Boehringer Ingelheim, AstraZeneca, Novartis, and Dako. The authors declare no other competing interests.

Additional information

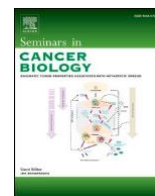
Correspondence should be addressed to Vassiliki A. Boussiotis.

Peer review information *Nature Immunology* thanks Ping-Chih Ho, Judith Varner and the other, anonymous, reviewer(s) for their contribution to the peer review of this work. Ioana Visan was the primary editor on this article and managed its editorial process and peer review in collaboration with the rest of the editorial team.

Reprints and permissions information is available at www.nature.com/reprints.

Publisher's note Springer Nature remains neutral with regard to jurisdictional claims in published maps and institutional affiliations.

© Springer Nature America, Inc. 2022



Immune cellular components and signaling pathways in the tumor microenvironment

Sasitorn Yenyuwadee^{a,b,c,1}, Konstantinos Aliazis^{a,b,1}, Qi Wang^{a,b}, Anthos Christofides^{a,b},
Rushil Shah^{a,b}, Nikolaos Patsoukis^{a,b,d,*}, Vassiliki A. Boussiotis^{a,b,d,*}

^a Division of Hematology-Oncology, Beth Israel Deaconess Medical Center

^b Department of Medicine Beth Israel Deaconess Medical Center, Harvard Medical School

^c Department of Dermatology, Faculty of Medicine Siriraj Hospital, Mahidol University, Bangkok, Thailand

^d Cancer Center, Beth Israel Deaconess Medical Center, Harvard Medical School Boston, MA 02215, USA

ARTICLE INFO

Keywords:

Tumor microenvironment
Signaling pathways
Checkpoint inhibitors

ABSTRACT

During the past decade there has been a revolution in cancer therapeutics by the emergence of antibody-based and cell-based immunotherapies that modulate immune responses against tumors. These new therapies have extended and improved the therapeutic efficacy of chemo-radiotherapy and have offered treatment options to patients who are no longer responding to these classic anti-cancer treatments. Unfortunately, tumor eradication and long-lasting responses are observed in a small fraction of patients, whereas the majority of patients respond only transiently. These outcomes indicate that the maximum potential of immunotherapy has not been reached due to incomplete knowledge of the cellular and molecular mechanisms that guide the development of successful anti-tumor immunity and its failure. In this review, we discuss recent discoveries about the immune cellular composition of the tumor microenvironment (TME) and the role of key signaling mechanisms that compromise the function of immune cells leading to cancer immune escape.

1. Cancer immunosurveillance pathways and the tumor microenvironment

The exploitation of the immune system for the treatment of cancer

has been investigated for many years. However, enthusiasm waxed and waned based on discoveries that supported or opposed the hypothesis that cancer can be subjected to immune-mediated control. It is currently understood that not only the immune system can control cancer growth

Abbreviations: HLA, human leukocyte antigens; IDO, indoleamine 2,3-dioxygenase; VEGF, vascular endothelial growth factor; TGF- β , transforming growth factor- β ; PD-1, programmed cell death protein 1; CTLA-4, cytotoxic T-lymphocyte-associated protein 4; ROR γ t, retinoic acid-related orphan receptor γ ; FLT3L, FMS-like tyrosine kinase 3 ligand; IRF4, interferon regulatory factor 4; CXCL9, CXC chemokine ligand 9; CXCL10, CXC chemokine ligand 10; CXCL11, CXC chemokine ligand 11; CCL2, C-C motif chemokine ligand 2; CCL5, C-C motif chemokine ligand 5; XCL1, X-C motif chemokine ligand 1; COX1, cyclooxygenase 1; COX2, cyclooxygenase 2; CXCR3, CXC chemokine receptor 3; G-CSF, granulocyte colony-stimulating factor; PGE₂, prostaglandin E₂; CXCL1, CXC motif chemokine ligand 1; TNF α , tumor necrosis factor alpha; NF- κ B, nuclear factor-kappaB; SHP-2, Src homology domain-containing phosphatase-2; TIM-3, T-cell immunoglobulin mucin-3; TLR3, Toll-like receptor 3; TLR7, Toll-like receptor 7; TLR9, Toll-like receptor 9; TIM-4, T-cell immunoglobulin mucin-4; IRF8, interferon regulatory factor 8; Th17, T helper 17 cell; MIP-1b, macrophage inflammatory protein-1 β ; CCL4, C-C motif chemokine ligand 4; RANTES, regulated on activation, normal T cell expressed and secreted; IFN- α , interferon alpha; ICOS-L, inducible costimulator ligand; AML, acute myeloid leukemia; VISTA, V-domain Ig suppressor of T-cell activation; mPGES1, microsomal prostaglandin E synthase-1; pSTAT1-IRF1, phosphorylated signal transducer and activator of transcription 1- interferon regulatory factor 1; HIF-1 α , hypoxia-inducible factor 1; CXCL12, CXC chemokine ligand 12; B7-H4, B7 homolog 4; SREBP1, sterol regulatory element-binding protein-1; PARP, poly adenosine diphosphate-ribose polymerase; Arg-1, arginase 1; iNOS, inducible nitric oxide synthase; GBM, glioblastoma multiforme; LAG-3, lymphocyte activation gene-3; VSIG-3, V-set and immunoglobulin domain containing 3; PSGL-1, P-selectin glycoprotein ligand-1; GITR, glucocorticoid-induced tumor necrosis factor receptor family-related receptor; mTOR, mammalian target of rapamycin; CCR7, C-C chemokine receptor type 7; VHL, von Hippel Lindau; TIGIT, T cell immunoreceptor with immunoglobulin and ITIM domain; HCMV, human cytomegalovirus; AOM/DSS, azoxymethane/dextran sodium sulfate; PDAC, pancreatic ductal adenocarcinoma; cSCCs, cutaneous squamous cell carcinomas.

* Correspondence to: Beth Israel Deaconess Medical Center, 330 Brookline Avenue Dana 513, Boston, MA 02215, USA.

E-mail addresses: npatouk@bidmc.harvard.edu (N. Patsoukis), vboussio@bidmc.harvard.edu (V.A. Boussiotis).

¹ These authors contributed equally.

<https://doi.org/10.1016/j.semcan.2022.08.004>

Received 24 June 2022; Accepted 12 August 2022

Available online 18 August 2022

1044-579X/© 2022 Published by Elsevier Ltd.

but has an important role in shaping the immunogenicity of cancer cells via immunoeediting [1]. During early stages of cancerous differentiation of normal cells, continuous immune surveillance results in the identification and elimination of these malignant populations through generation of adaptive anti-tumor immune responses. Tumor-associated macrophages (TAMs) have a central role in this process by mediating phagocytosis and clearance of cancer cells [2] and the presentation of cancer neoantigens to T cells [3]. Through continuous control, the immune system keeps cancer under check achieving equilibrium, even without complete elimination. The adaptive antitumor immune system can efficiently recognize neoantigens resulting from tumor-specific somatic mutations, antigens derived from oncogenic viruses, and antigens whose expression is shared with tissues at immune-privileged sites [4]. When cancer antigens yield peptides capable of binding to an individual's HLA alleles (neoepitopes), they can elicit CD4⁺ and CD8⁺ T cell responses [5,6] as evidenced by the presence and prognostic significance of immune infiltrates in human tumors [7–9]. However, under the continuous immune pressure cancer cells develop alterations to overcome immune attack, resulting in escape and growth of tumors that are resistant to the physiological immune mechanisms utilized to recognize and present antigens thereby engaging adaptive immune responses.

Escape mechanisms include tumor cell-intrinsic adaptations such as

downregulation of tumor neoantigens and induction of protective mechanisms rendering tumors resistant to cytotoxic cells of adaptive immunity. In that regard, it has been determined that genomic alterations and changes of neoantigen load are linked to diminished immune responses [10]. Escape may also result from the development of immunosuppressive mechanisms of the TME, with the production of soluble factors such as IDO, VEGF, and TGF- β [11,12]. Alterations in the cellular populations of the TME such as recruitment of immunosuppressive myeloid-derived suppressor cells (MDSCs) that are produced during cancer-driven emergency myelopoiesis, regulatory T cells (Tregs) and tumor associated macrophages (TAMs) have important roles in shaping the properties of the TME (Fig. 1) [13]. Changes also occur in dendritic cells (DC) which lose their ability to process and present tumor antigens to T cells [14]. Expression of co-inhibitory molecules in these immune populations shapes the signaling landscape of the TME, generating primarily pro-tumorigenic cues by suppressing critical functions of myeloid cells and TAMs, such as phagocytosis and antigen presentation, and compromising the ability of T cells to mount immune responses. These signaling pathways have a key role in cancer immune escape but also represent targets for immune-based treatments that have re-shaped modern cancer therapy. Among the coinhibitory receptors, inhibitory targeting PD-1 and its ligands with blocking antibodies has been the cornerstone of cancer immunotherapy and together with

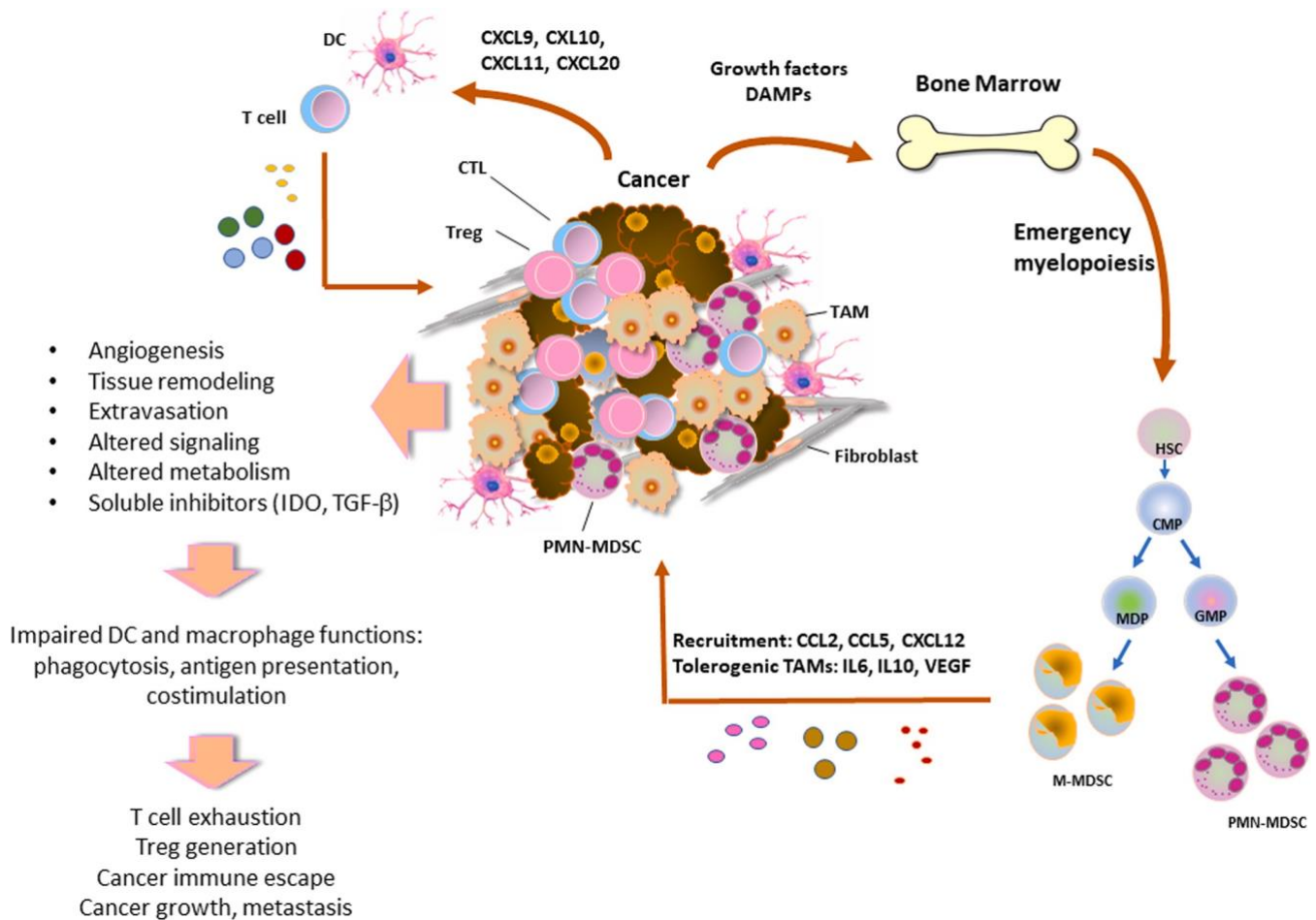


Fig. 1. During tumorigenesis, growth factors, such as M-CSF and GM-CSF, and damage-associated molecular patterns (DAMPs) produced by cancer cells due to rapid replication and apoptosis, act on bone marrow myeloid progenitors inducing emergency myelopoiesis and output of immature myelosuppressive PMN-MDSCs and M-MDSCs, which are recruited to the tumor via chemokines such as CCL2, CCL5 and CXCL12. In the TME, PMN-MDSCs and M-MDSCs directly induce immunosuppression, whereas M-MDSCs are also converted into tolerogenic and pro-tumorigenic TAMs by the function of soluble factors such as IL-6, IL-10 and VEGF. TAMs lose the physiologic properties of macrophages such as phagocytosis and together with MDSCs and soluble factors produced in the TME suppress the antigen presenting function of DCs, leading to impaired activation of tumor-specific T cells and generation of Treg cells. These orchestrated changes in the properties of immune cells promote cancer immune escape.

CTLA-4 blocking agents have revolutionized cancer treatment. In this review, we provide a concise summary of how key coinhibitory receptors shape the function of the immune components of the TME and discuss the role of immune populations during tumorigenesis and cancer evolution.

2. Dendritic cells are key mediators of tumor antigen presentation

Dendritic cells (DC) are professional antigen-presenting cells (APC) that play an important role in the tumorigenic and non-tumorigenic environment by activating CD8⁺ T cells and enhancing antitumor responses. DCs make up a small minority of the tumor-infiltrating leukocytes [15]. In both human and mice, four different major subsets of DCs have been characterized: the classical DC1 (cDC1), the heterogeneous population cDC2, the monocyte-derived DC (mo-DC), and the plasmacytoid DC (pDC) [16]. cDC1 expresses a distinct gene expression profile and specific markers [17]. It has been reported that cDC1 are critical for priming CD8⁺ T cells whereas cDC2 are responsible for priming CD4⁺ T cells [18] and support Th17 responses [19]. The DC2 group is a more heterogeneous population consisting of two different types of DCs, cDC2 and DC3 [20]. In agreement to that, another study revealed two distinct cDC2 populations by transcriptional analysis, cDC2A and cDC2B which express T-bet and RORγt respectively and are conserved across both human and mice [21] and might correspond to cDC2 and DC3 [22]. In humans, DC2 and DC3 derive from progenitors with differential expression of IRF8, where high expression led to the development of cDC1 and DC2, whereas low expression of IRF8 led to the development of DC3 and monocytes [23]. In contrast to cDC2 which require FLT3L for expansion, DC3 expanded and differentiated in the presence of granulocyte-macrophage stimulating factor (GM-CSF) but not FLT3L, providing further evidence that DC3s forms a distinct population within the cDC2 compartment [24]. Mo-DC can either derive directly from CD34⁺ precursors or from monocytes [25,26]. Studies have indicated

that IRF4 might be required for the differentiation of cDC2 and mo-DC, however, mo-DC do not share the same precursors as cDC2 [27,28]. Lastly, pDC are a distinct subpopulation of DC deriving from the common DC progenitors, secrete IFN-α/β and play an important role in viral infections [28].

Chemokines are mainly responsible for cDC1 recruitment and retention in the TME (Fig. 1). Tumors secrete several chemokines including CXCL9, CXCL10, and CXCL11, which can recruit Th1 and CD8⁺ T cells, CCL20 which recruits Th17 and immature DC, and CCL2 or CCL5 which recruit monocytes [29]. NK cells can also recruit cDC1 to the TME by secretion of CCL5 and XCL1, an effect abrogated by prostaglandin E2 (PGE₂) production [30]. Inhibition of PGE₂ production by ablation of COX1 or COX2 leads to increased accumulation of cDC1, tumor eradication, and increased sensitivity of tumor towards anti-PD-1 treatment [31]. Cytokines also play a role in the positioning of the DC in the TME. FLT3L secreted by NK cells and lymphocytes in mouse and human tumors has an active role in the recruitment and localization of cDC1 [32].

Generation of anti-tumor CD8⁺ T cell responses requires cross-presentation of tumor peptides to naïve CD8⁺ T cells on MHC class I molecules by the DC (Fig. 2A). Although priming of naïve T cells occurs in the tumor-draining lymph nodes, studies have shown that cross-presentation can also occur within the TME [33]. The antigens can travel to the lymph node either on cell debris or after their engulfment by migratory CD103⁺ cDC1 found in the TME, which then migrate to the tumor-draining lymph node and cross-present tumor antigens to naïve T cells, either directly or through antigen exchange to resident myeloid cells [34]. However, only the migratory CD103⁺ cDC1, but not the lymph node resident CD8⁺ cDC1, can prime naïve CD8⁺ T cells [35]. CCR7 is required for cDC1 migration to the tumor-draining lymph node and ablation of CCR7 expression results in a significantly smaller migratory effect of cDC1 to tumor-draining lymph node and a diminished T cell activation profile [36]. In human tumors, CCR7 expression positively correlates with greater DC infiltration and increased patient

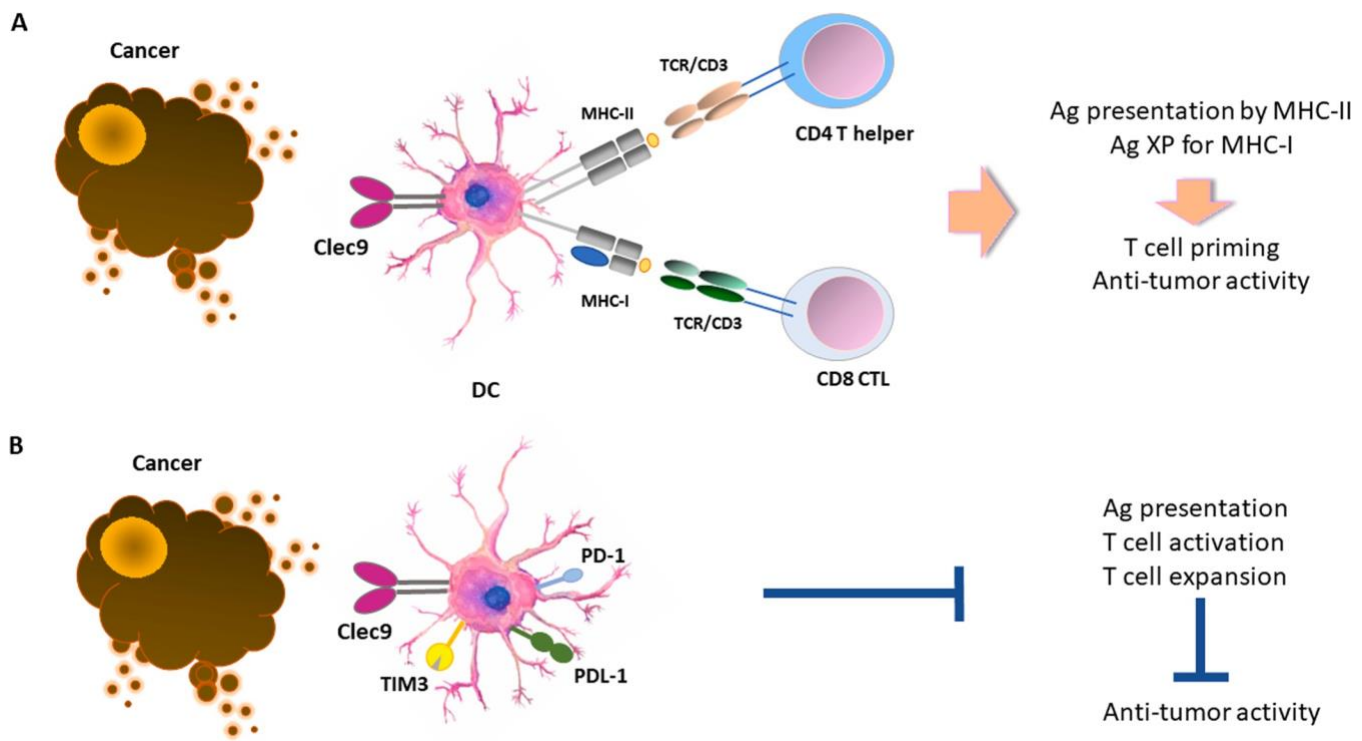


Fig. 2. DCs, particularly the cDC1 subset, can capture and process tumor-associated antigens and present them to CD4⁺ T cells by MHC-II molecules. cDC1 can also cross-present (XP) tumor-associated antigens to CD8⁺ T cells by MHC-I molecules (A). Expression of checkpoint inhibitors such PD-1, PDL-1 and TIM-3, compromise these functions leading to impaired T cell activation, T cell expansion and anti-tumor immunity.

survival [36].

Within the TME, CD103⁺ cDC1 secrete CXCL9 and CXCL10 which recruit CXCR3⁺CD8⁺ effector T cells to the tumor [37]. In non-tumor models, CXCR3 has been previously shown to drive CD4⁺ and CD8⁺ T cell recruitment into the lymph nodes and in close contact to DC for T cell priming [38]. In a melanoma mouse model, CXCL9 and CXCL10 secreted by CD103⁺ cDC1 were responsible for the recruitment of effector T cells and for controlling tumor growth [39]. CD103⁺ cDC1 are located at distal regions of the tumor and despite their sparsity, they are good CTL activators [15]. Furthermore, cDC1 can uptake and cross-present tumor antigens to T cells more efficiently than other myeloid cells, which can also engulf tumor cells and uptake tumor antigens [15]. These CD103⁺ cDC1 also secrete increased levels of IL-12 but not IL-10 suggesting a dominant role in facilitating increased cytotoxic function of intratumoral CD8⁺ T cells [15].

Tumors have developed several mechanisms of immune evasion which restrict the function of cDC1 [40]. One such mechanism involves reducing the number of cDC1 in the TME. Tumors in breast and pancreatic cancers secrete the G-CSF thereby inhibiting the expression of IRF8 which is responsible for the generation of DC progenitors [41]. Similarly, reduction of FLT3L production within the tumor limits the differentiation, expansion, and survival of intratumoral cDC1 [35]. The reduced tumor infiltration by DC might also result from an impaired chemoattractant profile in the TME. PGE₂ production leads to impaired NK viability and consequently impaired CCL5 and CXCL1 chemokine production, both of which act as chemoattractants for cDC1 [30].

Impairment of cDC1 function is also possible through direct inhibition of cDC1. In a breast cancer model, IL-10 which is secreted mainly by tumor-associated macrophages in the TME, resulted in low levels of IL-12 cDC1-mediated secretion [42]. Similarly, PGE₂ reduced the production of IL-12 by cDC1 and downregulated the expression of co-stimulatory molecules [31]. In murine tumor models, lipid accumulation led to decreased ability of DC to translocate the peptide-MHC class I complex to the cell surface resulting in decreased antigen-presentation ability and T cell stimulation [43]. Tumor-derived TGF- β also inhibited the antigen presentation capacity of DC, impaired their ability to stimulate T cells, and decreased their migration capacity to the draining lymph nodes [44].

Suppression of cDC1 responses in the context of cancer is also driven by the inhibitory receptors present on the surface of DC (Fig. 2B). In patients with hepatocellular carcinoma, PD-1⁺ DC circulate in their peripheral blood, making them potentially prone to inhibition by PD-L1, the ligand of PD-1, present in the TME [45]. PD-L1 is highly expressed on both tumor cells and immune cells present in the TME [46]. PD-L1 expression in tumor infiltrating DC might be stabilized by phosphorylation mediated by the enzyme casein kinase 2 (CK2) [47], which is highly expressed in multiple cancers and is linked to increased cell growth, proliferation and inhibition of apoptosis [48]. Inhibition of CK2 decreased PD-L1 expression on DC and resulted in tumor suppression through release of CD80 from DC thereby allowing T cells to receive CD80-mediated co-stimulatory signals and become activated [47]. In PD-L1-deficient tumors, tumor-associated DC upregulated PD-L1 expression [49]. The authors hypothesized that this upregulation could be an escape mechanism of the tumor by which immune cells receive inhibitory signals through the PD-L1-PD-1 axis. PD-L1 deletion on DC enhanced CD8⁺ anti-tumor T cell responses despite the higher number of tumor-associated macrophages in the TME [50]. In addition to its canonical interaction with PD-1 in *trans*, PD-L1 can also bind to CD80 in *cis* [51,52] and this interaction disrupts the PD-1: PD-L1 axis and prevents T cell inactivation [53,54]. Blocking of PD-L1 on DC allows CD80 to re-engage with CD28 on T cells and enhance T cell priming [55]. In ovarian tumor-infiltrating DC, PD-1 inhibited the secretion of TNF α and IL-6, and downregulated the expression of CD80, CD40, and MHC class I molecules [56]. PD-1 regulated multiple NF- κ B targets by recruiting the SHP-2 to the cytoplasmic domain tyrosine-based switch motif (ITSM) of PD-1 [56]. Anti-PD-1 reversed the suppressive effect of

PD-1 on cytokines but had no effect on the expression of the co-stimulatory and antigen-presenting molecules [56]. Together these studies provide evidence about the critical role of DC-expressed PD-L1 in the induction of PD-1-mediated T cell immunosuppression in the context of cancer.

TIM-3, a T cell checkpoint inhibitory receptor, is highly expressed on DCs in the TME compared to normal tissues and inhibits innate immune responses through recognition of nucleic acids via the pattern recognition receptors TLR3, TLR7, and TLR9 [57]. A combination of CK2 and a TIM-3 inhibitors led to greater tumor suppression and longer survival times for the mice [47]. TIM-3 was also highly expressed on intratumoral cDC1 in a mouse model for breast cancer [58]. Antibody blockade of TIM-3 led to increased granzyme B expression by CD8⁺ T cells and enhanced expression of CXCL9 by cDC1 [58]. Moreover, deletion of TIM-3 on DCs resulted in strong anti-tumoral CD8⁺ T cell responses and inflammasome activation [59]. TIM-4, a receptor responsible for engulfment of dead cells, is highly expressed in normal lung cDC1, however, inhibition of this receptor results in incomplete activation of anti-tumorigenic CD8⁺ T cells and increased tumor growth [60].

cDC2 cells have been historically considered to derive from monocytes and are recognized as cells responsible for Th2 and Th17 responses [61,62]. As mentioned earlier, they are recognized as a heterogeneous group which can be broken down into two different subsets, DC2 and DC3 [22]. In the context of cancer, these cells can travel from the tumor to the tumor-draining lymph nodes and present tumor antigens to CD4⁺ T cells [63]. Depletion of Treg leads to increased cDC2 ability to induce strong T cell responses and increased ratio of cDC2 to Treg is correlated with better clinical outcome and responsiveness to anti-PD-1 therapy [63]. DC3 are poorly characterized in the context of cancer. They rise from granulocyte-monocyte-DC progenitors and express low levels of IRF8 [23]. They are present in human papillomavirus-associated oropharyngeal squamous cell carcinoma tumors, are potent Th1 activators, and can secrete high levels of IL-12 and IL-18 which have the potential to drive anti-tumor responses [64]. It has been reported that DC3 bear signatures of both DC and monocyte-derived DC [22]. DC3 can stimulate memory T cells to produce IL-17 and differentiate naïve T cells into Th17 [65]. The differentiation program of these cells is regulated by GM-CSF [24]. Similarly, mo-DC can be generated in vitro from CD34⁺ precursors by culture with GM-CSF and TNF- α or monocytes by culture with GM-CSF and IL-4 [25,26]. However, only Mo-DC generated in vitro express the DC marker *Zbtb46*, providing evidence that these in vitro generated populations might not be the true counterparts of mo-DC differentiated in vivo [66]. The role of mo-DC in the presentation of tumor antigens is currently unclear. It was reported that although mo-DC can uptake antigen they have impaired capacity to induce potent T cell responses due to increased nitric oxide (NO) production [67]. However, in a different experimental system it was found that mo-DC could induce strong anti-tumor CD8⁺ T cell responses, which were impaired by blockade of monocyte entry to tumors [68]. Further studies are needed to fully characterize the cDC2, DC3 and mo-DC roles in the context of cancer.

pDCs are found in higher frequencies in human cancers and their presence is associated with poor prognosis and decreased survival [69]. Although pDCs normally produce IFN- α , in tumor settings including ovarian cancer, breast cancer, and melanoma, cancer-associated pDC have impaired IFN- α secretion [70]. This effect might be mediated by TNF- α and TGF- β present in the TME, which affect production of other cytokines such as IL-6, MIP-1b (CCL4) and RANTES [70]. In human ovarian cancer, pDCs are present in the tumor -but not ascites- can induce IL-10 secretion by naïve allogeneic T cells, and correlate with relapse [70]. Furthermore, when pDCs were cultured in medium from head and neck squamous cell carcinoma their ability to secrete IFN- α after TLR stimulation was significantly limited by IL-10 present in the medium, supporting the hypothesis that immunosuppressive cytokines in the TME contribute to the anti-inflammatory profile of tumor

infiltrating immune cells [71]. Lastly, pDCs express the ICOS-L which can stimulate ICOS-expressing Foxp3⁺ Treg which in turn secrete IL-10 in the TME and suppress immune responses [72]. Together, these immunological, signaling and functional features of DCs underline the pivotal role of this immune cell population in the development of anti-tumor responses and explain why DC-targeting signaling alterations in the TME might have a significant impact in anti-tumor immunity.

3. Myeloid derived suppressor cells (MDSC) inhibit anti-tumor T cell responses

The constant and prolonged secretion of danger-associated molecular patterns (DAMPs) and cytokines from the tumor cells has a direct effect on the bone marrow, through a process that is called in emergency myelopoiesis. During emergency myelopoiesis, immature myeloid cells, named MDSCs, with potent immunosuppressive properties, are produced and accumulate in the tumor microenvironment and peripheral organs. High numbers of these cells are associated with poor treatment outcome and worse clinical prognosis in various cancer types [73]. Two major subsets of MDSCs have been described in mice: Polymorphonuclear MDSCs (PMN-MDSCs) monocytic-MDSCs (M-MDSCs), which resemble morphologically and phenotypically to neutrophils and monocytes, respectively. PMN-MDSCs are identified as CD11b⁺Ly6G⁺Ly6C^{lo} in mice and CD11b⁺CD14⁺CD15⁺/CD66b⁺ in humans, while M-MDSCs are identified as CD11b⁺Ly6G[−]Ly6C^{hi} in mice and CD14⁺CD15⁺HLA-DR^{lo/−} in humans [74].

Among the mechanisms proposed for MDSC-mediated suppression function and subsequent cancer immune evasion, checkpoint inhibitors might have an important role. MDSCs isolated from patients with AML express high levels of VISTA and siRNA-mediated VISTA deletion attenuated MDSC-mediated inhibition of CD8⁺ T cells [75]. VISTA, a B7 family ligand, is predominantly expressed on the hematopoietic compartment, with highest expression observed in myeloid cells, including monocytic and granulocytic cells, and weaker expression on T cells [76]. VISTA was also identified as a homolog of PD-1, a member of the CD28 superfamily, indicating a potential function both as a ligand and a receptor [77]. VISTA transcription can be induced by HIF-1 α suggesting that hypoxia is implicated in VISTA upregulation in MDSCs located in hypoxic regions of the TME [78]. VISTA deletion in MDSCs had no effects in T cell proliferation in vitro. However, VISTA deletion resulted in increased T cell proliferation under hypoxia, suggesting that regulation of MDSC function by VISTA might occur only under oxygen deprivation [78]. Furthermore, VISTA blockade in tumor-bearing mice altered the tumor infiltrating immune cell populations by decreasing MDSCs and increasing T cells with anti-tumor properties [79].

The MDSCs suppression capacity is also affected by the PD-1/PD-L1 pathway. Compared to MDSCs localized in non-cancerous tissues, tumor infiltrating MDSCs express high levels of PD-L1, which is regulated by the COX2/mPGES1/PGE₂ pathway, pSTAT1-IRF1 axis and hypoxia-induced HIF-1 α [80–82]. Consistent with an active role of these pathways in MDSC function, PD-L1 blockade under hypoxia diminished the ability of MDSCs to suppress T cell activation by reducing the production of IL-10 and IL-6 [82]. Notably, conditional deletion of PD-1 in the myeloid compartment in tumor-bearing mice, resulted in diminished NO production and attenuated suppressive capacity of M-MDSCs indicating that PD-1 blockade or deletion counteracts the generation of immunosuppressive immature myeloid cells [83].

Due to their potent immunosuppressive properties, MDSCs have been associated with the limited efficacy of immunotherapy and standard chemotherapy in mouse tumor models and cancer patients. Conversely, selective depletion of MDSC reversed resistance to anti-CTLA4 Ab treatment in tumor bearing mice and increased the numbers of cytotoxic CD8⁺ T cells in tumor-draining lymph nodes and TME [84]. Doxycycline-induced suppression of MDSCs improved the efficacy of PD-1 inhibitors [85]. Similarly, in a mouse model of gastric cancer, 5-fluorouracil and oxaliplatin combination, which decreased

MDSCs, augmented CD8⁺ tumor infiltrating T cells and improved the therapeutic efficacy of anti-PD-1 treatment [86]. Furthermore, epigenetic targeting of MDSC in mice bearing immunotherapy-resistant tumors resulted in tumor eradication after anti-PD-1/anti-CTLA4 combined immunotherapy [87].

4. Generation of pro-tumorigenic tumor-associate macrophages (TAMs)

After egress from the bone marrow, monocytes (or M-MDSCs) are recruited to the TME via chemokines of the CC and CXC families, such as CCL2, CCL5, and CXCL12 [88] produced by cancer cells at early stages of the cancer immunity cycle and convert to bone marrow-derived tumor associated macrophages (Fig. 1), which, together with embryonically-derived tissue resident macrophages, form the population of TAMs. TAMs represent the most abundant immune population of the TME, consisting ~50% of hematopoietic cells and have predominantly pro-tumorigenic functions [89]. Pro-tumorigenic TAMs are immunosuppressive, lose the natural ability of macrophages to mediate phagocytosis and antigen presentation [83,90,91] and are characterized by expression of inhibitory molecules such as PD-1, PD-L1, VISTA, B7-H4 and TIM-3 [83,90–96].

The TME has a causative role in promoting the differentiation of pro-tumorigenic TAMs in a stepwise manner [97]. As a consequence of the malignant transformation of normal epithelial cells into cancerous cells by oncogenes and driver mutations, soluble factors, such as hematopoietic growth factors (e.g., M-CSF, GM-CSF) cytokines (e.g., IL-6, IL-1, and IL-8) and chemokines (e.g., CCL2, CCL5, CXCL12), are produced during cancer evolution (Fig. 1). For example, in pancreatic adenocarcinoma, KRAS^{G12D} mutation induces secretion of GM-CSF, which is correlated with an increased tumor infiltration by myeloid cells and immunosuppressive function [98,99]. p53 mutation has been documented to induce cancer-related inflammation by suppressing the production of IL-1 receptor antagonist [100]. In human melanoma, BRAF^{V600E}, a highly oncogenic mutated form of BRAF, and STAT3, a potent transcription factor often linked to oncogenic signaling, have been shown to drive expression of IL-6, IL-10 and VEGF, which promote a tolerogenic differentiation of bone marrow derived monocytes [101]. BRCA1-associated triple negative breast cancer induces pro-tumorigenic TAMs, by reprogramming glycolysis and SREBP1-mediated lipid metabolism, a metabolic signature associated with resistance to PARP inhibitors [102]. These mechanisms induce a unique differentiation program of TAMs, which lose the normal properties of healthy macrophages and obtain pro-tumorigenic features.

The immunophenotypic and metabolic properties of TAMs were previously streamlined in the simplified concept that TAMs have a differentiation program resembling M2 macrophages, characterized by expression of CD206, CD204, VEGF, CD163 and Arg-1 [103]. This is in contrast to the expression of classical markers of M1 polarized macrophage including CD80, CD86, MHC-II, iNOS and CD68, which correlated with effector function of macrophages and tumoricidal function of TAMs [103]. The M1/M2 programs rely mainly on metabolism, since proinflammatory M1 macrophages are supported by glycolysis, whereas anti-inflammatory M2 macrophages utilize mainly fatty acid oxidation (FAO)[104]. This concept is no further considered appropriate, but such differentiation profiles remain useful in the characterization of TAMs because there is extensive experience regarding the correlation between the expression of such immune marker combinations and prognosis in various cancers [97,105].

Live cell imaging allowing assessment of the spatial interaction of TAMs with other cells of the TME has significantly improved our understanding about the role of TAMs in tumor evolution. In a breast cancer mouse model, multiphoton microscopy studies showed that TAMs interact with mammary cancer cells, facilitating their intravasation and subsequent metastasis. Tumor cells closer to TAMs are more motile and are directed toward TAMs of the perivascular area

where they interact with blood vessels and enter the blood stream [106, 107]. Real time imaging provided evidence about the role of perivascular Tie2^{hi} TAMs in promoting transient vascular permeabilization and tumor intravasation, thereby facilitating metastasis [108]. In a model of GBM, intravital 2-photon microscopy showed two distinct TAM subtypes with morphological and functional differences: microglial cells which are large, highly branched and less motile, and bone marrow-derived macrophages which are smaller, less branched and less motile [109]. The differential properties of the spatially distinct subsets of TAMs might form attractive targets for therapeutic intervention.

Beyond the impact of oncogenes in regulating the production of tumor-derived soluble factors that regulate monocyte recruitment and TAM generation, the mutational landscape of tumor cells alter other immune cell types that are recruited in the TME. Colorectal cancer (CRC) serves as a paradigm for this process. Based on gene expression studies, CRC can be classified into four molecular subtypes (CMS1–4) [110]. CRC-CMS1 has DNA mismatch-repair defects, which cause microsatellite instability and hypermutation. These tumors are densely infiltrated by CD4⁺ and CD8⁺ T cells with high expression of immune checkpoint inhibitors including CTLA-4, PD-1, and PD-L1 and display favorable responses to checkpoint immunotherapy [111]. In contrast, CRC-CMS4 is characterized by tumor cells with a mesenchymal-like phenotype, an RNA sequencing profile dominated by signatures of the TGF-β pathway, Th17 pathway, monocyte/macrophage infiltration, and resistance to checkpoint immunotherapy [111]. Thus, cancer-specific

properties have a significant impact on the quantitative and qualitative inflammatory infiltrate of the TME and in regulating the crosstalk between myeloid cells and the adaptive immune system.

5. Tumor-associated T cells and signaling pathways shaping their function

A critical determinant of tumor containment and progression over time is the number and function of T cells within the TME. For this reason, T cells are the key targets of antibody-based and cell-based immunotherapies in cancer. During the phase of cancer escape from immune control, T cells that can recognize tumor-associated antigens and control tumor growth, lose the ability to mediate this function due to mechanisms related with tumor-induced tolerance and immunosuppression (Fig. 1) [112]. These dysfunctional T cells are characterized by features of T cell exhaustion (T_{EX}) observed in chronic viral infections [113] such as high surface expression of inhibitory receptors CTLA-4, PD-1, TIM-3, LAG-3, loss of expansion ability, and impaired effector function as determined by the diminished production of cytokines such as IFNγ and TNF-α (Fig. 3) [114]. The T_{EX} state might be reversible or irreversible [115] and a central goal of novel immunotherapies is to achieve re-invigoration of tumor-specific T_{EX} cells. The development of T_{EX} state is mediated primarily by T cell-extrinsic factors that lead to persistent T cell activation by tumor antigens [116].

The co-inhibitory molecules such as PD-1 (CD279) and CTLA-4

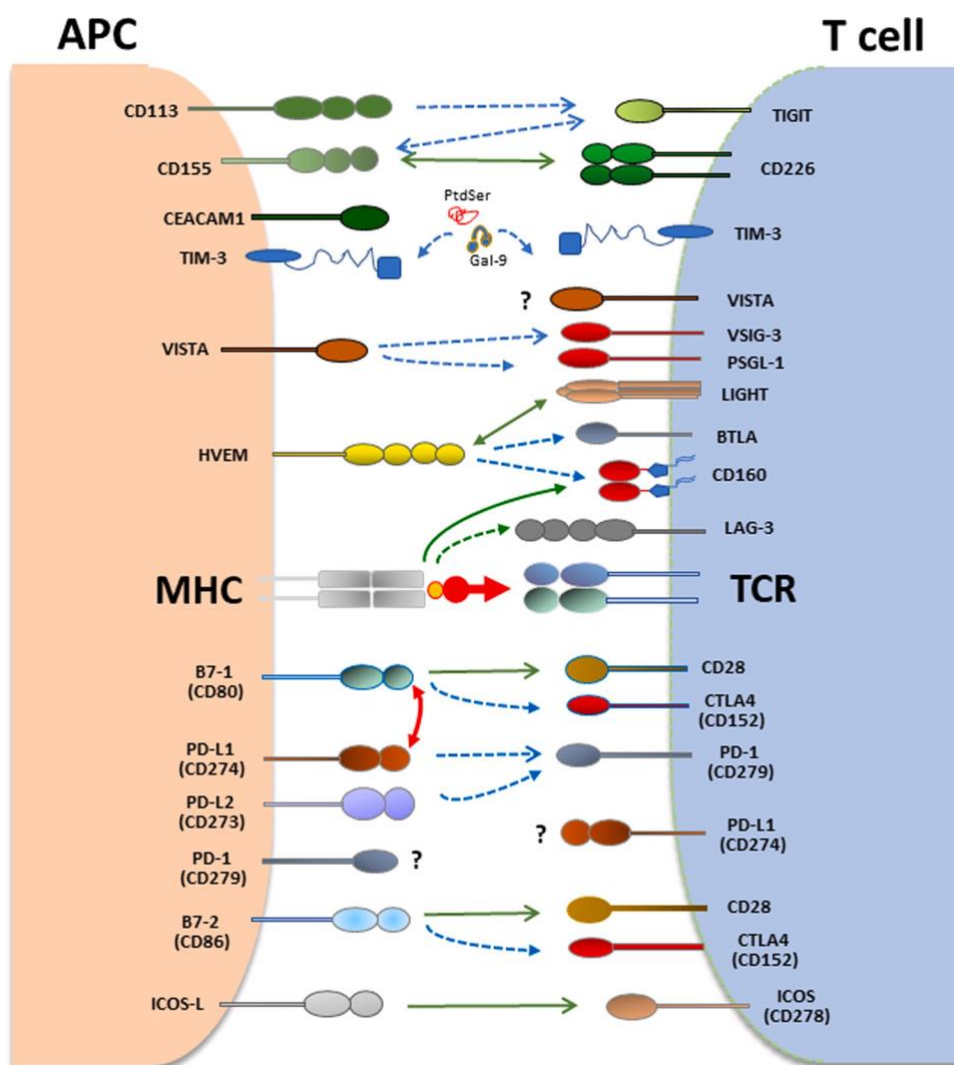


Fig. 3. Coinhibitory pathways in T cells and APC. T cell activation is initiated by recognition of antigens presented by antigen-presenting cells (APCs) to the T cell receptor (TCR)/CD3 complex. CD28 is the prototype costimulatory receptor in T cells and interacts with CD80 and CD86. Many coinhibitory receptors are up-regulated upon T cell activation and can attenuate TCR and costimulatory signals. CTLA4 and PD-1 are the prototype co-inhibitory receptors expressed in T cells. CTLA-4 interacts with B7-1 (CD80) and B7-2 (CD86) whereas PD-1 (CD279) interacts with PD-L1 (CD274) and PD-L2 (CD273) to inhibit T cell responses. In addition to canonical interaction of PD-L1 with PD-1 in *trans*, PD-L1 interacts with B7-1 (CD80) *in cis*, when co-expressed on the same APC leading to diminished availability of PD-L1 for canonical interaction with PD-1 in *trans*. VISTA, TIM-3 and PD-1 are expressed both in T cells and APC and can regulate immune responses by altering the properties of myeloid cells and T cells.

(CD152) are induced during physiologic T cell stimulation to tame activation signals. CTLA-4 being upregulated and acting early during T cell activation, is the high affinity receptor of CD80/CD86. CTLA-4 directly competes with CD28 for binding on CD80/CD86, and its binding on CD80/CD86 ligands on APC can result in the depletion of CD80/CD86 by trans-endocytosis [117] while simultaneously releasing free PD-L1 by eliminating availability of CD80 for PD-L1 engagement in PD-L1: CD80 interaction [118]. PD-1 is also induced upon TCR-mediated activation. Engagement of PD-1 by its ligands PD-L1 (B7-H1 or CD274) and/or PD-L2 (B7-DC or B7-H3) counteracts TCR signaling and CD28-mediated co-stimulation [119,120]. PD-1 and CTLA-4 are the prototype inhibitory receptors, known as immune checkpoints, and are the most extensively utilized therapeutic targets in cancer immunotherapy [121].

After engagement with its ligands PD-L1 or PD-L2, but also via tonic signaling [122], PD-1 inhibits T cell functions by recruiting phosphatases, predominantly SHP-2 but also SHP-1, to the immunoreceptor tyrosine-based switch motif (ITSM) and immunoreceptor tyrosine-based inhibitory motif (ITIM), expressed in PD-1 cytoplasmic tail, which antagonize TCR and CD28-mediated activation signals [123–126]. This TCR proximal signaling blockade results in inhibition of key downstream pathways including PI3K/Akt and Ras leading to altered biochemical, transcriptional and metabolic T cell reprogramming [127–129]. Constitutive PD-1 expression on T cells induced by persistent antigen stimulation during cancer promotes immune evasion, and blockade of the PD-1 pathway can improve T cell function and reduce tumor burden in multiple experimental tumor models and multiple types of human cancers [130,131].

The expression status of PD-L1 on tumor cells has served as a factor for patient stratification for anti-PD-1 therapy. However, in several clinical studies, there were patients with undetectable PD-L1 on tumors, who also responded to anti-PD-1 therapy [132]. This effect can be explained by the fact that, other cell types in the TME, such as macrophages, DCs, tumor-associated fibroblasts and myeloid cells also express PD-L1, creating an immunosuppressive TME for T cells and supporting tumor cell growth. Therefore, the relative contribution of PD-L1 on tumor cells and other cell types in limiting anti-tumor responses in the TME remains under investigation. PD-L1 expression on tumor cells can locally inhibit CD8⁺ T cell activation and protect PD-L1⁺, but not PD-L1⁻ tumors from eradication by the immune system, indicating a critical role for tumor PD-L1 in suppressing antitumor immunity [133]. By genetic deletion of PD-L1 in tumor cells and host mice, a different study showed comparable contribution of PD-L1 on each of these compartments to immune suppression, suggesting that PD-L1 expression in either of these compartments can be predictive of responses to PD-1/PD-L1 blockade therapy [134]. However by using conditional deletion of PD-L1 in tumor cells and dendritic cells-, transplantation chimeras, as well as various approaches of antibody blockade, it was determined by several investigators that PD-L1 expressed in APC, rather than tumor cells, has a causative role in compromising anti-tumor T cell responses and this APC-mediated PD-1 ligation and T cell immunosuppression is the dominant interaction targeted by checkpoint blockade therapy [95,135]. Since DCs mediate CD4⁺ T cell priming and cross-presentation of tumor antigens to CD8⁺ T cells, upregulation of PD-L1 on dendritic cells can attenuate cytotoxic T cell activity and compromise antitumor responses [136,137].

Recently, in *cis* interaction of PD-L1 and B7-1, on the same cell surface of APC, has been reported by several studies [51–54]. The in *cis* interaction of B7-1 with PD-L1 impairs the interaction of PD-L1 with PD-1 in *trans* (Fig. 3) resulting in reduced PD-1 signaling (reviewed in [138]). Blockade of the in *cis* interaction of PD-L1/B7-1 by B7-1-specific antibodies could increase PD-1-mediated T cell suppression and alleviate autoimmunity in several mouse models [139]. Among tumor-infiltrating myeloid cells, PD-L1-expressing DCs have a dominant role in regulating antitumor T cell responses via in *cis* interaction of PD-L1/B7-1 on DCs and PD-L1/PD-1 interactions between DCs and T

cells. These findings suggest a new therapeutic mechanism of PD-L1 checkpoint blockade acting on DCs to induce enhanced antigen presentation for T cell priming and simultaneous clonal expansion [137]. A more comprehensive understanding of these mechanisms will be necessary to optimize PD-1/PD-L1 targeting immunotherapy.

While the PD1/PD-L1 axis has been extensively investigated, other inhibitory pathways are also exploited by tumor cells, contributing to the generation of an immunosuppressive TME and escape of immunosurveillance [140]. VISTA (B7-H5, PD-1 H, Gi24, Dies1, SISP1 and DD1 α) has increasingly become a promising target for overcoming resistance to anti-PD-1 immunotherapy [141]. In addition to the ability of VISTA to regulate the immunosuppressive function of MDSC under hypoxia, as mentioned above [78], VISTA can function as an inhibitory regulator of naïve T cells, critical for steady-state maintenance of immune quiescence and peripheral tolerance (Fig. 3) [142]. Notably, VISTA can mitigate pathogenesis and progression of murine lupus by transmitting inhibitory signals on both T cells and myeloid cells [143, 144].

Although few studies have reported VISTA expression on tumor cells [145,146], VISTA expression on intratumoral myeloid cells and stromal cells has been recognized as a potential mediator of acquired resistance to anti-PD-1 and anti-CTLA-4 immunotherapies in patients with metastatic melanoma and pancreatic ductal adenocarcinoma [147–149]. Therapeutic blockade of the VISTA pathway has been limited by its unknown binding partners and their function. A recent study identified VSIG-3 as a putative ligand of VISTA to inhibit T cell activation and cytokine production [150]. While at physiological pH VISTA interacts mainly with VSIG-3, in acidic pH, VISTA serves as a selective ligand for PSGL-1 receptor on T cells suppressing T cell function (Fig. 3) [151]. This unique pH-dependent VISTA/PSGL-1 interaction suggests that engineering pH-sensitive antibodies might enable selective targeting of VISTA within the acidic TME to reverse cancer-mediated immune suppression without compromising self-tolerance and inducing autoimmunity [151]. Thus, targeting the VISTA pathway can be achieved in a context-dependent manner to overcome the immunosuppressive TME and reinvigorate responses of tumor-specific T cells.

5.1. T regulatory cells of the TME and implications in cancer immunotherapy

It has been previously established that inhibition of Akt and its downstream target mTOR is required to induce Treg differentiation and sustain Treg suppressor function [152,153]. PD-1 ligation inhibits Akt activation [127] and synergizes with TGF- β to induce FoxP3⁺ iTreg cells with potent suppressive capacity [154]. Moreover, PD-1 promotes fatty acid oxidation [128], a metabolic program that supports the differentiation, survival and function of Treg cells [155]. Based on these, one would anticipate that PD-1 promotes Treg generation and suppressor function. However, recent studies revealed an unexpected connection between PD-1 expression in Treg cells and the outcome of PD-1 pathway blockade [156]. In humans, FoxP3⁺CD4⁺ Treg cells represent a heterogeneous population that can be subdivided into three functionally and phenotypically distinct subsets [157]. Thymus derived naïve Tregs (nTreg: CD45RA⁺ FOXP3^{lo}) and activated effector-Tregs (eTreg: CD45RA⁻ FOXP3^{hi}) are highly suppressive while the CD45RA⁻ FOXP3^{lo} Treg cells represent a non-Treg population with a potential of inflammatory cytokine production. Among these Treg subsets, FoxP3⁺ Tregs infiltrating the TME in most cancers are predominantly the eTreg cells [158]. Expression of PD-1 was found in eTreg cells and the frequency of PD-1⁺ eTreg cells was higher in tumor samples from patients who did not respond to PD-1-blocking immunotherapy. Notably, blockade of the PD-1: PD-L1 pathway induced activation of eTreg in TILs, as determined by upregulation of CTLA-4, GITR and ICOS and these Treg obtained a more potent suppressor function. These results highlight a previously unappreciated role of PD-1 signaling in Tregs and suggest that PD-1 blockade enhances the suppressive activity of Tregs that express high

levels of PD-1. While blocking PD-1 in PD-1⁺ CD8⁺ T cells converts them to CD8⁺ Teff cells that have potent effector function leading to tumor regression, blocking PD-1 in PD-1⁺ Treg converts them to activated eTreg that have potent suppressor function leading to tumor progression. Thus, PD-1 expression balance between CD8⁺ Teff cells and eTreg in the TME that might predict the clinical efficacy of PD-1 blocking immunotherapy.

6. T cell differentiation and cancer immunosurveillance

CD8⁺ T cells play an important role in the adaptive immune response to intracellular pathogens and cancer [159]. Therapeutic responses to PD-1 checkpoint immunotherapy correlate with expansion of CD8⁺ memory T cells in mouse tumor models and patients [160]. Immunometabolic programs have a causative role in T cell differentiation and their immune function [161,162]. This is particularly important in the metabolically stressful TME where nutrient competition, hypoxia, excess ROS and metabolic byproducts of cancer cells create uniquely hostile conditions under which T cell activation by and cytotoxic function should be operated [163–165]. Although glycolysis has been intimately linked to effector function [166,167], augmenting glycolytic flux drives CD8⁺ T cells toward a terminally differentiated state, while its inhibition preserves the formation of long-lived T_M CD8⁺ T cells [168]. Thus, multiple signaling pathways and mediators of metabolic reprogramming, such as mTOR, SREBP, Myc [169–172], have important roles in immune-mediated tumor control by guiding differentiation and function of T cells in the context of cancer [172–175]. After stimulation with antigen, CD8⁺ naive T cells expand and differentiate into T_{EFF} cells and distinct T_M cell subsets, including T_{SCM}, T_{CM}, and T_{EM} [176]. Preclinical studies using adoptive transfer of purified CD8⁺ T cell populations revealed that less-differentiated T cells with features of T_{SCM} and T_{CM} mediate enhanced antitumor and antiviral responses compared with more-differentiated T_{EM} and T_{EFF} cells [177–179]. Preservation of T_{SCM} and T_{CM} cells with a quiescent phenotype and increased proliferative and survival capacities enhance T cell ability to maintain sustained anti-tumor control [180]. For example, Wnt signaling prevents T_{EFF} differentiation, while promoting the generation of T_{SCM} that maintain stemness and pluripotency and display long-lasting potent anti-tumor properties [179].

7. Tissue resident memory cells (T_{RM}) are novel regulators of anti-tumor immunity

Memory T cells have been classically divided into two subsets [181]. T_{EM} cells create immediate effector function to inflamed tissues whereas central memory T cells (T_{CM}) accumulate in secondary lymphoid organs and generate protective immunity [181,182]. Recently, a distinct T memory cell population, named tissue-resident memory T cells (T_{RM}) were identified and classified by their unique phenotype and properties. These cells reside permanently in peripheral non-lymphoid tissues and provide a protective effect against infections and cancer [183,184]. T_{RM} cells have been identified and investigated both in mice and humans in many tissues including skin, gut, brain and liver [185–187]. Although T_{RM} cells were defined as either CD4⁺ or CD8⁺, only CD8⁺ T_{RM} play a major role in cancer immunosurveillance and tumor prognosis [188–190]. Traditionally, CD8⁺ T_{RM} are defined by the co-expression of CD103, CD69 and/or CD49 [191], and downregulation of receptors that promote T cell recirculation including S1pr1, CD62L (L-selectin) and CCR7 [192–194]. CD103 integrin, formed by αE (CD103) and β7 subunits, promotes T_{RM} cells retention and homing to epithelial tissue and tumors [195–197]. T_{RM} cells have an established role in protective immunity in bacterial, viral infections and autoimmune diseases, including *Listeria monocytogenes* and Herpes Simplex infections and vitiligo.

An important role of T_{RM} in cancer is currently evolving. In a model of melanoma-associated vitiligo (MAV), using adoptive pmel cells which have a TCR that can detect melanoma gp100 antigen, it was shown that

adoptively transferred pmel T cells acquired a T_{RM} immunological profile with a CD103⁺CD69⁺CD62L^{lo} phenotype in the skin, draining lymph nodes, lung, and liver [198]. In this context, T_{RM} cells had a protective function against metastasis and expressed transcripts different from T_{CM} cells, characterized by features of effector function and lipid metabolism. In a mouse model of epidermal melanoma, it was also determined that T_{RM} have a role in promoting melanoma immune equilibrium [189]. Mice that did not develop melanoma (non-developer group) had higher numbers of CD69⁺CD103⁺ T_{RM} cells than tumor-developer mice. In addition, intact skin from the non-developer group, peritumoral area, and tumoral area showed higher number of T_{RM} cells. Notably, both CD69 and CD103 knock-out mice are more susceptible to melanoma formation than wild type counterparts, indicating the causative role of CD69 and CD103 proteins in regulating T_{RM} development and anti-tumor function [189]. Other studies have shown that CD103⁺ T_{RM} cells can protect against melanoma re-exposure providing evidence for the long-lasting ability of T_{RM} to provide cancer immunosurveillance [199]. In many types of cancer, CD8⁺ T_{RM} cells display robust production of cytokines such as granzyme B, granzyme A, perforin, and IFN-γ [198,200–203]. Importantly, recent work, using a VHL deficiency mouse model, provided evidence for a link between HIF-1α and CD103 expression and showed that HIF-1α expression supported enhanced differentiation of T_{RM} cells with cytotoxic function [200,203]. These findings link HIF-1α, a key signature molecule of the TME, with T_{RM} differentiation and function and underline the direct relevance of T_{RM} in anti-tumor immunity.

T_{RM} cells express checkpoint receptors, and might serve as markers for prognosis prediction. In melanoma patients, T_{RM} express PD-1, TIM-3, and PD-L1 at higher levels than peripheral blood T cells. Single-cell RNA sequencing of T cells isolated from human breast cancer demonstrated a high number of T_{RM} cells with a high level of TIM-3, PD-1, CTLA-4, TIGIT, and LAG-3 expression [190]. In lung cancer, PD-1, TIM-3, and CD137 are highly expressed [202,204]. After ex vivo pharmacologic stimulation of PD-1⁺CD103⁺ CD8 TILs from ovarian cancer, these T_{RM}-like cells highly expressed TIM-3, CTLA-4, and LAG-3 [205, 206]. In lung cancer patients, after anti-PD-1 treatment, T_{RM} cells upregulated PD-1, CTLA-4, TIM-3, TIGIT, and CD39 [207], whereas in melanoma patients PD-1 checkpoint immunotherapy resulted in T_{RM}-specific upregulation of PD-1 and LAG-3 [208]. Notably, the number of T_{RM} cells is correlated with a better response to PD-1 checkpoint immunotherapy and a favorable prognosis in multiple cancers including melanoma, breast cancer, lung cancer, urothelial cancer, ovarian cancer and cervical cancer [205,208–215]. The unravelling role of T_{RM} cells in cancer evolution and response to immunotherapy suggest that T_{RM} might be a promising novel target for therapeutic exploitation in cancer.

8. Innate lymphoid cells and their role in cancer immunotherapy

Innate lymphoid cells (ILCs), which lack antigen-specific receptors, are considered as the innate equivalents of T cells. The most recent nomenclature classifies ILCs into five groups, namely ILC1s, ILC2s, ILC3s which are the equivalent of Th1, Th2, and Th17 CD4⁺ T helper (Th) cells, respectively, natural killer (NK) cells, which are the equivalent of CD8⁺ cytotoxic T cells, and lymphoid tissue-inducer cells (LTis), a unique subset involved in the development of secondary lymphoid organs [216]. With the exception of the highly mobile and constantly circulating NK cells, ILCs are largely tissue-resident cells. Besides their main role of immune surveillance and tissue homeostasis, ILCs have emerged as critical players in cancer growth and therapy [217]. ILCs express a plethora of activating and inhibitory receptors [218]. Among the latter, checkpoint inhibitory receptors increasingly raise attention due to their role in tumor immunotherapy. Here, we summarize the current knowledge on the role of checkpoint inhibitory receptors in ILCs in the context of cancer.

8.1. Natural Killer (NK) cells

NK cells belong to a highly diverse subset of ILCs that circulate between peripheral organs, exerting cytotoxic activity that can directly eliminate cancer cells or cells undergoing microbial infections [219–221]. In healthy adults, NK cells comprise about 5–15% of circulating lymphocytes with the majority of healthy tissues mainly consisting of the mature highly cytolytic CD56^{dim} NK cell subset, while the immature and poorly cytolytic CD56^{bright} subset, although also present in healthy tissues, it becomes significantly enriched in cancer [222]. A plethora of activating and inhibitory receptors regulate NK cell development and function, with the dominant signal being inhibitory, resulting primarily from the interactions of certain NK cell inhibitory receptors with major histocompatibility complex class I (MHC-I) molecules [223,224]. These “classical” NK inhibitory receptors include the group of Killer Ig-like receptors (KIRs) in humans and the LY49 group of receptors in rodents, as well as the CD94/NKG2A receptor (Fig. 4A), which also recognizes HLA-E in humans and Qa-1b in mice [218, 223–228]. According to the “missing self” hypothesis [229], these inhibitory receptors have the unique ability to prevent NK cell responses against self, and allow NK cells to exert their cytotoxic activity against cells that have reduced or absent expression of MHC-I molecules. However, in the context of cancer, these NK inhibitory receptors hamper NK cell responses and contribute to tumor cell escape from elimination. Blocking antibodies, usually termed “immune checkpoint inhibitors” against KIRs (lirilumab) [230] and NKG2A (monalizumab) [231], which aim to improve NK cell function, are in phase I/II clinical trials against a range of hematologic malignancies and solid tumors either as mono- or combination therapy [232,233]. In addition, adoptive transfer of NK cells engineered to downregulate NKG2A in immunodeficient mice, efficiently prevented HLA-E⁺ tumor-mediated suppression leading to increased anti-tumor activity, suggesting this as a promising approach to be tested in a clinical setting [234].

Besides the classical inhibitory receptors, NK cells also express checkpoint inhibitory receptors (Fig. 4A). Expression of programmed cell death 1 (PD-1) was found on NK cells from healthy individuals correlating with prior HCMV infection [235]. Notably, PD-1 expression has been found to be restricted to the fully mature CD56^{dim} or to the CD56^{neg} NK compartment and not to the immature CD56^{bright} NK cell subset [236]. PD-1 is also expressed on NK cells in the context of cancer. PD-1⁺ NK cells were detected in the peripheral blood of patients with multiple myeloma, Kaposi sarcoma and lung cancer patients [237–239],

in pleural effusions from primary mesothelioma or metastatic adenocarcinoma patients [240], in the peritoneal fluid of high-grade peritoneal carcinomatosis patients [241], and in the peripheral blood and ascitic fluid of ovarian carcinoma patients, with both mRNA and protein PD-1 levels to be higher in the CD56^{dim} NK cell subset [242]. In contrast, PD-1 expression was found to be higher in CD56^{bright} than CD56^{dim} mature NK cells from blood and tissues from patients with Hodgkin lymphoma [243]. As in T cells, blockade of the PD-1/PD-L1 axis in NK cells could improve anti-tumor activity [243,244]. Interestingly, glucocorticoids present in the TME were found to be indispensable for PD-1 induction on human NK cells, particularly when combined with the inflammatory cytokines interleukin (IL)—12, IL-15 and IL-18, which are abundant at the tumor site [245]. In addition, expression of the PD-1 ligand, PD-L1, on NK cells has been associated with a regulatory function, limiting DC-mediated tumor antigen cross-presentation to CD8⁺ cells and resulting in impaired memory responses [246].

The inhibitory receptor cytotoxic T-lymphocyte-associated protein 4 (CTLA-4) has also been detected on NK cells from mice [247], in the blood from healthy donors and in the blood and tissues from cancer patients [248,249]. Similarly to PD-1, CTLA-4 was found to be predominantly expressed on CD56^{dim} NK cells from the blood of healthy individuals and was associated with decreased NK cell functionality [249]. These findings explain why CTLA-4 blockade, besides T cells, was also found to favor NK cell infiltration and antitumor function [250]. Of note, treatment with anti-CTLA-4 antibody could favor NK cell anti-tumor function indirectly, by depleting CTLA-4-expressing intratumoral regulatory T cells (Treg) [247].

Other checkpoint inhibitory receptors such as TIM-3, LAG-3, TIGIT, CD96 (TACTILE) have also been identified in NK cells (Fig. 4A). Although mostly considered as an inhibitory receptor [251,252], TIM-3 has also been reported to have an activation role in NK cells [253]. Higher TIM-3 expression has been observed on the CD56^{dim} NK cell subset, while on the CD56^{bright} cell subset it may be upregulated upon cytokine stimulation [251]. In the context of cancer, TIM-3 has been detected in NK cells from patients with advanced melanoma [254,255], gastric cancer [256], lung adenocarcinoma [257], and bladder cancer [258]. Increased TIM-3 expression was found in both CD56^{dim} and CD56^{bright} NK cell subsets, correlating with shorter overall survival [257]. Conversely, blockade of TIM-3 signals with TIM-3-specific antibodies improved NK cell functions in vitro [254,257].

LAG-3 acts synergistically with PD-1 and contributes to T cell and NK cell dysfunction, exhaustion [259] and tumor escape [260]. Several

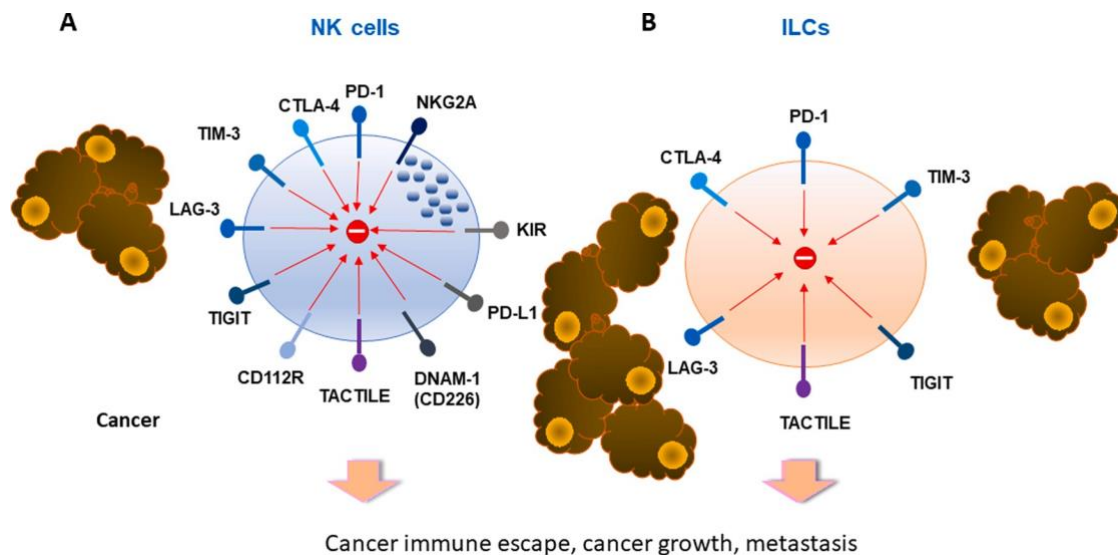


Fig. 4. NK cells and ILCs express multiple inhibitory receptors. NK cells express the classical inhibitory receptors KIR and NKG2A. Both NK cells and ILC express multiple checkpoint inhibitors. These receptors and their ligands offer new therapeutic opportunities to improve NK cell functions for cancer immunotherapy.

years of efforts testing LAG-3 as promising checkpoint blockade therapy recently led to the first approval of LAG-3 blocking antibody (relatlimab-rmbw) for combination therapy together with PD-1 antibody nivolumab (Opdualag) for the treatment of patients with unresectable or metastatic melanoma. An alternative approach used a LAG-3-Ig fusion protein (IMP321) as a soluble high affinity MHC-II agonist to enhance antigen presenting function. Treatment with IMP321 as monotherapy enhanced IFN- γ and TNF- α production in NK cells from control donors and cancer patients *ex vivo* [261], and was also shown to increase the number and activation of NK cells in the blood of breast cancer patients in combination with standard chemotherapy [262].

A separate group of receptors, also referred to as novel NK cell immune checkpoints, includes the inhibitory receptors TIGIT and CD112R [263] as well as the costimulatory receptor CD226 (DNAM-1) [264], and CD96 (TACTILE) for which both inhibitory and costimulatory functions have been reported [265,266]. These receptors interact with molecules of the nectin family CD155 (PVR) and CD112 (Nectin-2) (Fig. 4A) [267], two ligands with ubiquitous low level expression, often up-regulated in cancer cells [268,269] and myeloid suppressor cells within the TME [270,271]. TIGIT is expressed by activated T cells and NK cells and binds its ligands CD155 and CD112 expressed on antigen presenting cells (APC) [272]. Expression of these ligands by several cancer types results in T cell and NK cell exhaustion, impaired tumor immune infiltration and compromised antitumor function [273–275]. The TIGIT pathway and its related receptors and ligands offer new options for antibody-based blocking strategies, which have shown to improve tumor control in mice particularly when combined with PD-1/PD-L1 or CTLA-4 blockade [276].

8.2. Helper ILCs

Recent studies suggest that checkpoint receptors are involved in the immune responses of helper ILC subsets and have important implications in anti-tumor immunity (Fig. 4B). However, little information is currently available regarding the mechanisms by which these receptors regulate helper ILC functions. Although not detected in helper ILCs from healthy human tissue samples [277], PD-1 is expressed on tumor-associated helper ILC populations [278]. It was recently reported that helper ILC subsets are present in human malignant pleural effusions, with a notable PD-1 expression level on the ILC3 subset [240]. Another study, using single-cell RNA sequencing and a CRC mouse model associated with AOM/DSS-induced colitis, identified high-PD-1-expressing ILC2 infiltrates and demonstrated the importance of this specific subset in tumor progression [279]. Furthermore, PD-1⁺ ILC2 cells were present in most human PDAC tissues as well as in orthotopic PDAC tumors in mice, in which PD-1 blockade, resulted in ILC2 expansion and improved antitumor immunity [280]. These findings suggest the potential role of ILC2 cells as tissue-specific enhancers of cancer immunity that may amplify the efficacy of anti-PD-1 immunotherapy.

Similarly to PD-1, CTLA-4 expression was found to be very low in helper ILCs from healthy donors [281], but is increased in helper ILC subsets within tumor tissues [278]. High CTLA-4 expression has also been reported on intratumoral ILC1 subsets in mice [282]. Although TIM-3 has been detected on ILC3s from human decidua during pregnancy and inhibiting IL-22 production [283], currently very limited information is known regarding TIM-3 expression on helper ILCs in the context of cancer. Transcriptomic and immunophenotyping analyses in mouse and human cSCCs identified infiltration of functionally impaired NK and ILC1 cells characterized by reduced cytotoxicity and IFN- γ secretion, which correlated with decreased expression of activating receptors and increased expression of exhaustion markers including TIGIT on NK cells, and PD-1 and TIM-3 on ILC1s [284]. LAG-3 expression has not been reported in resting ILCs, but in the context of cancer and upon TGF- β -mediated conversion of NK to ILC1 cells, several checkpoint receptors were upregulated, among which LAG-3, TIGIT and CD96

expression has been documented [282]. The functional effects of blocking these receptors on helper ILCs remain to be determined.

9. Concluding remarks

Profiling the immune cells in the TME of patients with evolving techniques has revealed significant information regarding the immune cell composition of the TME in experimental animal models and patients with various types of cancer. It is increasingly understood that the immune cellular components of the TME, including DCs, TAMs and MDSCs have decisive roles in regulating cancer evolution and immune escape but also the outcomes of cancer therapy including chemotherapy, checkpoint immunotherapy and cancer vaccines. Although in healthy tissues these myeloid cells provide defense against insults mediated by pathogens, in the TME these cells lose their protective immune functions and convert to pro-tumorigenic mediators that support cancer growth and metastasis. Via such changes, myeloid cell populations fail to recruit T cells, present tumor antigens and mediate anti-tumor T cell responses. Instead, these myeloid cells suppress T cell activation by blunting recognition of tumor antigens, eliminating engagement of costimulatory pathways, upregulating the expression of inhibitory receptors and their ligands, and producing inhibitory soluble mediators thereby creating an immunosuppressive milieu. Engagement of inhibitory receptors on T cells of the TME impairs signaling events mediated by T cell receptor and costimulatory pathways and promotes generation of T_{EX} tumor-specific cells that are unable to mount anti-tumor responses. The TME also promotes differentiation of iTreg by T cell receptor engagement by tumor antigens and concomitant ligation of coinhibitory receptors, and production of Treg-promoting soluble factors such as TGF- β and IL-10. Together these mechanisms abrogate cancer immunosurveillance and support cancer evolution and immune escape. Although checkpoint blockade and cell-based therapies have achieved significant progress, challenges ahead include advancing the outcome of immunotherapy by targeting changes of the TME that compromise the function of key immune populations and preclude their ability to recognize and respond to tumor antigens. Such tentative targets for intervention include metabolic alterations, vasculature abnormalities and soluble inhibitors produced in the TME. Such efforts might repurpose available drugs previously used in the clinic, which can be administered together or sequentially with immunomodulating immunotherapies and cell-based therapies. In doing so, an additional challenge will be to achieve cancer elimination while preserving self-tolerance and preventing autoimmunity.

CRedit authorship contribution statement

SY, KA, QW, AC, RS wrote the main sections of the manuscript. NP generated sections of the manuscript and prepared figures. VAB generated sections of the manuscript, prepared figures, guided the co-authors and was responsible for the organization of the document.

Competing interests

VAB has patents on the PD-1 pathway licensed by Bristol-Myers Squibb, Roche, Merck, EMD-Serono, Boehringer Ingelheim, AstraZeneca, Novartis, and Dako. The authors declare no other competing interests.

Acknowledgments

This work was supported by NIH grants R01CA238263, R01CA229784, R01CA212605 (VAB); and grants JDRF (International 1-INO-2002-1119-A-N) and Sanofi (iAwards SRA 2020-0033) (NP).

Conflict of interest

VAB has patents on the PD-1 pathway licensed by Bristol-Myers Squibb, Roche, Merck, EMD-Serono, Boehringer Ingelheim, AstraZeneca, Novartis, and Dako. The authors declare no other competing interests.

References

- [1] R.D. Schreiber, L.J. Old, M.J. Smyth, Cancer immunoeediting: integrating immunity's roles in cancer suppression and promotion, *Science* 331 (6024) (2011) 1565–1570.
- [2] M. Lecoultré, V. Dutoit, P.R. Walker, Phagocytic function of tumor-associated macrophages as a key determinant of tumor progression control: a review, *J. Immunother.* *Cancer* 8 (2020) 2.
- [3] D. Hirayama, T. Iida, H. Nakase, The phagocytic function of macrophage-enforcing innate immunity and tissue homeostasis, *Int. J. Mol. Sci.* 19 (1) (2017).
- [4] T.N. Schumacher, W. Scheper, P. Kvistborg, Cancer neoantigens, *Annu. Rev. Immunol.* 37 (2019) 173–200.
- [5] N.A. Rizvi, et al., Cancer immunology. Mutational landscape determines sensitivity to PD-1 blockade in non-small cell lung cancer, *Science* 348 (6230) (2015) 124–128.
- [6] A. Snyder, et al., Genetic basis for clinical response to CTLA-4 blockade in melanoma, *New Engl. J. Med.* 371 (23) (2014) 2189–2199.
- [7] G. Bindea, et al., Spatiotemporal dynamics of intratumoral immune cells reveal the immune landscape in human cancer, *Immunity* 39 (4) (2013) 782–795.
- [8] R.S. Herbst, et al., Predictive correlates of response to the anti-PD-L1 antibody MPDL3280A in cancer patients, *Nature* 515 (7528) (2014) 563–567.
- [9] J. Galon, et al., Type, density, and location of immune cells within human colorectal tumors predict clinical outcome, *Science* 313 (5795) (2006) 1960–1964.
- [10] W.C. Hahn, et al., An expanded universe of cancer targets, *Cell* 184 (5) (2021) 1142–1155.
- [11] S. Spranger, et al., Up-regulation of PD-L1, IDO, and T(regs) in the melanoma tumor microenvironment is driven by CD8(+) T cells, *Sci. Transl. Med.* 5 (200) (2013) 200ra116.
- [12] M.S. Rooney, et al., Molecular and genetic properties of tumors associated with local immune cytolytic activity, *Cell* 160 (1–2) (2015) 48–61.
- [13] M. Binnewies, et al., Understanding the tumor immune microenvironment (TIME) for effective therapy, *Nat. Med.* 24 (5) (2018) 541–550.
- [14] T.L. Murphy, K.M. Murphy, Dendritic cells in cancer immunology, *Cell Mol. Immunol.* 19 (1) (2022) 3–13.
- [15] M. Broz, et al., Dissecting the tumor myeloid compartment reveals rare activating antigen-presenting cells critical for T cell immunity, *Cancer Cell* 26 (5) (2014) 638–652.
- [16] L. Amon, et al., The ontogenetic path of human dendritic cells, *Mol. Immunol.* 120 (2020) 122–129.
- [17] M. Collin, V. Bigley, Human dendritic cell subsets: an update, *Immunology* 154 (1) (2018) 3–20.
- [18] K. Hildner, et al., Batf3 deficiency reveals a critical role for CD8alpha+ dendritic cells in cytotoxic T cell immunity, *Science* 322 (5904) (2008) 1097–1100.
- [19] I. Leal Rojas, et al., Human blood CD1c+ dendritic cells promote Th1 and Th17 effector function in memory CD4+ T cells, *Front Immunol.* 8 (2017) 971.
- [20] A. Villani, et al., Single-cell RNA-seq reveals new types of human blood dendritic cells, monocytes, and progenitors, *Science* 356 (6335) (2017) eaah4573.
- [21] C. Brown, et al., Transcriptional basis of mouse and human dendritic cell heterogeneity, *Cell* 179 (4) (2019) 846–863.e24.
- [22] E. Kvedaraitė, F. Ginhoux, Human dendritic cells in cancer, *Sci. Immunol.* 7 (70) (2022) eabm9409.
- [23] U. Cytlak, et al., Differential IRF8 transcription factor requirement defines two pathways of dendritic cell development in humans, *Immunity* 53 (2) (2020) 353–370.e8.
- [24] P. Bourdely, et al., Transcriptional and functional analysis of CD1c+ human dendritic cells identifies a CD163+ subset priming CD8+CD103+ T Cells, *Immunity* 53 (2) (2020) 335–352.e8.
- [25] C. Caux, et al., GM-CSF and TNF-alpha cooperate in the generation of dendritic Langerhans cells, *Nature* 360 (6401) (1992) 258–261.
- [26] F. Sallusto, A. Lanzavecchia, Efficient presentation of soluble antigen by cultured human dendritic cells is maintained by granulocyte/macrophage colony-stimulating factor plus interleukin 4 and downregulated by tumor necrosis factor alpha, *J. Exp. Med.* 179 (4) (1994) 1109–1118.
- [27] A. Lehtonen, et al., Differential expression of IFN regulatory factor 4 gene in human monocyte-derived dendritic cells and macrophages, *J. Immunol.* 175 (10) (2005) 6570–6579.
- [28] F. Geissmann, et al., Development of monocytes, macrophages, and dendritic cells, *Science* 327 (5966) (2010) 656–661.
- [29] N. Nagarsheth, M. Wicha, W. Zou, Chemokines in the cancer microenvironment and their relevance in cancer immunotherapy, *Nat. Rev. Immunol.* 17 (9) (2017) 559–572.
- [30] J. Böttcher, et al., NK cells stimulate recruitment of cDC1 into the tumor microenvironment promoting cancer immune control, *Cell* 172 (5) (2018) 1022–1037.e14.
- [31] S. Zelenay, et al., Cyclooxygenase-dependent tumor growth through evasion of immunity, *Cell* 162 (6) (2015) 1257–1270.
- [32] K. Barry, et al., A natural killer-dendritic cell axis defines checkpoint therapy-responsive tumor microenvironments, *Nat. Med.* 24 (8) (2018) 1178–1191.
- [33] P. Shrikant, M. Mescher, Control of syngeneic tumor growth by activation of CD8+ T cells: efficacy is limited by migration away from the site and induction of nonresponsiveness, *J. Immunol.* 162 (5) (1999) 2858–2866.
- [34] K. Asano, et al., CD169-positive macrophages dominate antitumor immunity by crosspresenting dead cell-associated antigens, *Immunity* 34 (1) (2011) 85–95.
- [35] H. Salmon, et al., Expansion and activation of CD103(+) dendritic cell progenitors at the tumor site enhances tumor responses to therapeutic PD-L1 and BRAF inhibition, *Immunity* 44 (4) (2016) 924–938.
- [36] E. Roberts, et al., Critical role for CD103(+)/CD141(+) dendritic cells bearing ccr7 for tumor antigen trafficking and priming of T cell immunity in melanoma, *Cancer Cell* 30 (2) (2016) 324–336.
- [37] M. Mikucki, et al., Non-redundant requirement for CXCR3 signalling during tumoricidal T-cell trafficking across tumour vascular checkpoints, *Nat. Commun.* 6 (2015) 7458.
- [38] M. Kurachi, et al., Chemokine receptor CXCR3 facilitates CD8(+) T cell differentiation into short-lived effector cells leading to memory degeneration, *J. Exp. Med.* 208 (8) (2011) 1605–1620.
- [39] S. Spranger, et al., Tumor-residing Batf3 dendritic cells are required for effector T cell trafficking and adoptive T cell therapy, *Cancer Cell* 31 (5) (2017) 711–723.e4.
- [40] D. Hanahan, Hallmarks of cancer: new dimensions, *Cancer Discov.* 12 (1) (2022) 31–46.
- [41] M. Meyer, et al., Breast and pancreatic cancer interrupt IRF8-dependent dendritic cell development to overcome immune surveillance, *Nat. Commun.* 9 (1) (2018) 1250.
- [42] B. Ruffell, et al., Macrophage IL-10 blocks CD8+ T cell-dependent responses to chemotherapy by suppressing IL-12 expression in intratumoral dendritic cells, *Cancer Cell* 26 (5) (2014) 623–637.
- [43] D. Herber, et al., Lipid accumulation and dendritic cell dysfunction in cancer, *Nat. Med.* 16 (8) (2010) 880–886.
- [44] J. Kobbie, et al., Transforming growth factor beta inhibits the antigen-presenting functions and antitumor activity of dendritic cell vaccines, *Cancer Res* 63 (8) (2003) 1860–1864.
- [45] T. Lim, et al., PD-1 expression on dendritic cells suppresses CD8+ T cell function and antitumor immunity, *Oncotarget* 5 (3) (2016), e1085146.
- [46] V. Boussiotis, Molecular and biochemical aspects of the PD-1 checkpoint pathway, *New Engl. J. Med.* 375 (18) (2016) 1767–1778.
- [47] X. Zhao, et al., Phosphorylation and stabilization of PD-L1 by CK2 suppresses dendritic cell function, *Cancer Res* (2022) p. canres.2300.2021.
- [48] M. Gapany, et al., Association of elevated protein kinase CK2 activity with aggressive behavior of squamous cell carcinoma of the head and neck, *Mol. Med* 1 (6) (1995) 659–666.
- [49] J. Lau, et al., Tumour and host cell PD-L1 is required to mediate suppression of anti-tumour immunity in mice, *Nat. Commun.* 8 (2017) 14572.
- [50] S. Oh, et al., PD-L1 expression by dendritic cells is a key regulator of T-cell immunity in cancer, *Nat. Cancer* 1 (7) (2020) 681–691.
- [51] A. Chaudhri, et al., PD-L1 Binds to B7-1 Only In Cis on the Same Cell Surface, *Cancer Immunol. Res* 6 (8) (2018) 921–929.
- [52] S. Haile, et al., Tumor cell programmed death ligand 1-mediated T cell suppression is overcome by coexpression of CD80, *J. Immunol.* 186 (12) (2011) 6822–6829.
- [53] Y. Zhao, et al., Antigen-presenting cell-intrinsic PD-1 neutralizes PD-L1 in cis to attenuate PD-1 signaling in T cells, *Cell Rep.* 24 (2) (2018) 379–390.e6.
- [54] D. Sugiura, et al., Restriction of PD-1 function by cis-PD-L1/CD80 interactions is required for optimal T cell responses, *Science* 364 (6440) (2019) 558–566.
- [55] M. Mayoux, et al., Dendritic cells dictate responses to PD-L1 blockade cancer immunotherapy, *Sci. Transl. Med.* 12 (534) (2020) eaav7431.
- [56] L. Karyampudi, et al., PD-1 blunts the function of ovarian tumor-infiltrating dendritic cells by inactivating NF-κB, *Cancer Res* 76 (2) (2016) 239–250.
- [57] S. Chiba, et al., Tumor-infiltrating DCs suppress nucleic acid-mediated innate immune responses through interactions between the receptor TIM-3 and the alarmin HMGB1, *Nat. Immunol.* 13 (9) (2012) 832–842.
- [58] A. de Mingo Pulido, et al., TIM-3 regulates CD103+ dendritic cell function and response to chemotherapy in breast cancer, *Cancer Cell* 33 (1) (2018) 60–74.e6.
- [59] K. Dixon, et al., TIM-3 restrains anti-tumour immunity by regulating inflammasome activation, *Nature* 595 (7865) (2021) 101–106.
- [60] N. Caronni, et al., TIM4 expression by dendritic cells mediates uptake of tumor-associated antigens and anti-tumor responses, *Nat. Commun.* 12 (1) (2021) 2237.
- [61] D. Anderson, et al., Genetic models of human and mouse dendritic cell development and function, *Nat. Rev. Immunol.* 21 (2) (2021) 101–115.
- [62] L. Amon, et al., Transcriptional control of dendritic cell development and functions, *Int. Rev. Cell Mol. Biol.* 349 (2019) 55–151.
- [63] M. Binnewies, et al., Unleashing type-2 dendritic cells to drive protective antitumor CD4+ T cell immunity, *Cell* 177 (3) (2019) 556–571.e16.
- [64] D. Mittag, et al., Human dendritic cell subsets from spleen and blood are similar in phenotype and function but modified by donor health status, *J. Immunol.* 186 (11) (2011) 6207–6217.
- [65] E. Segura, et al., Human inflammatory dendritic cells induce Th17 cell differentiation, *Immunity* 38 (2) (2013) 336–348.
- [66] X. Wu, et al., MafB lineage tracing to distinguish macrophages from other immune lineages reveals dual identity of Langerhans cells, *J. Exp. Med.* 213 (12) (2016) 2553–2565.

- [67] D. Laoui, et al., The tumour microenvironment harbours ontogenically distinct dendritic cell populations with opposing effects on tumour immunity, *Nat. Commun.* 7 (2016) 13720.
- [68] S. Kuhn, J. Yang, F. Ronchese, Monocyte-derived dendritic cells are essential for CD8(+) T cell activation and antitumor responses after local immunotherapy, *Front Immunol.* 6 (2015) 584.
- [69] I. Treilleux, et al., Dendritic cell infiltration and prognosis of early stage breast cancer, *Clin. Cancer Res* 10 (22) (2004) 7466–7474.
- [70] S. Labidi-Galy, et al., Quantitative and functional alterations of plasmacytoid dendritic cells contribute to immune tolerance in ovarian cancer, *Cancer Res* 71 (16) (2011) 5423–5434.
- [71] K. Bruchhage, et al., IL-10 in the microenvironment of HNSCC inhibits the CpG ODN induced IFN- α secretion of pDCs, *Oncol. Lett.* 15 (3) (2018) 3985–3990.
- [72] C. Conrad, et al., Plasmacytoid dendritic cells promote immunosuppression in ovarian cancer via ICOS costimulation of Foxp3(+) T-regulatory cells, *Cancer Res* 72 (20) (2012) 5240–5249.
- [73] F. Veglia, E. Sanseviero, D.I. Gabrilovich, Myeloid-derived suppressor cells in the era of increasing myeloid cell diversity, *Nat. Rev. Immunol.* (2021).
- [74] V. Bronte, et al., Recommendations for myeloid-derived suppressor cell nomenclature and characterization standards, *Nat. Commun.* 7 (2016) 12150.
- [75] L. Wang, et al., VISTA is highly expressed on MDSCs and mediates an inhibition of T cell response in patients with AML, *Oncoimmunology* 7 (9) (2018), e1469594.
- [76] L. Wang, et al., VISTA, a novel mouse Ig superfamily ligand that negatively regulates T cell responses, *J. Exp. Med* 208 (3) (2011) 577–592.
- [77] D.B. Flies, et al., Cutting edge: a monoclonal antibody specific for the programmed death-1 homolog prevents graft-versus-host disease in mouse models, *J. Immunol.* 187 (4) (2011) 1537–1541.
- [78] J. Deng, et al., Hypoxia-induced VISTA promotes the suppressive function of myeloid-derived suppressor cells in the tumor microenvironment, *Cancer Immunol. Res.* 7 (7) (2019) 1079–1090.
- [79] I. Le Mercier, et al., VISTA regulates the development of protective antitumor immunity, *Cancer Res* 74 (7) (2014) 1933–1944.
- [80] V. Prima, et al., COX2/mPGES1/PGE2 pathway regulates PD-L1 expression in tumor-associated macrophages and myeloid-derived suppressor cells, *Proc. Natl. Acad. Sci. USA* 114 (5) (2017) 1117–1122.
- [81] C. Lu, et al., The expression profiles and regulation of PD-L1 in tumor-induced myeloid-derived suppressor cells, *Oncoimmunology* 5 (12) (2016), e1247135.
- [82] M.Z. Noman, et al., PD-L1 is a novel direct target of HIF-1 α , and its blockade under hypoxia enhanced MDSC-mediated T cell activation, *J. Exp. Med* 211 (5) (2014) 781–790.
- [83] L. Strauss, et al., Targeted deletion of PD-1 in myeloid cells induces antitumor immunity, *Sci. Immunol.* 5 (43) (2020).
- [84] P.E. Clavijo, et al., Resistance to CTLA-4 checkpoint inhibition reversed through selective elimination of granulocytic myeloid cells, *Oncotarget* 8 (34) (2017) 55804–55820.
- [85] Y. Li, et al., Targeting myeloid-derived suppressor cells to attenuate vasculogenic mimicry and synergistically enhance the anti-tumor effect of PD-1 inhibitor, *iScience* 24 (12) (2021), 103392.
- [86] W. Kim, et al., PD-1 signaling promotes tumor-infiltrating myeloid-derived suppressor cells and gastric tumorigenesis in mice, *Gastroenterology* 160 (3) (2021) 781–796.
- [87] K. Kim, et al., Eradication of metastatic mouse cancers resistant to immune checkpoint blockade by suppression of myeloid-derived cells, *Proc. Natl. Acad. Sci. USA* 111 (32) (2014) 11774–11779.
- [88] A. Mantovani, et al., Chemokines in the recruitment and shaping of the leukocyte infiltrate of tumors, *Semin Cancer Biol.* 14 (3) (2004) 155–160.
- [89] A. Robinson, et al., Monocyte regulation in homeostasis and malignancy, *Trends Immunol.* 42 (2) (2021) 104–119.
- [90] S.R. Gordon, et al., PD-1 expression by tumour-associated macrophages inhibits phagocytosis and tumor immunity, *Nature* 545 (7655) (2017) 495–499.
- [91] M. Qorraj, et al., The PD-1/PD-L1 axis contributes to immune metabolic dysfunctions of monocytes in chronic lymphocytic leukemia, *Leukemia* 31 (2017) 470–478.
- [92] S. Chiba, et al., Tumor-infiltrating DCs suppress nucleic acid-mediated innate immune responses through interactions between the receptor TIM-3 and the alarmin HMGB1, *Nat. Immunol.* 13 (9) (2012) 832–842.
- [93] K.O. Dixon, et al., TIM-3 restrains anti-tumour immunity by regulating inflammasome activation, *Nature* 595 (7865) (2021) 101–106.
- [94] W.I. Seo, et al., Expression of VISTA on tumor-infiltrating immune cells correlated with short intravesical recurrence in non-muscle-invasive bladder cancer, *Cancer Immunol. Immunother.* 70 (11) (2021) 3113–3122.
- [95] H. Lin, et al., Host expression of PD-L1 determines efficacy of PD-L1 pathway blockade-mediated tumor regression, *J. Clin. Invest* 128 (2) (2018) 805–815.
- [96] D. Dangaj, et al., Novel recombinant human b7-h4 antibodies overcome tumoral immune escape to potentiate T-cell antitumor responses, *Cancer Res* 73 (15) (2013) 4820–4829.
- [97] A. Sica, et al., Macrophage polarization in tumour progression, *Semin Cancer Biol.* 18 (5) (2008) 349–355.
- [98] Y. Pylayeva-Gupta, et al., Oncogenic Kras-induced GM-CSF production promotes the development of pancreatic neoplasia, *Cancer Cell* 21 (6) (2012) 836–847.
- [99] L.J. Bayne, et al., Tumor-derived granulocyte-macrophage colony-stimulating factor regulates myeloid inflammation and T cell immunity in pancreatic cancer, *Cancer Cell* 21 (6) (2012) 822–835.
- [100] V. Ubertini, et al., Mutant p53 gains new function in promoting inflammatory signals by repression of the secreted interleukin-1 receptor antagonist, *Oncogene* 34 (19) (2015) 2493–2504.
- [101] H. Sumimoto, et al., The BRAF-MAPK signaling pathway is essential for cancer-immune evasion in human melanoma cells, *J. Exp. Med* 203 (7) (2006) 1651–1656.
- [102] A.K. Mehta, et al., Targeting immunosuppressive macrophages overcomes PARP inhibitor resistance in BRCA1-associated triple-negative breast cancer, *Nat. Cancer* 2 (1) (2021) 66–82.
- [103] F.O. Martinez, et al., Macrophage activation and polarization, *Front Biosci.* 13 (2008) 453–461.
- [104] L.A. O'Neill, E.J. Pearce, Immunometabolism governs dendritic cell and macrophage function, *J. Exp. Med* 213 (1) (2016) 15–23.
- [105] S.D. Jayasingam, et al., Evaluating the polarization of tumor-associated macrophages into M1 and M2 phenotypes in human cancer tissue: technicalities and challenges in routine clinical practice, *Front Oncol.* 9 (2019) 1512.
- [106] J.B. Wyckoff, et al., Direct visualization of macrophage-assisted tumor cell intravasation in mammary tumors, *Cancer Res* 67 (6) (2007) 2649–2656.
- [107] M.J. Pittet, Behavior of immune players in the tumor microenvironment, *Curr. Opin. Oncol.* 21 (1) (2009) 53–59.
- [108] A.S. Harney, et al., Real-time imaging reveals local, transient vascular permeability, and tumor cell intravasation stimulated by TIE2hi macrophage-derived VEGFA, *Cancer Disco* 5 (9) (2015) 932–943.
- [109] Z. Chen, J.L. Ross, D. Hambarzumyan, Intravital 2-photon imaging reveals distinct morphology and infiltrative properties of glioblastoma-associated macrophages, *Proc. Natl. Acad. Sci. USA* 116 (28) (2019) 14254–14259.
- [110] J. Guinney, et al., The consensus molecular subtypes of colorectal cancer, *Nat. Med* 21 (11) (2015) 1350–1356.
- [111] E. Picard, et al., Relationships between immune landscapes, genetic subtypes and responses to immunotherapy in colorectal cancer, *Front Immunol.* 11 (2020) 369.
- [112] G. Willmsky, T. Blankenstein, Sporadic immunogenic tumours avoid destruction by inducing T-cell tolerance, *Nature* 437 (7055) (2005) 141–146.
- [113] C.U. Blank, et al., Defining 'T cell exhaustion', *Nat. Rev. Immunol.* 19 (11) (2019) 665–674.
- [114] K.E. Pauken, et al., Epigenetic stability of exhausted T cells limits durability of reinvigoration by PD-1 blockade, *Science* 354 (6316) (2016) 1160–1165.
- [115] S.J. Im, et al., Defining CD8+ T cells that provide the proliferative burst after PD-1 therapy, *Nature* 537 (7620) (2016) 417–421.
- [116] A. Schietinger, et al., Tumor-specific T cell dysfunction is a dynamic antigen-driven differentiation program initiated early during tumorigenesis, *Immunity* 45 (2) (2016) 389–401.
- [117] O.S. Qureshi, et al., Trans-endocytosis of CD80 and CD86: a molecular basis for the cell-extrinsic function of CTLA-4, *Science* 332 (6029) (2011) 600–603.
- [118] M. Tekguc, et al., Treg-expressed CTLA-4 depletes CD80/CD86 by trogocytosis, releasing free PD-L1 on antigen-presenting cells, *Proc. Natl. Acad. Sci. USA* 118 (30) (2021).
- [119] E. Hui, et al., T cell costimulatory receptor CD28 is a primary target for PD-1-mediated inhibition, *Science* 355 (6332) (2017) 1428–1433.
- [120] R. Mizuno, et al., PD-1 primarily targets TCR signal in the inhibition of functional T cell activation, *Front Immunol.* 10 (2019) 630.
- [121] S.H. Baumeister, et al., Coinhibitory pathways in immunotherapy for cancer, *Annu Rev. Immunol.* 34 (2016) 539–573.
- [122] R.A. Fernandes, et al., Immune receptor inhibition through enforced phosphatase recruitment, *Nature* 586 (7831) (2020) 779–784.
- [123] J.M. Chemnitz, et al., SHP-1 and SHP-2 associate with immunoreceptor tyrosine-based switch motif of programmed death 1 upon primary human T cell stimulation, but only receptor ligation prevents T cell activation, *J. Immunol.* 173 (2) (2004) 945–954.
- [124] T. Yokosuka, et al., Programmed cell death 1 forms negative costimulatory microclusters that directly inhibit T cell receptor signaling by recruiting phosphatase SHP2, *J. Exp. Med.* 209 (6) (2012) 1201–1217.
- [125] N. Patsoukis, et al., Interaction of SHP-2 SH2 domains with PD-1 ITSM induces PD-1 dimerization and SHP-2 activation, *Commun. Biol.* 3 (1) (2020) 128.
- [126] J. Celis-Gutierrez, et al., Quantitative interactomics in primary T cells provides a rationale for concomitant PD-1 and BTLA coinhibitor blockade in cancer immunotherapy, *Cell Rep.* 27 (11) (2019) 3315–3330.e7.
- [127] N. Patsoukis, et al., Selective effects of PD-1 on Akt and Ras pathways regulate molecular components of the cell cycle and inhibit T cell proliferation, *Sci. Signal* 5 (230) (2012) ra46.
- [128] N. Patsoukis, et al., PD-1 alters T-cell metabolic reprogramming by inhibiting glycolysis and promoting lipolysis and fatty acid oxidation, *Nat. Commun.* 6 (2015) 6692.
- [129] V.A. Boussiotis, N. Patsoukis, Effects of PD-1 signaling on immunometabolic reprogramming, *Immunometabolism* 4 (2) (2022).
- [130] K. Bardhan, T. Anagnostou, V.A. Boussiotis, The PD1:PD-L1/2 pathway from discovery to clinical implementation, *Front Immunol.* 7 (2016) 550.
- [131] S.L. Topalian, et al., Immunotherapy: the path to win the war on cancer? *Cell* 161 (2) (2015) 185–186.
- [132] W. Zou, J.D. Wolchok, L. Chen, PD-L1 (B7-H1) and PD-1 pathway blockade for cancer therapy: Mechanisms, response biomarkers, and combinations, *Sci. Transl. Med* 8 (328) (2016) 328rv4.
- [133] V.R. Juneja, et al., PD-L1 on tumor cells is sufficient for immune evasion in immunogenic tumors and inhibits CD8 T cell cytotoxicity, *J. Exp. Med* 214 (4) (2017) 895–904.
- [134] J. Lau, et al., Tumour and host cell PD-L1 is required to mediate suppression of anti-tumour immunity in mice, *Nat. Commun.* 8 (2017) 14572.
- [135] H. Tang, et al., PD-L1 on host cells is essential for PD-L1 blockade-mediated tumor regression, *J. Clin. Invest* 128 (2) (2018) 580–588.

- [136] Q. Peng, et al., PD-L1 on dendritic cells attenuates T cell activation and regulates response to immune checkpoint blockade, *Nat. Commun.* 11 (1) (2020) 4835.
- [137] S.A. Oh, et al., PD-L1 expression by dendritic cells is a key regulator of T-cell immunity in cancer, *Nat. Cancer* 1 (7) (2020) 681–691.
- [138] N. Patsoukis, et al., Revisiting the PD-1 pathway, *Sci. Adv.* 6 (38) (2020).
- [139] D. Sugiura, et al., PD-1 agonism by anti-CD80 inhibits T cell activation and alleviates autoimmunity, *Nat. Immunol.* 23 (3) (2022) 399–410.
- [140] L.P. Andrews, H. Yano, D.A.A. Vignali, Inhibitory receptors and ligands beyond PD-1, PD-L1 and CTLA-4: breakthroughs or backups, *Nat. Immunol.* 20 (11) (2019) 1425–1434.
- [141] L. Yuan, et al., VISTA: a mediator of quiescence and a promising target in cancer immunotherapy, *Trends Immunol.* 42 (3) (2021) 209–227.
- [142] M.A. ElTanbouly, et al., VISTA is a checkpoint regulator for naive T cell quiescence and peripheral tolerance, *Science* 367 (6475) (2020).
- [143] X. Han, et al., PD-1H (VISTA)-mediated suppression of autoimmunity in systemic and cutaneous lupus erythematosus, *Sci. Transl. Med.* 11 (522) (2019).
- [144] M.A. ElTanbouly, et al., VISTA Re-programs Macrophage Biology Through the Combined Regulation of Tolerance and Anti-inflammatory Pathways, *Front Immunol.* 11 (2020), 580187.
- [145] K. Mulati, et al., VISTA expressed in tumour cells regulates T cell function, *Br. J. Cancer* 120 (1) (2019) 115–127.
- [146] S.R. Rosenbaum, et al., FOXD3 Regulates VISTA Expression in Melanoma, *Cell Rep.* 30 (2) (2020) 510–524, e6.
- [147] J. Gao, et al., VISTA is an inhibitory immune checkpoint that is increased after ipilimumab therapy in patients with prostate cancer, *Nat. Med.* 23 (5) (2017) 551–555.
- [148] J. Blando, et al., Comparison of immune infiltrates in melanoma and pancreatic cancer highlights VISTA as a potential target in pancreatic cancer, *Proc. Natl. Acad. Sci. USA* 116 (5) (2019) 1692–1697.
- [149] H. Kakavand, et al., Negative immune checkpoint regulation by VISTA: a mechanism of acquired resistance to anti-PD-1 therapy in metastatic melanoma patients, *Mod. Pathol.* 30 (12) (2017) 1666–1676.
- [150] J. Wang, et al., VSIG-3 as a ligand of VISTA inhibits human T-cell function, *Immunology* 156 (1) (2019) 74–85.
- [151] R.J. Johnston, et al., VISTA is an acidic pH-selective ligand for PSGL-1, *Nature* 574 (7779) (2019) 565–570.
- [152] S. Haxhinasto, D. Mathis, C. Benoist, The AKT-mTOR axis regulates de novo differentiation of CD4⁺Foxp3⁺ cells, *J. Exp. Med.* 205 (3) (2008) 565–574.
- [153] G.M. Delgoffe, et al., The mTOR kinase differentially regulates effector and regulatory T cell lineage commitment, *Immunity* 30 (6) (2009) 832–844.
- [154] L.M. Francisco, et al., PD-L1 regulates the development, maintenance, and function of induced regulatory T cells, *J. Exp. Med.* 206 (13) (2009) 3015–3029.
- [155] L.Z. Shi, et al., HIF1 α -dependent glycolytic pathway orchestrates a metabolic checkpoint for the differentiation of TH17 and Treg cells, *J. Exp. Med.* 208 (7) (2011) 1367–1376.
- [156] S. Kumagai, et al., The PD-1 expression balance between effector and regulatory T cells predicts the clinical efficacy of PD-1 blockade therapies, *Nat. Immunol.* (2020).
- [157] M. Miyara, et al., Functional delineation and differentiation dynamics of human CD4⁺ T cells expressing the FoxP3 transcription factor, *Immunity* 30 (6) (2009) 899–911.
- [158] J.B. Wing, A. Tanaka, S. Sakaguchi, Human FOXP3(+) Regulatory T Cell Heterogeneity and Function in Autoimmunity and Cancer, *Immunity* 50 (2) (2019) 302–316.
- [159] M.A. Williams, M.J. Bevan, Effector and memory CTL differentiation, *Annu Rev. Immunol.* 25 (2007) 171–192.
- [160] A. Ribas, et al., PD-1 blockade expands intratumoral memory T cells, *Cancer Immunol. Res.* 4 (3) (2016) 194–203.
- [161] N.J. MacIver, J.C. Rathmell, Editorial overview: metabolism of T cells: integrating nutrients, signals, and cell fate, *Curr. Opin. Immunol.* 46 (2017) viii–xi.
- [162] V.A. Gerriets, et al., Foxp3 and Toll-like receptor signaling balance Treg cell anabolic metabolism for suppression, *Nat. Immunol.* 17 (12) (2016) 1459–1466.
- [163] C. Herbel, et al., Clinical significance of T cell metabolic reprogramming in cancer, *Clin. Transl. Med.* 5 (1) (2016) 29.
- [164] C.H. Chang, et al., Metabolic competition in the tumor microenvironment is a driver of cancer progression, *Cell* 162 (6) (2015) 1229–1241.
- [165] S. Daneshmandi, et al., Blockade of 6-phosphogluconate dehydrogenase generates CD8(+) effector T cells with enhanced anti-tumor function, *Cell Rep.* 34 (10) (2021), 108831.
- [166] K.A. Frauwirth, C.B. Thompson, Regulation of T lymphocyte metabolism, *J. Immunol.* 172 (8) (2004) 4661–4665.
- [167] C.H. Chang, et al., Posttranscriptional control of T cell effector function by aerobic glycolysis, *Cell* 153 (6) (2013) 1239–1251.
- [168] M. Sukumar, et al., Inhibiting glycolytic metabolism enhances CD8⁺ T cell memory and antitumor function, *J. Clin. Invest.* 123 (10) (2013) 4479–4488.
- [169] T. Porstmann, et al., PKB/Akt induces transcription of enzymes involved in cholesterol and fatty acid biosynthesis via activation of SREBP, *Oncogene* 24 (43) (2005) 6465–6481.
- [170] K. Duvel, et al., Activation of a metabolic gene regulatory network downstream of mTOR complex 1, *Mol. Cell* 39 (2) (2010) 171–183.
- [171] T. Porstmann, et al., SREBP activity is regulated by mTORC1 and contributes to Akt-dependent cell growth, *Cell Metab.* 8 (3) (2008) 224–236.
- [172] R. Wang, et al., The transcription factor Myc controls metabolic reprogramming upon T lymphocyte activation, *Immunity* 35 (6) (2011) 871–882.
- [173] S.C. Cheng, et al., mTOR- and HIF-1 α -mediated aerobic glycolysis as metabolic basis for trained immunity, *Science* 345 (6204) (2014) 1250684.
- [174] H. Zeng, H. Chi, mTOR signaling and transcriptional regulation in T lymphocytes, *Transcription* 5 (2) (2014), e28263.
- [175] T. Le Bourgeois, et al., Targeting T cell metabolism for improvement of cancer immunotherapy, *Front Oncol.* 8 (2018) 237.
- [176] S.M. Kaech, W. Cui, Transcriptional control of effector and memory CD8⁺ T cell differentiation, *Nat. Rev. Immunol.* 12 (11) (2012) 749–761.
- [177] C.A. Klebanoff, et al., Central memory self/tumor-reactive CD8⁺ T cells confer superior antitumor immunity compared with effector memory T cells, *Proc. Natl. Acad. Sci. USA* 102 (27) (2005) 9571–9576.
- [178] L. Gattinoni, et al., Acquisition of full effector function in vitro paradoxically impairs the in vivo antitumor efficacy of adoptively transferred CD8⁺ T cells, *J. Clin. Invest.* 115 (6) (2005) 1616–1626.
- [179] L. Gattinoni, et al., Wnt signaling arrests effector T cell differentiation and generates CD8⁺ memory stem cells, *Nat. Med.* 15 (7) (2009) 808–813.
- [180] C.A. Klebanoff, L. Gattinoni, N.P. Restifo, CD8⁺ T-cell memory in tumor immunology and immunotherapy, *Immunol. Rev.* 211 (2006) 214–224.
- [181] F. Sallusto, et al., Two subsets of memory T lymphocytes with distinct homing potentials and effector functions, *Nature* 401 (6754) (1999) 708–712.
- [182] E.J. Wherry, et al., Viral persistence alters CD8 T-cell immunodominance and tissue distribution and results in distinct stages of functional impairment, *J. Virol.* 77 (8) (2003) 4911–4927.
- [183] D. Masopust, A.G. Soerens, Tissue-resident T cells and other resident leukocytes, *Annu Rev. Immunol.* 37 (2019) 521–546.
- [184] K.D. Omilusik, A.W. Goldrath, Remembering to remember: T cell memory maintenance and plasticity, *Curr. Opin. Immunol.* 58 (2019) 89–97.
- [185] L. Kok, et al., A committed tissue-resident memory T cell precursor within the circulating CD8⁺ effector T cell pool, *J. Exp. Med.* 217 (10) (2020).
- [186] D. Masopust, et al., Preferential localization of effector memory cells in nonlymphoid tissue, *Science* 291 (5512) (2001) 2413–2417.
- [187] E.M. Steinert, et al., Quantifying memory CD8 T cells reveals regionalization of immunosurveillance, *Cell* 161 (4) (2015) 737–749.
- [188] E. Menares, et al., Tissue-resident memory CD8(+) T cells amplify anti-tumor immunity by triggering antigen spreading through dendritic cells, *Nat. Commun.* 10 (1) (2019) 4401.
- [189] S.L. Park, et al., Author correction: tissue-resident memory CD8(+) T cells promote melanoma-immune equilibrium in skin, *Nature* 566 (7745) (2019), E10.
- [190] P. Savas, et al., Publisher correction: single-cell profiling of breast cancer T cells reveals a tissue-resident memory subset associated with improved prognosis, *Nat. Med.* 24 (12) (2018) 1941.
- [191] S. Corgnac, et al., The emerging role of CD8(+) tissue resident memory T (TRM) cells in antitumor immunity: a unique functional contribution of the CD103 integrin, *Front Immunol.* 9 (2018) 1904.
- [192] C.N. Skon, et al., Transcriptional downregulation of S1pr1 is required for the establishment of resident memory CD8⁺ T cells, *Nat. Immunol.* 14 (12) (2013) 1285–1293.
- [193] A. Bai, et al., Kruppel-like factor 2 controls T cell trafficking by activating L-selectin (CD62L) and sphingosine-1-phosphate receptor 1 transcription, *J. Immunol.* 178 (12) (2007) 7632–7639.
- [194] G.F. Debes, et al., Chemokine receptor CCR7 required for T lymphocyte exit from peripheral tissues, *Nat. Immunol.* 6 (9) (2005) 889–894.
- [195] G. Gofru, J. Rivera-Nieves, K. Ley, Role of beta7 integrins in intestinal lymphocyte homing and retention, *Curr. Mol. Med.* 9 (7) (2009) 836–850.
- [196] P.J. Kilshaw, S.J. Murant, A new surface antigen on intraepithelial lymphocytes in the intestine, *Eur. J. Immunol.* 20 (10) (1990) 2201–2207.
- [197] M.P. Schön, et al., Mucosal T lymphocyte numbers are selectively reduced in integrin alpha E (CD103)-deficient mice, *J. Immunol.* 162 (11) (1999) 6641–6649.
- [198] A.K. Molodtsov, et al., Resident memory CD8(+) T cells in regional lymph nodes mediate immunity to metastatic melanoma, *Immunity* 54 (9) (2021) 2117–2132, e7.
- [199] B.T. Malik, et al., Resident memory T cells in the skin mediate durable immunity to melanoma, *Sci. Immunol.* 2 (10) (2017).
- [200] I. Liikanen, et al., Hypoxia-inducible factor activity promotes antitumor effector function and tissue residency by CD8⁺ T cells, *J. Clin. Invest.* 131 (7) (2021).
- [201] J. Han, et al., Resident and circulating memory T cells persist for years in melanoma patients with durable responses to immunotherapy, *Nat. Cancer* 2 (3) (2021) 300–311.
- [202] A.P. Ganesan, et al., Tissue-resident memory features are linked to the magnitude of cytotoxic T cell responses in human lung cancer, *Nat. Immunol.* 18 (8) (2017) 940–950.
- [203] X. Mei, et al., The emerging role of tissue-resident memory CD8(+) T lymphocytes in human digestive tract cancers, *Front Oncol.* 11 (2021), 819505.
- [204] F. Djenidi, et al., CD8⁺CD103⁺ tumor-infiltrating lymphocytes are tumor-specific tissue-resident memory T cells and a prognostic factor for survival in lung cancer patients, *J. Immunol.* 194 (7) (2015) 3475–3486.
- [205] J.R. Webb, K. Milne, B.H. Nelson, PD-1 and CD103 are widely coexpressed on prognostically favorable intraepithelial CD8 T cells in human ovarian cancer, *Cancer Immunol. Res.* 3 (8) (2015) 926–935.
- [206] F.L. Komdeur, et al., CD103⁺ tumor-infiltrating lymphocytes are tumor-reactive intraepithelial CD8⁺ T cells associated with prognostic benefit and therapy response in cervical cancer, *Oncoimmunology* 6 (9) (2017), e1338230.
- [207] J.X. Caushi, et al., Transcriptional programs of neoantigen-specific TIL in anti-PD-1-treated lung cancers, *Nature* 596 (7870) (2021) 126–132.
- [208] J. Edwards, et al., CD103(+) tumor-resident CD8(+) T cells are associated with improved survival in immunotherapy-naïve melanoma patients and expand

- significantly during anti-PD-1 treatment, *Clin. Cancer Res* 24 (13) (2018) 3036–3045.
- [209] T. Murray, et al., Very late antigen-1 marks functional tumor-resident CD8 T cells and correlates with survival of melanoma patients, *Front Immunol.* 7 (2016) 573.
- [210] P. Savas, et al., Single-cell profiling of breast cancer T cells reveals a tissue-resident memory subset associated with improved prognosis, *Nat. Med* 24 (7) (2018) 986–993.
- [211] Z.Q. Wang, et al., CD103 and intratumoral immune response in breast cancer, *Clin. Cancer Res* 22 (24) (2016) 6290–6297.
- [212] T. Duhén, et al., Co-expression of CD39 and CD103 identifies tumor-reactive CD8 T cells in human solid tumors, *Nat. Commun.* 9 (1) (2018) 2724.
- [213] J.R. Webb, et al., Tumor-infiltrating lymphocytes expressing the tissue resident memory marker CD103 are associated with increased survival in high-grade serous ovarian cancer, *Clin. Cancer Res* 20 (2) (2014) 434–444.
- [214] J. Koh, et al., Prognostic implications of intratumoral CD103+ tumor-infiltrating lymphocytes in pulmonary squamous cell carcinoma, *Oncotarget* 8 (8) (2017) 13762–13769.
- [215] B. Wang, et al., CD103+ tumor infiltrating lymphocytes predict a favorable prognosis in urothelial cell carcinoma of the bladder, *J. Urol.* 194 (2) (2015) 556–562.
- [216] E. Vivier, et al., Innate lymphoid cells: 10 years on, *Cell* 174 (5) (2018) 1054–1066.
- [217] L. Ducimetiere, M. Vermeer, S. Tugues, The interplay between innate lymphoid cells and the tumor microenvironment, *Front. Immunol.* 10 (2019) 2895.
- [218] S. Guia, et al., Activating and inhibitory receptors expressed on innate lymphoid cells, *Semin. Immunopathol.* 40 (4) (2018) 331–341.
- [219] A. Horowitz, et al., Genetic and environmental determinants of human NK cell diversity revealed by mass cytometry, *Sci. Transl. Med* 5 (208) (2013) 208ra145.
- [220] A.G. Freud, et al., The broad spectrum of human natural killer cell diversity, *Immunity* 47 (5) (2017) 820–833.
- [221] K.J. Malmberg, et al., Natural killer cell-mediated immunosurveillance of human cancer, *Semin. Immunol.* 31 (2017) 20–29.
- [222] P. Carrega, et al., CD56(bright)perforin(low) noncytotoxic human NK cells are abundant in both healthy and neoplastic solid tissues and recirculate to secondary lymphoid organs via afferent lymph, *J. Immunol.* 192 (8) (2014) 3805–3815.
- [223] A. Moretta, et al., Activating receptors and coreceptors involved in human natural killer cell-mediated cytotoxicity, *Annu. Rev. Immunol.* 19 (2001) 197–223.
- [224] H.J. Pegram, et al., Activating and inhibitory receptors of natural killer cells, *Immunol. Cell Biol.* 89 (2) (2011) 216–224.
- [225] S. Sivori, et al., CD94 functions as a natural killer cell inhibitory receptor for different HLA class I alleles: identification of the inhibitory form of CD94 by the use of novel monoclonal antibodies, *Eur. J. Immunol.* 26 (10) (1996) 2487–2492.
- [226] J.J. Perez-Villar, et al., The CD94/NKG2A inhibitory receptor complex is involved in natural killer cell-mediated recognition of cells expressing HLA-G1, *J. Immunol.* 158 (12) (1997) 5736–5743.
- [227] V.M. Braud, et al., HLA-E binds to natural killer cell receptors CD94/NKG2A, B and C, *Nature* 391 (6669) (1998) 795–799.
- [228] L. Chiossone, et al., Natural killer cell immunotherapies against cancer: checkpoint inhibitors and more, *Semin. Immunol.* 31 (2017) 55–63.
- [229] K. Karre, et al., Selective rejection of H-2-deficient lymphoma variants suggests alternative immune defence strategy, *Nature* 319 (6055) (1986) 675–678.
- [230] F. Romagne, et al., Preclinical characterization of 1-7F9, a novel human anti-KIR receptor therapeutic antibody that augments natural killer-mediated killing of tumor cells, *Blood* 114 (13) (2009) 2667–2677.
- [231] T. van Hall, et al., Monalizumab: inhibiting the novel immune checkpoint NKG2A, *J. Immunother. Cancer* 7 (1) (2019) 263.
- [232] H.E. Kohrt, et al., Anti-KIR antibody enhancement of anti-lymphoma activity of natural killer cells as monotherapy and in combination with anti-CD20 antibodies, *Blood* 123 (5) (2014) 678–686.
- [233] P. Andre, et al., Anti-NKG2A mAb is a checkpoint inhibitor that promotes anti-tumor immunity by unleashing both T and NK cells, *Cell* 175 (7) (2018) 1731–1743, e13.
- [234] T. Kamiya, et al., Blocking expression of inhibitory receptor NKG2A overcomes tumor resistance to NK cells, *J. Clin. Invest* 129 (5) (2019) 2094–2106.
- [235] M. Della Chiesa, et al., Features of memory-like and PD-1(+) human NK cell subsets, *Front. Immunol.* 7 (2016) 351.
- [236] S. Pesce, et al., Identification of a subset of human natural killer cells expressing high levels of programmed death 1: a phenotypic and functional characterization, *J. Allergy Clin. Immunol.* 139 (1) (2017) 335–346, e3.
- [237] D.M. Benson Jr., et al., The PD-1/PD-L1 axis modulates the natural killer cell versus multiple myeloma effect: a therapeutic target for CT-011, a novel monoclonal anti-PD-1 antibody, *Blood* 116 (13) (2010) 2286–2294.
- [238] A. Beldi-Ferchiou, et al., PD-1 mediates functional exhaustion of activated NK cells in patients with Kaposi sarcoma, *Oncotarget* 7 (45) (2016) 72961–72977.
- [239] C. Niu, et al., PD-1-positive natural killer cells have a weaker antitumor function than that of PD-1-negative natural killer cells in lung cancer, *Int. J. Med. Sci.* 17 (13) (2020) 1964–1973.
- [240] N. Tumino, et al., Presence of innate lymphoid cells in pleural effusions of primary and metastatic tumors: Functional analysis and expression of PD-1 receptor, *Int. J. Cancer* 145 (6) (2019) 1660–1668.
- [241] S. Pesce, et al., Different features of tumor-associated NK cells in patients with low-grade or high-grade peritoneal carcinomatosis, *Front. Immunol.* 10 (2019) 1963.
- [242] F.R. Mariotti, et al., PD-1 in human NK cells: evidence of cytoplasmic mRNA and protein expression, *Oncoimmunology* 8 (3) (2019) 1557030.
- [243] F. Vari, et al., Immune evasion via PD-1/PD-L1 on NK cells and monocyte/macrophages is more prominent in Hodgkin lymphoma than DLBCL, *Blood* 131 (16) (2018) 1809–1819.
- [244] M.P. Trefny, et al., PD-1(+) natural killer cells in human non-small cell lung cancer can be activated by PD-1/PD-L1 blockade, *Cancer Immunol. Immunother.* 69 (8) (2020) 1505–1517.
- [245] L. Quatrini, et al., Glucocorticoids and the cytokines IL-12, IL-15, and IL-18 present in the tumor microenvironment induce PD-1 expression on human natural killer cells, *J. Allergy Clin. Immunol.* 147 (1) (2021) 349–360.
- [246] X.L. Iraolagoitia, et al., NK cells restrain spontaneous antitumor CD8+ T cell priming through PD-1/PD-L1 interactions with dendritic cells, *J. Immunol.* 197 (3) (2016) 953–961.
- [247] A. Stojanovic, et al., CTLA-4 is expressed by activated mouse NK cells and inhibits NK Cell IFN-gamma production in response to mature dendritic cells, *J. Immunol.* 192 (9) (2014) 4184–4191.
- [248] J. Russick, et al., Natural killer cells in the human lung tumor microenvironment display immune inhibitory functions, *J. Immunother. Cancer* 8 (2) (2020).
- [249] F. Esen, G. Deniz, E.C. Aktas, PD-1, CTLA-4, LAG-3, and TIGIT: The roles of immune checkpoint receptors on the regulation of human NK cell phenotype and functions, *Immunol. Lett.* 240 (2021) 15–23.
- [250] F.J. Kohlhapp, et al., NK cells and CD8+ T cells cooperate to improve therapeutic responses in melanoma treated with interleukin-2 (IL-2) and CTLA-4 blockade, *J. Immunother. Cancer* 3 (2015) 18.
- [251] L.C. Ndhlovu, et al., Tim-3 marks human natural killer cell maturation and suppresses cell-mediated cytotoxicity, *Blood* 119 (16) (2012) 3734–3743.
- [252] H. Komita, et al., Expression of immune checkpoint molecules of T cell immunoglobulin and mucin protein 3/galectin-9 for NK cell suppression in human gastrointestinal stromal tumors, *Oncol. Rep.* 34 (4) (2015) 2099–2105.
- [253] M.K. Gleason, et al., Tim-3 is an inducible human natural killer cell receptor that enhances interferon gamma production in response to galectin-9, *Blood* 119 (13) (2012) 3064–3072.
- [254] I.P. da Silva, et al., Reversal of NK-cell exhaustion in advanced melanoma by Tim-3 blockade, *Cancer Immunol. Res.* 2 (5) (2014) 410–422.
- [255] A. Gallois, et al., Reversal of natural killer cell exhaustion by TIM-3 blockade, *Oncoimmunology* 3 (12) (2014), e946365.
- [256] Z. Wang, et al., The clinical significance of abnormal Tim-3 expression on NK cells from patients with gastric cancer, *Immunol. Invest.* 44 (6) (2015) 578–589.
- [257] L. Xu, et al., Increased Tim-3 expression in peripheral NK cells predicts a poorer prognosis and Tim-3 blockade improves NK cell-mediated cytotoxicity in human lung adenocarcinoma, *Int. Immunopharmacol.* 29 (2) (2015) 635–641.
- [258] W. Zhang, et al., The functional potency of natural killer cells in response to IL-2/IL-15/IL-21 stimulation is limited by a concurrent upregulation of Tim-3 in bladder cancer, *Exp. Cell Res.* 372 (2) (2018) 92–98.
- [259] A. Merino, et al., Chronic stimulation drives human NK cell dysfunction and epigenetic reprogramming, *J. Clin. Invest* 129 (9) (2019) 3770–3785.
- [260] S.R. Woo, et al., Immune inhibitory molecules LAG-3 and PD-1 synergistically regulate T-cell function to promote tumoral immune escape, *Cancer Res.* 72 (4) (2012) 917–927.
- [261] C. Brignone, et al., A soluble form of lymphocyte activation gene-3 (IMP321) induces activation of a large range of human effector cytotoxic cells, *J. Immunol.* 179 (6) (2007) 4202–4211.
- [262] C. Brignone, et al., First-line chemoimmunotherapy in metastatic breast carcinoma: combination of paclitaxel and IMP321 (LAG-3Ig) enhances immune responses and antitumor activity, *J. Transl. Med.* 8 (2010) 71.
- [263] F. Xu, et al., Blockade of CD112R and TIGIT signaling sensitizes human natural killer cell functions, *Cancer Immunol. Immunother.* 66 (10) (2017) 1367–1375.
- [264] C. Bottino, et al., Identification of PVR (CD155) and Nectin-2 (CD112) as cell surface ligands for the human DNAM-1 (CD226) activating molecule, *J. Exp. Med* 198 (4) (2003) 557–567.
- [265] C.J. Chan, et al., The receptors CD96 and CD226 oppose each other in the regulation of natural killer cell functions, *Nat. Immunol.* 15 (5) (2014) 431–438.
- [266] E.Y. Chiang, et al., CD96 functions as a co-stimulatory receptor to enhance CD8(+) T cell activation and effector responses, *Eur. J. Immunol.* 50 (6) (2020) 891–902.
- [267] B. Sanchez-Correa, et al., DNAM-1 and the TIGIT/PVRIG/TACTILE axis: Novel immune checkpoints for natural killer cell-based cancer immunotherapy, *Cancers (Basel)* 11 (6) (2019).
- [268] A. Fuchs, M. Colonna, The role of NK cell recognition of nectin and nectin-like proteins in tumor immunosurveillance, *Semin. Cancer Biol.* 16 (5) (2006) 359–366.
- [269] Y. Takai, et al., Nectins and nectin-like molecules: roles in contact inhibition of cell movement and proliferation, *Nat. Rev. Mol. Cell Biol.* 9 (8) (2008) 603–615.
- [270] D. Sarhan, et al., Adaptive NK cells with low TIGIT expression are inherently resistant to myeloid-derived suppressor cells, *Cancer Res.* 76 (19) (2016) 5696–5706.
- [271] S. Whelan, et al., PVRIG and PVRL2 are induced in cancer and inhibit CD8(+) T-cell function, *Cancer Immunol. Res.* 7 (2) (2019) 257–268.
- [272] A.C. Anderson, N. Joller, V.K. Kuchroo, Lag-3, Tim-3, and TIGIT: Co-inhibitory receptors with specialized functions in immune regulation, *Immunity* 44 (5) (2016) 989–1004.
- [273] R.J. Johnston, et al., The immunoreceptor TIGIT regulates antitumor and antiviral CD8(+) T cell effector function, *Cancer Cell* 26 (6) (2014) 923–937.
- [274] S. Nishiwada, et al., Clinical significance of CD155 expression in human pancreatic cancer, *Anticancer Res.* 35 (4) (2015) 2287–2297.

- [275] Q. Zhang, et al., Blockade of the checkpoint receptor TIGIT prevents NK cell exhaustion and elicits potent anti-tumor immunity, *Nat. Immunol.* 19 (7) (2018) 723–732.
- [276] S.J. Blake, et al., Molecular pathways: Targeting CD96 and TIGIT for cancer immunotherapy, *Clin. Cancer Res* 22 (21) (2016) 5183–5188.
- [277] Y. Simoni, et al., Human innate lymphoid cell subsets possess tissue-type based heterogeneity in phenotype and frequency, *Immunity* 46 (1) (2017) 148–161.
- [278] M. Salimi, et al., Activated innate lymphoid cell populations accumulate in human tumour tissues, *BMC Cancer* 18 (1) (2018) 341.
- [279] S. Wang, et al., Transdifferentiation of tumor infiltrating innate lymphoid cells during progression of colorectal cancer, *Cell Res.* 30 (7) (2020) 610–622.
- [280] J.A. Moral, et al., ILC2s amplify PD-1 blockade by activating tissue-specific cancer immunity, *Nature* 579 (7797) (2020) 130–135.
- [281] G. Ercolano, et al., Distinct and shared gene expression for human innate versus adaptive helper lymphoid cells, *J. Leukoc. Biol.* 108 (2) (2020) 723–737.
- [282] Y. Gao, et al., Tumor immunoevasion by the conversion of effector NK cells into type 1 innate lymphoid cells, *Nat. Immunol.* 18 (9) (2017) 1004–1015.
- [283] P. Vacca, et al., PD-1 is expressed by and regulates human group 3 innate lymphoid cells in human decidua, *Mucosal Immunol.* 12 (3) (2019) 624–631.
- [284] C. Luci, et al., Cutaneous squamous cell carcinoma development is associated with a temporal infiltration of ILC1 and NK cells with immune dysfunctions, *J. Invest. Dermatol.* 141 (10) (2021) 2369–2379.

Unanswered questions and future directions

- It has been experimentally demonstrated in the past that tumor growth results in the accumulation of MDSCs in distal organs (e.g. lungs), contributing to the formation of metastatic niches, whereas prevention of MDSCs migration restricts the metastatic potential of the primary tumor. In our studies, we showed that blockade of PD-1 – SHP-2 axis in myeloid cells, induced differentiation of MDSCs, improving their anti-tumor properties and limiting their suppression capacity. In the future, we plan to examine how the deletion of PD-1 or SHP-2 in myeloid cells can alter the formation of the metastatic niches, in organs distal to the primary tumor. In our study, we showed that SHP-2 or PD-1 deletion improved anti-tumor immunity and decelerated tumor progression. However, this was tested only in “hot-tumors”, which are infiltrated by immune cells. It is unclear whether the blockade of PD-1 – SHP-2 axis in myeloid cells in the context of “cold-tumors” can lead to the repopulation of the TME with immune cells and change their response to immunotherapy. We will inject cold tumors to WT, *Shp2^{f/f}LysMCre* and *Pdcd1^{f/f}LysMCre* mice, and then, we will assess the tumor progression and immune response.
- Deletion of SHP-2 or PD-1 in the myeloid cells of tumor bearing mice resulted in the accumulation of differentiated myeloid cells, including MDSC and TAMs, with pro-immunogenic properties, and enhancement of anti-tumor immunity. However, it is unclear which specific myeloid compartment had the greatest contribution on this outcome. In the future, we will investigate this question using a step-by-step depletion strategy of specific

myeloid subsets, using anti-GR1 antibody for MDSC depletion and clodronate-liposome for TAMs depletion.

- We showed that blockade of PD-1 – SHP-2 axis in myeloid cells alleviated the suppression capacity of MDSCs and activated T cells, however, it is still unknown how the suppression capacity of Tregs is affected. For an in vitro Treg suppression assay, the proliferation of naive T cells will be assessed in the presence of APC and graded numbers of Treg cells. We will examine how SHP-2 or PD-1 deletion in myeloid cells affects Treg suppression capacity by performing in vitro suppression assay, and using APC from WT, PD-1 KO or SHP-2 KO mice.
- In our study, we described how the immune cell populations are affected by the deletion of the PD-1 – SHP-2 axis in the myeloid cells, but we did not examine how the tumor cells are changing at a functional level. In the future, we will perform in vitro functional assays to assess basic properties of tumor cells such as migration and proliferation.

Key findings

- SHP-2 deletion in myeloid cells enhances anti-tumor immunity.
- SHP-2 ablation in myeloid cells promotes activation and differentiation of MDSCs in tumor bearing mice.
- Deletion of SHP-2 in myeloid cells results in increased infiltration of monocytes in the tumor microenvironment, and subsequent recruitment and activation of T cells, alternating the tumor immune microenvironment.
- SHP-2 ablation reprograms TAMs, resulting in more differentiated cells with enhanced proinflammatory properties and antigen presentation capacity.
- Monocytes isolated from SHP-2 deficient tumor bearing mice possess long lasting anti-tumor immunity.
- In myeloid progenitors, PD-1 interacts with SHP-2, and PD-1–SHP-2 axis alters HOXA10 and IRF8 phosphorylation in response to GM-CSF and IL-3.
- PD-1 or SHP-2 ablation in myeloid cells had similar effects in myeloid differentiation signatures and anti-tumor function.
- The augmented anti-tumor ability of the immune system after deletion of either PD-1 or SHP-2 is at least partially mediated by IL-10.

Citations

1. Mattiuzzi C, Lippi G. Current Cancer Epidemiology. *J Epidemiol Glob Health*, 2019;9:217-22. 10.2991/jegh.k.191008.001
2. Falzone L, Salomone S, Libra M. Evolution of Cancer Pharmacological Treatments at the Turn of the Third Millennium. *Front Pharmacol*, 2018;9:1300. 10.3389/fphar.2018.01300
3. Dagher OK, Schwab RD, Brookens SK, Posey AD, Jr. Advances in cancer immunotherapies. *Cell*, 2023;186:1814- e1. 10.1016/j.cell.2023.02.039
4. Boussiotis VA. Molecular and Biochemical Aspects of the PD-1 Checkpoint Pathway. *N Engl J Med*, 2016;375:1767-78. 10.1056/NEJMra1514296
5. Das M, Zhu C, Kuchroo VK. Tim-3 and its role in regulating anti-tumor immunity. *Immunol Rev*, 2017;276:97-111. 10.1111/imr.12520
6. Gao X, Zhu Y, Li G, Huang H, Zhang G, Wang F, *et al.* TIM-3 expression characterizes regulatory T cells in tumor tissues and is associated with lung cancer progression. *PLoS One*, 2012;7:e30676. 10.1371/journal.pone.0030676
7. Zhong W, Liu X, Zhu Z, Li Q, Li K. High levels of Tim-3(+)Foxp3(+)Treg cells in the tumor microenvironment is a prognostic indicator of poor survival of diffuse large B cell lymphoma patients. *Int Immunopharmacol*, 2021;96:107662. 10.1016/j.intimp.2021.107662
8. Du W, Yang M, Turner A, Xu C, Ferris RL, Huang J, *et al.* TIM-3 as a Target for Cancer Immunotherapy and Mechanisms of Action. *Int J Mol Sci*, 2017;1810.3390/ijms18030645

9. Wen J, Mao X, Cheng Q, Liu Z, Liu F. A pan-cancer analysis revealing the role of TIGIT in tumor microenvironment. *Sci Rep*, 2021;11:22502. 10.1038/s41598-021-01933-9
10. Jantz-Naeem N, Bottcher-Loschinski R, Borucki K, Mitchell-Flack M, Bottcher M, Schraven B, *et al.* TIGIT signaling and its influence on T cell metabolism and immune cell function in the tumor microenvironment. *Front Oncol*, 2023;13:1060112. 10.3389/fonc.2023.1060112
11. Chauvin JM, Zarour HM. TIGIT in cancer immunotherapy. *J Immunother Cancer*, 2020;8:10.1136/jitc-2020-000957
12. Annese T, Tamma R, Ribatti D. Update in TIGIT Immune-Checkpoint Role in Cancer. *Front Oncol*, 2022;12:871085. 10.3389/fonc.2022.871085
13. Huo JL, Wang YT, Fu WJ, Lu N, Liu ZS. The promising immune checkpoint LAG-3 in cancer immunotherapy: from basic research to clinical application. *Front Immunol*, 2022;13:956090. 10.3389/fimmu.2022.956090
14. Sauer N, Szlasa W, Jonderko L, Oslizlo M, Kunachowicz D, Kulbacka J, *et al.* LAG-3 as a Potent Target for Novel Anticancer Therapies of a Wide Range of Tumors. *Int J Mol Sci*, 2022;23:10.3390/ijms23179958
15. Mair MJ, Kiesel B, Feldmann K, Widhalm G, Dieckmann K, Wohrer A, *et al.* LAG-3 expression in the inflammatory microenvironment of glioma. *J Neurooncol*, 2021;152:533-9. 10.1007/s11060-021-03721-x
16. Aggarwal V, Workman CJ, Vignali DAA. LAG-3 as the third checkpoint inhibitor. *Nat Immunol*, 2023;24:1415-22. 10.1038/s41590-023-01569-z

17. Cho JS, Hsu JV, Morrison SL. Localized expression of GITR-L in the tumor microenvironment promotes CD8+ T cell dependent anti-tumor immunity. *Cancer Immunol Immunother*, 2009;58:1057-69. 10.1007/s00262-008-0622-2
18. Burckhart T, Thiel M, Nishikawa H, Wuest T, Muller D, Zippelius A, *et al.* Tumor-specific crosslinking of GITR as costimulation for immunotherapy. *J Immunother*, 2010;33:925-34. 10.1097/CJI.0b013e3181f3cc87
19. Schaer DA, Budhu S, Liu C, Bryson C, Malandro N, Cohen A, *et al.* GITR pathway activation abrogates tumor immune suppression through loss of regulatory T cell lineage stability. *Cancer Immunol Res*, 2013;1:320-31. 10.1158/2326-6066.CIR-13-0086
20. Yum JI, Hong YK. Terminating Cancer by Blocking VISTA as a Novel Immunotherapy: Hasta la vista, baby. *Front Oncol*, 2021;11:658488. 10.3389/fonc.2021.658488
21. Mulati K, Hamanishi J, Matsumura N, Chamoto K, Mise N, Abiko K, *et al.* VISTA expressed in tumour cells regulates T cell function. *Br J Cancer*, 2019;120:115-27. 10.1038/s41416-018-0313-5
22. Kuklinski LF, Yan S, Li Z, Fisher JL, Cheng C, Noelle RJ, *et al.* VISTA expression on tumor-infiltrating inflammatory cells in primary cutaneous melanoma correlates with poor disease-specific survival. *Cancer Immunol Immunother*, 2018;67:1113-21. 10.1007/s00262-018-2169-1
23. Lee J, Ahn E, Kissick HT, Ahmed R. Reinvigorating Exhausted T Cells by Blockade of the PD-1 Pathway. *For Immunopathol Dis Therap*, 2015;6:7-17. 10.1615/ForumImmunDisTher.2015014188
24. Pardoll DM. The blockade of immune checkpoints in cancer immunotherapy. *Nat Rev Cancer*, 2012;12:252-64. 10.1038/nrc3239

25. Ribas A, Wolchok JD. Cancer immunotherapy using checkpoint blockade. *Science*, 2018;359:1350-5. 10.1126/science.aar4060
26. Ramos-Casals M, Brahmer JR, Callahan MK, Flores-Chavez A, Keegan N, Khamashta MA, *et al.* Immune-related adverse events of checkpoint inhibitors. *Nat Rev Dis Primers*, 2020;6:38. 10.1038/s41572-020-0160-6
27. Yan T, Yu L, Shangguan D, Li W, Liu N, Chen Y, *et al.* Advances in pharmacokinetics and pharmacodynamics of PD-1/PD-L1 inhibitors. *Int Immunopharmacol*, 2023;115:109638. 10.1016/j.intimp.2022.109638
28. Strauss L, Mahmoud MAA, Weaver JD, Tijaro-Ovalle NM, Christofides A, Wang Q, *et al.* Targeted deletion of PD-1 in myeloid cells induces antitumor immunity. *Sci Immunol*, 2020;5:10.1126/sciimmunol.aay1863
29. Gordon SR, Maute RL, Dulken BW, Hutter G, George BM, McCracken MN, *et al.* PD-1 expression by tumour-associated macrophages inhibits phagocytosis and tumour immunity. *Nature*, 2017;545:495-9. 10.1038/nature22396
30. Klocke K, Sakaguchi S, Holmdahl R, Wing K. Induction of autoimmune disease by deletion of CTLA-4 in mice in adulthood. *Proc Natl Acad Sci U S A*, 2016;113:E2383-92. 10.1073/pnas.1603892113
31. Ibis B, Aliazis K, Cao C, Yenyuwadee S, Boussiotis VA. Immune-related adverse effects of checkpoint immunotherapy and implications for the treatment of patients with cancer and autoimmune diseases. *Front Immunol*, 2023;14:1197364. 10.3389/fimmu.2023.1197364

32. Tekguc M, Wing JB, Osaki M, Long J, Sakaguchi S. Treg-expressed CTLA-4 depletes CD80/CD86 by trogocytosis, releasing free PD-L1 on antigen-presenting cells. *Proc Natl Acad Sci U S A*, 2021;11810.1073/pnas.2023739118
33. Saad P, Kasi A. Ipilimumab. *StatPearls*. Treasure Island (FL) ineligible companies. Disclosure: Anup Kasi declares no relevant financial relationships with ineligible companies.; 2023.
34. Yang L, Ning Q, Tang SS. Recent Advances and Next Breakthrough in Immunotherapy for Cancer Treatment. *J Immunol Res*, 2022;2022:8052212. 10.1155/2022/8052212
35. Mitra A, Barua A, Huang L, Ganguly S, Feng Q, He B. From bench to bedside: the history and progress of CAR T cell therapy. *Front Immunol*, 2023;14:1188049. 10.3389/fimmu.2023.1188049
36. Sterner RC, Sterner RM. CAR-T cell therapy: current limitations and potential strategies. *Blood Cancer J*, 2021;11:69. 10.1038/s41408-021-00459-7
37. Dagar G, Gupta A, Masoodi T, Nisar S, Merhi M, Hashem S, *et al.* Harnessing the potential of CAR-T cell therapy: progress, challenges, and future directions in hematological and solid tumor treatments. *J Transl Med*, 2023;21:449. 10.1186/s12967-023-04292-3
38. Tang TCY, Xu N, Nordon R, Haber M, Micklethwaite K, Dolnikov A. Donor T cells for CAR T cell therapy. *Biomark Res*, 2022;10:14. 10.1186/s40364-022-00359-3
39. Kazemi MH, Sadri M, Najafi A, Rahimi A, Baghernejadan Z, Khorramdelazad H, *et al.* Tumor-infiltrating lymphocytes for treatment of solid tumors: It takes two to tango? *Front Immunol*, 2022;13:1018962. 10.3389/fimmu.2022.1018962

40. Zhao Y, Deng J, Rao S, Guo S, Shen J, Du F, *et al.* Tumor Infiltrating Lymphocyte (TIL) Therapy for Solid Tumor Treatment: Progressions and Challenges. *Cancers (Basel)*, 2022;1410.3390/cancers14174160
41. Esfahani K, Roudaia L, Buhlaiga N, Del Rincon SV, Papneja N, Miller WH, Jr. A review of cancer immunotherapy: from the past, to the present, to the future. *Curr Oncol*, 2020;27:S87-S97. 10.3747/co.27.5223
42. Lin MJ, Svensson-Arvelund J, Lubitz GS, Marabelle A, Melero I, Brown BD, *et al.* Cancer vaccines: the next immunotherapy frontier. *Nat Cancer*, 2022;3:911-26. 10.1038/s43018-022-00418-6
43. Conlon KC, Miljkovic MD, Waldmann TA. Cytokines in the Treatment of Cancer. *J Interferon Cytokine Res*, 2019;39:6-21. 10.1089/jir.2018.0019
44. Kartikasari AER, Huertas CS, Mitchell A, Plebanski M. Tumor-Induced Inflammatory Cytokines and the Emerging Diagnostic Devices for Cancer Detection and Prognosis. *Front Oncol*, 2021;11:692142. 10.3389/fonc.2021.692142
45. Lan T, Chen L, Wei X. Inflammatory Cytokines in Cancer: Comprehensive Understanding and Clinical Progress in Gene Therapy. *Cells*, 2021;1010.3390/cells10010100
46. Rallis KS, Corrigan AE, Dadah H, George AM, Keshwara SM, Sideris M, *et al.* Cytokine-based Cancer Immunotherapy: Challenges and Opportunities for IL-10. *Anticancer Res*, 2021;41:3247-52. 10.21873/anticancer.15110
47. Berraondo P, Sanmamed MF, Ochoa MC, Etxeberria I, Aznar MA, Perez-Gracia JL, *et al.* Cytokines in clinical cancer immunotherapy. *Br J Cancer*, 2019;120:6-15. 10.1038/s41416-018-0328-y

48. Rosenberg SA. IL-2: the first effective immunotherapy for human cancer. *J Immunol*, 2014;192:5451-8. 10.4049/jimmunol.1490019
49. Shalhout SZ, Miller DM, Emerick KS, Kaufman HL. Therapy with oncolytic viruses: progress and challenges. *Nat Rev Clin Oncol*, 2023;20:160-77. 10.1038/s41571-022-00719-w
50. Zahavi D, Weiner L. Monoclonal Antibodies in Cancer Therapy. *Antibodies (Basel)*, 2020;910.3390/antib9030034
51. Ordonez-Reyes C, Garcia-Robledo JE, Chamorro DF, Mosquera A, Sussmann L, Ruiz-Patino A, *et al.* Bispecific Antibodies in Cancer Immunotherapy: A Novel Response to an Old Question. *Pharmaceutics*, 2022;1410.3390/pharmaceutics14061243
52. van de Donk N, Zweegman S. T-cell-engaging bispecific antibodies in cancer. *Lancet*, 2023;402:142-58. 10.1016/S0140-6736(23)00521-4
53. de Visser KE, Joyce JA. The evolving tumor microenvironment: From cancer initiation to metastatic outgrowth. *Cancer Cell*, 2023;41:374-403. 10.1016/j.ccell.2023.02.016
54. Yenyuwadee S, Aliasis K, Wang Q, Christofides A, Shah R, Patsoukis N, *et al.* Immune cellular components and signaling pathways in the tumor microenvironment. *Semin Cancer Biol*, 2022;86:187-201. 10.1016/j.semcancer.2022.08.004
55. Christofides A, Strauss L, Yeo A, Cao C, Charest A, Boussiotis VA. The complex role of tumor-infiltrating macrophages. *Nat Immunol*, 2022;23:1148-56. 10.1038/s41590-022-01267-2

56. Salmaninejad A, Valilou SF, Soltani A, Ahmadi S, Abarghan YJ, Rosengren RJ, *et al.* Tumor-associated macrophages: role in cancer development and therapeutic implications. *Cell Oncol (Dordr)*, 2019;42:591-608. 10.1007/s13402-019-00453-z
57. Ghouse SM, Vadrevu SK, Manne S, Reese B, Patel J, Patel B, *et al.* Therapeutic Targeting of Vasculature in the Premetastatic and Metastatic Niches Reduces Lung Metastasis. *J Immunol*, 2020;204:990-1000. 10.4049/jimmunol.1901208
58. Veglia F, Sanseviero E, Gabrilovich DI. Myeloid-derived suppressor cells in the era of increasing myeloid cell diversity. *Nat Rev Immunol*, 2021;21:485-98. 10.1038/s41577-020-00490-y
59. Del Prete A, Salvi V, Soriani A, Laffranchi M, Sozio F, Bosisio D, *et al.* Dendritic cell subsets in cancer immunity and tumor antigen sensing. *Cell Mol Immunol*, 2023;20:432-47. 10.1038/s41423-023-00990-6
60. Ma Y, Shurin GV, Peiyuan Z, Shurin MR. Dendritic cells in the cancer microenvironment. *J Cancer*, 2013;4:36-44. 10.7150/jca.5046
61. Gupta YH, Khanom A, Acton SE. Control of Dendritic Cell Function Within the Tumour Microenvironment. *Front Immunol*, 2022;13:733800. 10.3389/fimmu.2022.733800
62. Yu S, Liu C, Su K, Wang J, Liu Y, Zhang L, *et al.* Tumor exosomes inhibit differentiation of bone marrow dendritic cells. *J Immunol*, 2007;178:6867-75. 10.4049/jimmunol.178.11.6867
63. Lin B, Du L, Li H, Zhu X, Cui L, Li X. Tumor-infiltrating lymphocytes: Warriors fight against tumors powerfully. *Biomed Pharmacother*, 2020;132:110873. 10.1016/j.biopha.2020.110873

64. Kumar S, Singh SK, Rana B, Rana A. Tumor-infiltrating CD8(+) T cell antitumor efficacy and exhaustion: molecular insights. *Drug Discov Today*, 2021;26:951-67. 10.1016/j.drudis.2021.01.002
65. Jin X, Cai Y, Xue G, Que J, Cheng R, Yang Y, *et al.* Identification of shared characteristics in tumor-infiltrating T cells across 15 cancers. *Mol Ther Nucleic Acids*, 2023;32:189-202. 10.1016/j.omtn.2023.03.007
66. Yu P, Fu YX. Tumor-infiltrating T lymphocytes: friends or foes? *Lab Invest*, 2006;86:231-45. 10.1038/labinvest.3700389
67. Vignali DA, Collison LW, Workman CJ. How regulatory T cells work. *Nat Rev Immunol*, 2008;8:523-32. 10.1038/nri2343
68. Togashi Y, Shitara K, Nishikawa H. Regulatory T cells in cancer immunosuppression - implications for anticancer therapy. *Nat Rev Clin Oncol*, 2019;16:356-71. 10.1038/s41571-019-0175-7
69. Ishida Y, Agata Y, Shibahara K, Honjo T. Induced expression of PD-1, a novel member of the immunoglobulin gene superfamily, upon programmed cell death. *EMBO J*, 1992;11:3887-95. 10.1002/j.1460-2075.1992.tb05481.x
70. Riley JL. PD-1 signaling in primary T cells. *Immunol Rev*, 2009;229:114-25. 10.1111/j.1600-065X.2009.00767.x
71. Chemnitz JM, Parry RV, Nichols KE, June CH, Riley JL. SHP-1 and SHP-2 associate with immunoreceptor tyrosine-based switch motif of programmed death 1 upon primary human T cell stimulation, but only receptor ligation prevents T cell activation. *J Immunol*, 2004;173:945-54. 10.4049/jimmunol.173.2.945

72. Patsoukis N, Duke-Cohan JS, Chaudhri A, Aksoylar HI, Wang Q, Council A, *et al.* Interaction of SHP-2 SH2 domains with PD-1 ITSM induces PD-1 dimerization and SHP-2 activation. *Commun Biol*, 2020;3:128. 10.1038/s42003-020-0845-0
73. Marasco M, Berteotti A, Weyershaeuser J, Thorausch N, Sikorska J, Krausze J, *et al.* Molecular mechanism of SHP2 activation by PD-1 stimulation. *Sci Adv*, 2020;6:eaay4458. 10.1126/sciadv.aay4458
74. Yokosuka T, Takamatsu M, Kobayashi-Imanishi W, Hashimoto-Tane A, Azuma M, Saito T. Programmed cell death 1 forms negative costimulatory microclusters that directly inhibit T cell receptor signaling by recruiting phosphatase SHP2. *J Exp Med*, 2012;209:1201-17. 10.1084/jem.20112741
75. Rota G, Niogret C, Dang AT, Barros CR, Fonta NP, Alfei F, *et al.* Shp-2 Is Dispensable for Establishing T Cell Exhaustion and for PD-1 Signaling In Vivo. *Cell Rep*, 2018;23:39-49. 10.1016/j.celrep.2018.03.026
76. Tartaglia M, Niemeyer CM, Fragale A, Song X, Buechner J, Jung A, *et al.* Somatic mutations in PTPN11 in juvenile myelomonocytic leukemia, myelodysplastic syndromes and acute myeloid leukemia. *Nat Genet*, 2003;34:148-50. 10.1038/ng1156
77. Lindsey S, Huang W, Wang H, Horvath E, Zhu C, Eklund EA. Activation of SHP2 protein-tyrosine phosphatase increases HoxA10-induced repression of the genes encoding gp91(PHOX) and p67(PHOX). *J Biol Chem*, 2007;282:2237-49. 10.1074/jbc.M608642200
78. Zhu C, Lindsey S, Konieczna I, Eklund EA. Constitutive activation of SHP2 protein tyrosine phosphatase inhibits ICSBP-induced transcription of the gene encoding gp91PHOX during myeloid differentiation. *J Leukoc Biol*, 2008;83:680-91. 10.1189/jlb.0807514

79. Huang W, Saberwal G, Horvath E, Zhu C, Lindsey S, Eklund EA. Leukemia-associated, constitutively active mutants of SHP2 protein tyrosine phosphatase inhibit NF1 transcriptional activation by the interferon consensus sequence binding protein. *Mol Cell Biol*, 2006;26:6311-32. 10.1128/MCB.00036-06
80. Netherby CS, Messmer MN, Burkard-Mandel L, Colligan S, Miller A, Cortes Gomez E, *et al.* The Granulocyte Progenitor Stage Is a Key Target of IRF8-Mediated Regulation of Myeloid-Derived Suppressor Cell Production. *J Immunol*, 2017;198:4129-39. 10.4049/jimmunol.1601722
81. Lindsey S, Zhu C, Lu YF, Eklund EA. HoxA10 represses transcription of the gene encoding p67phox in phagocytic cells. *J Immunol*, 2005;175:5269-79. 10.4049/jimmunol.175.8.5269